

**Treatment of azo dyes in industrial wastewater using  
microbial fuel cells**

**Eustace Fernando**

Faculty of Science and Technology

This is an electronic version of a PhD thesis awarded by the University of Westminster. © The Author, 2014.

This is an exact reproduction of the paper copy held by the University of Westminster library.

---

The WestminsterResearch online digital archive at the University of Westminster aims to make the research output of the University available to a wider audience. Copyright and Moral Rights remain with the authors and/or copyright owners.

Users are permitted to download and/or print one copy for non-commercial private study or research. Further distribution and any use of material from within this archive for profit-making enterprises or for commercial gain is strictly forbidden.

---

Whilst further distribution of specific materials from within this archive is forbidden, you may freely distribute the URL of WestminsterResearch:  
(<http://westminsterresearch.wmin.ac.uk/>).

In case of abuse or copyright appearing without permission e-mail  
[repository@westminster.ac.uk](mailto:repository@westminster.ac.uk)

# **TREATMENT OF AZO DYES IN INDUSTRIAL WASTEWATER USING MICROBIAL FUEL CELLS**

By

**EUSTACE FERNANDO**

University of Westminster

Faculty of Science and Technology

A thesis submitted in partial fulfilment of the requirements of  
the University of Westminster for the degree of  
Doctor of Philosophy

March 2014

## Abstract

Due to the extensive use of xenobiotic azo dyes in the colour industry and their proven mutagenic and cytotoxic nature, their treatment prior to discharge is essential and is legally enforced. However, currently used wastewater treatment technologies such as activated sludge systems, anaerobic digestion, electrochemical destruction, adsorption and membrane filtration are ineffective in removing azo dyes due to reasons such as inefficient dye degradation, slow degradation kinetics, toxic metabolite formation, inhibitory costs and generation of secondary waste streams. Therefore, in this study, microbial fuel cells (MFCs) were studied as possible systems that could effectively degrade azo dyes with an additional benefit of concomitant biogenic electricity generation.

The co-metabolic degradation of the model azo dye Acid Orange-7 (AO-7) using *Shewanella oneidensis* and mixed anaerobic cultures in MFC was carried out with particular emphasis on AO-7 degradation kinetics in the initial study. The effect of using various carbon sources including cheaper complex ones such as molasses and corn steep liquor as electron donors for azo dye degradation in MFCs was also investigated. The outcomes of this study demonstrated that fast AO-7 reductive degradation kinetics using cheap, sustainable co-substrate types can be achieved with concomitant bioelectricity generation in two-chamber MFCs. Power densities up-to 37 mWm<sup>-2</sup> were observed in the two-chamber MFC system during AO-7 decolourisation.

Co-metabolic reductive degradation of azo dye mixtures using dye acclimated mixed microbial populations under industrially relevant conditions (high temperatures and salinities) and changes in microbial community structure in the MFCs in presence of complex azo dye mixtures in two-chamber MFCs was investigated. The outcomes of this work demonstrated that efficient colour and organic content removal can be achieved under high temperatures and moderate salinities using azo dye adapted mixed microbial populations in two-chamber MFCs. Microbial community analysis of the original anaerobic consortium and the azo dye adapted microbial culture following MFC operation indicated that both cultures were dominated by bacteria belonging to the phylum Firmicutes. However, bacteria belonging to phyla Proteobacteria and Bacteroidetes also became selected following MFC operation. Peak power densities up-to 27 mWm<sup>-2</sup> were observed in this study during decolourisation of complex azo dye mixtures.

The complete degradation of the azo dye AO-7 using a sequential reductive – oxidative bioprocess in a combined MFC-aerobic bioreactor system operating at ambient temperature in continuous mode was studied. The outcomes of this study demonstrated that the azo dye AO-7 can be fully decolourised and degraded into non-toxic and simpler metabolites. Maximum power densities up-to 52 mWm<sup>-2</sup> were observed during azo dye degradation. A modular scale-up version (with a volumetric scale-up factor of 6) of the two stage integrated bioreactor system demonstrated the capability to efficiently treat two types of real wastewater originating from colour industry without any apparent deterioration of reactor performance in terms of dye decolourisation and COD removal.

The use of applied external resistance ( $R_{ext}$ ) and redox mediators as tools for enhancing azo dye degradation kinetics in dual chamber MFCs was studied. The outcomes of this work suggest that azo dye reductive degradation kinetics in MFC anodes can be influenced by varying  $R_{ext}$ . Furthermore, AO-7 reductive degradation kinetics was improved in a concentration-dependent manner by exogenous addition of two electron shuttling compounds anthraquinone-2,6-disulfonic acid and anthraquinone-2-sulfonic acid in MFC anodes.

The overall outcomes of this study implies that MFCs could be successfully applied for achieving enhanced azo dye reductive biodegradation kinetics in MFC anodes coupled with concomitant bioelectricity generation. It further demonstrated that MFC systems can be successfully integrated with existing wastewater treatment technologies such as activated sludge systems for complete degradation and toxicity removal of azo dyes and their biotransformation metabolites.

# Table of Contents

Chapter 1 - General introduction .....	1
1.1. Dyes and the history of the colour industry .....	2
1.2. Types of synthetic dyes and their uses in the colour industry .....	4
1.2.1. Basic dyes (cationic dyes) .....	4
1.2.2. Acid dyes .....	4
1.2.3. Direct dyes .....	5
1.2.4. Reactive dyes .....	5
1.2.5. Disperse dyes .....	6
1.3. Azo compounds and their chemistry .....	6
1.3.1. Azo dyes and colour .....	7
1.3.2. Azobenzenes and the effect of chemical substituent groups of the aryl rings on colour .....	8
1.3.3. The extent of production and usage of azo dyes in colour industry .....	9
1.3.4. Azo dye contaminated wastewater disposal and legislation pertaining to colour industry wastewater discharge .....	9
1.4. Problem statement .....	12
1.5. Current methods for treatment of colour industry wastewater .....	13
1.5.1. Physico-chemical dye removal methods .....	13
1.5.2. Electrochemical removal of synthetic dyes .....	15
1.5.3. Biological degradation methods .....	17
1.5.4. Reductive degradation of azo dyes .....	17
1.6. Use of Bioelectrochemical systems for azo dye removal .....	22
1.6.1. Bio-electrochemical systems and microbial fuel cells (MFC) .....	22
1.6.2. Microbial fuel cells and the history of Bioelectrochemical systems .....	22
1.6.3. Working principle of MFCs .....	24
1.6.4. Thermodynamics of MFCs .....	26
1.6.5. Internal losses of MFCs and OCV .....	28
1.6.6. Types of Microbial fuel cells .....	30
1.6.7. Microbial electrolysis cells .....	34
1.6.8. The use of BES for pollutant removal .....	35
1.7. Hypothesis .....	39
1.8. Aims and objectives of the current project .....	39
1.8.1. Specific objectives .....	40
Chapter 2 - Materials and Methods .....	44
2.1. Chemicals .....	45

2.2. Bacterial strains, their maintenance and MFC anode culture media.....	49
2.3. Bio-electrochemical systems and operation.....	54
2.4. Experimental design.....	64
2.5. Analytical procedure.....	67
2.5.1. AO7 decolourisation and kinetic study.....	67
2.5.2. Assessment of decolourisation of the azo dye mix containing simulated wastewater .....	68
2.5.3. COD removal .....	69
2.5.4. Extraction of AO-7 degradation products .....	70
2.5.5. Detection of degradation products using HPLC .....	71
2.5.6. Identification of degradation metabolites using HPLC-MS .....	71
2.5.7. Quantification of 4-aminobenzenesulfonic acid and 1-amino-2-naphthol .....	72
2.5.8. Fourier Transform Infra-Red (FTIR) analysis.....	73
2.5.9. Toxicity assessment.....	74
2.5.10. Mutagenicity assessment using Ames test.....	75
2.5.11. Electrochemical monitoring .....	79
2.5.12. Microbial community analysis .....	82
2.6. Statistical analysis of data.....	87
<b>Chapter 3 - Co-metabolic reductive degradation of Acid Orange - 7 in microbial fuel cell anodes .....</b>	<b>88</b>
3.2. Results and discussion .....	90
3.2.1. Anodic decolourisation of AO7 and kinetics of AO7 removal.....	90
3.2.2. The effect of co-substrate type on decolourisation kinetics of AO7 .....	94
3.2.3. The effect of pH on AO-7 co-metabolic degradation in MFC anodes by <i>S.oneidensis</i> .....	95
3.2.4. Decolourisation metabolites of AO7 and COD removal during MFC operation .....	97
3.2.6. Assessment of mutagenic potential of the AO7 decolourisation metabolites using the Ames test. ....	100
3.2.7. Assessment of electrochemical parameters during AO7 decolourisation .....	103
3.3. Concluding remarks .....	105
<b>Chapter 4 - Co-metabolic decolourisation of azo dye mixtures by dye-acclimated mixed microbial populations in MFCs .....</b>	<b>106</b>
4.2. Results and Discussion .....	108
4.2.1. Decolourisation of azo dye mixtures during fed-batch MFC operation.....	108
4.2.2. Decolourisation and COD removal performance during MFC fed-batch operation.....	109

4.2.3. Decolourisation and bio-electrochemical system performances under thermophilic and saline conditions .....	113
4.2.3. Bacterial 16s rDNA community analysis of the original anaerobic digested sludge and azo dye/MFC adapted dye degrading culture .....	116
4.3. Concluding remarks .....	121
<b>Chapter 5 - An integrated MFC – aerobic bioreactor process for complete degradation of Acid Orange-7 .....</b>	<b>122</b>
5.2. Results and discussion .....	124
5.2.1. AO7 degradation, colour removal and soluble COD reduction during two-stage reactor operation .....	124
5.2.2. Aminobenzene formation during the MFC stage and amine removal in the subsequent aerobic stage .....	126
5.2.3. Toxicity reduction during the two stage reactor operation .....	129
5.2.4. Biogenic electricity generation during AO-7 degradation.....	130
5.2.5. Degradation of aminobenzenes in the aerobic second stage .....	132
5.2.6. Putative biodegradation pathway of AO-7.....	134
5.2.7. The effect of shock AO-7 loadings on MFC operation .....	139
5.3. Concluding remarks .....	140
<b>Chapter 6 - The scale up tubular air-breathing MFCs and treatment of real colour industry wastewater .....</b>	<b>141</b>
6.2. Results and discussion.....	143
6.2.1. Decolourisation and COD removal in AO-7 containing model wastewater in the scaled up MFC-aerobic reactor system.....	143
6.2.2. Decolourisation of real colour industry wastewater in the scaled up system...	144
6.2.3. Electrochemical performance of the parallel connected MFC modules during real and simulated wastewater treatment.....	149
6.2.4. Degradation of colouring agents in real colour industry wastewater in the MFC – aerobic two stage process .....	152
6.3. Concluding remarks .....	155
<b>Chapter 7 - External resistance and redox mediators as potential tools for influencing azo dye reductive decolourisation kinetics in MFCs.....</b>	<b>156</b>
7.2. Results and discussion.....	158
7.2.1. Azo dye degradation kinetics and MFC external resistance .....	158
7.2.2. Simultaneous power production in MFCs coupled to azo dye degradation under various external resistances .....	162
7.2.3. COD reduction in MFCs during azo dye reductive decolourisation under various external resistances .....	163
7.2.4. Microbial community variations in MFCs under different external resistances	164

7.2.5. The effect of exogenous addition of synthetic redox mediators on azo dye decolourisation in MFC anodes.....	170
7.3. Concluding remarks .....	175
<b>Chapter 8 - Conclusions .....</b>	<b>176</b>
<b>Chapter 9 - Future work.....</b>	<b>183</b>
9.1. Development of biocathodes for colour industry wastewater treatment .....	184
9.2. The use of enzymes as the cathode catalyst in MFCs for simultaneous azo dye degradation and bioelectricity generation.....	185
9.3. Integrating advanced oxidation processes (AOP) with MFCs for complete azo dye degradation .....	186
9.4. Incorporating molecular and synthetic biology approaches for engineering microbes that are better capable of extracellular electron transfer.....	187
<b>References .....</b>	<b>189</b>
<b>List of publications.....</b>	<b>212</b>
<b>Appendix 1 .....</b>	<b>213</b>
<b>Appendix 2 .....</b>	<b>214</b>

# List of Figures

## Chapter 1

**Figure 1.1:** Bismarck Brown, one of the first synthetic azo dyes

**Figure 1.2:** Sir William Henry Perkins

**Figure 1.3:** Acid dyes belonging to different chemical classes

**Figure 1.4:** Two compounds exemplifying A) an alkyl azo compound and B) an aryl azo compound.

**Figure 1.5:** The bathochromic shift of –OH substituted azobenzene

**Figure 1.6:** A highly coloured wastewater stream from the textile industry being released unlawfully into a natural waterway

**Figure 1.7:** Modes of azo dye reductive degradation in biotic environments under anaerobic conditions

**Figure 1.8:** Current and proposed methods for removal of synthetic dyes from industrial wastewater

**Figure 1.9:** The working principle of a microbial fuel cell (MFC) and microbial electrolysis cell (MEC)

**Figure 1.10:** Regions of a polarisation curve used to assess the MFC performance depicting the energy losses.

**Figure 1.11:** Types of two-chambered microbial fuel cells

**Figure 1.12:** The working principle of a benthic MFC system

**Figure 1.13:** Different types of single chamber microbial fuel cells

## Chapter 2

**Figure 2.1:** Acid Orange 7 structure

**Figure 2.2:** Schematic diagram of the two-chamber MFC set-up

**Figure 2.3:** Schematic diagram and the hydraulic-flow of the integrated MFC – aerobic bioreactor system

**Figure 2.4:** The experimental set-up during the start-up stage of the continuous run of the two-stage integrated MFC-aerobic bioreactor system

**Figure 2.5:** The up-scaled two stage MFC-aerobic reactor system



**Figure 2.6:** The parallel configured external electrical circuit of the three combined MFC modules

**Figure 2.7:** Components and the hydraulic flow of the up-scaled two-stage integrated bioreactor system

**Figure 2.8:** The scaled up tubular MFC modules for real wastewater treatment

**Figure 2.9:** *Vibrio fischeri* acute cytotoxicity assay standard dose-response curve

**Figure 2.10:** Positive controls for Ames mutagenicity tests using  $\text{NaN}_3$

**Figure 2.11:** The bacterial 16s rRNA gene

## Chapter 3

**Figure 3.1:** AO-7 reductive decolourisation

**Figure 3.2:** (A) The first order logarithmic decay models of AO7 removal

**Figure 3.3:** AO7 removal using different inocula and the MFC electrochemical performance

**Figure 3.4:** The effect of pH on AO-7 co-metabolic decolourisation by *S.oneidensis* in MFC anodes

**Figure 3.5:** The effect of pH variation on MFC power output during AO-7 decolourisation by *S.oneidensis*

**Figure 3.6:** HPLC profile of fully decolourised effluents from MFC anodes

**Figure 3.7:** COD removal during MFC operation within a 48 hour period

**Figure 3.8:** Mean His<sup>+</sup> revertant colonies of *S.typhimurium* TA1535 and TA1538 from Ames tests

**Figure 3.9:** *S.typhimurium* TA1535 and TA1538 His<sup>+</sup> revertants fold increase above background from Ames tests

**Figure 3.10:** MFC electrochemical performance during AO-7 decolourisation

## Chapter 4

**Figure 4.1:** UV-Visible scans of the feed solution and the decolourised samples

**Figure 4.2:** Decolourisation of azo dye mixtures, COD reduction of the feed solution and the MFC voltage generation during MFC operation

**Figure 4.3:** 16s rDNA PCR-DGGE profile differences between the original un-acclimated mixed culture and the culture after MFC operation

**Figure 4.4:** Phylogenetic relationships of the identified bacteria

## Chapter 5

**Figure 5.1:** AO-7 removal during the two stage operation at various AO-7 loading rates

**Figure 5.2:** Removal of amines within the MFC stage and the aerobic stage

**Figure 5.3:** *Vibrio fischeri* luminescence-based toxicity determinations

**Figure 5.4:** MFC current production during the tubular MFC

**Figure 5.5:** Current-power plot and a polarisation curve indicating the tubular MFC performance during azo dye treatment

**Figure 5.6:** HPLC gradient elution profile of the effluent of the aerobic treatment and FTIR spectra of metabolites formed

**Figure 5.7:** Putative aerobic biodegradation pathways of 4-aminobenzenesulfonic acid and 1-amino-2-naphthol

**Figure 5.8:** The recovery of the MFC stage from a shock AO-7 loading of 400 mgL<sup>-1</sup> (200 mL batch tests)

## Chapter 6

**Figure 6.1:** Decolourisation of the model wastewater containing AO7 in the scaled up reactor

**Figure 6.2:** Decolourisation of real wastewater from wool colouring industry

**Figure 6.3:** Decolourisation performance of the scaled up MFC reactor system

**Figure 6.4:** Decolourisation of real wastewater from leather tanning industry

**Figure 6.5:** Decolourisation performance of the scaled up MFC-aerobic reactor

**Figure 6.6:** Current production in scaled – up MFC modules during AO-7 decolourisation

**Figure 6.7:** The average individual electrochemical performance of the three parallel MFC modules

**Figure 6.8:** The power – current plot and polarisation curve of the parallel connected MFCs

**Figure 6.9:** Overlay of HPLC chromatograms of real wastewater from wool colouring industry at different treatment stages

**Figure 6.10:** Overlay of HPLC chromatograms of real wastewater from the leather tanning industry at different treatment stages

## Chapter 7

**Figure 7.1:** Decolourisation kinetic constants of azo dyes at various external resistances

**Figure 7.2:** The variation of maximum power densities obtainable from MFCs under various  $R_{\text{exts}}$

**Figure 7.3:** COD reduction performance of MFC systems under various  $R_{\text{ext}}$

**Figure 7.4:** DGGE fingerprints during AO-7 decolourisation in MFCs operating under various  $R_{\text{exts}}$

**Figure 7.5:** Phylogenetic tree of the bacterial communities selected in MFC anodes under various  $R_{\text{exts}}$

**Figure 7.6:** Cyclic voltammograms of AO-7 containing MFC anodes following the addition of synthetic redox mediators AQDS and AQS

**Figure 7.7:** The concentration-dependant effect of the exogenous supplementation of the redox mediator AQDS on AO-7 degradation kinetics

**Figure 7.8:** The concentration dependant effect of the exogenous supplementation of the redox mediator AQS on AO-7 degradation kinetics

**Figure 7.9:** The non-linear relationship between the mediator concentration and decolourisation kinetic constant ( $k$ )

# List of Tables

## Chapter 1

**Table 1.1:** Typical properties of untreated textile wastewater

**Table 1.2:** A summary of current studies utilising BES for the purpose of removal of recalcitrant pollutants.

## Chapter 2

**Table 2.1:** The composition of azo dye mixture used in the experiments involving azo dye adapted mixed microbial consortium

**Table 2.2:** Typical characteristics of the real industrial wastewater used in this study.

**Table 2.3:** Synthetic redox mediators used

**Table 2.4:** The three model azo dyes used in the current study, their structures, molecular weights and absorbance maxima

**Table 2.5:** Components of the vitamin mix stock solution used in this study

**Table 2.6:** Components of the trace elements stock solution used in this study

**Table 2.7:** Composition of Oceanibulbus medium for *V.fischeri*

**Table 2.8:** The composition of the Vogel-Bonner minimal medium-E (50X stock)

**Table 2.9:** Components used for the preparation of VBE glucose agar plates

**Table 2.10:** Soft-top agar overlay composition

**Table 2.11:** Trace stock solution composition for soft top agar overlay

**Table 2.12:** composition of the denaturing gels (8% acrylamide) used in microbial community analysis

## Chapter 3

**Table 3.1:** Comparison of AO7 removal rates and first order kinetic constants of decolourisation

**Table 3.2:** Comparison of AO7 decolourisation kinetic constants and maximum power densities with different co-substrate types

**Table 3.3:** Comparison of initial and final COD values at various AO7 concentrations

## Chapter 4

**Table 4.1:** The effect of operating temperature on colour removal, COD removal and electrochemical performance of the MFC system

**Table 4.2:** The effect of salinity on colour removal, COD removal and electrochemical performance of the MFC system

**Table 4.3:** Phylogenetic affiliations of PCR-DGGE sequences of the un-adapted anaerobic culture and azo dye adapted culture

## Chapter 7

**Table 7.1:** Phylogenetic affiliations of the 16s rDNA sequences obtained from experiments conducted under various  $R_{\text{exts}}$

# ACKNOWLEDGEMENTS

I would like to express my sincerest gratitude to my director of studies Dr. Godfrey Kyazze for his guidance and his expert advice throughout these years. His passion for research has been a source of inspiration and his guidance and friendship during difficult times was of immense help. I would also like to express my heartfelt gratitude to Professor Tajalli Keshavarz for his guidance, expert advice and having belief in me throughout my study. His knowledge and experience has been a precious contribution. I would like to express my sincere gratitude to the University of Westminster scholarship committee for awarding me a research studentship.

I would like to thank all my friends and colleagues (past and present) at the University of Westminster for their friendship and unwavering support. Special thanks to my friends Rana Amache, Adelaja Seun, Maryam Safari, Hafiz Iqbal, Pradeep Kumar Sachitharan and Artun Sukan. It has been a truly unique experience and life would have been dull without your company. I would like to thank all the technical staff at Cavendish Campus who assisted me in various ways during my work; especially, Dr. Thakor Tandel and Neville Antonio for their incessant assistance whenever the need arose. I would also like to express my heartfelt gratitude to Shivani Sivarajah for her unconditional support, encouragement and precious advice during toughest times.

Many thanks to Hafiz Iqbal, Dr. Pamela Greenwell and Carlos Balcazar Lopez for their help, advice and support for arranging FTIR analysis and Sanger sequencing during my study.

Finally, I would like to thank my parents and my brother for their unconditional love, encouragement and support. I am indebted to them for having understanding and belief in me throughout my struggles and triumphs alike. Without your love, encouragement and sacrifice, this research would not have been possible.

# Author's Declaration

I declare that the present work was carried out in accordance with the Guidelines and Regulations of the University of Westminster.

This thesis is entirely my own work and that where any material could be construed as the work of others, it is fully cited and referenced, and/or with appropriate acknowledgement given.

Until the outcome of the current application to the University of Westminster, the work will not be submitted for any such qualification at another university or similar institution.

Signed : *Eustace Fernando*

Date: 29<sup>th</sup> March 2014

**Eustace Fernando**

*To my beloved parents and brother*

“It is not the answer that enlightens, but the question”

**Eugene Ionesco**



## List of abbreviations

- ANOVA – Analysis of variance
- AO-7 – Acid Orange 7
- AOP – advanced oxidation processes
- APHA – American Public Health Association
- AQDS - anthraquinone-2,6-disulfonic acid
- AQS - anthraquinone-2-sulfonic acid
- ATP – Adenosine Triphosphate
- BDD – Boron doped diamond
- BES – Bio-electrochemical system
- BLAST – Basic Local Alignment Search Tool
- BOD – Biochemical oxygen demand
- CE – Coulombic efficiency
- COD – Chemical oxygen demand
- CoTMPP - cobalt tetramethylphenylporphyrin
- DAF – dissolved air flotation
- DE – Decolourisation efficiency
- DEFRA – Department for Environment Food and Rural Affairs
- DF – Dilution factor
- DGGE – Denaturing gradient gel electrophoresis
- DI – De-ionised
- DNA – Deoxyribonucleic acid
- DY-106 – Direct Yellow 106
- $E'_0$  = Standard reduction potential
- $E^0_{\text{emf}}$  – Electromotive force at standard conditions
- $E_{\text{anode}}$  – Anode potential
- $E_{\text{cathode}}$  – Cathode potential
- $E_{\text{cell}}$  = Cell voltage
- EDTA - Ethylenediaminetetraacetic acid
- $E_{\text{emf}}$  – Electromotive force
- EET – Extracellular electron transfer
- ESI – Electrospray ionisation
- F - Faraday's constant ( $9.64853 \times 10^4 \text{ C mol}^{-1}$ )
- FAS – Ferrous ammonium sulphate

- FTIR – Fourier Transform Infrared Spectroscopy
- $g$  – Gravitational force
- HPLC – High Performance Liquid Chromatography
- HPLC-MS - High Performance Liquid Chromatography – Mass Spectrometry
- HRT – Hydraulic retention time
- $IC_{50}$  – Half maximal inhibitory concentration
- $IR\Omega$  – sum of all Ohmic losses
- $K$  – Decolourisation kinetic constant
- kDa – Kilo Dalton
- LB – Luria-Bertani growth medium
- MEC – Microbial electrolysis cell
- MFC – Microbial fuel cell
- NADH – Nicotinamide Adenine Dinucleotide reduced form
- NADPH – Nicotinamide Adenine Dinucleotide Phosphate reduced form
- NCBI – National Center for Biotechnology Information
- NCIMB - National Collection of Industrial, food and Marine Bacteria
- NIST – National Institute of Standards and Technology
- NTA – Nitrilotriacetic acid
- OCV – Open circuit potential
- ORP – Oxidation/reduction potential
- PABA – p-aminobenzoic acid
- PC – phthalocyanine
- PCR – Polymerase chain reaction
- PDA – Photodiode array
- $P_{max}$  – Maximum power density
- $pO_2$  – Oxygen partial pressure
- PTFE – Polytetrafluoroethylene
- PVC – Polyvinyl chloride
- $R$  – Universal gas constant ( $8.31447 \text{ J mol}^{-1} \text{ K}^{-1}$ )
- rDNA – Ribosomal DNA
- RE – Removal efficiency
- $R_{ext}$  – External resistance
- $R_{int}$  – Internal resistance

- RR-3 – Reactive Red 3
- $R_t$  – Retention time
- SD – Standard deviation
- T – Absolute temperature (Kelvins)
- TAE – Tris- Acetate EDTA buffer
- TDS – Total dissolved solids
- UASB – up-flow anaerobic sludge blanket
- UPGMA - Unweighted Pair-Group Method with Arithmetic Mean
- UV – ultraviolet
- V/V – Volume per volume
- VBE – Vogel-Bonner minimal medium – E
- W/V – Weight per volume
- WFD – Water Framework Directive
- $\Delta G_r^0$  - Gibbs free energy (Joules) at standard conditions (298.15 K temperature, 1 bar pressure and 1M concentrations of all chemical species)
- $\Delta G_r$  - Gibbs free energy (Joules)
- $\lambda_{\max}$  – Absorbance maximum
- $\Pi$  - Reaction quotient
- $\Sigma\eta_a$  - anode related overpotential
- $\Sigma\eta_c$  - Cathode related overpotential

*This page intentionally left blank*

# **Chapter 1 - General introduction**

## 1.1. Dyes and the history of the colour industry

Dyes impart colour to various materials such as textile, paper and leather in a way that the colour is not readily altered by factors such as washing, light or heat. Prior to the industrial revolution, all dyes that were in human use were produced from natural sources. Written records of the first use of dyes and colouring agents run as far back in history as 4600 years in ancient China and ancient Egypt. When Alexander the Great's army conquered the Persian capital of Susa in 331 BCE, they took custody of vast stocks of magnificent purple dyed royal robes. By the time of the Alexander the Great's conquest of the Persian Empire, the colour industry utilising many natural dyes was a thriving industry in that part of the ancient world. A myriad of colours were provided by natural sources. A bright yellow/flavonoid colour originating from *Reseda luteola* (weld) seeds and blue/indigo colour originating from *Indigofera tinctoria* (indigo plant) leaves are a few examples of natural dyes that were used to colour textiles, walls and other materials throughout the ancient world.

Following the industrial revolution, synthetic dyes started to replace the natural dyes from colour industry processes. In 1856, William Henry Perkins (Figure 1.2) synthesised the first synthetic dyestuff –aniline based cationic dye called Mauveine while trying to synthesize the antimalarial drug quinine (Tyagi and Yadav, 2001). The first synthetic azo dye Bismarck Brown was synthesised by the German industrial chemist Johann Peter Griess in the year 1858 (Figure 1.1).

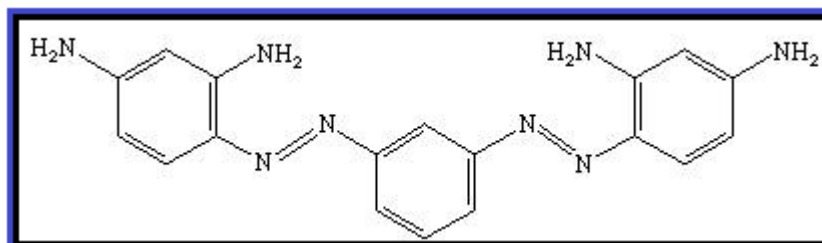


**Figure 1.1:** Bismarck Brown, one of the first synthetic azo dyes

The emergence of a vast variety of synthetic dyes including azo dyes soon followed after these discoveries and transformed the colour industry in a major way. Synthetic dyes were cheaper to produce, offered a large variety of colours and could be made available in vast quantities for the rapidly expanding and highly profitable colour industry. These advancements displaced the natural dyes from the industrial market and synthetic dyes replaced them rapidly.

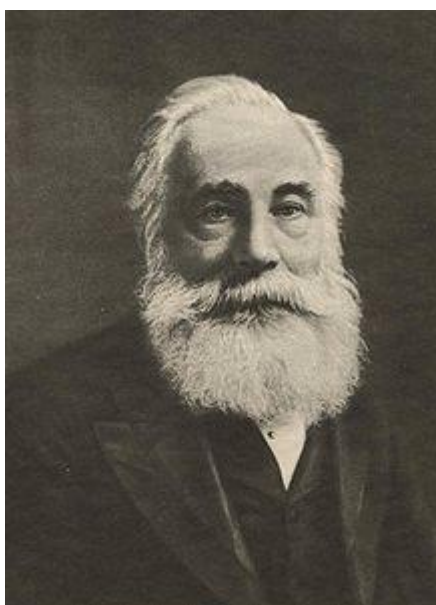


**Figure 1.2:** Sir William Henry Perkin is considered as the father of the synthetic colour industry due to his invention of the first ever synthetic dye Mauveine. (Image adapted from - [http://en.wikipedia.org/wiki/William\\_Henry\\_Perkin](http://en.wikipedia.org/wiki/William_Henry_Perkin))

Since the industrial revolution, thousands of different types of synthetic dyes bearing a vast variety of properties are chemically synthesised and are made available in substantial quantities for the colour industry. The extent of the use of

synthetic dyes spans from textile industry, where it is used in most quantities to paper and leather industries. Other industrial sectors using synthetic dyes include food, petroleum and pharmaceutical industries.

## **1.2. Types of synthetic dyes and their uses in the colour industry**

### **1.2.1. Basic dyes (cationic dyes)**

Basic dyes are cationic in nature and carry cationic groups such as  $-NR_3^+$  and  $=NR_2^+$ . They are mostly aniline based synthetic dyes (Christie, 2001). Due to the cationic nature of the basic dyes, they are well suited for dyeing anionic fibres such as acrylic fibres and less well used in dyeing wool or nylon. However, basic dyes are known for their intrinsic poor lightfastness and poor adherence to fibre substrates (Shah and Jain, 1983). Common basic dyes include methylene blue, safranin and crystal violet.

### **1.2.2. Acid dyes**

Acid dyes are organic dyes bearing sulfonic, carboxylic or phenol groups that exhibit affinity to cationic sites of fibres. The fixation of the dye during the dyeing process is mainly due to salt formation between the anionic groups of the dye and cationic groups of the fibre substrate (Christie, 2001). During the dyeing process using acid dyes, the pH value of the dye bath is often reduced in order to maintain the amino groups of the fibre substrate in protonated state, hence, increasing the fixation of acid dyes to the fibres substrate (Carpar et al, 2006). Acid dyes are often effective at dyeing wool, silk and nylon fibres, whereas they are ineffective when used with cellulosic fibre types such as cotton. Acid dyes comprises of synthetic dyes belonging to anthraquinone, azobenzene and triphenylmethane chemical classes (Figure 1.3).



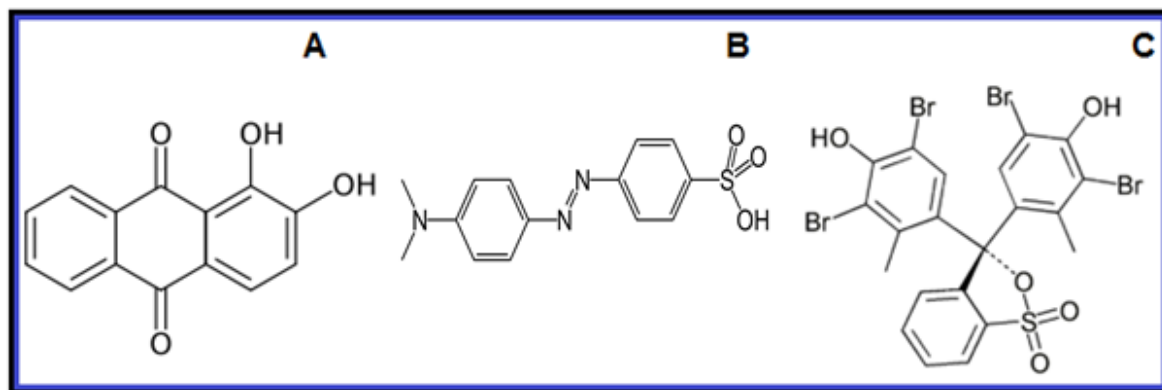


**Figure 1.3:** Acid dyes belonging to different chemical classes (A) anthraquinone (Alizarin) (CAS No- 72-48-0) (B) azobenzene (Methyl Orange) (CAS No- 547-58-0) and (C) Triphenylmethane (Bromocresol green) (CAS No- 76-60-8)

### 1.2.3. Direct dyes

Direct dyes generally are relatively large dye molecules that are adhered to the fibre substrate by hydrogen bonding and Van der Waals attractions. Hence, slightly alkaline media and temperatures close to boiling point are used in dye baths in order to ensure good affinity of the direct dye to its fibre substrate. Furthermore, salts such as  $\text{Na}_2\text{SO}_4$ ,  $\text{NaCl}$  and  $\text{Na}_2\text{CO}_3$  are often used in order to drive the direct dye on to the fibre substrate. Direct dyes are mostly used for cellulosic fibre substrates such as cotton and jute. However, due to the weak bonding affinities between the direct dye and the fibre substrate, they are known for poor washfastness and excessive dye wastage and discharge during dyeing processes (Christie, 2001).

### 1.2.4. Reactive dyes

Reactive dyes possess chemical substituent groups that can directly react and form covalent linkages with the fibre substrate. The covalent linkage of reactive dyes to their substrates gives them excellent washfastness. Moreover, cold reactive dyes enable the use of reactive dyes at room temperature. Unlike disperse dyes where high temperatures are required for dyeing process, cold

reactive dyes allow high affinity to its fibre substrate under milder conditions. Therefore, reactive dyes are the most favoured type of dye class amongst all dye types used in the colour industry and have seen widespread use within the industry (Chiou and Li, 2003). Common commercial examples of reactive dyes include Reactive Black-5 (CAS No - 17095-24-8) and Reactive Red-3 (CAS No- 23211-47-4).

#### **1.2.5. Disperse dyes**

Disperse dyes are highly conjugated planer structures that are often insoluble in water. Disperse dyes are often finely ground with a dispersing agent and made available for dyeing in the form of aqueous suspensions (Neamtu et al, 2004). Due to the absence of ionising groups and planer structures of disperse dyes, they are well suited for dyeing hydrophobic synthetic fibres such as acrylic, nylon, polyester and cellulose triacetate. Some examples of commercially used disperse azo dyes include Disperse Red-1 (CAS No- 2872-52-8) and Disperse Orange-1 (CAS No- 2581-69-3).

### **1.3. Azo compounds and their chemistry**

Majority of the synthetic dyes currently being used in the colour industry belong to the azo chemical class (Pandey et al, 2007). Azo compounds are characterized by its possession of one or more azo chemical moieties ( $-N=N-$ ). The azo linkages in a chemical compound could be flanked by alkyl or aryl groups. Despite azo chemical groups ( $-N=N-$ ) being known as chromophoric (colour bearing) chemical groups, for azo dyes to exhibit vividly different colours, several prerequisite chemical properties are necessary.

### 1.3.1. Azo dyes and colour

In addition to bearing the azo chromophore, azo dyes are required to exhibit resonance of electrons (de-localised p-orbital electrons) in a conjugated aromatic ring system (Abraham, 1977).

When comparing the chromogenic properties of following two compounds, it becomes apparent that the presence of an azo chemical moiety alone would not allow an organic compound to confer properties of a dye.

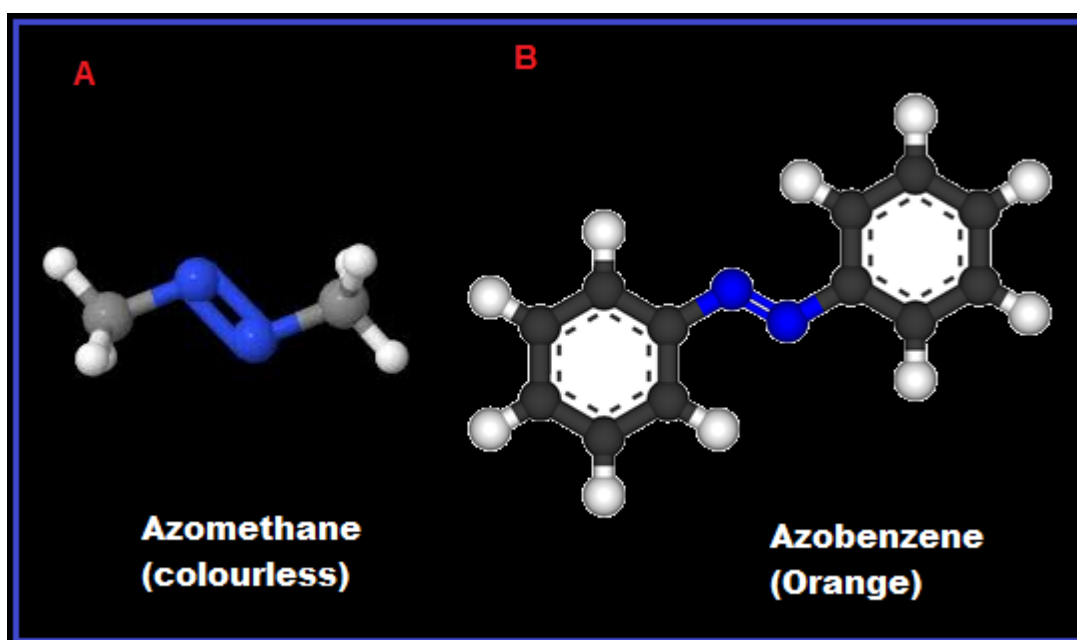


**Figure 1.4:** Two compounds exemplifying an A) an alkyl azo compound and B) an aryl azo compound.

The chromogenic properties of the aforementioned two compounds are distinctly different because the alkyl azo compound lacks a conjugated system and resonance of electrons. Hence, alkyl azomethane is colourless whereas aryl azobenzene is orange in colour (Figure 1.4).

### 1.3.2. Azobenzenes and the effect of chemical substituent groups of the aryl rings on colour

In addition to possessing chromophoric groups, many organic dyes including azo dyes possess auxochromes which cause the colour of a dye to shift towards either end of the visible spectrum. Examples of auxochromes include carboxylic and sulfonic acid groups, amino, nitro and hydroxyl substituent groups of the aryl rings. Therefore, auxochromes are used as aryl ring substituents that can give target colours in organic dyes. Furthermore, auxochromes are used to influence the water solubility of the organic dye. For an example, substituting an aryl ring of an azo dye with electron donating chemical groups (such as  $\text{-NH}_2$ ) prompts the dye to exhibit a bathochromic shift (shift of the emission spectrum towards a longer wavelength). By contrast, the presence of an electron withdrawing chemical groups (such as  $\text{-OH}$  groups) on azo dye aryl rings prompts the opposite effect (Hypsochromic shift) (Towns, 1999). This becomes apparent by observing the bathochromic shift of absorbance maxima ( $\lambda_{\text{max}}$ ) of structurally similar azo dyes carrying different substituent groups at the same position of the aryl ring (Figure 1.5).

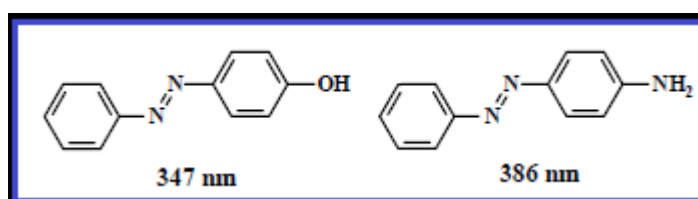


**Figure 1.5:** The bathochromic shift of  $\text{-OH}$  substituted azobenzene from 347nm to 386nm when azobenzene is substituted with  $\text{-NH}_2$  group at the same position of the aryl ring.

### **1.3.3. The extent of production and usage of azo dyes in colour industry**

As of 2009, the annual global production of synthetic dyes exceeded 900,000 tonnes (Chequer et al, 2009) and is expected to be well over a million tonnes per annum at present. Nearly two-thirds (60% - 70%) of all synthetic dyes are azo dyes (Van der Zee et al, 2001). Therefore, azo dyes are considered as the most commonly used dyestuff in the colour industry. Moreover, a vast variety numbering over 10,000 chemically different azo dyes are currently being used in the colour industry. Most azo dye precursors are produced from primary aromatic products obtained from the distillation process of coal tar. Diazotization reactions of aromatic diazonium compounds are mainly used for synthesis of many azo dyes (Tyagi and Yadav, 1990).

The preference for azo dyes over other dye types in the colour industry is due to their industrially desirable properties such as ease and low cost of synthesis and being available in vast variety of colours. Other desirable properties include high washfastness and lightfastness.

### **1.3.4. Azo dye contaminated wastewater disposal and legislation pertaining to colour industry wastewater discharge**

During the dyeing processes in colour industry, up-to 50% of the used dyes may not be fixed to their fibre substrates and hence may be washed out to form highly coloured effluent streams (Figure1.6). The discharge of synthetic dye containing wastewater is not desirable due to several reasons. Firstly, the high colour intensity of many synthetic dyes may interfere with penetration of sunlight when mixed with natural waterstreams and may hinder photosynthesis and disrupt ecosystems. Hence, highly coloured waterstreams are undesirable in terms of

aesthetic and biodiversity perspectives. Secondly, majority of synthetic dyes are highly recalcitrant in the natural environment. They are not naturally encountered by the microbes in the environment and hence, are not easily biodegraded. Furthermore, synthetic dyes are resistant to photolysis and can withstand high temperatures. Therefore, they tend to accumulate in the environment and impart harmful effects in the biosphere. Recalcitrant azo dyes may undergo partial biotransformation into other compounds if discharged untreated. The dyes themselves and/or their biotransformation products are demonstrated to be toxic and in many instances carcinogenic in nature (Mansour et al, 2009). Benzidine and 1-phenylazo-2-hydroxynaphthalene (Sudan dyes) based dyes are especially noted for their genotoxic and mutagenic potential (Weber, 1991). The genotoxic nature of these dyes and their biotransformation products is often attributed to their planar structure and their ability to intercalate between DNA double helices (Mansour et al, 2009). Therefore, the use of benzidine based azo dyes is banned in Europe.

For example, in Turkey, where its textile products accounts for up-to 14% of the total European textile imports, it is estimated that approximately 150 million tonnes of dye contaminated wastewater is produced annually (Ozkan-Yucel and Gokcay, 2013). Therefore, treatment of effluent water containing synthetic dyes (and other pollutants) from industries such as textile, leather/tannery, paper printing and cosmetic industries is environmentally important and enforced legally. Recently there has been an increase in environmental awareness from the public leading to more stringent legislation pertaining to uncontrolled industrial waste release into the natural environment (Christie, 2007).



**Figure 1.6:** A highly coloured wastewater stream from the textile industry being released unlawfully into a natural waterway (source – [www.sophied.net](http://www.sophied.net))

The discharge of azo compounds, along with other pollutants, into water streams is one of the concerns highlighted in the Water Framework Directive (WFD 2000/60/EC) and is strictly regulated by environmental regulatory agencies such as the UK Environment Agency. Regulations specified under (EC) 1907/2006 directive prohibits discharge of many industrially used azo compounds to the environment (Christie, 2007). The permissible standards for textile colouring industry effluent as specified by Water Framework Directive (WFD) and DEFRA (Department for Environment Food and Rural Affairs) are as follows; pH 5.5-9, Chemical Oxygen Demand (COD) –  $250 \text{ mgL}^{-1}$  and Biochemical Oxygen Demand (BOD) –  $30 \text{ mgL}^{-1}$  (eco-web.com). However, typical untreated textile industry effluent has been reported to possess characteristics shown in table 1.1. Hence, treatment is essential prior to discharge into natural water streams.

**Table 1.1:** Typical properties of untreated textile wastewater (Adel et al, 2004)

Parameters	Values
pH	7.0– 12.0
Biochemical Oxygen Demand ( $\text{mgL}^{-1}$ )	80 – 6,000
Chemical Oxygen Demand ( $\text{mgL}^{-1}$ )	150 – 12,000
Total Suspended Solids ( $\text{mgL}^{-1}$ )	15 – 8,000
Total Dissolved Solids ( $\text{mgL}^{-1}$ )	2,900 -3,100
Chloride ( $\text{mgL}^{-1}$ )	1000 - 1600
Total Kjeldahl Nitrogen ( $\text{mgL}^{-1}$ )	70 – 80
Colour (Pt-Co scale)	50 - 2500

#### 1.4. Problem statement

Due to the low levels of fixation of azo dyes to their substrate, up to 50% of the initial dye mass used may remain in the spent dye bath in a form which no longer has affinity for the substrate. Since the dyes cannot be reused in the dyeing process, they are usually discarded, along with other process wastewater, as effluent. Azo dyes are mostly regarded as recalcitrant environmental pollutants due to their xenobiotic nature. Hence they can accumulate in ecosystems, be transferred along food chains and may cause harmful effects to human health. Some azo dyes such as dinitroaniline orange and orthonitroaniline orange are reported to be mutagenic and some have been shown to be linked to basal cell carcinoma (a common type of skin cancer) (Engel et al., 2008). Benzidine-derived azo dyes are carcinogens and their use is discontinued from western industrialised countries (Pandey et al, 2007). Wastewater containing azo dyes is usually



intensely coloured and this not only affects the aesthetics of the receiving water bodies but also reduces the solubility of oxygen in water. Azo dye concentrations as low as  $1 \text{ mgL}^{-1}$  are highly visible and therefore, the colour intensity prevents sunlight from penetrating through the water to reach plants, algae and other photosynthetic organisms growing on river beds, thus affecting aquatic life. Azo dye containing wastewater is usually complex and may contain particulates, high salt concentrations and low/high pH all of which pose problems to conventional wastewater treatment methods. Due to these environmental risks of synthetic dye wastewater discharge and already stringent legal requirements, it is imperative that colour industry wastewater is treated to an acceptable standard recognised by environment agencies before being released to the environment.

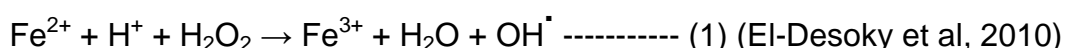
## **1.5. Current methods for treatment of colour industry wastewater**

Due to environmental risks and legal obligations, colour industry wastewater needs to be treated for colour, organic compounds including toxic ones, inorganic ions such as nitrates, sulphates and phosphates and heavy metal ions. Several technologies are currently in use for colour and organics removal. These range from physico-chemical degradation methods to biological degradation methods (Figure 1.8).

### **1.5.1. Physico-chemical dye removal methods**

Advanced oxidation processes (AOP) utilising various strong oxidants is the most common physico-chemical approach to industrial dye removal (Erkurt, 2010). Oxidation of the azo ( $\text{-N=N-}$ ) bond and the flanking aryl rings has been achieved by subjecting the azo bond or the aryl rings to attack by free radicals such as  $\text{OH}^\bullet$

created by free radical generating chemical species such as  $O_3$  and  $H_2O_2$ . UV light has been used in combination with strong oxidising agents in order to increase the efficiency of degradation process by photolysis; combinations such as  $O_3/H_2O_2$ ,  $UV/H_2O_2$ ,  $UV/O_3$ , are currently in use for chemical treatment of azo dyes. In addition, Fenton's reagent ( $Fe^{2+}/H_2O_2$ ) has been used to oxidize azo dye contaminated effluent waters (Petrova et al, 2008). The Fenton's reaction is as follows;



The oxidative free radical generating properties of  $H_2O_2$  is enhanced by the presence of  $Fe^{2+}$  that acts as a catalyst in mildly acidic solution. Hydroxyl radicals generated act as powerful non-specific oxidising agents that are capable of degrading a wide range of environmental pollutants including synthetic dyes. Other chemical AOP methods utilise oxidising agents such as sodium hypochlorite. Chemical AOP methods are not sustainable at larger industrial scales due to high cost of oxidising reagents such as hydrogen peroxide and sodium hypochlorite. Moreover, the exact chemical nature of the products generated from chemical AOP oxidation of various environmental pollutants can be unpredictable (Dos Santos et al, 2007, Robinson et al, 2001). Therefore, the disposal of the resultant effluent can be problematic.

Chemical reduction of azo dyes into their constituent aminobenzenes is also possible using reductant chemical species such as sulphide, cysteine and  $Fe^{2+}$  (Ozkan-Yucel and Gokcay, 2013).

Many industrial dye users in the UK use coagulation/flocculation methods coupled to dissolved air floatation (DAF). DAF processes are almost always combined to a coagulation/flocculation process where coagulants such as  $AlCl_3$  or  $FeCl_3$  are used

to coagulate the pollutants and air saturation of the aqueous medium containing the dye pollutant wastewater is used for phase separation. Using physico-chemical means such as DAF to treat azo dye contaminated industrial effluents is high in energy expenditure, costly due to the high cost of chemical coagulants used and produces large amounts of sludge (Mu et al, 2009). Coagulation/flocculation processes can be slow depending on the operational conditions such as pH and hence, it is difficult to implement to larger dye wastewater volumes (Vandevivere et al, 1998).

Adsorption of synthetic dyes is another physico-chemical method that utilises a range of adsorbents such as activated carbon, wood chips, clay, rice hulls and inactivated microbial biomass. Adsorption and biosorption methods using support materials such as activated carbon and inactivated biomass also leads to disposal problems of the spent sorbent. Using adsorbents such as activated carbon is known to be particularly costly and regeneration of the sorbent material can be a problem (Robinson et al, 2001). Adsorption of polar and charged dyes such as reactive dyes however, have proven to be problematic with conventional low-cost adsorbents such as wood chips and inactivated biomass due to the excessively hydrophilic nature of charged dyes (Ozkan-Yucel and Gokcay, 2013). Membrane filtration has also been used but it is very expensive and leaves a concentrated dye stream which requires further treatment prior to disposal. Membrane filtration is also known to be rapid and highly successful at laboratory scales but ineffective at larger industrial scales due to high cost and intrinsic pitfalls of the process such as membrane fouling and clogging (Wu et al, 1998).

### **1.5.2. Electrochemical removal of synthetic dyes**

Electrochemical removal of environmental pollutants including azo dyes involves passing an electrical current via electrodes through an aqueous solution

containing the target pollutant that will result in oxidation or reduction reactions. In addition to electro-oxidation and electro-reduction, processes such as electro-coagulation and electro-flocculation could also lead to removal of target pollutants (Banat et al, 1996). Conventional coagulation phase separation techniques used for dye removal involves the introduction of  $\text{Fe}^{3+}$  or  $\text{Al}^{3+}$  ions and hydroxyl ions in the form of NaOH or soda lime into the contaminated water, leading to precipitation of dye pollutants. In electrocoagulation methods however, Fe or Al sacrificial anodes are routinely employed so that during the electrochemical process,  $\text{Fe}^{3+}$  or  $\text{Al}^{3+}$  ions are generated at the anode and  $\text{OH}^-$  ions are generated at the cathode and they act as coagulants of dye pollutants (Tarr, 2003). Varying the current density of the electrochemical cell can be used as a control measure for the release of metal ions required for coagulation reactions from the sacrificial anodes.

Electrochemical cells in which reductive and oxidative degradation of synthetic dyes takes place, several electrode materials can be utilised. Activated carbon, graphite felt, platinum, titanium (Chou et al, 2011), steel, polypyrrole and boron doped diamond (BDD) (Lopes et al, 2004) are the most common types of electrodes used for electrochemically assisted dye removal.

Other electrochemical methods such as electro-Fenton processes photo-assisted electro-Fenton processes where hydrogen peroxide and  $\text{Fe}^{2+}$  are generated in-situ within the electrochemical cell have also gained considerable interest for synthetic dye removal from wastewater (Guivarch et al, 2003, Xie et al, 2006). All electrochemical methods however, require a large input of electrical energy in order to achieve pollutant removal or degradation of the target pollutant.

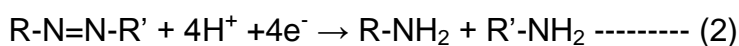
### 1.5.3. Biological degradation methods

Biological methods are attractive in the sense that they require low energy input, low cost and are environmentally more acceptable than physico-chemical methods. Whole cell microorganisms and fungi as well as enzymes have been used. The dyes can be degraded reductively or oxidatively.

### 1.5.4. Reductive degradation of azo dyes

Reduction of azo bonds by various microorganisms under anaerobic conditions leads to the formation of aminobenzenes which may subsequently be mineralised oxidatively. Reductive degradation of azo moieties in synthetic dyes leads to the formation of corresponding aminobenzenes as shown in the expression 2.

Reduction can be carried out by different mechanisms such as enzymes, redox mediators (mediated electron transfer into the  $-N=N-$  moiety) and biogenic reductant molecules such as sulfide (Pandey et al, 2007) (Figure 1.7). Several species of bacterial genera such as *Clostridium*, *Eubacterium* and some yeasts and fungi are capable of producing NADPH/NADH dependant non-specific Azobenzene reductases that have the capability of reducing azo bonds (Pandey et al, 2007). Azo bonds are proposed to be operational as an electron sink or a terminal electron acceptor during the process of anaerobic ATP generation for cellular energy requirements (Chengalroyan and Dabbs, 2013, Doble and Kumar, 2005). Biological and chemical reduction of the azo moiety can be represented in the following general formula.



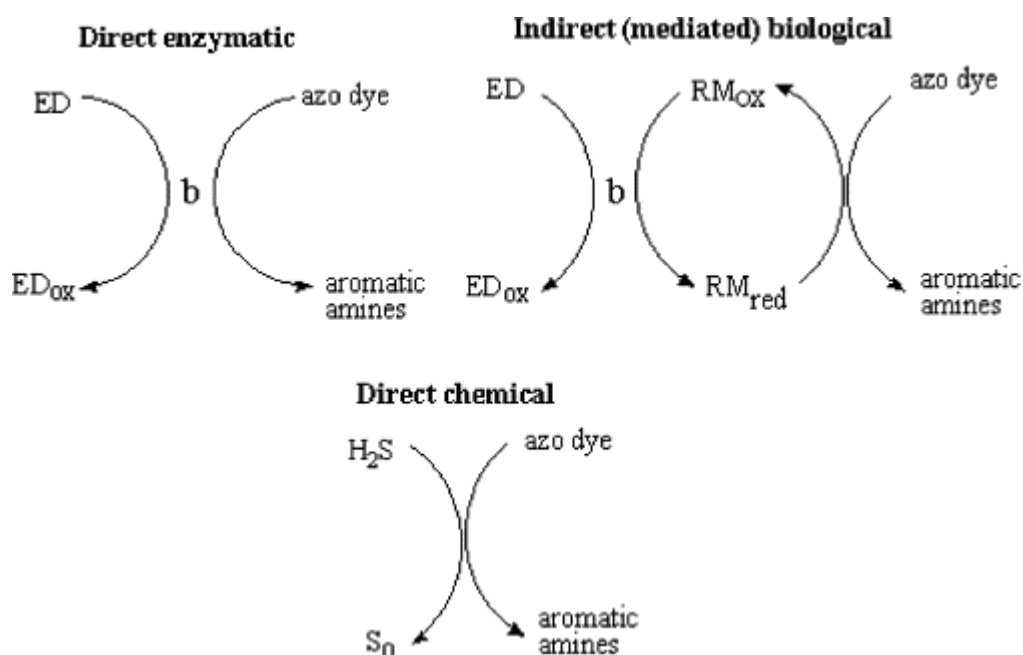


**Figure 1.7:** Modes of azo dye reductive degradation in biotic environments under anaerobic conditions. Biogenic sulphide present in sulphate reducing anaerobic environments leads to direct chemical reduction of azo moieties (adapted from – Pandey et al, 2007).

The reductive equivalents for the azo bond reduction could be provided from the oxidation of numerous carbon sources. Sugars such as glucose, sucrose, lactose (Jain et al, 2012), organic acids such as pyruvate, acetate and benzoic acid (Murali et al, 2013) and amino acids such as cysteine (Logan et al, 2005) were reported as the carbon sources for azo dye degradation in several previous studies. Several complex unrefined electron donors such as molasses, rapeseed cake, corn-steep liquor and starch (Jain et al, 2012) were also reported.

It is widely accepted that the anaerobic reductive cleavage only leads to the decolourisation of an azo compound rather than its mineralisation. Anaerobic azo dye reduction is routinely reported in literature in both immobilised (e.g. Upflow Anaerobic Sludge Blanket-UASB) and suspended biophase reactors. However, the rate of subsequent mineralization (i.e. of aminobenzenes) under anaerobic conditions is very slow.

Although colourless, the direct discharge of aminobenzene containing wastewater is not legally permitted due to high toxicity of aminobenzenes. The environmental toxicity of aminobenzenes ranks very high among other well-known environmental pollutants. The toxicity of mono-substituted benzenes to acetoclastic methanogens were found to be in the following order:  $\text{COOH} < \text{H} < \text{OH} < \text{NH}_2 < \text{NO}_2$ , (Razo-Flores, 1997) where nitrobenzenes are also converted to aminobenzenes under anaerobic conditions. This clearly shows the highly toxic nature of aminobenzenes and hence it is necessary they are further broken down to other less toxic compounds. Ortho substituted aminophenols such as 1-amino-2-naphthol are thought to be toxic and mutagenic (Gottlieb et al, 2003, Ruiz-Arias et al, 2010). However, the toxic/mutagenic nature of such aminobenzenes is not well established and is subject to debate. Therefore, it is necessary to explore the environmental toxicity of these aminobenzenes.

Metabolic oxidation of the dyes by bacteria is reported to be very difficult as the molecules are too big to be assimilated through the cell membranes of most wild-type microorganisms used to date. Genetically engineered bacteria such as *Xenophilus azovorans* KF46F and *Pseudomonas aeruginosa* K22 are two examples that are capable of azo dye degradation under aerobic conditions (Pandey et al, 2007). However, it is thought that the decolourisation occurs under microaerophilic conditions in isolated microaerophilic zones within the culture broth by reductive cleavage of the azo moiety. Several non-specific enzymes, isolated from aerobic organisms such as *Bacillus* spp, *Pseudomonas aeruginosa* and *Staphylococcus aureus*, have been reported to possess the capability of reducing azo bonds (Ooi et al, 2007). It is widely known that most azo dyes pass unchanged through aerobic wastewater treatment processes such as activated sludge systems. It is known that conventional biological wastewater treatment

technologies such as anaerobic digesters or activated sludge systems are incapable of effectively neutralising the environmental toxicity of majority of the synthetic dyes. Combined anaerobic - aerobic processes were shown to degrade azo dyes in previous studies (Khehra et al, 2006), however the anaerobic process is too slow and some of the produced amines may be toxic to the aerobes in the subsequent process. The aerobic further degradation of monocyclic aminobenzenes is thought to proceed via the formation of catechol derivatives as shown in several previous studies (Junker et al, 1994, Kalme et al, 2007). The aromatic ring activation reactions carried out by mono-oxygenase and di-oxygenase enzymes prompt aromatic ring opening and further degradation of amines. Highly substituted aminobenzenes however, can exhibit extensive resistance to biodegradation and therefore, could pose environmental problems.

An extensive amount of work exists on oxidation of dyes using fungal species, especially white rot fungi such as *Pleurotus ostreatus* and *Trametes versicolor* (Fu and Viraragharan, 2001; [www.sophied.net](http://www.sophied.net)) or their enzymes – laccases, peroxidases (Teerapatsakul et al, 2008). Although fungal oxidases are reported to be able to act non-specifically on many azo dyes, the terminal degradation products of fungal oxidation of azo compounds could be more toxic than the parent dyes. Another drawback with fungal cultures is that they require rather long growth phases before actually producing high amounts of active enzymes.

Therefore, it is clear that novel and innovative avenues of better treating colour industry wastewater must be sought in order to alleviate the environmental damage caused by the uncontrolled discharge of synthetic dyes. The current methods that are employed for colour industry wastewater treatment are summarised in figure 1.8.



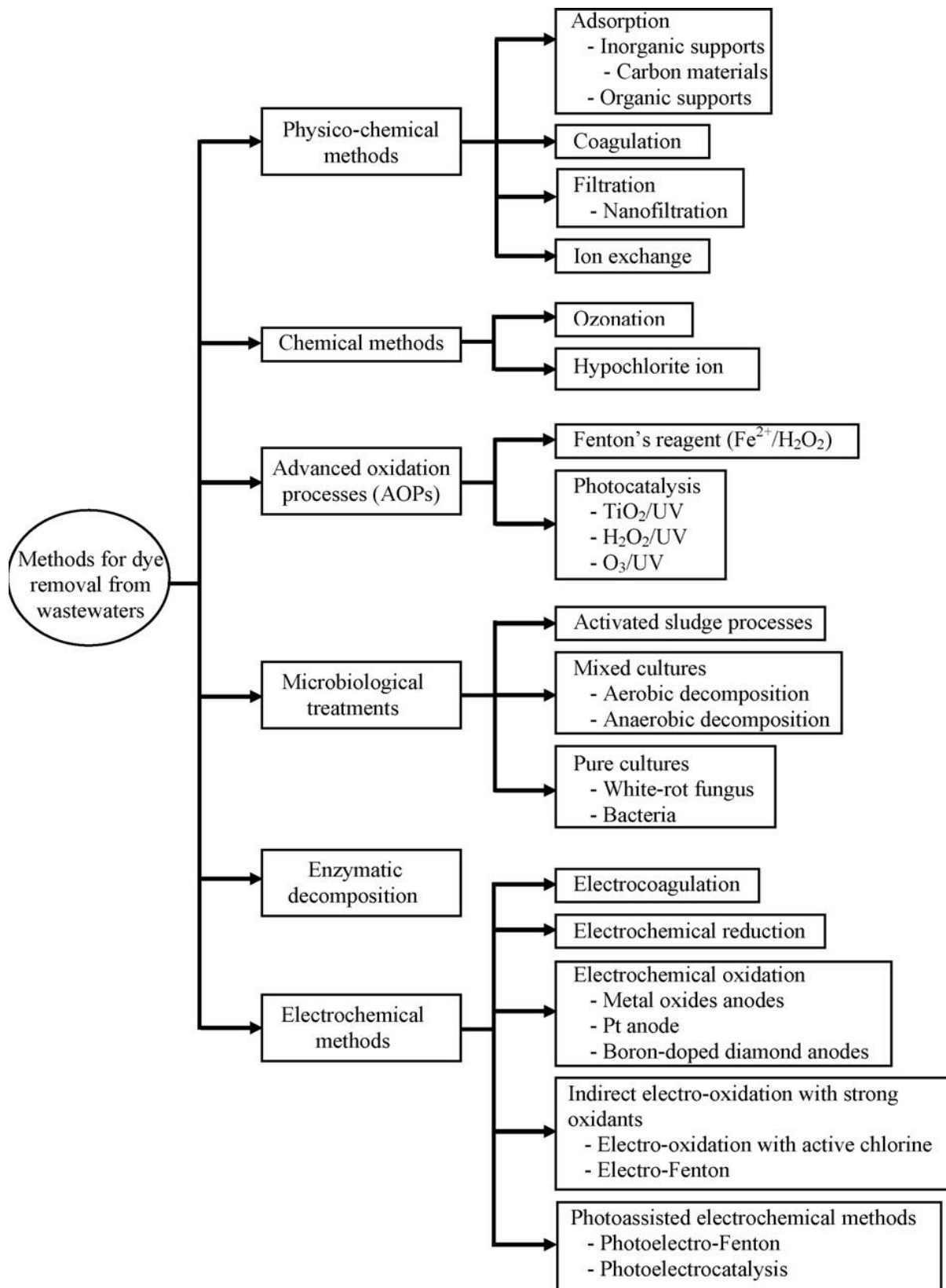


**Figure 1.8:** Current and proposed methods for removal of synthetic dyes from industrial wastewater (adapted from – Martinez-Huitle and Brillas, 2009)

## **1.6. Use of Bioelectrochemical systems for azo dye removal**

From the foregoing discussion, it is apparent that there is need to develop more effective and eco-friendly treatment methods for azo dye containing wastewater due to the limitations of current wastewater treatment technologies when used for the treatment of azo dye contaminated wastewater. Recently, Bioelectrochemical systems (BES) have been proposed as a promising alternative of not only wastewater treatment but also concomitant energy production (Rozendal et al, 2008; Hawkes et al, 2010).

### **1.6.1. Bio-electrochemical systems and microbial fuel cells (MFC)**

Bio-electrochemical systems use microbes to catalyse oxidation and reduction reactions at the anode and cathodes respectively in electrochemical cells. They are unique systems that could convert the chemical energy of biodegradable organic contaminants in wastewater to biogenic electricity (MFCs) or to hydrogen/value-added chemical products in microbial electrolysis cells (MECs) (Pant et al, 2012).

### **1.6.2. Microbial fuel cells and the history of Bioelectrochemical systems**

Microbial fuel cells are BES that utilise micro-organisms e.g. *Shewanella*, *Geobacter*, *Rhodospirillum rubrum*, yeasts and mixed microbial populations to catalyse an oxidation and reduction reaction at an anode and cathode electrode respectively and can produce electricity when connected to a load/resistor via an external circuit (Figure 1.9a).

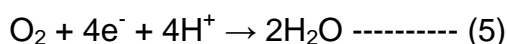
Observations of electrochemical phenomena relating to biological systems are not new. In 1771, the Italian physicist Luigi Galvani observed that a dead frog's legs would twitch when a small current was passed through it with the aid of electrodes. This observation is widely regarded as the first reported instance of a bioelectrical phenomenon (Ieropoulos et al, 2005). Thereafter, in 1911, M.C Potter demonstrated that electrical energy can be produced in electrochemical cells by living cultures of *Escherichia coli* and *Saccharomyces cerevisiae* with the aid of platinum electrodes (Potter, 1911). Potter's study is currently regarded as the first instance where the concept of MFCs was experimentally demonstrated. Subsequent to this breakthrough study by Potter in 1911, the concept of electrochemical phenomena involving microbes was largely overlooked or neglected for many decades. Aside from a handful of studies such as Cohen, 1931 and Berk et al, 1964, very little scientific interest was given to the electrochemical phenomena involving microbial metabolism until early 1980s. Following the intense debate on the looming energy crisis and the current extent of the environmental damage occurring due to industrialisation and extensive fossil fuel burning, a renewed interest was placed on environmentally cleaner and more sustainable alternatives for energy generation and environmental remediation. In this context, biofuels and other alternative environmentally sustainable technologies were given the primary emphasis. Research on MFCs and other BES was reinvigorated due to aforementioned reasons by many leading research institutions world-wide after many years of lapse following the breakthrough study by Potter. MFCs and BES had an additional appeal of environmental remediation and contaminant removal coupled with concomitant electricity/biohydrogen generation. In this view, MFCs are unique systems that are capable of converting the chemical energy of contaminants to usable biogenic electrical energy.

### 1.6.3. Working principle of MFCs

MFCs generally comprise of an anode, a cathode, an external circuit and an ion selective membrane separating the anode and the cathode (Figure 1.9). In brief, organic substrates such as glucose and acetate are oxidised at the anode end of the MFCs by microorganisms in the anode compartment. Electrons and protons are released due to the microbial catabolism of organic substrates.



The electrons are picked up by the anode electrode and flow through the external circuit into the cathode end of the MFC, where, a chemical species with a high redox potential such as oxygen or ferricyanide will accept electrons to undergo reduction. The protons produced in the process permeate into the cathode side of the MFC through an ion permeable membrane placed between the anode and cathode compartments. In the cathode, atmospheric oxygen is most often used as the electron acceptor where it undergoes reduction as follows.



In order to catalyse the above reaction, various oxygen reducing catalyst materials are employed. The most common cathode catalyst material is Platinum. However, due to the high cost of platinum catalyst material, the use of alternative cheaper catalyst materials is preferred for MFCs. Alternative cheaper cathode catalysts demonstrated to have a promising potential include cobalt tetramethylphenylporphyrin (CoTMPP) (Cheng et al, 2005), metal phthalocyanine (PC) derivatives such as FePC, activated carbon (HaoYu et al, 2007) and biological catalyst materials such as peroxidase enzymes such as laccases (Schaetzle et al, 2009).

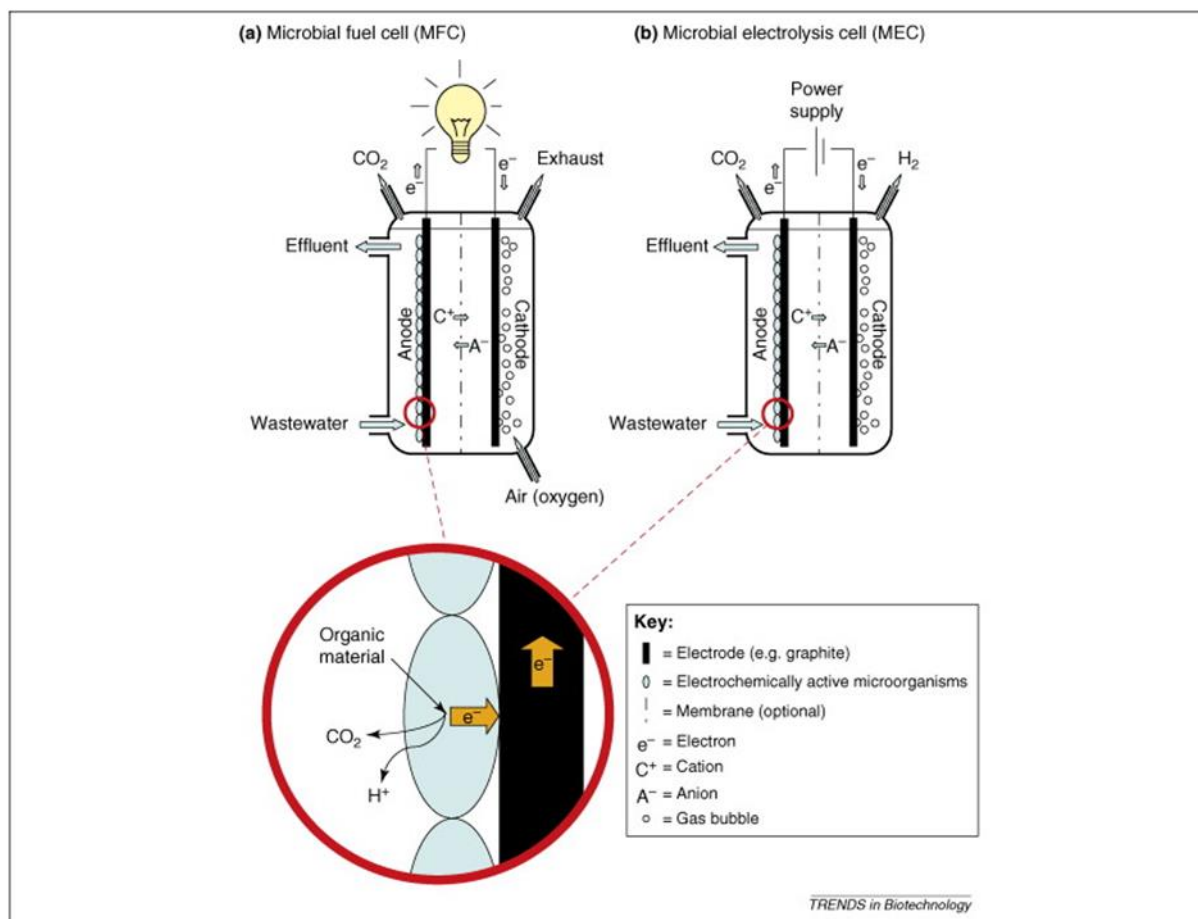


**Figure 1.9:** The working principle of a microbial fuel cell (MFC) and microbial electrolysis cell (MEC) and microbially catalysed direct electron transfer from substrate oxidation onto electrode surfaces (image adapted from Rozendal et al, 2008)

Electron transfer to the anode electrode is thought to occur by several different mechanisms. Electron transfer could be mediated through various natural or synthetic electron shuttles or redox mediators. Natural electron shuttles include compounds such as riboflavin (Velasquez-Orta et al, 2010) and humic acid (Thygesen et al, 2009). Well studied synthetic electron shuttles include anthraquinone-2,6-disulfonic acid (AQDS) (Aeschbacher et al, 2009) and anthraquinone-2-sulfonic acid (AQS) (Tsujimura et al, 2001). Direct electron transfer to the anode occurs through microbial membrane-bound electron transfer proteins such as Mtr cytochrome protein complexes and so-called nanowires,

microbial pilli-like extracellular electrically conductive appendages (Schroder et al, 2007).

#### 1.6.4. Thermodynamics of MFCs

In order to produce electrical energy in MFCs, the overall reaction of the bio-electrochemical cell must be thermodynamically favourable. Gibbs free energy of the electrochemical reaction is a measure that can be used in order to assess the feasibility of an MFC system to produce electricity. Gibbs free energy is calculated as follows.

$$\Delta G_r = \Delta G_r^0 + RT \ln \Pi \text{ ----- (6)}$$

Where,  $\Delta G_r$  is the Gibbs free energy (J) of the reaction at specific conditions,  $\Delta G_r^0$  is the Gibbs free energy (J) at standard conditions (298.15 K temperature, 1 bar pressure and 1M concentrations of all chemical species), R is the universal gas constant ( $8.31447 \text{ J mol}^{-1} \text{ K}^{-1}$ ), T (Kelvins) is the absolute temperature and  $\Pi$  is the equilibrium constant.

The amount of useful work that can be obtained from the electrochemical reactions of an MFC is related to the electromotive force ( $E_{emf}$ ) of the system. Electromotive force is also defined as the potential difference between the anode and the cathode of an electrochemical cell.

$$E_{emf} = - \Delta G_r / nF \text{ ----- (7)}$$

Where, n is the number of electrons transferred per reaction and F is the Faraday's constant ( $9.64853 \times 10^4 \text{ C mol}^{-1}$ ).

Under standard conditions (where  $\Pi = 1$ ), the EMF can be written as follows.

$$E_{emf}^0 = - \Delta G_r^0 / nF \text{ ----- (8)}$$

Where,  $E_{\text{emf}}^0$  is the EMF at standard conditions.

Therefore, from equations (7) and (8) the EMF for the overall reaction could be written as:

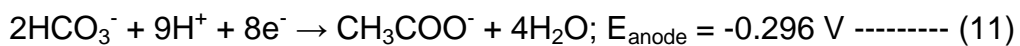
$$E_{\text{emf}} = E_{\text{emf}}^0 - (RT/nF) \ln(\Pi) \text{ ----- (9)}$$

When individual anode and cathode half cells of the MFC are considered:

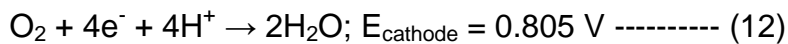
$$E_{\text{emf}} = E_{\text{cathode}} - E_{\text{anode}} \text{ ----- (10)}$$

For an MFC operating under ideal conditions utilising 5mM acetate at pH 7 in the anode as the sole electron donor and a cathode utilising oxygen as the sole electron acceptor at atmospheric pressure ( $p\text{O}_2 = 0.2$ ) at pH 7:

Anode



Cathode



From equation (10),  $E_{\text{emf}}$  of this MFC is:

$$= 0.805 - (-) 0.296 = 1.106 \text{ V}$$

Therefore, MFCs utilising acetate as the electron donor and atmospheric oxygen as the sole electron acceptor under aforementioned conditions, it is widely accepted that theoretical electromotive force or open circuit potential (OCV) would never exceed 1.1 Volts (Logan et al, 2006). In an ideal MFC therefore, the open circuit potential would equal to the thermodynamic  $E_{\text{emf}}$  value calculated using the potentials of anode and cathode half cells.

### **1.6.5. Internal losses of MFCs and OCV**

In real MFCs however, the OCV never reaches the thermodynamically calculated theoretical value due to several inherent limitations of BES. These limitations are referred to as overpotentials. Therefore, in order to reduce the effect of overpotentials and to optimise the energy efficiency of bioelectrochemical systems, a good level of understanding relating to internal losses of BES is needed. The overpotentials in MFC systems are categorised into four main areas. They are activation overpotentials, Ohmic losses, bacterial metabolic losses and concentration polarisation losses (Rabaey and Verstraete, 2005).

Activation overpotentials are related to the activation energies of anodic and cathodic oxidation/reduction reactions. Activation losses could relate to the compounds undergoing oxidation in the anode and where the microbially catalysed electron transfer occurs. This could be related to electron carrying cell surface proteins or electron shuttling mediator compounds. Activation losses could also occur at the cathode where electrons are coupled with a final electron acceptor. Improving electrode catalysis and increasing electrode surface areas are general strategies used in order to circumvent the adverse effects of activation losses to MFC performance.

Concentration losses occur mainly due to mass transport limitations of the reactants to or from the electrodes and due to the formation of concentration gradients perpendicular to the plane of the electrode. When sufficient mixing of the surrounding electrolyte is absent, the process of simple diffusion becomes inadequate for efficiently transporting reactants to the electrode and products away from the electrode. This leads to the formation of concentration gradients of reactants and products and is a major contributor for concentration losses in



MFCs. Therefore, adequate mixing of the bulk electrolyte is essential for minimising the concentration related losses in MFC systems.

Ohmic losses of an MFC system is related to the resistance to flow of electrons and counter ions through electrodes, external circuit, electrode interconnections, ion selective membranes and the electrolyte. Electrode spacing and solution conductivity are primarily important in reducing Ohmic losses. It has been shown that electrode spacing and Ohmic losses exhibit an inverse relationship (Rozendal et al, 2008). Other factors such as high resistivity of the ion selective membrane and poor electrical interconnections (especially at the electrodes) could also contribute to high Ohmic losses in MFCs.

Bacterial metabolic action in the anode results in release of electrons and protons from the organic substrates and the electrons being transferred down a redox potential gradient to a terminal electron acceptor. In MFCs, the anode electrode acts as the terminal electron acceptor. When electrons are transferred from reduced substrates such as acetate ( $E'_0 = -0.296\text{V}$ ) or reduced electron carriers such as NADH ( $E'_0 = -0.32\text{V}$ ), the higher the potential difference between the electron donor and the electron acceptor (i.e. the anode) the energy gain for the anode microorganism will be higher. However, the voltage output of the MFC system will be lower. In order to maximise the OCV of the MFC, the potential of the anode must be kept as low as possible. Under very low anode potentials however, the anode bacteria may seek alternative terminal electron acceptors in the anolyte solution and the electrons may be diverted to fermentative or methanogenic metabolic pathways (Logan et al, 2006). Polarisation plots of MFCs are routinely used to assess the system performance and the energy losses occurring due to overpotentials can be approximately represented graphically as shown in figure 1.10.

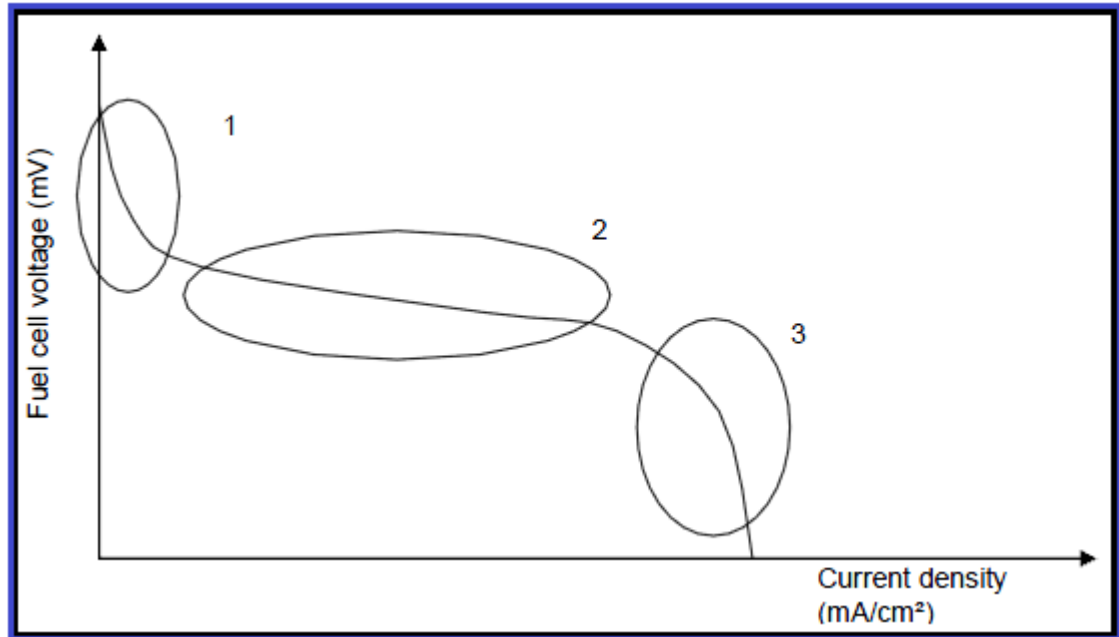


**Figure 1.10:** Regions of a polarisation curve used to assess the MFC performance depicting the energy losses. Zone-1- activation losses, zone-2- Ohmic losses, Zone-3- concentration losses (adapted from- Rabaey et al, 2005)

As shown in the following equation, the observed cell voltage can be expressed as the difference between thermodynamically calculated electromotive force and the sum of anodic overpotential, cathodic overpotential and Ohmic losses of the MFC system.

$$E_{\text{cell}} = E_{\text{emf}} - (\Sigma\eta_a + \Sigma\eta_c + IR_{\Omega}) \text{ ----- (13)}$$

Where,  $\Sigma\eta_a$  and  $\Sigma\eta_c$  respectively are anode and cathode related overpotentials and  $IR_{\Omega}$  is the sum of all Ohmic losses which are proportional to the current drawn from the MFC system.

### 1.6.6. Types of Microbial fuel cells

Architecture and the material of construction of MFCs differentiated and evolved over many years of MFC related research. The design and construction of MFCs can make a considerable influence in terms of optimal performance, internal energy losses and the mode of operation (i.e. batch or continuous operation). One

of the very first MFC designs included the conventional H-type configuration where two glass bottles were held clamped together between a glass bridge. The junction held an ion specific membrane or an agar salt bridge and the glass compartments house the anode and cathode electrodes (Figure 1.11-A). There are several variations of the two chamber system where attempts were made to increase the available membrane surface area, electrode surface area and to reduce the distance between electrodes (Figure 1.11-B) (Logan et al, 2006). The two-chamber system is mostly suitable for fundamental studies due to its intrinsic limitations such as very high internal resistances and consequently, high internal energy losses and the limited ability to operate in the continuous-flow mode, hence, reducing its practical applicability for larger-scale real wastewater treatment processes. Other variations of two chamber MFCs include miniaturised reactors which are well suited for remote sensing applications (Ringeisen et al, 2006). In almost all two-chamber MFCs utilising atmospheric oxygen as the terminal electron acceptor, the catholyte is actively aerated in order to circumvent the low solubility of oxygen in the aqueous catholyte. This demands a further energy input into the operation of the MFC system and hence, reduces its energy efficiency.



**Figure 1.11:** Types of two chambered microbial fuel cells (A) the conventional H-type (B) the rectangular type two-chamber systems with high membrane surface areas

Single-chamber MFCs are a later development where the cathode was removed from the catholyte and was placed exposed to atmospheric oxygen and is passively aerated (Logan et al, 2006). The anode is housed within the single reactor compartment containing the anolyte medium (Figure 1.13). The single chamber type MFCs are more energy efficient compared to their two-chamber counterparts due to several reasons. The distance between the anode and the cathode is significantly reduced and no energy expenditure is required for active oxygenation of the catholyte as the cathode is passively aerated. Furthermore, anode and cathode surface areas could be considerably increased compared to two-chamber systems. Mono-chamber MFC systems could be considered as innovative reactor designs due to their efficiency and versatility they offer in terms of performance and operational standpoints. Hence, single-chamber air cathode type MFCs routinely register higher power performance and are more sustainable compared to their two-chamber counterparts. Single chamber MFC systems (such as tubular up-flow systems in particular) are well suited for continuous-flow mode reactor operation.

Other less commonly utilised MFC types include benthic/sediment deployed MFCs where the anode resides in the sediment and the cathode is exposed to atmospheric oxygen. The benthic MFCs use the sediment as the source of substrate as well as the source of microbial inoculum. The sediment is rich in various microbial communities including ones that are capable of extracellular electron transfer. The electrochemically active microbes residing within the sediment oxidise naturally found decomposing organic substrate and transfer a portion of the electrons released on-to the anode electrode of the benthic MFC, placed within the sediment. The electrons are then drawn towards the cathode electrode (placed exposed to atmospheric oxygen) via the external circuit. The

current generated within the external circuit is used to power various remote-sensing devices. The major advantage of this type of MFCs is that they can be deployed for powering remote sensing and environmental monitoring devices as a reliable source of power and can be left unattended unlike using conventional batteries (Figure 1.12).

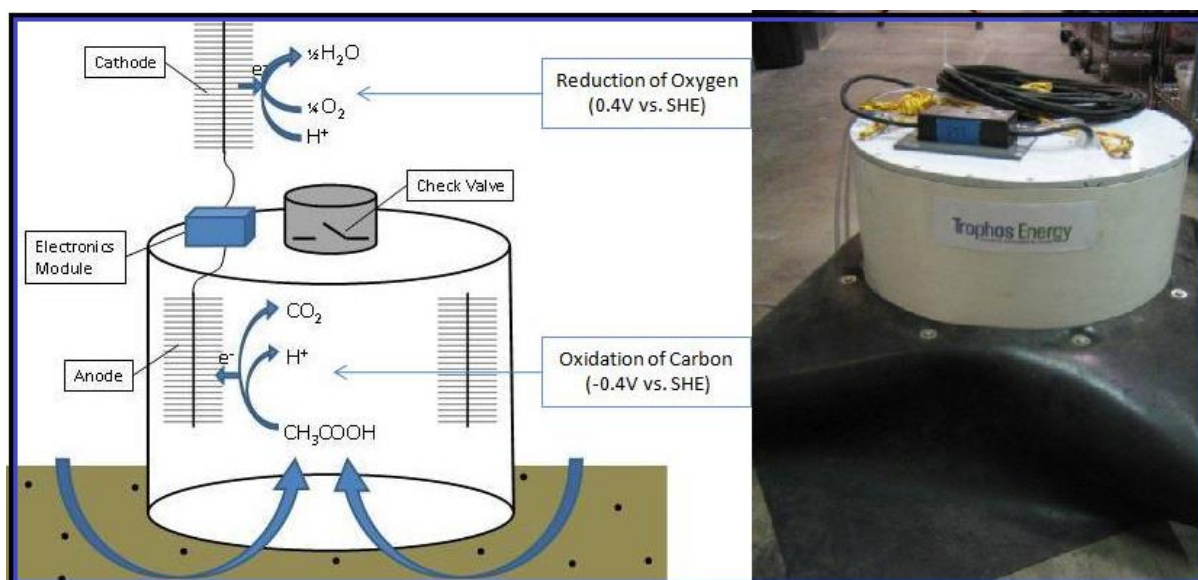


**Figure 1.12:** The working principle of a benthic MFC system and a benthic MFC system being readied for deployment in marine sediment for remote sensing applications (Guzman et al, 2010).

Sediment/benthic MFCs have gained much research interest in recent times due to their potential remote sensing applications in environmental, marine and military sectors.

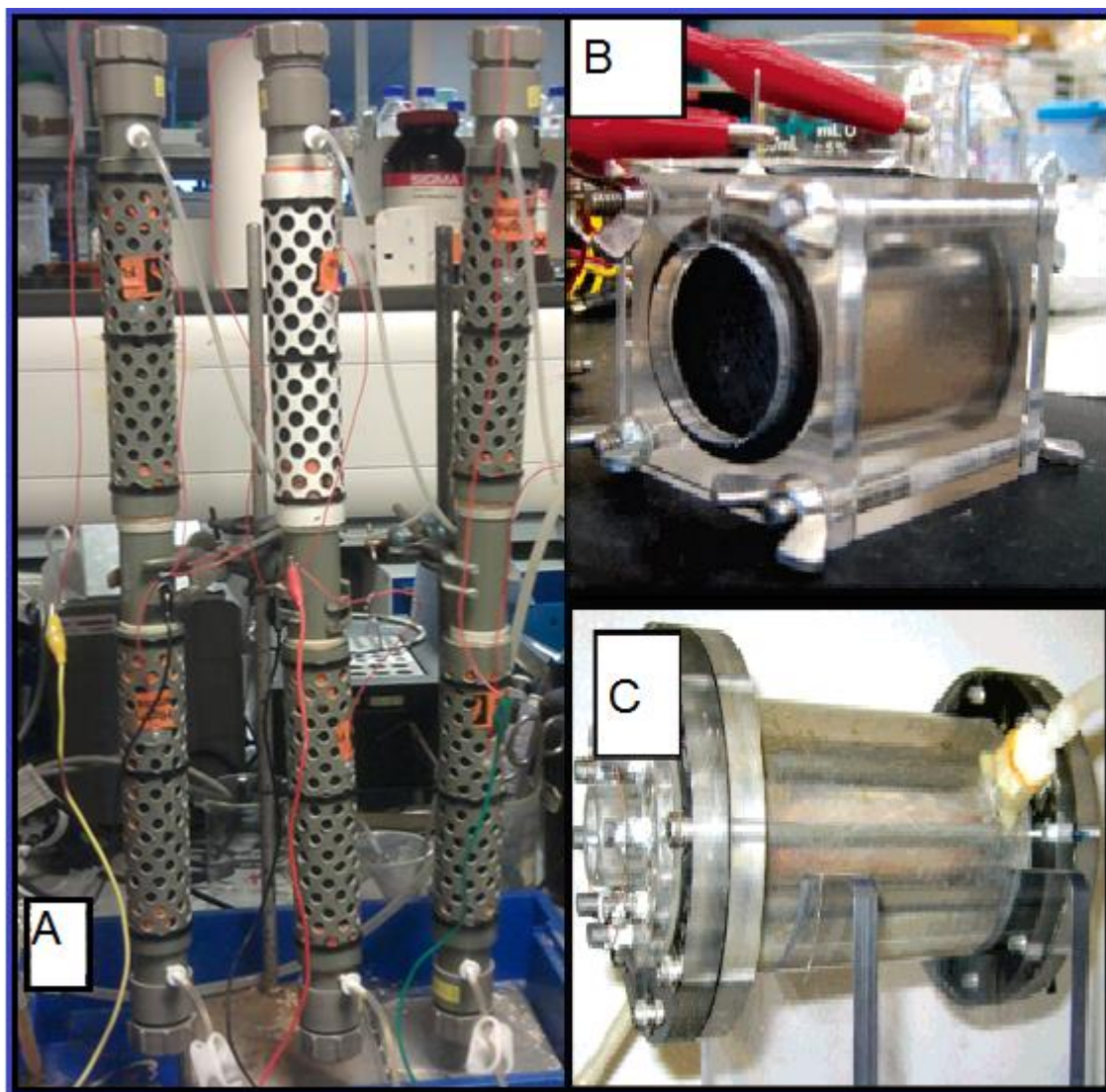


**Figure 1.13:** (A) tubular up-flow type single chamber MFC systems for continuous flow operation (used in this study) (B) rectangular type single chamber systems for batch operation (Logan et al, 2006) (C) single chamber MFC with an inner concentric cathode for continuous flow operation (Logan et al, 2006).

### 1.6.7. Microbial electrolysis cells

Microbial electrolysis cells (MECs) are similar to MFCs but instead of the external load, they utilise a small external power source to bias the thermodynamics of the reactions occurring in the anode and cathode of BES (Figure 1.9b). MECs are mainly utilised for production of biohydrogen by microbially assisted electrolysis of water at the cathode of an MEC. Furthermore, MEC systems are also utilised for the production of value added products such as Sodium hydroxide (Chen et al,

2012), hydrogen peroxide (Foley et al, 2010), recovery of precious metals, and microbially assisted desalination (Luo et al, 2010). MECs may be useful in terms of (forcefully) transferring electrons into the (-N=N-) moiety of azo pollutants, resulting in reductive cleavage of the dye pollutant (Mu et al, 2009). Especially when the electron accepting azo dye possessing a low redox potential, an external power supply would be useful for biasing thermodynamics towards the reductive azo moiety degradation (as shown in expression 2).

#### **1.6.8. The use of BES for pollutant removal**

Although the primary aim of the majority of research involving BES is to enhance the generation of biogenic electricity (in the case of MFCs) and cathodic hydrogen evolution (in the case of MECs), significant and growing amount of research is currently being devoted towards a variety of other applications of BES. Apart from the use of BES for the removal of more readily oxidisable organics such as sugars, fatty acids and amino acids present in wastewater, increasing attention is now diverted towards the removal of more recalcitrant waste types. Particularly, the organic and inorganic wastes originating from various chemical industries tend to be more recalcitrant compared to wastes originating from the agricultural sector or the food industry. Different types of MFCs were used in either batch or continuous flow modes and both anodic and cathodic chambers were used in several previous studies that demonstrated the ability of MFC systems to effectively degrade and in some instances, detoxify recalcitrant environmental pollutants. Some of the recent studies highlighting the use of BES systems used for pollutant removal are summarised in Table 1.2.

**Table 1.2:** A summary of current studies utilising BES for the purpose of removal of recalcitrant pollutants. Particular attention has been paid for the studies involving azo dyes as the environmental pollutant.

Recalcitrant pollutant	BES type and compartment used	Microbial culture	Reference
Furfural	Single chamber type MFC anode compartment	Pre-acclimated mixed microbial culture	Luo et al, 2010
Microcrystalline cellulose	Two-chamber MFC anode	Bovine rumen mixed microbial culture	Rismani-Yazdi et al, 2007
Phenol	Two-chamber MFC anode	Pre-acclimated mixed microbial culture	Luo et al, 2010
Nitrobenzene	Two-chamber MFC cathode	Mixed anaerobic consortium	Mu et al, 2009
1,2-dichloroethane	Two-chamber MFC anode	Pre-acclimated mixed microbial culture	Pham et al, 2009
4-nitrophenol	Two-chamber MFC cathode	Anaerobic sludge	Zhu and Ni, 2009
Petroleum hydrocarbon contaminated soil	U-tube type soil MFC	Mixed microbial community from saline, petroleum contaminated soil	Wang et al, 2012
Brilliant Red X-3B (azo dye)	Single chamber MFC anode with glucose as co-substrate	Mixture of anaerobic and aerobic sludge inoculum	Sun et al, 2009
Congo-Red (azo dye)	Two-chamber MFC anode with glucose as the co-substrate	Anaerobically digested sludge	Li et al, 2010
Methyl Orange, Orange-1 and Orange-2 (azo dyes)	*Two-chamber MFC cathode compartment	<i>Klebsiella pneumoniae</i> strain L17	Liu et al, 2009



Methyl Orange (azo dye)	**Two-chamber MFC cathode compartment	Anaerobic sludge	Ding et al, 2010
Amaranth (azo dye)	‡Two-chamber MFC cathode compartment	Anaerobic mixed culture	Fu et al, 2010
Orange-2 (azo dye)	Microbially assisted electrolysis of the azo dye at the cathode	MFC enriched mixed microbial consortium	Mu et al, 2009
Brilliant Red X-3B	Constructed wetland up-flow type MFC anode	Anaerobic sludge in addition to the soil microbial community	Fang et al, 2013

---

***\*The pH of the cathode was maintained at 3.0.***

***\*\*The cathode compartments was irradiated with visible light and Rutile coated graphite cathodes were used.***

***‡Cathode compartment was capable of in-situ  $H_2O_2$  generation and exogenously supplemented with  $Fe^{2+}$  in order to form Fenton's reagent***

In addition to the removal of organic xenobiotic environmental pollutants as listed above, several studies used BES for the purpose of removal of industrially important inorganic pollutants such as sulphide (Rabaey et al, 2006) sulphate (Zhao et al, 2008) and Nitrate (Virdis et al, 2008). In the aforementioned studies carried out involving azo dyes however, (Liu et al, 2009, Ding et al, 2010, Mu et al, 2009 and Fu et al, 2010), MFCs were employed only for reductive degradation of azo dyes in either anode or the cathode compartments. Means for further degradation and detoxification of the resulting aminobenzenes were not explored in any of the studies. Furthermore, in some studies (Mu et al, 2009), azo dye reduction process was assisted by exogenous supply of electrical energy. Therefore, means for full degradation and detoxification of azo dyes and their biotransformation products coupled with a sustainable approach (i.e. with no

exogenous supply of electrical energy and utilising waste material as the energy source for BES) should be the focus of developing BES for treatment of colour industry wastewater.

The removal of pollutants from wastewater in a sustainable fashion has always been one of the top priorities for methods used for recalcitrant waste removal. In this view, most physico-chemical waste treatment methods score poorly due to their intrinsic pitfalls such as very high energy expenditure, high cost of application and operation and generation of secondary waste products that lead to further disposal problems.

Concomitant energy recovery in the form of electricity while removing azo dye pollutants from simulated effluent water has been reported in recent literature and is an interesting development in terms of the use of BES to achieve pollutant removal (Liu et al, 2009).

Most BES research involved the use of carbohydrates and organic acids e.g. acetate as a substrate. However, due to cost considerations, it is preferable to use unrefined substrate types such as nutrient rich agricultural wastes (eg. molasses, lignocellulosic material and rapeseed cake) for concomitant bioremediation of environmental pollutants and concomitant recovery of biogenic electrical energy in MFCs.

Current drawbacks of BES systems include low growth rate of microbes, electron diversion to methane formation, membrane pH gradients and electrode potential losses (Rabaey et al, 2005). The microorganisms utilised in BES are unique in the sense that they can transfer electrons (from oxidation of organic matter) extracellularly to an insoluble electron acceptor (e.g. electrode). The redox potential of the electron accepting chemical species or the electrode in BES is of

paramount importance in the view of efficient electron transfer from the oxidised organic substrate. The redox potential of the electron accepting electrode can be biased by suitable choice of oxidant in the cathode or by a power supply to improve electron transfer (i.e. MECs).

The redox potential of the dyes/electron acceptor was highlighted as a predictive measure of their biodegradability when dye degradation was studied oxidatively using laccases or reductively using yeast (Zille et al, 2004). The addition of redox mediators is a possible way by which electron transfer (hence azo dye reductive degradation and MFC electrochemical performance) could be improved. Bioaugmentation is a widely used strategy in bioremediation but it has not been fully exploited in BES (Saratale et al, 2010; [www.biofuture.ie](http://www.biofuture.ie)). The use of process integration by coupling different treatment systems together e.g. MFC + activated sludge could also aid the mineralization of azo dyes. Ultimately a system that is able to operate on real wastewaters on a large scale is required. So the influence of scale up on the performance of BES needs investigation. Since BES is a recent development, very little information exists regarding their potential for treatment of azo dye containing wastewater. (Liu et al., 2009; Sun et al., 2009 and Li et al., 2010).

## **1.7. Hypothesis**

Azo dye compounds in polluted industrial effluent water can be fully degraded into non-toxic intermediates using either BES alone or in conjunction with already existing wastewater treatment technologies.

## **1.8. Aims and objectives of the current project**

The overall aim of this project is to investigate the technical feasibility of bioelectrochemical systems, as a standalone system or in conjunction with

conventional wastewater treatment processes, for treatment of azo dye-containing industrial wastewater.

In order to achieve the aforementioned aim, research was directed through following specific objectives.

### **1.8.1. Specific objectives**

#### **1. *To investigate the co-metabolic reductive degradation of azo dyes in the anode of microbial fuel cells.***

For the initial study, the model mono azo dye Acid Orange-7 (AO-7) was selected. Azo dyes are known to pass through aerobic biotreatment systems unchanged (Pandey et al, 2007). Hence, the best strategy of completely degrading azo dyes would be to employ a sequential reductive-oxidative degradation process. For this purpose, the reductive degradation of azo dyes with the aid of a co-substrate (i.e. electron donor for azo moiety reduction) in the anodes of MFCs was studied. Azo dyes that carry highly charged substituent groups (such as the sulfonate group in AO-7) and with high molecular weight (some exceeding 1 kDa) are highly unlikely to cross largely non-polar biological membranes and enter the cellular interior of bacterial cells. Therefore, the reduction of azo moieties by means of transfer of electrons is likely to occur in the extracellular milieu (Cervantes and Dos Santos, 2010, Pandey et al, 2007) with electrons coming from a co-substrate (i.e. glucose, acetate). Furthermore, the ability of MFCs to use oxygen indirectly as the terminal electron acceptor also confers MFCs an additional advantage over conventional anaerobic systems in terms of faster microbial metabolic rates and growth rates that could potentially be beneficial in achieving faster azo dye degradation kinetics in MFC anodes. The azo dye degradation was analysed with respect to the kinetics of degradation, the nature of degradation products formed and the toxicity

of the formed intermediates. A pure culture of *Shewanella oneidensis* MR-1 and anaerobic mixed cultures were used as inocula. The effect of using various un-refined co substrate types as well as different anode pH was also investigated.

***2. To investigate the co-metabolic decolourisation of azo dye mixtures under industrially relevant conditions using dye-acclimated mixed microbial populations***

In real industrial scenarios, it is very unlikely that single azo dyes are encountered and the industrial wastewater may exhibit certain extreme traits such as high temperatures and high salinities. Moreover, it is highly disadvantageous to utilise pure cultures for industrial wastewater treatment due to high cost and operational limitations. Therefore, in the second related study, the co-metabolic degradation of complex azo dye mixtures using a dye-acclimated mixed culture was investigated. Experimental conditions included a range of industrially relevant temperatures and salinities routinely encountered in colour industry wastewater. Microbial community dynamics during MFC operation were investigated using 16s rDNA microbial community profiling methods.

***3. To examine the effect of process integration on azo dye degradation.***

A complete degradation and detoxification of azo dyes and their intermediates is desired. The aminobenzenes yielding from the reductive degradation of AO-7 in the MFC stage are expected to be amenable to further degradation into less toxic intermediates if an aerobic treatment stage analogous to an activated sludge system is present. Therefore, a sequential MFC-aerobic integrated bioreactor system configuration was investigated for the full degradation of the model azo dye AO-7. Single-chamber tubular-type MFCs that are best suited for continuous flow operation were used for the study. An azo dye acclimated mixed microbial culture was used in the MFC stage in order to obtain optimum decolourisation of

the model azo dye. Other important aspects of operation such as the hydraulic retention time (HRT), dye loading rate, ability to operate at ambient temperature, long term operational stability of the integrated reactor system and the response of the reactor to sudden shock loadings of the azo dye were also investigated. The chemical nature and the toxicity of degradation products were also studied.

***4. To evaluate the influence of scale up on treatment of azo dyes in bioelectrochemical systems (tubular air-breathing MFCs).***

To assess the potential industrial applicability of the tested integrated MFC-aerobic integrated bioreactor system, it is essential to investigate the scalability of the system. For this purpose, a modular scale-up approach was used. The volumetric scale-up factor of 6 was used in the up-scaled reactor system. The reactor system was initially tested in continuous-flow mode at ambient temperature using AO-7 as the model azo dye. This was followed by feeding the reactor system with real industrial wastewater originating from colour industry. The real wastewater used included wastewater collected from an acid dyebath for wool and an acid dyebath for leather. Colour and COD removal and concomitant bio-electricity generation was monitored during the feeding cycles of the model wastewater containing AO-7 and the two types of real colour industry wastewater.

***5. To investigate the effects of the exogenous addition of redox mediators and the effect of external resistance on azo dye reductive degradation in MFCs.***

Other factors that could affect azo dye decolourisation rates in MFCs include the presence of redox mediators and the anode potential. Exogenous addition of synthetic redox mediators such as anthraquinone-2,6-disulfonic acid (AQDS) and anthraquinone-2-sulfonic acid (AQS) was investigated using a range of

concentrations of these two compounds on the reductive decolourisation of AO7 in MFC anodes.

The MFC anode potential is influenced by the applied external resistance and therefore, it could be used as a convenient tool to vary anode potential without exogenous polarisation of the anode compartment. The effect of a range of external resistances were tested on the reductive decolourisation of three model azo dyes AO-7, Reactive Red-3 (RR-3) and Direct Yellow 106 (DY-106) in the anode compartments of MFCs.

## **Chapter 2 - Materials and Methods**



## 2.1. Chemicals

AO7 Sodium salt (Figure 2.1) (purity  $\geq 98.0\%$ ), sodium pyruvate, sodium acetate, corn-steep liquor, sulfanilic acid and 1-amino-2-naphthol were purchased from Sigma Aldrich (UK). All chemicals were of analytical grade and were used without further purification. Ficodox Plus <sup>TM</sup> mixed COD reagent was purchased from Fisher Scientific (UK).

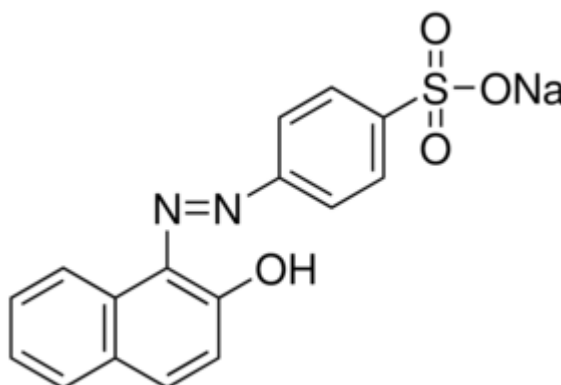


**Figure 2.1:** Acid Orange 7 structure

The dye mixtures used in simulated wastewater comprised of 18 structurally different dyes of commercial grade (Table 2.1). Molasses for the anolyte medium was purchased from Billington's, UK and the buffer salts (analytical grade) were purchased from Sigma Aldrich, UK. Ficodox Plus<sup>TM</sup> mixed COD reagent was purchased from Fisher Scientific, UK. Reagents and enzymes for PCR and were purchased from New England Biolabs (USA). All molecular biology grade reagents for denaturing gradient gel electrophoresis (DGGE) analysis were purchased from Sigma Aldrich, UK. Azo dyes except for AO-7, Methyl Orange, Reactive Black-5, Congo Red and Reactive Red -3 were obtained from industrial sources by a previous Europe-wide study relating to colour industry wastewater treatment (Sophied European project FP6 - <http://www.sophied.net/>).

**Table 2.1:** The composition of azo dye mixture used in chapter 4, their molecular weights and absorbance maxima ( $\lambda_{\max}$ )

Dye	CAS number	registry Molecular ( $\text{g mol}^{-1}$ )	weight $\lambda_{\max}$ (nm)
Acid Black 107	12218-96-1	N/A*	576
Acid Black 194	61931-02-0	461.38	570
Acid Black 210	99576-15-5	938.02	606
Acid Orange 7	633-96-5	350.32	484
Acid Red 266	57741-47-6	467.78	496
Acid Yellow 194	61814-52-6	N/A**	446
Acid Yellow 49	12239-15-5	426.28	396
Congo Red	573-58-0	696.65	497
Direct Blue 71	4399-55-7	1029.9	580
Direct Red 80	2610-10-8	1373	536
Direct Yellow 106	12222-60-5	1325	402
Disperse Blue 124	61951-51-7	377.42	466
Methyl Orange	547-58-0	327.33	464
Reactive Black 5	17095-24-8	991.82	596
Reactive Blue 222	93051-44-6	1460.91	610
Reactive Red 195	93050-79-4	1136.32	526
Reactive Red 3	23211-47-4	774.04	532
Reactive Yellow 145	93050-80-7	1026.3	418

***N/A – Molecular weight not available***

***\*Acid Black 107 structure unspecified and the molecular weight is not available***

***\*\*Acid Yellow 194 is a di-sulphonated co-complex dye (Espantaleón et al, 2003). The formula weight and the structure are not available.***

Molasses used as the co-substrate in the work described in chapters 4,5 and 6 was purchased from Billington's (UK).

The real industrial wastewater used in the work described in chapter 6 was obtained from a previous Europe-wide industrial study relating to colour industry wastewater treatment (Sophied project FP-6 <http://www.sophied.net/>). The industrial wastewater originated from two acid dyebaths in Europe used respectively for tanning of leather and colour fixation on wool fabrics. The exact dye content and other auxiliary components were unknown. Typical characteristics of the two industrial wastewaters are listed in Table 2.2.

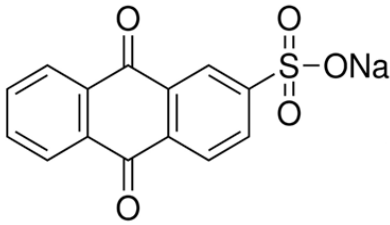
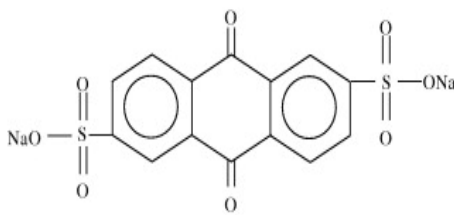
**Table 2.2:** Typical characteristics of the two colour industry wastewaters used in this study at unmodified state

Parameter	Acid dyebath wastewater for wool	Acid dyebath wastewater for leather
pH	7.75	7.2
Total dissolved solids (TDS)	161 mgL <sup>-1</sup>	146 mgL <sup>-1</sup>
Conductivity	3.15 ± 1.2 mScm <sup>-1</sup>	289 ± 33 µScm <sup>-1</sup>
Oxidation/reduction potential (ORP) vs Ag/AgCl	-53 mV	-18.9 mV
COD	1000 ± 60 mgL <sup>-1</sup>	1280 ± 40 mgL <sup>-1</sup>

Conductivity and TDS measurements were taken using an Oakton PC-700 (Oakton Instruments, UK) conductivity probe. ORP measurements were made using a BASi Ag/AgCl reference electrode (BASi reference electrodes, USA). The Ag/AgCl reference electrode contained 3M NaCl electrolyte and was +196 mV versus the standard hydrogen electrode (SHE) at 25°C.

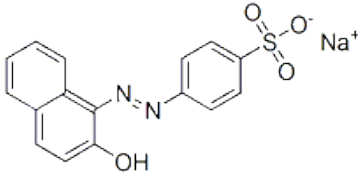
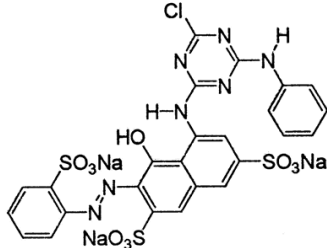
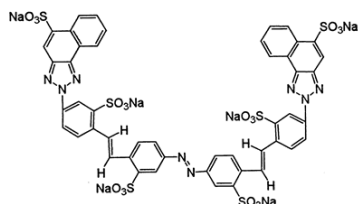
The two synthetic redox mediators Anthraquinone-2-sulfonic acid sodium salt (AQS) and Anthraquinone-2,6-disulfonic acid disodium salt (AQDS) used for the work presented in chapter 7 were purchased from Sigma Aldrich (UK) and Fisher Scientific (UK) respectively. The structures of the synthetic redox mediators used are indicated in table 2.3. All microbial growth medium components were purchased from Sigma Aldrich and used without further purification. Reagents used for molecular microbial profiling work were purchased from Sigma Aldrich (UK) and New England Biolabs (USA).

**Table 2.3:** Synthetic redox mediators used in chapter 7

Redox mediator	MW (Da)	Structure
Anthraquinone-2-sulfonic acid	310.27	
Anthraquinone-2,6-disulfonic acid	412.3	

The three model azo dyes Acid Orange-7 (AO7), Reactive Red-3 (RR3) and Direct Yellow-106 (DY106) (analytical grade) used in this study were purchased from Sigma Aldrich (UK). The three structurally different azo dyes and their absorbance maxima are shown in table 2.4.

**Table 2.4:** The three model azo dyes used in the work presented in chapter 7, their structures, molecular weights and absorbance maxima

Dye	MW (Da)	Structure	$\lambda_{\text{max}}$ (nm)
Acid Orange-7	350.32		484
Reactive Red-3	774.04		532
Direct Yellow 106	1325		402

## 2.2. Bacterial strains, their maintenance and MFC anode culture media

*Shewanella oneidensis* strain 14063 and *Vibrio fischeri* strain 13938 were purchased from NCIMB (UK) and cryopreserved stock cultures were maintained at -80°C. Anaerobic digested sludge samples were obtained from Mogden Sewage Treatment Works London (UK). Anaerobic sludge inoculum was initially grown in trypticase-soy broth and later sub-cultured into minimal medium (Tables 2.4 and 2.5) supplemented with sodium pyruvate and casein hydrolysate. *Vibrio fischeri* for bioluminescence toxicity assays was grown in oceanibulbus growth medium (NCIMB growth media catalogue) (Table 2.3). Histidine auxotroph strains *Salmonella typhimurium* strain TA 1535 and strain TA 1538 for the soft agar overlay Ames mutagenicity test were obtained from the University of Westminster culture collection. Both *S.typhimurium* strains were initially grown in Luria Bertani

(LB) medium (Sigma Aldrich) and maintained as glycerol cryopreserved stock cultures at -80°C.

The original anaerobic mixed microbial consortium for the study described in chapter 4 was obtained from Mogden Sewage Treatment Works London (UK). The anaerobic microbial consortium was initially acclimated at 30°C over a period of five months in a solution containing all 18 azo dyes (each dye at 10 mgL<sup>-1</sup>) in Winogradsky columns (column height – 42cm) supplemented with microcrystalline cellulose (1% w/v) (Sigma Aldrich) as a carbon source. Dyes were replenished in the Winogradsky columns approximately every week after complete decolourisation of the solution was observed.

The anolyte minimal salts medium for the study presented in chapter 3 consisted of (gL<sup>-1</sup>) NH<sub>4</sub>Cl, 0.46; KCl, 0.225; NaH<sub>2</sub>PO<sub>4</sub>, 2.5; Na<sub>2</sub>HPO<sub>4</sub>, 4.11; (NH<sub>4</sub>)<sub>2</sub>SO<sub>4</sub>, 0.225; 1% (V/V) of the trace element solution as described by Marsilli et al, 2008 and 0.3% (V/V) vitamin mix as described by Wolin et al, 1963. The anolyte minimal medium was supplemented with 500 mgL<sup>-1</sup> Casein hydrolysate (Sigma Aldrich UK) and 20mM Sodium pyruvate as the primary carbon source. The vitamin stock solution (100X concentrated) for minimal media comprised of the following (Table 2.5).

**Table 2.5:** Components of the vitamin mix stock solution used in this study

Component	Concentration (mgL <sup>-1</sup> )
P-aminobenzoic acid (PABA)	50
L-ascorbic acid	100
Folic acid	50
Riboflavin	10
Nicotinic acid	100
Pantothenic acid	100
Thiamine hydrochloride	10
Biotin	100

The trace elements stock solution (100X concentrated) used in this study comprised of the following (Table 2.6).

**Table 2.6:** Components of the trace elements stock solution used in this study

Component	Concentration (mgL <sup>-1</sup> )
Nitrilotriacetic acid (NTA)	1500
MnCl <sub>2</sub> ·4H <sub>2</sub> O	100
FeSO <sub>4</sub> ·7H <sub>2</sub> O	300
CoCl <sub>2</sub> ·6H <sub>2</sub> O	170
ZnCl <sub>2</sub>	170
CuSO <sub>4</sub> ·5H <sub>2</sub> O	40
AlK(SO <sub>4</sub> ) <sub>2</sub> ·12H <sub>2</sub> O	5
H <sub>2</sub> BO <sub>4</sub>	5
NaMoO <sub>4</sub>	90
NiCl <sub>2</sub>	120
NaWO <sub>4</sub> ·2H <sub>2</sub> O	20
NaSeO <sub>4</sub>	100

Simulated wastewater anolyte medium for the study presented in chapter 5 containing a mixture of all 18 azo dyes ( $20 \text{ mgL}^{-1}$  each dye, total dye content  $360 \text{ mgL}^{-1}$ ) and molasses ( $4 \text{ gL}^{-1}$ ) as a co-substrate was formulated in  $50 \text{ mM}$ , pH-7 phosphate buffer ( $21 \text{ mM NaH}_2\text{PO}_4$  and  $29 \text{ mM Na}_2\text{HPO}_4$ ).

The synthetic wastewater medium used for the work described in chapter 5 comprised of Molasses ( $2 \text{ gL}^{-1}$ ) as the electron donor, dissolved in tap water. Common auxiliary salts that are routinely present in textile wastewater  $\text{Na}_2\text{SO}_4 \cdot 10\text{H}_2\text{O}$  and  $\text{NaCl}$  were added ( $2\% \text{ W/V}$ ,  $1:1$  ratio) to the synthetic wastewater anolyte medium in order to provide the necessary ionic strength for MFC operation. The final pH of the anolyte medium feed was  $7.6 \pm 0.2$ . AO7 was supplemented into the synthetic wastewater from a stock solution. The synthetic wastewater was stripped of dissolved oxygen by sparging nitrogen gas for 10 minutes before being continuously fed into the MFC stage of the two-stage reactor system.

The MFCs used for the study described in chapter 5 were inoculated with the same azo dye acclimated mixed microbial population as described earlier from already operational MFCs treating simulated azo dye wastewater. The azo dye adapted mixed microbial culture was introduced into the MFC units at  $10\%$  of the total reactor working volume. During start-up, the inoculated MFCs were operated in fed-batch mode up-to three consecutive cycles in order to obtain reproducible MFC performance from all replicate reactors. The same synthetic medium without the azo dye was used during the start-up of MFC reactors.

For the work described in chapter 6, model wastewater containing AO-7 ( $35 \text{ mgL}^{-1}$ ) was prepared as described below. For the latter part of the study involving real industrial wastewater, the colour industry effluent was modified by supplementing it with  $2 \text{ gL}^{-1}$  of molasses to act as a co-substrate during colour removal. The real



wastewater influent for continuous reactor operation was autoclaved at 110°C for 15 minutes. The industrial wastewater influents from wool colouring and leather tanning indicated COD values of  $3950 \pm 40 \text{ mgL}^{-1}$  and  $4250 \pm 30 \text{ mgL}^{-1}$  following the supplementation of  $2 \text{ gL}^{-1}$  of molasses co-substrate. The MFC stage was inoculated with an azo dye adapted mixed microbial consortium from a continuously fed tubular MFC system treating AO-7 as described earlier.

The minimal growth medium used in the work described in chapter 7 was the same as described earlier but was supplemented with glucose ( $1 \text{ gL}^{-1}$ ) as the carbon source. For the experiments involving various external resistances, dyes were introduced into anode medium at a concentration of  $50 \text{ mgL}^{-1}$  from a filter sterilised stock solution before starting each experiment. For the experiments involving synthetic redox mediators, AQDS and AQS were supplemented into the anode growth medium at concentrations  $20 \text{ }\mu\text{M}$ ,  $50 \text{ }\mu\text{M}$  and  $150 \text{ }\mu\text{M}$  from filter sterilised  $10 \text{ mM}$  synthetic redox mediator stock solutions. All experiments with synthetic redox mediators were carried out using AO-7 as the model azo compound, supplemented into the anode medium at a concentration of  $210 \text{ mgL}^{-1}$  from a filter sterilised stock solution. All experiments were carried out in a temperature controlled environment ( $30^\circ\text{C}$ ) in an incubator.

The inoculum source for the two-chamber MFC system was the azo dye adapted mixed bacterial culture from an already operating fed-batch MFC system treating simulated azo dye wastewater as described earlier. The biomass was centrifuged, washed twice with sterile phosphate buffer before being introduced into the anode chamber at approximately  $90 \text{ mg}$  wet biomass per anode volume ( $150 \text{ mL}$ ).

The anolyte medium (apart from the vitamin solutions and redox mediators) and all MFC components were sterilised by autoclaving at  $121^\circ\text{C}$  for 15 minutes.

## 2.3. Bio-electrochemical systems and operation

For the study described in chapter 3, the H-type MFCs were constructed with two identical Duran glass bottles and were held together with an external metal clip. The anode and cathode compartments were separated with a cation exchange membrane (CMI-7000, Membranes International- USA). Two rubber gaskets were used to ensure a seal. The electrodes were constructed from carbon cloth (Figure 2.2). The cathode contained a Pt catalyst layer with a Pt loading of  $0.5 \text{ mgcm}^{-2}$ . Pt powder for the cathode was mixed with carbon black powder (Sigma Aldrich, UK) for a 10% (w/w) mixture. This mixture was suspended in Nafion ionomer solution (Sigma Aldrich) and the suspension was applied as a uniform coating on the cathode electrodes using a paint brush. Electrode connections were made by soldering insulated Copper wire onto the electrodes using Lead solder. All exposed connections were coated with non-conductive epoxy for insulation. Each electrode had a projected surface area of  $20 \text{ cm}^2$ . An external load of  $2200 \Omega$  was used in all experiments and the potential across the resistor was recorded using the Picolog ADC-24 (Pico Technology, UK) online data logging system.

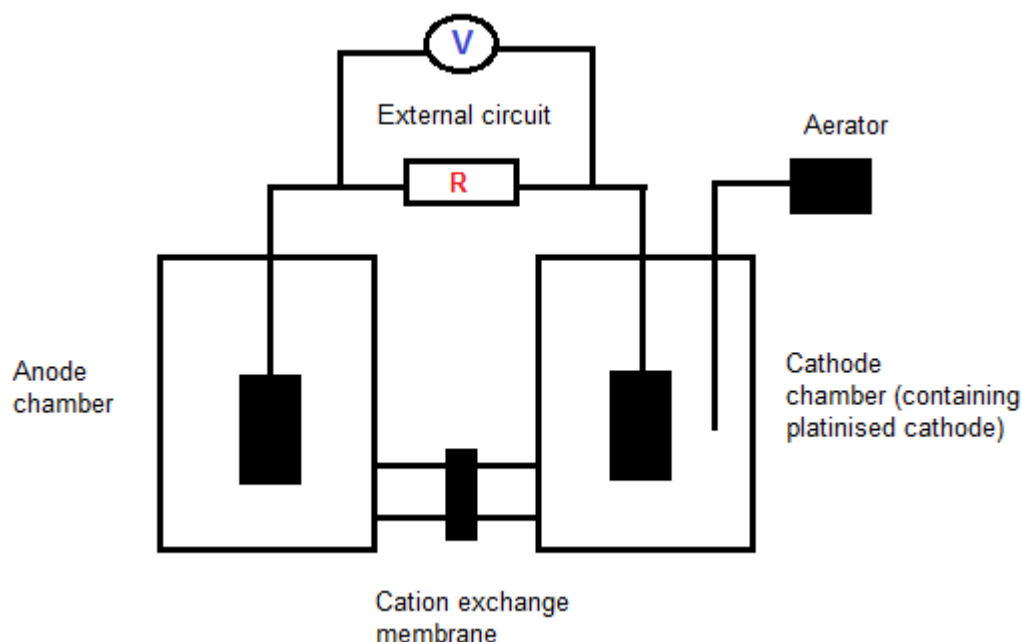


**Figure 2.2:** Schematic diagram of the two-chamber MFC set-up used throughout this work.

The catholyte and anolyte solutions were buffered to pH 7.0 using 50mM phosphate buffer (21mM -  $\text{NaH}_2\text{PO}_4$  and 29mM-  $\text{Na}_2\text{HPO}_4$ ) in all experiments.

The experiments were carried out in batch mode with a working volume of 150 mL in each MFC compartment. During start—up, the anode was seeded with actively growing *S. oneidensis* or anaerobically digested sludge seed culture (10% V/V of the total anolyte volume). The anolyte was purged with nitrogen gas for 10 minutes through a 0.22  $\mu\text{m}$  pore diameter filter prior to inoculation. The catholyte was actively aerated at an air flow rate of  $100 \text{ mLmin}^{-1}$  using an aquarium pump. All experiments were conducted at  $30^\circ\text{C}$  using a Stuart 160 incubator (Fisher Scientific, UK).

For the work described in chapter 4, the same H-type, two-chamber MFC configuration described earlier was used. An external resistance of  $1\text{k}\Omega$  was used in all experiments and the potential across the external resistance was recorded using a Picolog ADC-24 (Pico-Technology, UK) online data logging system. Prior

to inoculation, the anolyte medium was sparged with nitrogen gas for 10 minutes and the MFC headspace was also filled with nitrogen gas. The anode was seeded with the previously described azo dye adapted microbial consortium (10% v/v of the anode volume) from a Winogradsky column. The MFCs were operated in fed batch mode. Each fed-batch cycle was initiated when the MFC voltage fell below 50mV and 75% anode contents were removed and replenished with fresh dye-containing medium when starting new cycles. The catholyte was sparged continuously with air at a flow rate of 200 mLmin<sup>-1</sup>. All experiments were conducted in a temperature regulated Stuart 160 incubator (Fisher Scientific, UK).

Cylindrical single chamber MFCs were used in the work presented in chapter 5. They were constructed from polyvinyl chloride and had a working volume of 200mL. The reactor dimensions were 3.5 cm (internal diameter) and 30 cm length. Both electrodes were constructed from carbon fabric (PRF composite materials, Dorset, UK). The concentric anode had a projected surface area of 96cm<sup>2</sup> whereas the cathode had a surface area of 64 cm<sup>2</sup> (measured). The cathode contained a platinum catalyst layer on one side (Pt loading at 0.35 mgcm<sup>-2</sup>) and a Polytetrafluoroethylene (PTFE) diffusion layer on the other side in order to minimise water loss through the membrane. The cathode catalyst layer was applied as described earlier in section 2.1.4. and the PTFE gas diffusion layer was applied as described by Antolini et al, 2002. The connections on the electrodes were secured using insulated copper wire soldered to the electrodes and the connection interfaces were insulated with non-conductive epoxy. The anode and the cathode were separated by a CMI-7000 cation exchange membrane (Membranes International, USA). Electrode spacing between the anode and the cathode was approximately 1.3 cm. The external circuit of the MFCs were connected across a 1000 Ohm resistor to a data acquisition system (Picolog ADC-

24, Pico Technology, UK) in order to gather voltage data, set at a data recording interval of 10 minutes (Figures 2.3 and 2.4). All single-chamber MFCs were simultaneously and continuously fed using a multi-channel peristaltic pump (Watson-Marlow, UK) with an up-flow configuration. The outflowing effluent from the MFC stage was continuously fed-into the aerobic second stage of the reactor installed downstream to the MFC stage. The dye containing influent feeding rate was varied throughout the study.

The working volume of the subsequent aerobic stage was 1000 mL. The aerobic reactor was continuously aerated at an air sparging rate of 200 mL air per minute through a ceramic air stone sparger using an aquarium pump and was continuously agitated using a magnetic mixer. All constituent stages of the integrated reactor system were operated at ambient temperature without exogenous control of temperature. The temperature in the laboratory varied from 14.6°C (during winter) and 26°C (during summer).

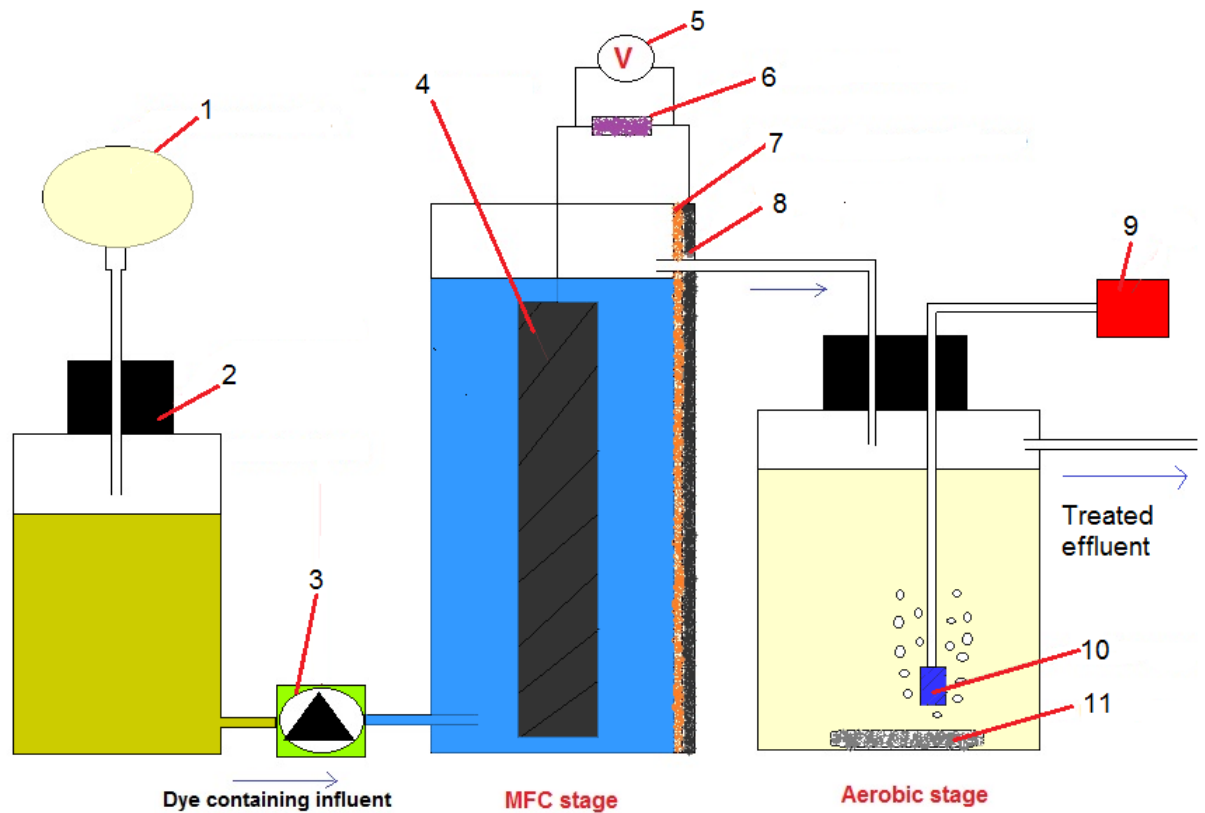


**Figure 2.3:** Schematic diagram and the hydraulic-flow of the integrated MFC – aerobic bioreactor system treating AO-7 containing synthetic wastewater. The components of the system are [1] nitrogen gas bag [2] synthetic wastewater feeding tank [3] peristaltic pump [4] carbon fabric anode [5] data logging system [6] external resistor [7] cation exchange membrane [8] platinised carbon cathode [9] air pump [10] air stone sparger [11] magnetic mixer



**Figure 2.4:** The experimental set-up during the start-up stage of the continuous run of the two-stage integrated MFC-aerobic bioreactor system for the treatment of the model colour industry wastewater containing AO-7.

For the work described in chapter 6, three MFC units were incorporated to produce a modular scale-up model for the initial MFC stage of the two-stage system. The system components and the hydraulic flow of the up-scaled system are shown in Figure 2.5. The MFCs were arranged in tandem but operated as a single unit in terms of hydraulic flow.

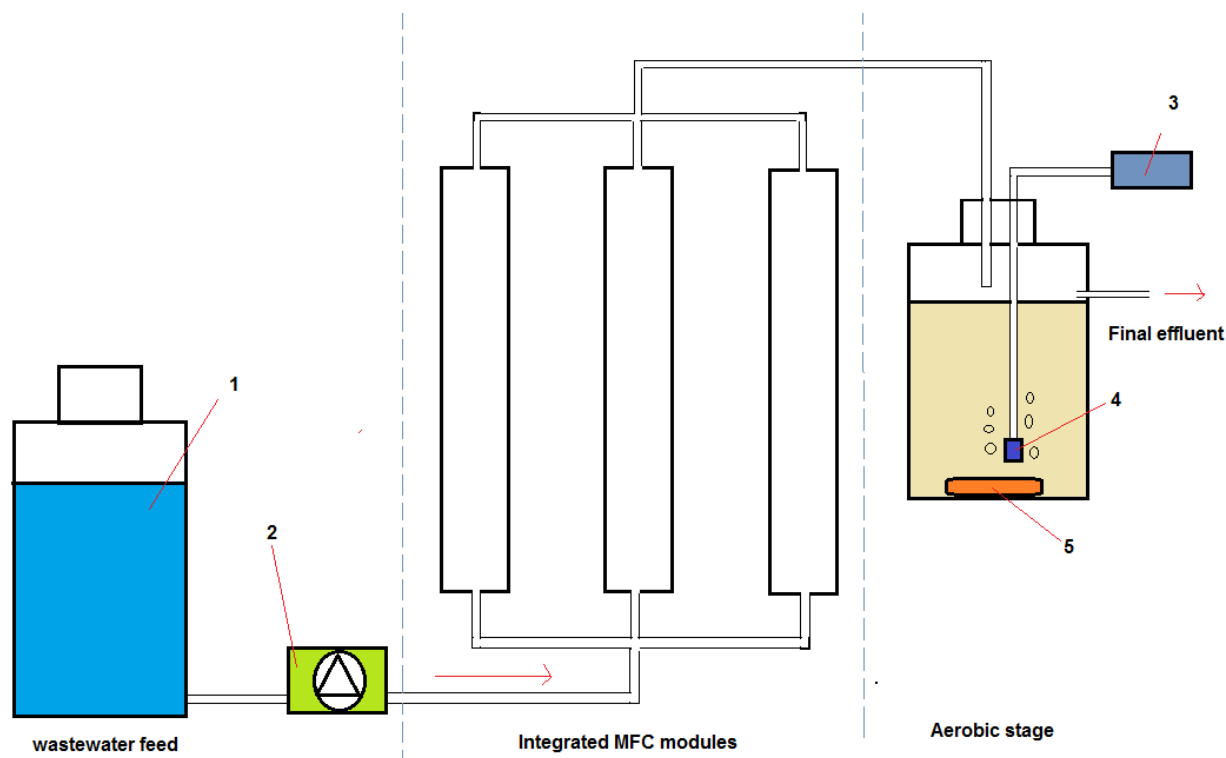


**Figure 2.5:** Components and the hydraulic flow of the up-scaled two-stage integrated bioreactor system featuring integrated MFC modules. (1) Wastewater feed (2) peristaltic pump (3) air pump (4) air stone sparger (5) magnetic mixer

The working volume of a single MFC module was 400 mL and had a combined working volume of 1200 mL in the integrated reactor system. The MFC reactor construction was of polyvinyl chloride (PVC) tubes and had an internal diameter of 3.5 cm and a length of 60 cm. The anode and the cathode were made of carbon paper (PRF composite materials, Dorset, UK) and had surface areas of 192 cm<sup>2</sup> (projected) and 128 cm<sup>2</sup> (measured) respectively. The electrode spacing between the anode and the cathode was approximately 1.3 cm. The hollow concentric anode ran through the length of the PVC tube. Platinum powder was used as the oxygen reduction catalyst in the cathode and was coated on to the cathode membrane-facing side at 0.35 mgcm<sup>-2</sup>. The air facing side of the cathode contained a PTFE diffusion layer in order to minimise water loss through the cation exchange membrane. The Pt catalyst layer and the PTFE diffusion layer was applied as described earlier. Electrical connections on the electrodes were secured



by soldering copper wire onto the electrodes and the exposed junctions were sealed with non-conductive epoxy. A cation exchange membrane (CMI-7000 – Membranes International, USA) separated the anode and the cathode in all three MFC modules. The spacing between the anode and the cathode was approximately 1.5 cm in each MFC module. Three MFC modules were connected in parallel to a 500 Ohm external resistor and the voltage across the resistance was monitored using a PicoLog ADC-24 (Pico Technology, UK) data logging system at a data recording interval of 10 minutes. The external electrical circuit in the system is indicated in Figure 2.6. Real or model dye wastewater was continuously fed with an up-flow configuration to the MFC modules using a peristaltic pump. The effluent from the MFC stage was collectively fed into the second aerobic stage of the integrated bioreactor system (Figures 2.7 and 2.9). The aerobic bioreactor stage was actively aerated continuously through an airstone sparger at an air flow rate of 400 mL air per minute. The aerobic reactor was continuously agitated using a magnetic mixer. The working volume of the aerobic stage was 2 L. The HRTs of the MFC stage and the subsequent aerobic stage respectively were 13.3 hours and 22.2 hours.

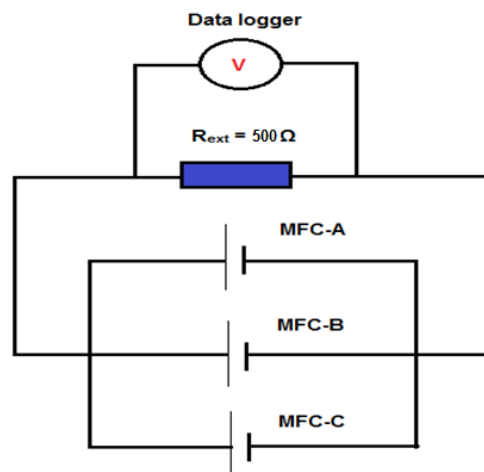


**Figure 2.6:** The parallel configured external electrical circuit of the three combined MFC modules used in this study.

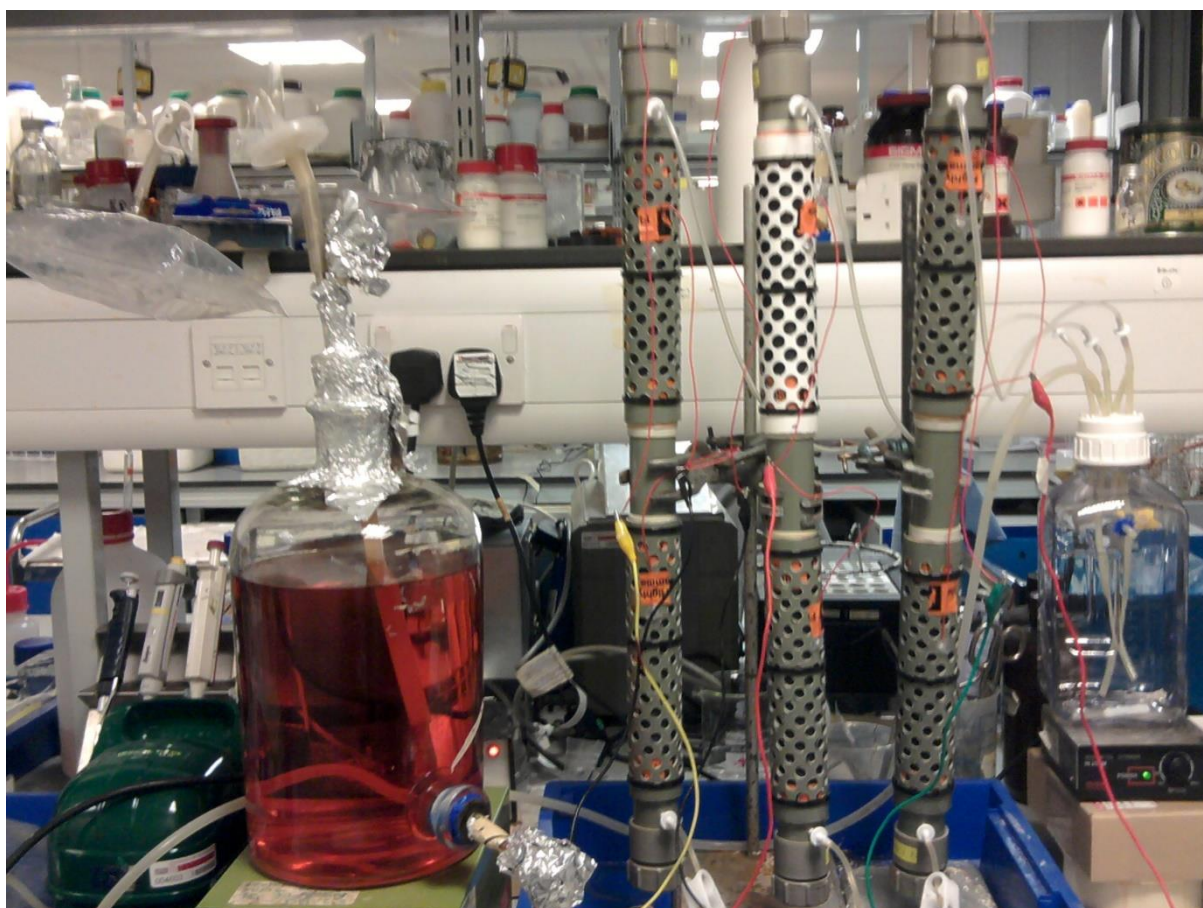


**Figure 2.7:** The up-scaled two stage MFC-aerobic reactor system (during start-up of the continuous run) used for the treatment of AO-7 containing model wastewater and two types of real colour industry wastewater

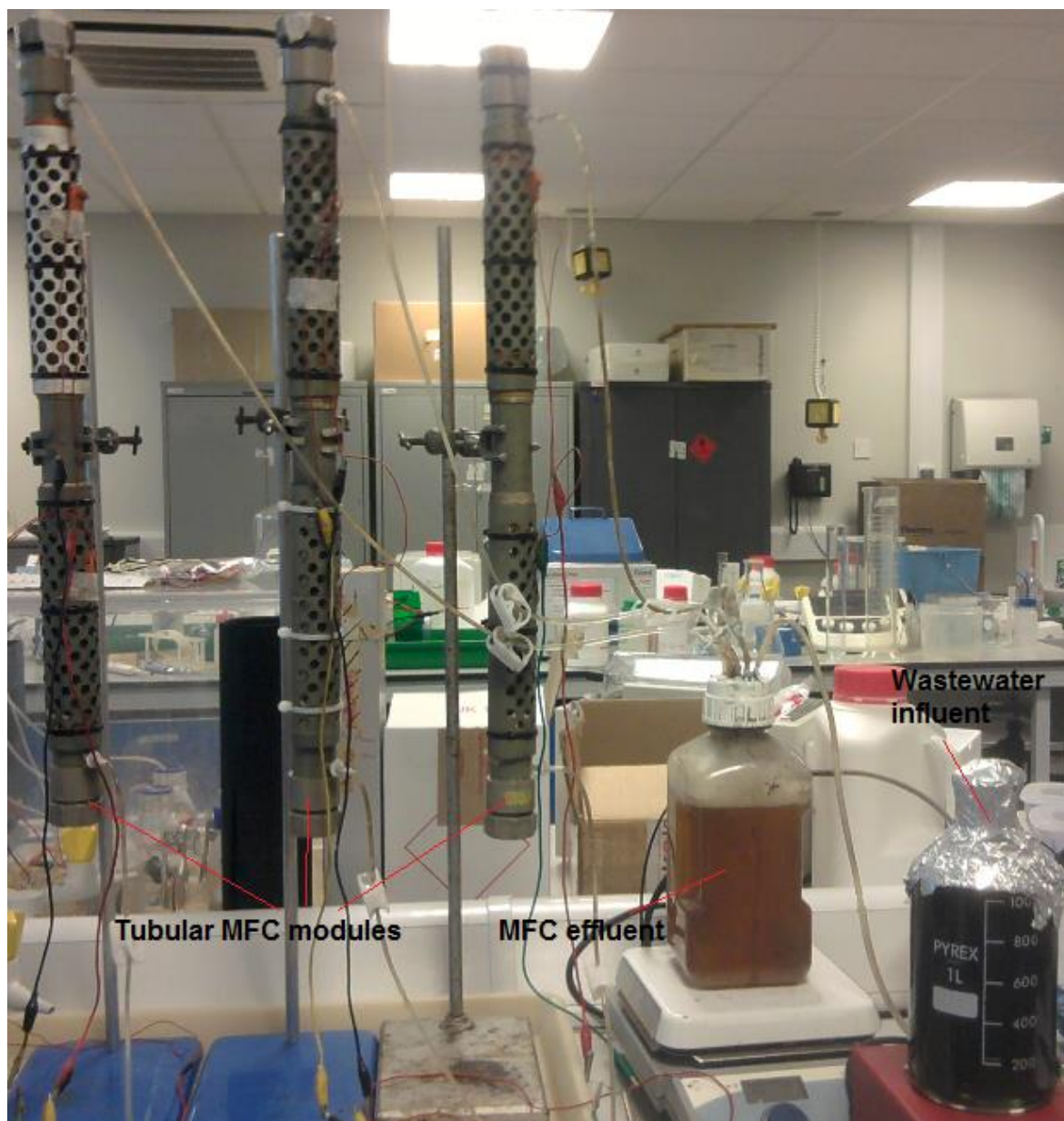


**Figure 2.8:** The scaled up tubular MFC modules (three reactors acting in unison) treating real colour industry wastewater from leather tanning.

The work presented in chapter 7 used the same conventional H-type MFC system described earlier. The anode and cathode chambers were operated with a working volume of 150 mL and the measured surface area of the electrodes was  $20 \text{ cm}^2$ . The cathode contained a platinum catalyst layer with a Pt loading of  $0.5 \text{ mgcm}^{-2}$ . The cathode catalyst layer was applied as described earlier. The anode and cathode chambers were separated by a cation exchange membrane (CMI 7000 – Membranes International, USA). For start-up of the system, the MFCs were

allowed to produce a stable voltage across a 1 k $\Omega$  resistor for three consecutive fed-batch cycles in dye-free media before being used in experiments.

## 2.4. Experimental design

In the first study described in chapter 3, investigated the kinetics of AO7 decolourisation by *S.oneidensis* in MFC anodes at AO7 concentrations ranging from 35 mgL<sup>-1</sup> to 350 mgL<sup>-1</sup> using dual chamber MFCs assembled and operated as described earlier. The effect of inoculum type on AO7 decolourisation (at an AO7 concentration of 35 mgL<sup>-1</sup>) was studied using *S.oneidensis*, anaerobic digested sludge and a mixed inoculum of anaerobic sludge and *S.oneidensis* at a volumetric ratio of 1:1 (the total inoculum was 10% V/V of the working volume of the anode). The control was an MFC containing AO7 (35 mgL<sup>-1</sup>) with no microorganism. The effect of pH on AO-7 decolourisation by *S.oneidensis* was investigated by changing the anolyte medium pH from pH-4 to pH-9 using 2N HCl or NaOH to adjust the anolyte pH. Starting AO-7 concentration was kept constant at 35 mgL<sup>-1</sup> throughout the set of experiments investigating the effect of pH on AO-7 decolourisation. The anolyte medium composition was the same as in other parts of this study (co-substrate – Sodium pyruvate at 20 mM concentration). The effect of co-substrate type on AO7 decolourisation kinetics was determined at AO7 concentrations of 35 mgL<sup>-1</sup> and 195 mgL<sup>-1</sup> in MFCs inoculated with *S. oneidensis*. The co-substrates chosen were sodium acetate, rapeseed cake, molasses and corn-steep liquor (Sigma Aldrich, UK) and were supplemented in the anolyte medium at a concentration of 300 mgL<sup>-1</sup>. The abiotic control experiments used in this work were not seeded with the microbial inoculum but used the same medium as the other experiments and were assembled and operated under the same conditions as the tests. The colour removal by adsorption in abiotic controls is presented in appendix 1.

The work described in chapter 4 was conducted in several separate experiments as indicated below.

**Experiment 1:** Long-term fed-batch operation of the MFC system containing the simulated wastewater was conducted at 30°C for 50 days. Microbial community analysis was carried out on samples collected at the end of the fed-batch operation (after 50 days) and un-adapted anaerobically digested sludge.

**Experiment 2:** The effect of operating temperature on decolourisation of azo dye mixtures was investigated at 20°C, 30°C, 40°C and 50°C respectively.

**Experiment 3:** The effect of salt concentration in the anode feed on decolourisation of the dye mixture was investigated using anolyte feed solutions containing salt contents ranging from 0% - 2.5% (w/v). Salts used were NaCl and Na<sub>2</sub>SO<sub>4</sub>·10H<sub>2</sub>O in a ratio of 1:1 (temperature controlled at 30°C at all salt concentrations).

The abiotic controls used in the experiments described in chapter 4 contained the same molasses medium and the azo dye mixture but were not seeded with the azo dye adapted microbial consortium. All abiotic control MFCs containing media and the dye mixture (360 mgL<sup>-1</sup>) were autoclaved at 121°C for 15 minutes and were used without inoculation. All experiments were conducted in duplicate and the values reported are means ± SD of the mean.

The assessment of azo dye adsorption: A separate test was carried out in order to assess the colour removal contribution from dye adsorption on to biomass and other surfaces in the MFC (eg. electrodes and membrane). Microbial cultures in MFCs that showed a stable voltage output after start-up (after 72 hours) were heat killed by autoclaving (121°C for 15 minutes). The azo dye mixture (sterilised at 121°C for 15 minutes) was introduced into the heat inactivated MFCs at the same

concentration ( $360 \text{ mgL}^{-1}$ ) and colour removal was assessed after 24 hours of incubation at  $30^{\circ}\text{C}$ .

In the work described in chapter 5, the MFC stage of the experimental set-up consisted of three identical MFC units operating in continuous flow mode, two of which were duplicate tests and the other was an open-circuit control. The azo dye loading rate was incrementally varied from  $70 \text{ g m}^{-3}\text{day}^{-1}$  to  $210 \text{ g m}^{-3}\text{day}^{-1}$  during the experiments. The hydraulic residence time (HRT) of the influent within the MFC stage of the integrated reactor system was 12 hours during all dye loading rates. Samples were drawn from all reactors at set time points throughout the experimental run (total length- 154 days). Sampling was conducted from the influent (i.e. feeding tank), the MFC reactors and the aerobic stage bioreactors. The HRT of the subsequent aerobic reactor stage was 60 hours. The values reported are means of duplicate experiments. The components of the integrated two stage MFC-aerobic reactor system treating AO-7 containing synthetic wastewater and its hydraulic flow is depicted in the schematic diagram (Figure 2.6). Following the two-stage continuous runs, the ability of the MFC stage of the system to recover from a sudden shock-load of AO-7 was investigated. AO-7 was spiked into the MFC reactor stage from a  $5 \text{ gL}^{-1}$  AO-7 stock solution to reach a final AO-7 concentration of  $400 \text{ mgL}^{-1}$  in the MFC stage. The recovery of the MFC stage was tracked in terms of colour and COD removal.

In the work described in chapter 6, experiments were designed and carried out with the aim of investigating the effect of scale-up of the integrated MFC-aerobic two-stage bioreactor system for azo dye removal and to investigate the reactor performance when used for the treatment of model and real industrial wastewaters. A modular scale-up was used in which the MFC stage comprised of three 400 mL MFC units acted in unison to act as the initial stage of the two-stage system.

During the initial experiment where model wastewater containing AO-7 was used, the AO-7 loading rate was maintained at  $126 \text{ gm}^{-3}\text{day}^{-1}$  (COD loading of  $5.76 \text{ kg CODm}^{-3}\text{day}^{-1}$ ). In the experiment where real colour industry wastewater was used, COD loadings of  $7.11 \text{ kgCODm}^{-3}\text{day}^{-1}$  (dye wastewater from wool colouring) and  $7.65 \text{ kgCODm}^{-3}\text{day}^{-1}$  (dye wastewater from leather tanning) respectively were maintained. Colour and COD removal performance of the reactor system during the experimental runs were monitored.

In the work described in chapter 7, separate experiments were carried out several at different applied external resistances  $10 \Omega$ ,  $510 \Omega$ ,  $2.2 \text{ k}\Omega$ ,  $10 \text{ k}\Omega$  and  $46 \text{ k}\Omega$  for each model azo dye. An open circuit control was run in parallel with all experiments for comparison purposes. All experiments were carried out in duplicate and the data presented are means  $\pm$  SD of duplicate tests. For the experiments involving synthetic redox mediators, the concentration of the two mediators tested (AQDS and AQS) were varied from  $20 \mu\text{M}$  to  $150 \mu\text{M}$ . The control experiment included all other components in the anolyte solution except for the synthetic redox mediator.

## 2.5. Analytical procedure

### 2.5.1. AO7 decolourisation and kinetic study

The decolourisation of AO7 in MFC anodes in work described in chapter 3, 5 and 7 were assessed using a UV-Visible spectrophotometer (Perkin-Elmer; Lambda-35). AO7 removal was quantified using spectrophotometric standard calibrations constructed at the peak absorbance ( $\lambda_{\text{max}}$ ) of the dye ( $484\text{nm}$ ). The AO7 removal efficiency (RE) was calculated as follows:

$$RE(\%) = \frac{C_{0,AO7} - C_{t,AO7}}{C_{0,AO7}} \times 100 \quad \text{-----} \quad 1$$



Where,  $C_{0AO7}$  and  $C_{tAO7}$  are AO7 concentrations (mM) at the start and at each time point respectively.

The kinetics of AO7 decolourisation was modelled using first order kinetic models. The first order rate constants ( $k$ ) for AO7 decolourisation reactions can be estimated using the integrated first order rate law.

$$\ln[C_t] = (-)kt + \ln[C_0] \text{ ----- 2}$$

Where,  $C_0$  and  $C_t$  respectively are AO7 concentrations of the starting sample and at each time point. Therefore,  $-k$  for the decolourisation of AO7 at each concentration would be equal to the slope of a linear plot of  $\ln[C_t/C_0]$  against time (t).

### **2.5.2. Assessment of decolourisation of the azo dye mix containing simulated wastewater**

The decolourisation of the azo dye mix containing feed solution used in the work described in chapter 4 was monitored spectrophotometrically using a Perkin-Elmer Lambda-35 UV-visible spectrophotometer. The peak area between wavelengths 400nm-650nm was used to monitor colour removal as described by Nigam et al, 2000; as compliance of different wavelengths within this range is required by environmental agencies dealing with such effluents. The decolourisation efficiency (DE) of the dye mixture was calculated as follows:

$$DE (\%) = \frac{A_0 - A_t}{A_0} \times 100 \text{ -----3}$$

Where,  $A_0$  and  $A_t$  are absorbance peak area values between the wavelength range 400 nm - 650 nm of UV-Visible spectra scans in the starting solution and at each time point respectively. Kinetics of dye decolourisation during MFC fed-batch operation was modelled using first order kinetic models. The first order kinetic



constants of decolourisation ( $K_{(\text{decol})}$ ) can be estimated using the integrated first-order rate law.

$$\ln(A_t) = -K_{(\text{decol})} * t + \ln(A_0) \text{ ----- 4}$$

Where,  $A_0$  and  $A_t$  are absorbance peak area values between the wavelength range 400 nm - 650 nm of UV-Visible spectra scans in the starting solution and at each time point respectively.

In order to assess the colour removal in more complex real industrial wastewater used in work described in chapter 7, UV – visible scans of real wastewater and the decolourised samples were used (Perkin – Elmer Lambda-35 UV-Visible spectrophotometer). The colour removal efficiencies were established by calculating the peak area reduction within the wavelength region 400 nm – 650 nm of the UV-vis scans of influent and effluent wastewater samples, as described earlier in equation 3.

Colour removal in the MFC anodes used in the work described in chapter 7 was assessed using a UV-visible spectrophotometer (Lambda-35, Perkin Elmer). Azo dye degradation was modelled into first order kinetics. The first-order decolourisation kinetic constants ( $k$ ) were estimated as described earlier in equation 2.

### **2.5.3. COD removal**

Chemical oxygen demand (COD) of the samples was determined using the closed reflux titrimetric method as described in Environment Agency (UK) Standard method 5220D (Westwood, 2007). Appropriately diluted 2 mL samples were used for each determination. Briefly, the samples were centrifuged at 6000 g for 10 minutes and the supernatant was filtered through a 0.22 µm PTFE filter in order to remove suspended biomass. Appropriately diluted 2 mL samples were added to

3.8 mL of Ficodox mixed COD reagent and was digested on a pre-heated heating block for 1.5 hours at 150°C in closed digestion tubes. A 0.025M ferrous ammonium sulphate (FAS) titrant was used with 2-3 drops of Ferroin indicator solution (Fisher Scientific, UK) in order to titrimetrically determine the residual Potassium dichromate contained in the Ficodox digestate following the digestion with the sample. The COD removal was calculated using the following equation:

$$COD (mgL^{-1}) = (V_b - V_s) * DF * M * 4000 \text{ ----- } 5$$

Where  $V_b$  and  $V_s$  are ferrous ammonium sulphate (FAS) titrant volumes for the blank and the sample respectively, DF is the sample dilution factor and M is the molarity of FAS titrant.

The percentage COD removal was calculated as follows:

$$Percentage \text{ COD removal} = \frac{COD_i - COD_s}{COD_i} \times 100 \text{ ----- } 6$$

Where,  $COD_i$  and  $COD_s$  are initial COD and sample COD value at each time point respectively.

The COD removal kinetic constants ( $K_{(CODrem)}$ ) in the work described in chapter 4 were determined as follows:

$$\ln (COD_s) = -k_{(CODrem)} * t + \ln (COD_i) \text{ ----- } 7$$

Where,  $COD_i$  and  $COD_s$  respectively are initial and sample COD concentration values at each time point.

The  $-k_{(CODrem)}$  is equal to the slope of linear plot of  $\ln(COD_s/COD_i)$  against time (t).

#### **2.5.4. Extraction of AO-7 degradation products**

In the work described in chapter 5, the final effluent samples collected at the end of the aerobic second stage were centrifuged at 8000 g for 10 minutes and filtered

through PTFE membrane filters (0.22  $\mu\text{m}$ ) in order to remove suspended biomass. The supernatant was then acidified to pH-2 using 3N HCl in order to precipitate soluble proteins. The solution was then centrifuged at 8000 g for 10 minutes and the supernatant was used for metabolite extraction. The metabolites in these samples were extracted into equal volumes of ethyl acetate. The extracts were concentrated by rotary evaporation and dried over anhydrous  $\text{Na}_2\text{SO}_4$  in a desiccator to obtain crystals. These crystals were then dissolved in 1 mL of HPLC grade methanol.

#### **2.5.5. Detection of degradation products using HPLC**

For the work presented in chapter 3, the degradation products of AO7 decolourisation were identified using HPLC according to the procedure described by Mu et al, 2009. The HPLC system (DIONEX GS50) was equipped with a Phenomenex Gemini C18 reversed phase column (5  $\mu\text{m}$ , 150 X 4.6 mm) and a Photodiode Array (PDA) detector (DIONEX PDA-100). The two standard compounds sulfanilic acid and 1-amino-2-naphthol were detected at wavelengths 248 nm and 284 nm respectively. The mobile phase consisted of 50% methanol and 50% 33 mM (pH 7) phosphate buffer. The mobile phase was pumped at a flow rate of 1  $\text{mLmin}^{-1}$  and the sample injection volume was 20  $\mu\text{L}$ . The presence of the two AO7 decolourisation metabolites Sulfanilic acid and 1-amino-2-naphthol were confirmed using the retention times ( $R_t$ ) of the standard compounds.

#### **2.5.6. Identification of degradation metabolites using HPLC-MS**

In the work described in chapter 5, the separation of AO7 degradation metabolites was carried out using HPLC (Dionex GS50). The HPLC system was equipped with a Phenomenex Gemini® reversed phase C18 column (5  $\mu\text{m}$ , 150 X 4.6 mm). The detection of the metabolites was done at 248 nm using a photodiode array detector (Dionex PDA-100). The mobile phases were 0.05% (V/V) formic acid in

Acetonitrile (mobile phase-A) and HPLC grade water (mobile phase-B). Subsequent to a 1 minute equilibration before injection, a linear gradient of 10% - 90% of mobile phase-A (0.05% formic acid in Acetonitrile) was used over 29 minutes. The sample injection volume was 20  $\mu\text{L}$  and a flow rate of 1  $\text{mLmin}^{-1}$  was used.

The HPLC system was interfaced with Surveyor® MSQ plus Z-spray electrospray ionisation (ESI) mass spectrometer. The mass spectrometer was operated in the positive mode with a cone voltage of 70 V and the probe temperature was 400°C. The needle voltage was maintained at 3 kV and the capillary temperature was set to 200°C. Nitrogen was used as the cone gas. The mass range selected was from 45 – 500 amu. Quasi-molecular ions formed in ESI-MS were identified using the NIST mass spectra database.

#### **2.5.7. Quantification of 4-aminobenzenesulfonic acid and 1-amino-2-naphthol**

Quantification of the two reductive degradation products of AO-7 4-aminobenzenesulfonic acid and 1-amino-2-naphthol (produced at the end of the MFC stage) in the work described in chapter 5 was carried out using HPLC. The authentic standards of both compounds (analytical grade) were purchased from Sigma Aldrich (UK). Samples from both MFC stage and the aerobic stage were analysed using a reversed phase Phenomenex Gemini® C18 column. The mobile phases were acetonitrile and HPLC grade water (60:40 V/V) pumped at a flow rate of 1  $\text{mLmin}^{-1}$ . The sample injection volume was 20  $\mu\text{L}$  and the detection of both compounds was conducted at 248 nm. For identification of 4-aminobenzenesulfonic acid and 1-amino-2-naphthol in samples, the retention times ( $R_t$ ) of the standard compounds were compared to those of samples. Standard curves for both compounds were constructed and the concentrations of

both compounds present in all samples were directly read from the standard curves.

HPLC gradient elution of the metabolites contained in the samples was carried out for the work described in chapter 6, in order to investigate the chemical changes that took place during the two-stage decolourisation process. The separation of metabolites using HPLC gradient elution was carried as described earlier. Briefly, the Dionex GS50 HPLC system was equipped with a Phenomenex Gemini® reversed phase C18 column (5  $\mu$ m, 150 X 4.6 mm). The detection of the metabolites was done at 248 nm using a photodiode array detector (Dionex PDA-100). The mobile phases were Acetonitrile (mobile phase-A) and HPLC grade water (mobile phase-B). Subsequent to a 1minute equilibration before injection, a linear gradient of 10% - 90% of mobile phase-A (Acetonitrile) was used over 29 minutes. The sample injection volume was 20  $\mu$ L and a flow rate of 1 mLmin<sup>-1</sup> was used.

#### **2.5.8. Fourier Transform Infra-Red (FTIR) analysis**

FTIR spectroscopy was carried out in order to further understand the chemical nature of the substituent groups present in the fully decolourised samples originating from the aerobic stage of the integrated reactor system. Ethyl acetate extracts obtained from the aerobic bioreactor stage of the reactor and the AO-7 containing influent were obtained using the procedure described in the section 2.7. The dry crystals obtained were finely ground to powder form and were mixed with spectroscopically pure KBr (5:95 ratio) (BDH chemicals, UK) and pressed into translucent pellets using a laboratory press. The KBr pellets were fixed in the sample holder and FTIR scans were conducted at the mid IR region ranging from 400 cm<sup>-1</sup> to 4000 cm<sup>-1</sup> at 16 scan speed (Perkin Elmer, Spectrum One) (Eastman Dental Institute, University College, London).

### 2.5.9. Toxicity assessment

*Vibrio fischeri* (NCIMB strain 13938) was initially grown in NCIMB growth medium 1537 (Oceanibulbus medium) (Table 2.7).

**Table 2.7:** Composition of Oceanibulbus medium for *V.fischeri* (13938)

Component	Concentration (gL <sup>-1</sup> )
Tryptone	10
Yeast extract	5
NaCl	10
Sigma Aldrich sea salts ready mixture (S9983)	14

*V.fischeri* was grown in Oceanibulbus medium for 72 hours (22°C, 150 rpm) before the cells were harvested by centrifugation at 4000 X g. The cell pellet was washed twice with sterile phosphate buffer (50 mM, pH 7.1) and was resuspended in a sterile 2% NaCl solution before being used in the toxicity assay.

Toxicity assays were conducted according to the Microtox® standard acute toxicity testing procedure (Gaudet, 1994). The luminescence inhibition cytotoxicity assessment procedure was checked using phenol solutions ranging from 5 mgL<sup>-1</sup> to 45 mgL<sup>-1</sup> (Figure 2.9) prior to be used for the determination of toxicity of the samples originating from this study. The luminescence inhibition was measured as described below.

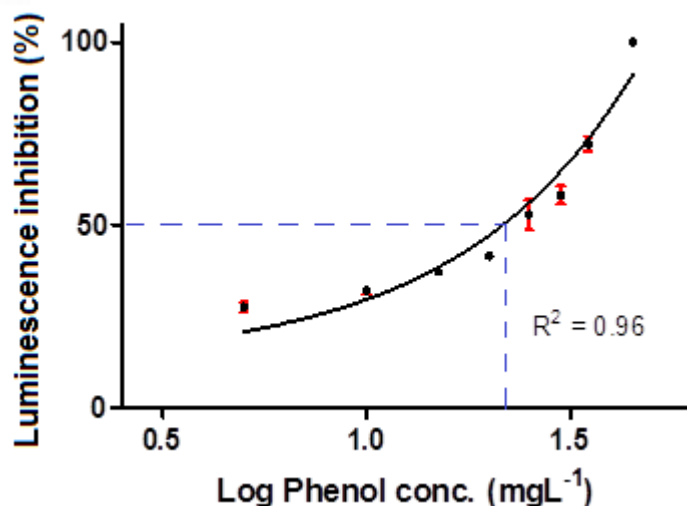


**Figure 2.9:** *Vibrio fischeri* acute cytotoxicity assay dose-response curve using phenol (5 mgL<sup>-1</sup> – 45 mgL<sup>-1</sup>).

For the acute toxicity work described in chapter 5, bioluminescence based toxicity assessment of samples was carried out using the standard Microtox® *V.fischeri* luminescence reduction assay as described earlier. The half maximal inhibitory concentrations (IC<sub>50</sub>) (indicating a reduction of half of the total luminescent intensity compared to controls) were expressed as a COD equivalent of the analysed samples. All samples for toxicity testing were obtained when the reactor system was operating at its highest AO-7 loading rate (210 gm<sup>-3</sup>day<sup>-1</sup>).

#### 2.5.10. Mutagenicity assessment using Ames test

Mutagenicity of the reductive decolourisation products generated following full colour removal in MFCs in experiments that contained AO-7 concentrations ranging from 35 mgL<sup>-1</sup> to 350 mgL<sup>-1</sup> was established using soft overlay agar Ames mutagenicity testing procedure as described by Maron and Ames, 1983. The two histidine auxotroph strains *S.typhimurium* TA 1535 and TA 1538 carry the following two mutations respectively in their histidine synthesis genes *hisG* (*hisG46* – a base-pair mutation) and *hisD* (*hisD3052* – a frame-shift mutation) (Maron and Ames, 1983). The two strains tested are unable to synthesise histidine

on their own and therefore, are unable to grow on histidine deficient growth media. The mutagenic potential of a tested chemical or physical mutagen is proportional to the rate of reversion of the tested strains from histidine auxotroph to a histidine prototroph (Maron and Ames, 1983). Where the reverted strain acquires the capability of synthesise histidine and grow on histidine deficient growth medium following exposure to a mutagen.

The mutagenicity tests were carried out on Vogel-Bonner minimal agar plates with a soft-top agar layer seeded with the test organism and the test chemicals. The composition of the Vogel-Bonner minimal medium-E (VBE) (50X concentrated) is shown in Table 2.8 (Pilatz et al, 2006).

**Table 2.8:** The composition of the Vogel-Bonner minimal medium-E (50X stock) used in the Ames mutagenicity study

Component	Concentration (gL <sup>-1</sup> )
MgSO <sub>4</sub> ·7H <sub>2</sub> O	10
Citric acid monohydrate	100
K <sub>2</sub> HPO <sub>4</sub>	500
Na(NH <sub>4</sub> )HPO <sub>4</sub>	175

For preparing VBE glucose agar plates, following components were used (Table 2.9)



**Table 2.9:** Components used for the preparation of VBE glucose agar plates

Component	Quantity
Agar	15 g
50X VBE from stock	20 mL
Glucose from a 40% (w/v) stock solution	50 mL
DI water to 1000 mL	

The composition of the soft top agar overlay is shown in Table 2.10.

**Table 2.10:** Soft-top agar overlay composition (for 600 mL)

Component	Quantity
VBE glucose agar solution	200 mL
NaCl	3 g
Trace stock solution	60 mL
DI water to 600 mL	

The composition of the trace stock solution is shown in Table 2.11.

**Table 2.11:** Trace stock solution composition for soft top agar overlay

Component	Quantity
Biotin	6.1 mg
Histidine	5.25 mg
DI water to 100 mL	

All components were autoclaved at 121°C for 15 minutes except the glucose stock solution and the trace stock solution for soft top agar overlays. Glucose stock was autoclaved at 110°C for 10 minutes and the trace stock solution was filter sterilised through a sterile 0.22 µm pore diameter PTFE filter.

Test culture strains *S.typhimurium* strains TA 1535 and TA 1538 were grown in LB media overnight and the overnight cultures were used for Ames mutagenicity testing.

VBE glucose agar (15 mL) was first poured in to petri dishes and allowed to set. The test organism (100 µL) and the test chemical (i.e. AO-7 degradation products or the unreduced dye) (100 µL) were added to 2 mL of molten soft-top agar and poured over the first layer of agar. When the top layer was set, the plates were incubated at 37°C for 72 hours. The revertant colonies developed on the soft agar overlay were counted using a semi-automatic bacterial colony counter (American Optical Quebec 3327). All tests were carried out in duplicate with sodium azide being used as a positive control (Figure 2.10) and sterilised deionised water being used for the background plate. The average background colony count was subtracted from all tests.

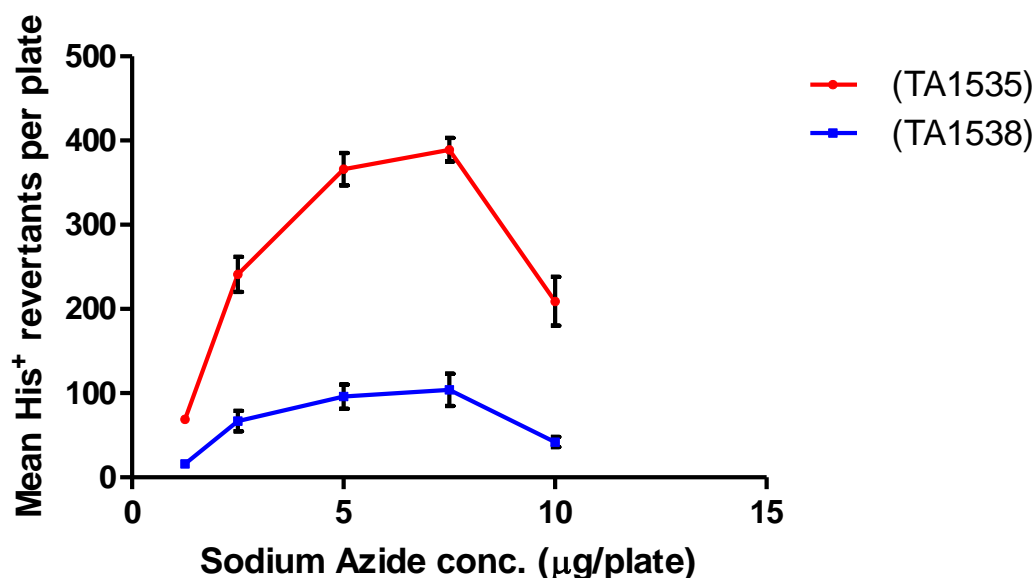


**Figure 2.10:** Positive controls for Ames mutagenicity tests using  $\text{NaN}_3$  as the known model mutagen for the two test strains of *S.typhimurium* TA 1535 and TA 1538.

### 2.5.11. Electrochemical monitoring

Polarization curves for determining power density vs current density plots were constructed using a range of external resistances spanning  $1\Omega$  -  $1\text{M}\Omega$ . The external circuit of the MFC was opened to connect various external resistances when the system exhibited a stable voltage across the initial  $2200\Omega$  external resistor. The current flowing through each external load was calculated using the Ohm's law.

$$I = E/R \text{ ----- } 8$$

Where, I is the current flowing through the load (mA), E is the potential across the resistor (mV) and R is the external resistance ( $\Omega$ ).

The power produced was calculated using the following equation:

$$P = EI \text{ ----- } 9$$

Where, P is Power produced (mW), E is the potential (mV) and I is the current (mA).

The current density and power density values were calculated by normalising current and power values to the projected surface area of the anode (20 cm<sup>2</sup>).

Coulombic efficiency (CE) was calculated by integrating the measured current over time based on the observed COD removal as follows (Logan et al, 2006):

$$CE (\%) = \frac{M \int_0^t I dt}{\Delta COD * F b V_{an}} \times 100 \text{ ----- } 10$$

Where, M is the molecular weight of Oxygen (32), I is current (A), F is the Faraday's constant (96485 Cmol<sup>-1</sup>), b is the number of electrons exchanged per mol of oxygen (4), V<sub>an</sub> is the working volume of the anode (L) and ΔCOD is the change of COD over time (t) (g CODL<sup>-1</sup>).

In the work described in chapter 5, the test MFC units were operated in closed circuit configuration with 500 Ω external resistances whereas the control MFC reactor was operated in open circuit configuration. Voltage data acquisition from all reactors was conducted using a Picolog (Pico Technology, UK) data logging system. The current flowing through the external circuit was calculated using the Ohm's law as previously described in equation 8. The Power produced by the MFC systems was calculated as previously described in equation 9. The current and power values obtained were normalised to the anode surface area (96 cm<sup>2</sup>) to construct polarisation curves and power-current plots. External circuits were opened at the end of the MFC operation in order to connect various external resistances ranging from 1 Ω to 1 MΩ. When the potential differences across each resistance reached a stable value, they were used to construct polarisation curves and power-current plots.

The external circuits of the three integrated MFC modules were connected in parallel configuration to a 500 Ohm load as shown in figure 2.6. The ADC-24 (Pico-Technology, UK) data logging system was connected in parallel across the 500 Ohm resistance. Polarisation curves of the collective three-module system were recorded by varying the external resistance from 1 Ohm to 1 Mega Ohm and recording the registered voltage across each external load. Current flowing across each resistance was calculated using the Ohm's law, as shown in equation 8. The power produced was calculated as earlier described according to equation 9. Current and power values were normalised to the anode surface area (192 cm<sup>2</sup>) and were used to construct power-current plots.

For the work described in chapter 7, the total internal resistance ( $R_{int}$ ) of the MFC systems were estimated using the polarisation slope method as described by Menicucci et al, 2006 and Fan et al, 2008. During each experiment, the external circuit of the MFCs were opened to connect various external resistances ranging from 1  $\Omega$  – 1 M $\Omega$ . When the potential across each resistance indicated a stable voltage value, it was used to construct polarisation curves and power-current plots as described earlier. The maximum power density ( $P_{max}$ ) of the MFC systems was obtained from power-current curves. The slope of the Ohmic polarisation region represents the total internal resistance ( $R_{int}$ ) (Menicucci et al, 2006, Liang et al, 2007 and Fan et al, 2008).

Cyclic voltammetry of the experiments involving synthetic redox mediators was carried out using a PG 581 potentiostat (UniScan Instruments, UK). MFC anodes were used as the working electrode whereas the cathode was used as the counter electrode. Ag/AgCl electrode (4M KCl, BASi reference electrodes, USA) was used as the reference electrode. A scan rate of 10 mVsec<sup>-1</sup> was used and the potential sweeps were carried out within the potential range of (-) 500 mV to 500 mV.

## 2.5.12. Microbial community analysis

For the work described in chapter 4, microbial community analysis was carried out by amplification and analysis of the V3 region of the 16s ribosomal DNA (rDNA) of bacteria (Figure 2.11) using PCR and DGGE. Total genomic DNA was extracted using the phenol-chloroform method (Ogram et al, 1987) from the original anaerobic digested sludge and the bulk culture liquid from an MFC fed with simulated wastewater containing the azo dye mixture operated in fed-batch mode for 50 days. Extracted total microbial genomic DNA was verified on 1% (w/v) agarose gels prior to PCR amplification. The DNA extracts were checked for purity using the  $A_{260}/A_{280}$  ratio and quantified using a Nano-Drop (Nano-1000, Thermo Scientific, USA) spectrophotometer. The 16s rDNA hypervariable V3 regions were then amplified using the following set of universal primers; F357-GC (*E.coli* numbering) (5'-CGC CCG CCG CGC GCG GCG GGC GGG GCG GGG GCA CGG GGG GCC TAC GGG AGG CAG CAG-3') and R518 (*E.coli* numbering) (5'-ATT ACC GCG GCT GCT GG-3') (Sun et al, 2012).

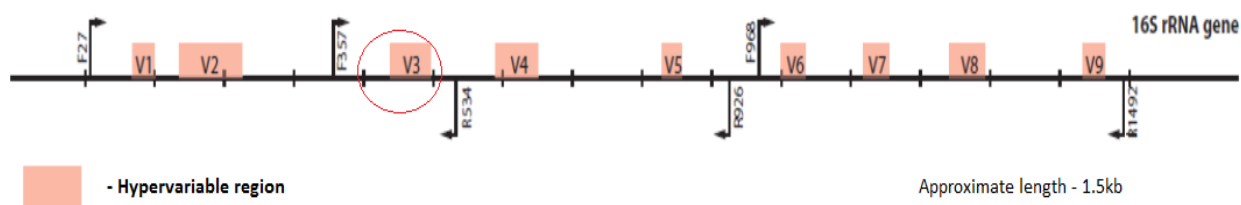


**Figure 2.11:** The bacterial 16s rRNA gene (approximate total length – 1.5 kb) and the hypervariable V3 region amplified for microbial community profiling in this study (shown within the red circle).

The PCR reaction mixture (50  $\mu$ L) included the following components:

2X PCR master mix (New England Biolabs) ----- 25  $\mu$ L

Nuclease free water ----- 22  $\mu$ L

Forward and Reverse primers ----- 1  $\mu$ L each

Template whole genomic DNA ----- 1  $\mu$ L

The PCR was performed using Bio-Rad PCR system MJ-Mini (UK) under following conditions: initial denaturation at 95 °C for 4 min, followed by 30 cycles of 95 °C for 0.5 min, 58 °C for 1 min, 72 °C for 0.5 min, and finally at 72°C for 7 min. PCR products were run on 1.5% (w/v) agarose gels for product size confirmation prior to DGGE runs.

DGGE was performed using CBS Scientific DASG-250 universal mutation detection system. PCR products were loaded and run on 8% (w/v) polyacrylamide gels (37.5:1 acrylamide:bis-acrylamide) with a denaturant gradient ranging from 30% - 60% across the gel (100% corresponding to 7M urea and 40% deionised formamide).

The components of the denaturing gel are listed in Table 2.12.

**Table 2.12:** composition of the denaturing gels (8% acrylamide) used in microbial community analysis

Component	Quantity		
	0%	30%	60%
Tris acetate EDTA (TAE) buffer 50X stock	0.5 mL	0.5 mL	0.5 mL
Acrylamide (40% 37.5:1 stock)	5 mL	5 mL	5 mL
Deionised Formamide	-	3 mL	6 mL
Urea	-	3.15 g	6.3 g
Glycerol	0.5 mL	0.5 mL	0.5 mL
Nuclease free water	To 25 mL	To 25 mL	To 25 mL

The solutions were cast within the glass plates using a gradient delivery system and the samples were loaded with a tracker dye (6X – Promega, USA) inside the wells.

Electrophoresis was conducted in 1X Tris-Acetate EDTA (TAE) buffer at 200 V for 5 hours at 60°C. Following electrophoresis, the gel was stained using SYBR Green-1 DNA stain (Sigma Aldrich, UK) and visualised using a transilluminator table. Bands of interest were excised out of the gel using sterile scalpels and incubated at 4°C in tubes containing 100 µL of sterile nuclease-free water for 48 hours. This solution was used as the template for the second round of PCR amplification using the universal primer set F338 (5'-ACT CCT ACG GGA GGC AGC AG-3') and R518 using the same PCR conditions indicated before. The amplified products were loaded in 40 µL volumes onto 1.5% agarose gels for verification. The bands were excised from agarose gels and PCR products were



purified using a QiaQuick gel extraction system (QiaGen, UK). Following the verification of PCR products on 1.5% agarose gels, the PCR amplicons were sequenced at the Wolfson Institute for Biomedical Research, University College London, UK.

The sequences obtained were compared with those in the NCBI GenBank 16s rDNA nucleotide sequence repository using NCBI BLAST nucleotide search tool (<http://blast.ncbi.nlm.nih.gov/Blast>). Phylogenetic analysis of the sequences was conducted using Mega-5.05 molecular evolutionary genetics analysis tool with neighbour joining method (with 1000 bootstrap replicates).

For the work described in chapter 7, changes in microbial communities during the experiments involving different external resistances were investigated using PCR-DDGE. The total genomic DNA from the samples obtained from MFCs operated under various  $R_{ext}$  was extracted using a Sigma Aldrich Gen-Elute bacterial DNA kit as per manufacturer's instructions. The whole genomic DNA isolates were verified on 1% (w/v) agarose gels prior to PCR amplifications. The hypervariable V3 region of the bacterial 16s rRNA gene was amplified using the following set of primers – F357-GC (5'-CGC CCG CCG CGC GCG GCG GGC GGG GCG GGG GCA CGG GGG GCC TAC GGG AGG CAG CAG-3') and R518 (5'-ATT ACC GCG GCT GCT GG-3') (Sun et al, 2013). The PCR conditions were the same as described earlier. The amplified sections were verified on 1.5% (w/v) agarose gels for correct product size confirmation prior to DGGE microbial community profiling.

Microbial community profiling was carried out using Bio-Rad D-Code universal mutation detection system (USA). Poly acrylamide gels (8%) with a denaturing gradient ranging from 30% to 60% (100% corresponding to 7M urea and 40% deionised formamide) were formulated from components as shown in table- 2.12 and were cast into the glass plates using the Bio-Rad model-475 gradient delivery

system. The samples were loaded into the wells in with a tracker dye (6X concentrated, Promega, USA) and run for 16 hours at 70 Volts. The temperature of the system was maintained at 60°C throughout the run. Following the DGGE run, the gels were stained using the DNA stain SYBR Green-1 (Sigma Aldrich- UK) and was visualised under polarised light using a transilluminator table.

The gel images were scanned and analysed using the gel image analysis software PhyElph© version 1.6. DGGE fingerprints were analysed for their differences in the band patterns using unweighted pair-group method with arithmetic mean (UPGMA) clustering method. UPGMA algorithm with Jaccard's coefficient was used to cluster the band distances on gel images. Dendrograms were created using UPGMA clustering algorithm (PhyElph© version 1.6).

Bands of interest were excised out of the DGGE gel using sterile scalpels and the cut-out gel blocks were incubated at 4°C for 24 hours in tubes containing 100 µL of nuclease free water. This was used as the template for second round of PCR amplification using the primer set F-338 (5'-ACT CCT ACG GGA GGC AGC AG-3') and R518 (Sun et al, 2012). The products were verified for products size on 1.5% (w/v) agarose gels and checked for concentration and purity using a Nano-Drop spectrophotometer (ND 1000, Thermo Scientific, USA). The DNA samples were sequenced at GATC Biotech, Germany.

The obtained 16s rDNA fingerprints were analysed using the NCBI GenBank 16s rDNA gene fingerprint repository (<http://blast.ncbi.nlm.nih.gov/Blast>) using the basic local alignment search tool (BLAST). Phylogenetic relationships of the 16s rDNA gene fingerprints were established using Mega 5.05 evolutionary genetics analysis tool with neighbour joining method (1000 bootstrap replicates were used).

## **2.6. Statistical analysis of data**

All experimental data indicated on the graphs are the means of duplicate experiments unless otherwise stated and the error bars represent the standard deviation of the mean (SD). Statistical analysis of data was conducted by one-way analysis of variance (ANOVA) with Tukey post-test using Prism GraphPad 5.0.

## **Chapter 3 - Co-metabolic reductive**

**degradation of Acid Orange - 7 in microbial fuel  
cell anodes**

## Summary

The decolourisation of acid orange 7 (AO7) (C.I.15510) through co-metabolism in a microbial fuel cell by *Shewanella oneidensis* strain 14063 was investigated with respect to the kinetics of decolourisation, extent of degradation and toxicity of biotransformation products. The aim of this work was to investigate the decolourisation of AO7 in the anode of a MFC through co-metabolism. Of particular interest were the kinetics of decolourisation, extent of degradation and the toxicity of biotransformation products.

Rapid decolourisation of AO7 (> 98% within 30 hours) was achieved at all tested dye concentrations with concomitant power production. The aminobenzene degradation products were recalcitrant under tested conditions. The first order kinetic constant of decolourisation ( $k$ ) decreased from  $0.709 \pm 0.05 \text{ h}^{-1}$  to  $0.05 \pm 0.01 \text{ h}^{-1}$  (co-substrate- pyruvate) when the dye concentration was raised from  $35 \text{ mgL}^{-1}$  to  $350 \text{ mgL}^{-1}$ . The use of unrefined co-substrates such as rapeseed cake, corn-steep liquor and molasses also indicated comparable or better AO7 decolourisation kinetic constant values. The fully decolourised solutions indicated increased toxicity as the initial AO7 concentration was increased.

This work highlights the possibility of using microbial fuel cells to achieve high kinetic rates of AO7 decolourisation through co-metabolism with concomitant electricity production and could potentially be utilised as the initial step of a two stage anaerobic/aerobic process for azo dye biotreatment.

The experimental outcomes of the work described in this chapter were published in, Fernando, E., Keshavarz, T., Kyazze, G., 2012. Enhanced bio-decolourisation of acid orange 7 by *Shewanella oneidensis* through co-metabolism in a microbial fuel cell. International Biodeterioration & Biodegradation 72, 1-9.

## 3.2. Results and discussion

### 3.2.1. Anodic decolourisation of AO7 and kinetics of AO7 removal

AO7 was rapidly decolourised in MFC anodes at low to moderate concentrations (the respective removal rates at AO7 concentrations  $35 \text{ mgL}^{-1}$  and  $70 \text{ mgL}^{-1}$  were  $254.6 \text{ mgL}^{-1}\text{day}^{-1}$  and  $500.4 \text{ mgL}^{-1}\text{day}^{-1}$ ). The rapid colour removal observed is associated with the reduction of the AO7 chromophore at 484 nm (Figure 3.1A).

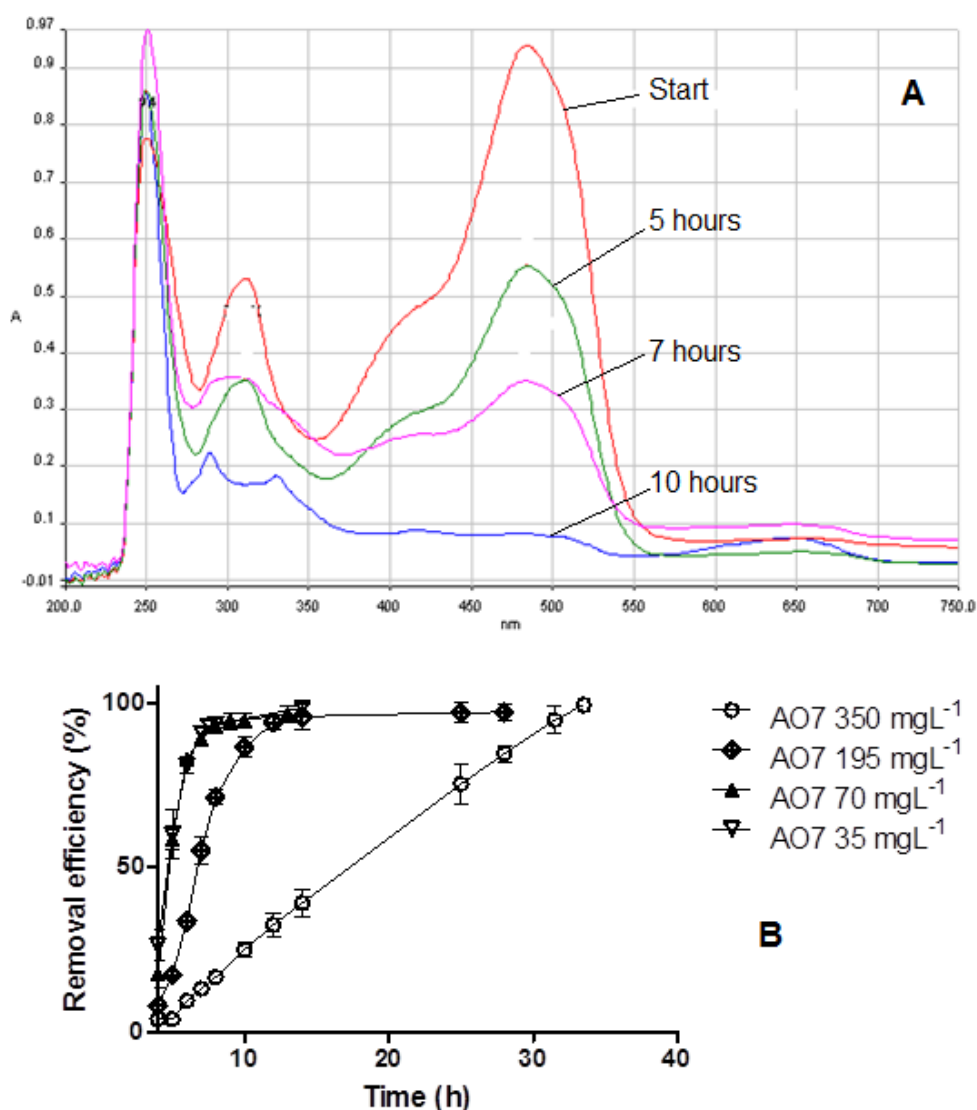


**Figure 3.1:** (A) Absorption spectra showing the reduction of peak intensity of the chromophore at 484 nm over a 10 hour period (starting AO7 conc- $70 \text{ mgL}^{-1}$ ) and (B). The effect of AO7 concentration on decolourisation rate in MFC anodes

The temporal AO7 removal reached > 90% at all tested dye concentrations after 30 hours of MFC operation (Figure 3.1B).

AO7 decolourisation kinetics could be fitted to a first order logarithmic decay model as described in equation 2 (Figure 3.2A). The reaction rate constants ( $k$ ) for the decolourisation reactions decreased with increasing AO7 concentration. A linear correlation can be observed between the rate constant ( $k$ ) of AO7 decolourisation and initial AO7 concentration (Figure 3.2B).

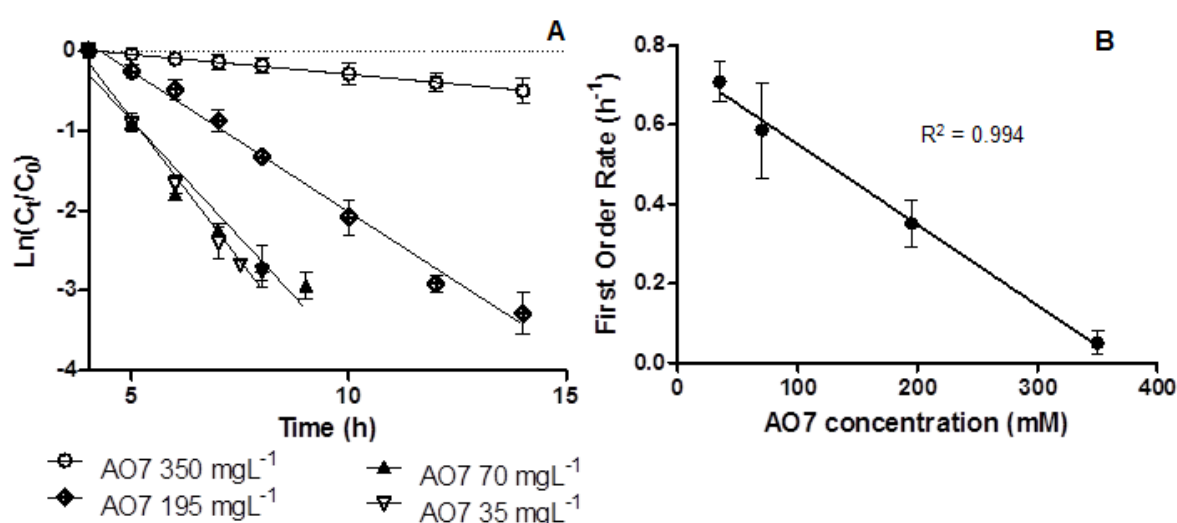


**Figure 3.2:** (A) The first order logarithmic decay models of AO7 removal in MFC anodes and (B) the linear relationship between the first order rate constant ( $k$ ) of AO7 removal and initial AO7 concentration

This effect may be attributed to the toxicity of the dye or its decolourisation metabolites when found in rising concentrations to the anode microbes. IsIk and Sponza 2004 and Inan Beydilli and Pavlostathis 2005 reported that accumulation of aminobenzene azo dye decolourisation metabolites induces an inhibitory effect on decolourisation rates.

Previously, in studies that utilised mixed anaerobic cultures, Van der Zee *et al*, 2001, Van der Zee *et al*, 2000 and Mendez-Paz *et al*, 2003 suggested that

anaerobic decolourisation of AO7 can be fitted to a first-order autocatalytic model due to the possible redox mediator role played by 1-amino-2-naphthol, one of the metabolites of AO7 reductive decolourisation. It was suggested that 1-amino-2-naphthol in its amino-quinone form may play a role as a redox mediator, catalysing the transfer of reducing equivalents to the azo moiety of AO7 molecules, leading to its accelerated decolourisation. However, this reported phenomenon was not evident at high AO7 concentrations in this study ( $k$  values did not increase as dye concentration increased), most probably due to the inhibitory effect to the anode microbial population caused by the toxicity of the dye or the accumulation of its decolourisation metabolites. Any possible inhibitory effect on microbial growth or metabolism may eventually lead to reduced rates of substrate oxidation and may hamper the release of reducing equivalents.

*S. oneidensis* utilised in this study indicated rapid AO7 decolourisation kinetics at low to moderate AO7 concentrations. The decolourisation kinetic constants ( $k$ ) observed in this study are comparable or better in comparison to that of other studies utilising pure or mixed microbial cultures (Table 3.1).



**Table 3.1:** Comparison of AO7 removal rates, first order kinetic constants of decolourisation, different inocula and reactor types reported in other studies

AO7 conc. (mgL <sup>-1</sup> )	Removal rate (mgL <sup>-1</sup> d <sup>-1</sup> ) (dye conc.)	Decolourisation kinetic constant, <i>k</i> (h <sup>-1</sup> ) (dye conc.)	Culture	Reactor type	Reference
30 to 300	NG*	0.1 (60mgL <sup>-1</sup> ) 0.08(300mgL <sup>-1</sup> )	Methanogenic and mixed anaerobic cultures	Anaerobic batch reactor	Bras et al, 2001
60 to 300	300	0.066(300mgL <sup>-1</sup> )	Anaerobic sludge from pulp and paper wastewater treatment plant	Up-flow anaerobic sludge blanket (UASB)	Carvalho et al, 2007
35 to 350	254.6 (35mgL <sup>-1</sup> ) 500.43 (70mgL <sup>-1</sup> ) 551 (195mgL <sup>-1</sup> ) 290 (350mgL <sup>-1</sup> )	0.709(35mgL <sup>-1</sup> ) 0.587(70mgL <sup>-1</sup> ) 0.352(195mgL <sup>-1</sup> ) 0.05(350mgL <sup>-1</sup> )	<i>Shewanella oneidensis</i>	Dual chamber MFC	<b>This study</b>
10 to 200	NG*	0.082(10mgL <sup>-1</sup> ) 0.047 (50mgL <sup>-1</sup> ) 0.04(100mgL <sup>-1</sup> ) 0.020 (200mgL <sup>-1</sup> )	<i>Alcaligenes faecalis</i> and <i>Rhodococcus erythropolis</i>	Erlenmeyer flasks	Mutafov et al, 2007

The decolourisation of AO7 improved marginally when anaerobic sludge was utilised as the inoculum ( $k = 0.781 \pm 0.021 \text{ h}^{-1}$  at AO7 conc. 35 mgL<sup>-1</sup>) (Figure 3.3A). This could be due to the action of biogenic sulphide produced by the sulphate reducing microbial communities that are ubiquitously found in anaerobic sludge. AO7 decolourisation rates were higher in UASB reactors inoculated with anaerobic granular sludge compared to chemical reduction of AO7 using sulphide at comparable concentrations as reported by Van der zee *et al*, 2001. Hence, the presence of biogenic sulphide may be responsible for the marginal increase of AO7 decolourisation rate observed in this study when anaerobic sludge was utilised to inoculate MFC anodes. However, the electrochemical performance of MFCs was markedly lower when anaerobic sludge was utilised (Figure 3.3B), possibly due to the diversion of electrons to methane generation pathways by

methanogenic bacteria usually found in anaerobic sludge (Mendez-Paz et al, 2005). Supplementing the anaerobic sludge inoculum with *S. oneidensis* pure culture resulted in restoration of the MFC performance to a limited extent ( $19 \pm 1.6$  mWm<sup>-2</sup>) while maintaining a high AO7 decolourisation rate ( $k= 0.713 \pm 0.017$  h<sup>-1</sup>) (Figures 3.3A and 3.3B).

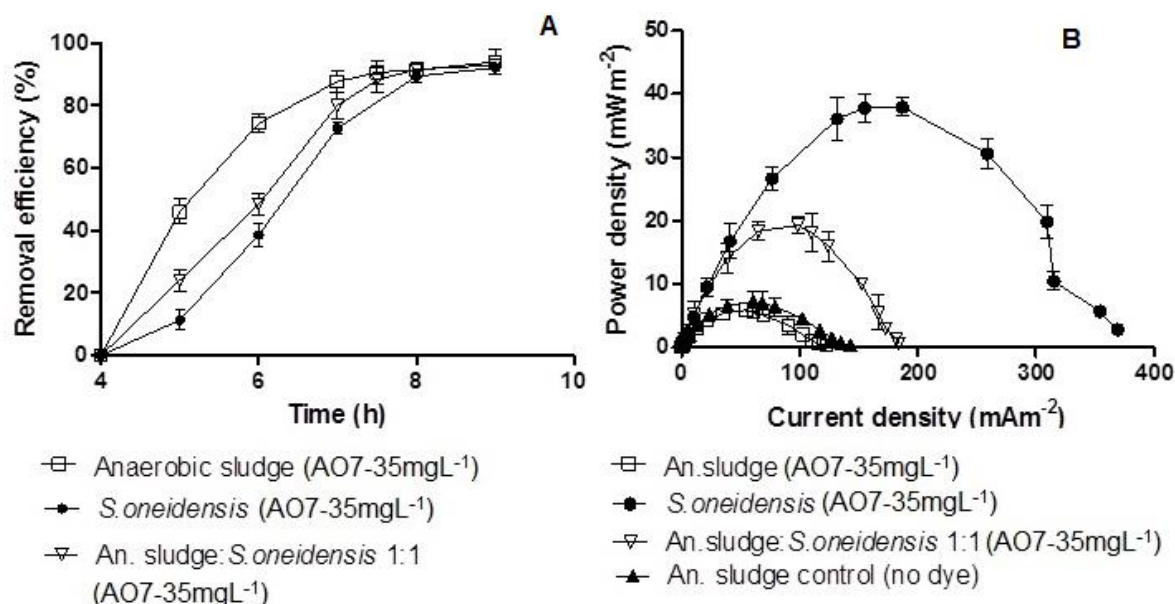


**Figure 3.3:** (A) AO7 removal using anaerobic sludge as the inoculum compared to AO7 removal using *S.oneidensis* pure culture and (B) comparison of MFC performance.

### 3.2.2. The effect of co-substrate type on decolourisation kinetics of AO7

The use of unrefined co-substrate types such as rapeseed cake, corn-steep liquor and molasses indicated high AO7 decolourisation kinetic constants (table 2). Acetate indicated the lowest decolourisation constant ( $k$ ) value. Identification of most suitable and efficient substrate types for biological wastewater treatment is of utmost importance in the view of sustainability and cost effectiveness of novel wastewater treatment processes. The high kinetic rates of AO7 decolourisation utilising unrefined co-substrate types such as rapeseed cake, corn-steep liquor

and molasses achieved in this study implies that these relatively cheap raw materials could potentially be used in novel textile wastewater treatment processes to effectively decolourise azo dyes using microbial fuel cells.

**Table 3.2:** Comparison of AO7 decolourisation kinetic constants ( $k$ ) and maximum power densities ( $P_{\max}$ ) with different co-substrate types

Co-substrate	AO7 at 35mgL <sup>-1</sup>		AO7 at 195mgL <sup>-1</sup>	
	$K$ (h <sup>-1</sup> )	$P_{\max}$ (mWm <sup>-2</sup> )	$K$ (h <sup>-1</sup> )	$P_{\max}$ (mWm <sup>-2</sup> )
<b>Rapeseed cake</b>	0.82 ± 0.02	33.4 ± 2.76	0.3 ± 0.013	15.22 ± 2.89
<b>Corn-steep liquor</b>	0.86 ± 0.014	39.2 ± 1.39	0.32 ± 0.012	19.28 ± 3.41
<b>Molasses</b>	0.69 ± 0.017	26.4 ± 3.16	0.29 ± 0.009	14.0 ± 2.2
<b>Acetate</b>	0.37 ± 0.011	29.4 ± 2.29	0.06 ± 0.003	17.29 ± 1.27

Values are means of duplicate experiments ± SD

### 3.2.3. The effect of pH on AO-7 co-metabolic degradation in MFC anodes by *S.oneidensis*

The best decolourisation performance was observed when the anolyte medium pH was close to the neutral pH value. At pH-7, over 90% AO-7 decolourisation was achieved within four hours whereas at low pH (pH-4) and high pH (pH-9), time to reach 90% AO-7 decolourisation increased substantially to 56 hours and 29 hours respectively (Figure 3.4).

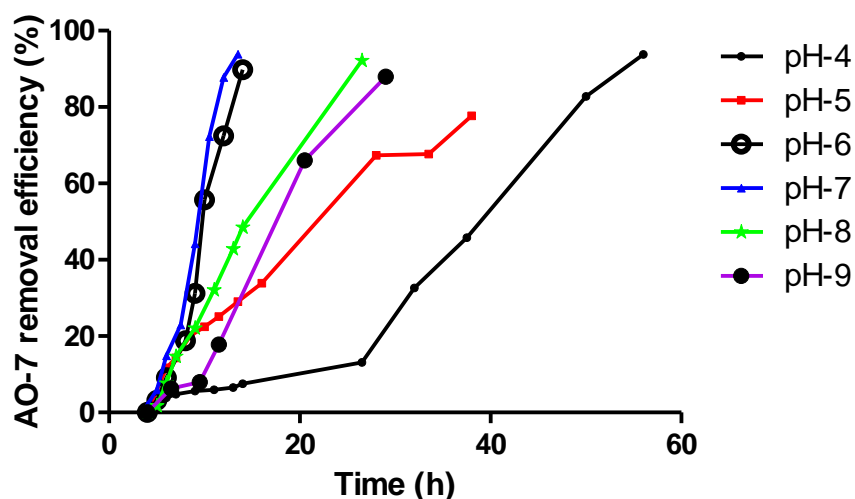


**Figure 3.4:** The effect of pH on AO-7 co-metabolic decolourisation by *S.oneidensis* in MFC anodes

This suggests that *S.oneidensis* is not capable of tolerating extreme high or extreme low pH values and its metabolic activity is severely restrained at these extremities. The hindrance of microbial metabolic action in turn severely affects the electron transfer into the azo moiety of AO-7 and its reductive decolourisation.

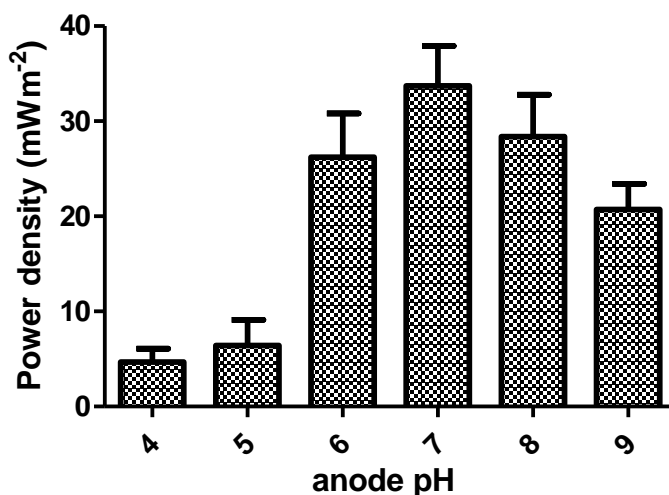


**Figure 3.5:** The effect of pH variation on MFC power output during AO-7 decolourisation by *S.oneidensis*.

The variations of pH away from neutral value induced serious adverse effects on MFC power output. As depicted on Figure 3.5, when pH shifts away from the neutral value towards the acidic end (pH 4) and alkaline end (pH 9) both exert a negative effect on MFC power densities. This suggests that adverse conditions such as high or low pH values greatly hinder the external electron transfer activity of *S.oneidensis*. This could be partly due to the reduced bacterial metabolic action of bacteria when encountered with adverse conditions such as extreme pH.

### **3.2.4. Decolourisation metabolites of AO7 and COD removal during MFC operation**

Aminobenzene products of AO7 reductive decolourisation - sulfanilic acid and 1-amino-2-naphthol - were detected upon analysis of the decolourised liquid using HPLC (Retention times 1.6 min and 4.3 min respectively) (Figure 3.6). The presence of the two compounds after full decolourisation of the anolyte (after ~ 30 hours) and after 48 hours, suggests that these degradation products are recalcitrant under the test conditions.

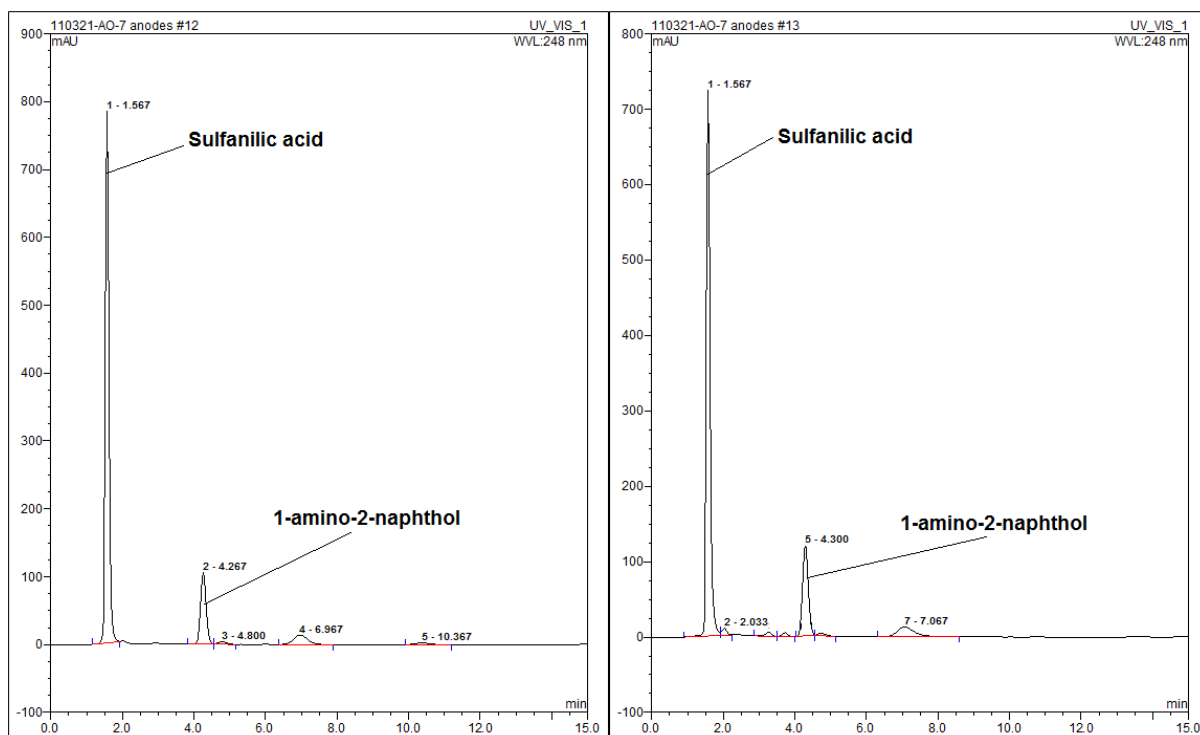


**Figure 3.6:** HPLC profile of fully decolourised effluents from MFC anodes (A) at 30 hours and (B) at 48 hours indicate the presence of Sulfanilic acid ( $R_t = 1.57$  min) and 1-amino-2-naphthol ( $R_t = 4.3$  min). The two decolourisation metabolites are persistent under test conditions (initial AO7 concentration before decolourisation –  $195 \text{ mgL}^{-1}$ ).

*Shewanella* species producing flavonoid compounds that are capable of enhancing extracellular electron transfer is reported in earlier studies (von Canstein et al, 2008). Therefore, a possible mechanism for the observed rapid biotransformation of AO7 into aminobenzenes would be the shuttling of electrons produced by microbial substrate oxidation into the azo moiety via microbial extracellular redox mediators such as flavin compounds.

The COD removal after 48 hours of MFC operation at the initial AO7 concentration of  $350 \text{ mgL}^{-1}$  was  $73.7 \pm 1.5\%$  compared to  $93.5 \pm 0.9\%$  COD removal in the control MFC, where no dye was added (Figure 3.7). The theoretical oxygen demand (ThOD) of AO7 (calculated using stoichiometric oxygen equivalent required for complete oxidation) at a concentration of  $1 \text{ mM}$  ( $350 \text{ mgL}^{-1}$ ) is  $672 \text{ mgL}^{-1}$ . The

remaining COD value of the fully decolourised AO7 solution (at 350 mgL<sup>-1</sup> initial dye concentration) after 48 hours was greater than the ThOD (table 3.3).

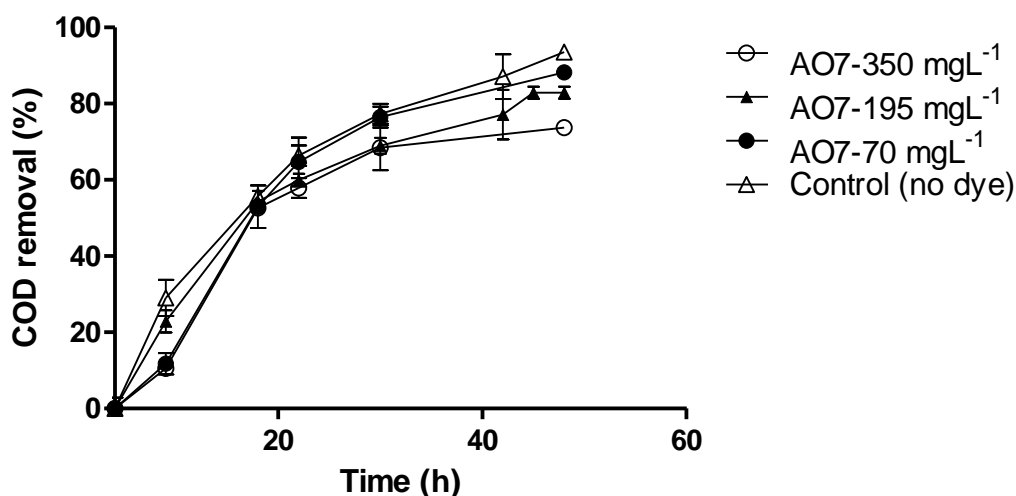


**Figure 3.7:** COD removal during MFC operation within a 48 hour period

Hence, the results indicate that the COD removal is primarily associated with the microbial oxidation of the primary carbon source (i.e. Pyruvate) rather than the utilisation of the dye pollutant as a carbon and energy source. This further indicates that the decolourisation metabolites of AO7 are persistent and do not easily catabolise under tested conditions.

**Table 3.3:** Comparison of initial and final (after 48 hour MFC operation) COD values at various initial AO7 concentrations

Initial AO7				
concentration	Control (no dye)	Test (70 mgL <sup>-1</sup> )	Test (195 mgL <sup>-1</sup> )	Test (350 mgL <sup>-1</sup> )
Initial COD (mgL <sup>-1</sup> )	2583 ± 23.7	2833.3 ± 61*	2916.6 ± 42.4**	3166.6 ± 47.7**
COD at 48 hours (mgL <sup>-1</sup> )	166.6 ± 2.57	332.3 ± 3.5*	501.7 ± 8**	833.3 ± 13.3**

The COD values are means of duplicate experiments  $\pm$  SD. Means are significantly different from control values at  $P < 0.05^*$ ,  $P < 0.01^{**}$  analysed by one way ANOVA in conjunction with Tukey post-test.

### **3.2.6. Assessment of mutagenic potential of the AO7 decolourisation metabolites using the Ames test.**

It was previously shown that many aminobenzenes resulting from azo dye reductive degradation harbour a significant mutagenic and carcinogenic potential (Chequer et al, 2011 and Ferraz et al, 2011). However, the toxicity and mutagenicity profiles of reductively decolourised AO7 solutions has not been widely characterised in earlier studies that reported the phenomenon of anaerobic decolourisation of AO7. Therefore, a more complete understanding of the mutagenicity of AO7 reductive biotransformation products is required. Furthermore, benzidine and 1-phenylazo-2-hydroxynaphthalene based azo dyes have been banned from commercial use in the European Union due to their high mutagenic potential (Mansour et al, 2009 and Pandey et al, 2007). They are mainly associated with hepatic and bladder cancers as shown in toxicology studies involving rodents (Pandey et al, 2007). Toxicological and mutagenic potential data obtained from animal models such as rodents can be extrapolated to humans (Stiborova et al, 2002). In this study, Ames mutagenicity testing was carried out using *S.typhimurium* histidine auxotrophs TA1535 and TA1538 on the influent feed solution containing unreduced AO-7 (at  $350 \text{ mgL}^{-1}$ ) and reductively decolourised AO-7 solutions that contained initial AO-7 concentrations ranging from  $35 \text{ mgL}^{-1}$  to  $350 \text{ mgL}^{-1}$ .



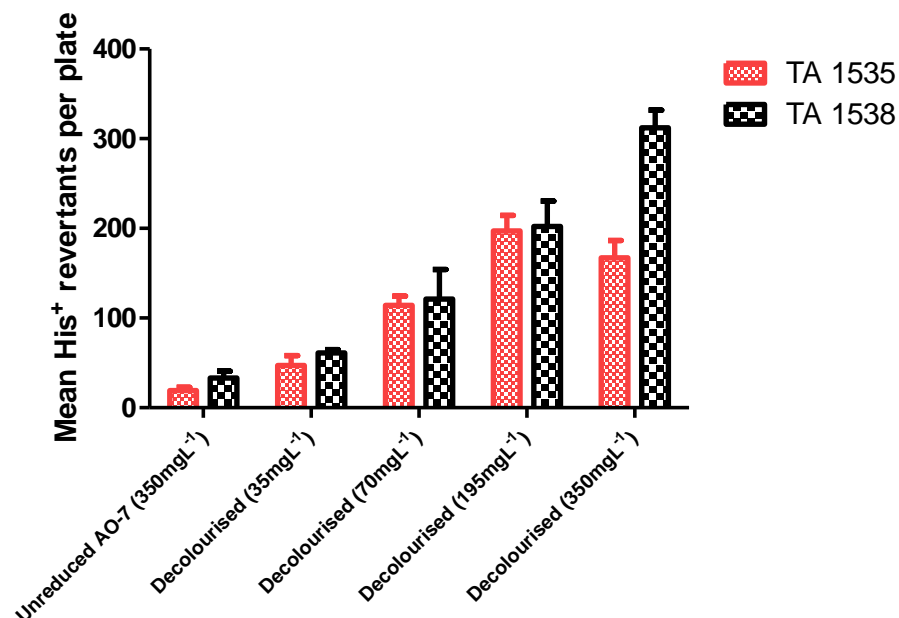


**Figure 3.8:** Mean His<sup>+</sup> revertant colonies of *S.typhimurium* TA1535 and TA1538 for unreduced AO-7 (at 350 mgL<sup>-1</sup>) and decolourised AO-7 at various initial AO-7 concentrations ranging from 35 mgL<sup>-1</sup> to 350 mgL<sup>-1</sup> during Ames mutagenicity test

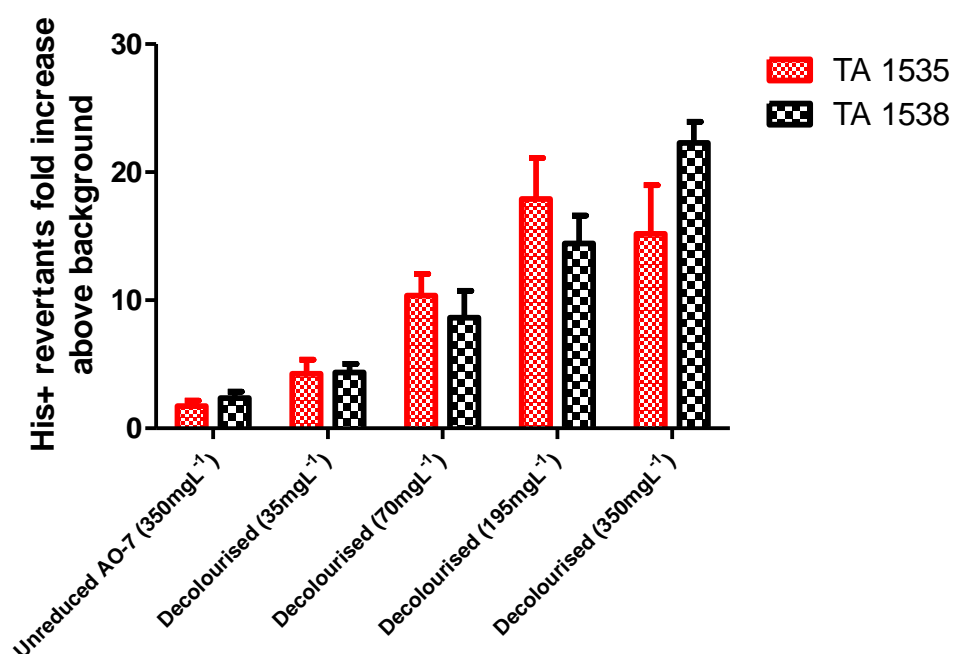


**Figure 3.9:** *S.typhimurium* TA1535 and TA1538 His<sup>+</sup> revertants fold increase above background (control) plate during Ames mutagenicity test of unreduced AO-7 (at 350 mgL<sup>-1</sup>) and decolourised AO-7 (initial AO-7 concentrations before decolourisation ranged from 35 mgL<sup>-1</sup> – 350 mgL<sup>-1</sup>)

The results of this study suggest that both *S.typhimurium* histidine auxotroph strains (TA1535 and TA1538) undergo reversion where both strains acquire the

capability to grow on Histidine deficient minimal growth medium when they are exposed to AO-7 decolourisation metabolites. The appearance His<sup>+</sup> revertants for both *S.typhimurium* strains indicated a concentration dependant effect where the lowest number of His<sup>+</sup> revertants was observed at the lowest AO-7 degradation metabolite concentration (35 mgL<sup>-1</sup>) and the highest number of His<sup>+</sup> revertants observed at the highest AO-7 degradation metabolite concentration (Figure 3.8). Unreduced AO-7 (at 350 mgL<sup>-1</sup>) indicated His<sup>+</sup> revertant fold increases of 1.72 and 2.35 respectively for the two strains TA1535 and TA1538 above the background plate. At 35 mgL<sup>-1</sup>, His<sup>+</sup> revertants fold increases above the background plate for TA1535 and TA1538 respectively were 4.27 and 4.35 fold. However, at high AO-7 concentrations (350 mgL<sup>-1</sup> – decolourised), the His<sup>+</sup> reversion rate fold increases stood significantly higher ( $p < 0.05$ , t-test) at 15.18 and 22.28 respectively for TA1535 and TA1538 compared to background (control) revertant plates (Figure 3.9).

The two Histidine auxotrophs tested in this study *S.typhimurium* TA1535 and TA1538 carry a base-pair mutation (point mutation) (*hisG46*) and a frame-shift mutation (*hisD3052*) respectively in their Histidine synthesis genes and therefore, are unable to grow on Histidine deficient growth media. The high reversion rates observed for both *S.typhimurium* Histidine auxotroph strains at high AO-7 decolourisation metabolite concentrations suggests that reductive degradation metabolites of AO-7 are capable of inducing both point mutations and frame-shift mutations in *S.typhimurium*. The mutagenic and carcinogenic potentials of these azo dye derivatives have been attributed to their planer aromatic structures, where they can intercalate between DNA double helixes with relative ease. Furthermore, it is generally accepted that non-polar and planer aromatic structures are more potent mutagens compared to aromatics substituted with polar and charged

substituent groups (Gottlieb et al, 2003). Sulfanilic acid (4-aminobenzenesulfonic acid) is one of the reductive degradation products of AO-7 and it is a highly charged aminobenzene due to the presence of the sulfonic acid group. Therefore, it can be expected in the case of AO-7 that high mutagenic potential of AO-7 reductive degradation metabolites detected by Ames test in this study, is mostly due to the relatively non polar naphthalene derivative 1-amino-2-naphthol.

### **3.2.7. Assessment of electrochemical parameters during AO7 decolourisation**

Electrochemical monitoring of the MFCs during AO7 decolourisation indicated a statistically significant ( $P < 0.05$ ) decline of power densities obtained from the system with increasing AO7 concentrations. The maximum power density reduced from  $37 \text{ mWm}^{-2}$  to  $19.3 \text{ mWm}^{-2}$  when the dye concentration was increased from  $70 \text{ mgL}^{-1}$  to  $350 \text{ mgL}^{-1}$  (Figure 3.10B). However, the presence of AO7 in the anode compartment up to a concentration of  $70 \text{ mgL}^{-1}$  had no apparent effect on MFC electrochemical performance compared to the control MFC with no AO7. This suggests that the anodic microbial population may tolerate low to moderate AO7 pollutant concentrations without any detrimental effect on the electrochemical performance (Figures 3.10A and 3.10B). The notable reduction of power densities at high dye concentrations indicate that a significant portion of the electrons released during microbial substrate oxidation is diverted to reducing the azo chromophore into aminobenzenes.

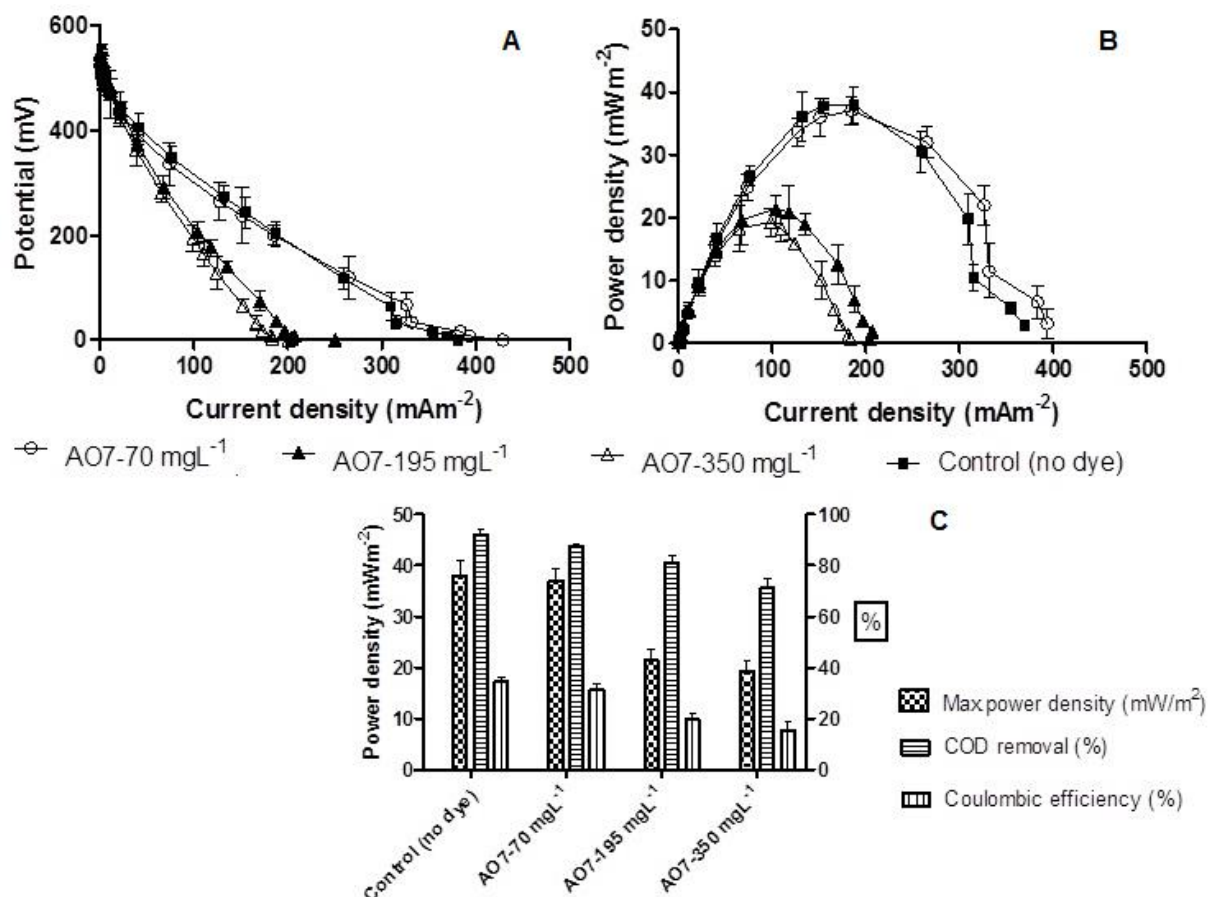


**Figure 3.10:** (A) polarisation curves and (B) Power density-current density plots during AO7 decolourisation (using pyruvate as the co-substrate) containing initial AO7 concentrations of 70 mgL<sup>-1</sup>, 195 mgL<sup>-1</sup> and 350 mgL<sup>-1</sup> (C) Comparison of maximum power densities, Coulombic efficiencies and percentage COD removal at different initial AO7 concentrations. Bars with asterisks indicate that they were significantly different (one way ANOVA,  $P < 0.05$  with Tukey post-test).

The presence of alternative electron acceptors in abundance (in this case AO7) for the anode bacterial population may greatly diminish the Coulombic efficiency. The statistically significant ( $P < 0.05$ ) reduction of Coulombic efficiency by almost half when the AO7 concentration was increased from 70 mgL<sup>-1</sup> to 350 mgL<sup>-1</sup> (Figure 3.10C) suggests that the observed drop in electrochemical performance may be caused by the competition for electrons by the dye pollutant. Another contributory factor for this effect could be the accumulation of toxic decolourisation metabolites of AO7.

Li et al, 2010 demonstrated the possibility of employing an MFC system utilising an aerobic bio-cathode to achieve more complete mineralisation of the model azo dye Congo Red operating in an anaerobic aerobic mode sequential manner. A two-step approach utilising aerobic biotreatment, oxidative enzymatic treatment such as laccase (Teerapatsakul et al, 2008) or photo-catalysed Fenton reactions (Aleboyeh et al, 2005 and Chacon et al, 2006) as a second treatment stage could hold promise in developing an industrially applicable system for treating azo dye polluted industrial effluents.

### **3.3. Concluding remarks**

This study demonstrated the possibility of utilising the electrochemically active bacterium *S. oneidensis* (strain 14063) to achieve enhanced kinetic rates of AO7 decolourisation and concomitant production of electrical energy using an MFC system. This work further demonstrates that unrefined, cheaper co-substrate types such as rapeseed cake, corn-steep liquor and molasses can be successfully utilised to achieve high decolourisation kinetics of azo dyes in MFCs. Therefore, the enhanced decolourisation kinetic rates achieved in this study utilising unrefined co-substrate types implies that MFCs could potentially be employed as the initial step of a two stage anaerobic/aerobic biological treatment process for treating azo dye contaminated industrial effluents.

# **Chapter 4 - Co-metabolic decolourisation of azo dye mixtures by dye-acclimated mixed microbial populations in MFCs**

## Summary

This study was focused on assessing the suitability of bio-electrochemical systems using azo dye adapted mixed cultures for decolourising complex azo dye mixtures at industrially relevant conditions. Of particular interest were the influence of operating conditions such as temperature and salinity and the bacterial community composition of the azo dye degrading adapted mixed culture.

In this study, azo dye adapted mixed microbial consortium was used to effectively remove colour from azo dye mixtures and to simultaneously generate bio-electricity using microbial fuel cells (MFCs). Operating temperature (20°C-50°C) and salinity (0.5% w/v - 2.5% w/v) were varied during experiments. Reactor operation at 50°C improved dye decolourisation and COD removal kinetic constants by approximately two fold compared to the kinetic constants at 30°C. Decolourisation and COD removal kinetic constants remained high (0.28 h<sup>-1</sup> and 0.064 h<sup>-1</sup> respectively) at moderate salinity (1% w/v) but deteriorated approximately four fold when the salinity was raised to 2.5% (w/v). Molecular phylogenetic analysis of microbial cultures used in the study indicated that both un-acclimated and dye acclimated cultures from MFCs were predominantly comprised of Firmicutes bacteria. This study demonstrates the possibility of using adapted microbial consortia in MFCs for achieving efficient bio-decolourisation of complex azo dye mixtures and concomitant bio-electricity generation under industrially relevant conditions.

The experimental outcomes of the work described in this chapter were published in, Fernando, E., Keshavarz, T., Kyazze, G., 2013. Simultaneous co-metabolic decolourisation of azo dye mixtures and bio-electricity generation under thermophilic (50°C) and saline conditions by an adapted anaerobic mixed culture in microbial fuel cells. *Bioresource Technology* 127, 1-8.

## **4.2. Results and Discussion**

### **4.2.1. Decolourisation of azo dye mixtures during fed-batch MFC operation**

The decolourisation of the feed solution containing the azo dye mixture was confirmed by visual observation and spectrophotometric scans, suggesting a rapid removal of azo chromophores of the dye mixture during MFC operation (Figure 4.1). The persistent high peak intensities near the UV region (220-300 nm) of the spectra scans of samples taken at 6, 20 and 36 hours can be attributed to the formation of colourless amines during azo dye decolourisation. Under anoxic condition, azo dyes are known to undergo reductive decolourisation into their respective aminobenzines by membrane bound non-specific reductase enzymes. In view of anionic nature and large molecular size of many azo dyes, it can be expected that they are incapable of crossing largely non-polar biological membranes into cellular interior. Hence, the rapid decolourisation of azo dye mixtures observed in this study can be attributed to extra-cellular co-metabolic reductive decolourisation by the anodic microbial community. However, it was difficult to identify the exact nature of the decolourisation metabolites in this study due to the complex nature of the dye mixture and the complex carbon source used (molasses).



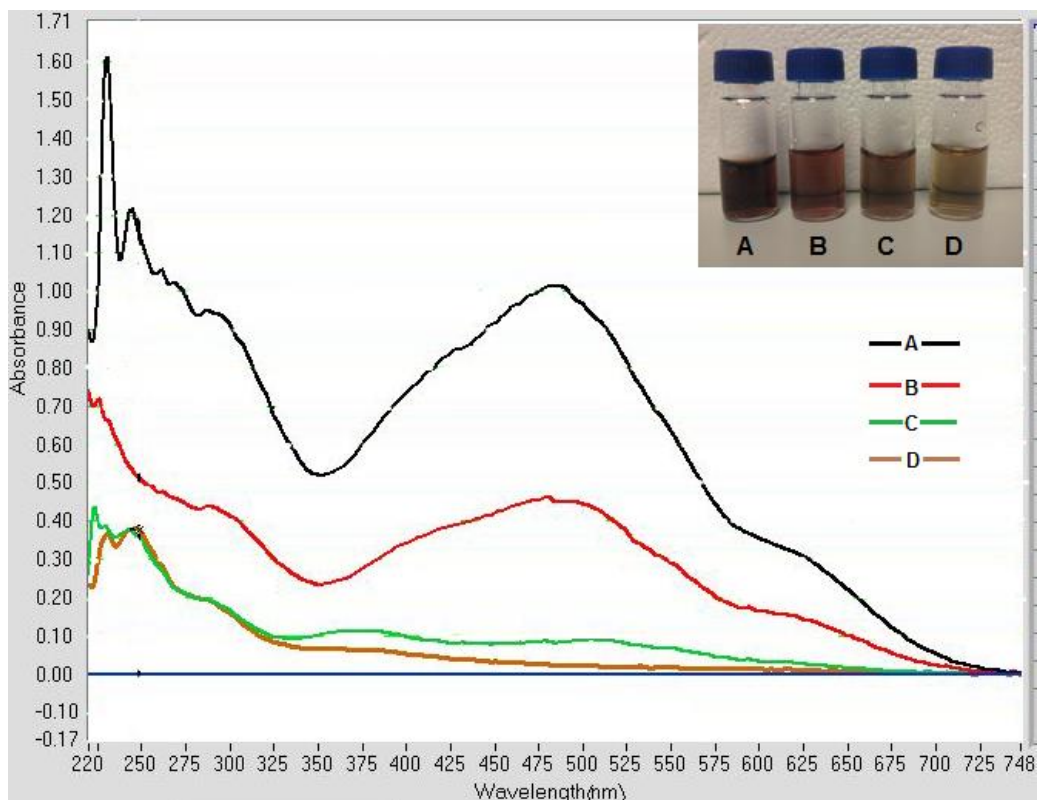


**Figure 4.1:** Absorption spectra of the feed solution (0 hours – spectrum-A) and samples taken at 6, 20 and 36 hours (spectra B, C and D) respectively indicate the decrease in peak intensity at the visible region of the spectrum over-time; indicating the decolourisation of the azo dye mixture. Inset: (A) fed-batch feed solution, (B), (C) and (D) are samples taken after 6, 20 and 36 hours of MFC operation respectively (temperature- 30°C, Experiment-1).

#### 4.2.2. Decolourisation and COD removal performance during MFC fed-batch operation

Decolourisation of the azo dye mixture and COD reduction in the influent feed solution reached over 90% in all of the cycles (Figure 4.2). This suggests that efficient and repeatable colour removal from azo dye mixtures is possible when adapted anaerobic microbial consortia are employed in fed-batch operation. When the colour removal by adsorption processes was assessed, the decolourisation was found to be as low as  $1.6\% \pm 0.21\%$  ( $n=3$ ) (appendix 2). Therefore, the contribution from adsorption to colour removal in this study was considered to be small. In the work presented in the previous chapter, it was demonstrated that

better decolourisation kinetics compared to other anaerobic systems (eg. UASB reactors) could be achieved for the model azo dye Acid Orange-7 (AO-7) in the electrochemically active environment of MFCs. This was attributed to the more effective transfer of reducing equivalents to the azo moiety in an electrochemically active environment of a MFC, eventually leading to rapid reductive decolourisation of the model azo dye. Sanroman et al, 2004 reported the possibility of electrochemical decolourisation of textile azo dye mixtures up-to 2-3 dyes. However, biological decolourisation of azo dye mixtures is rarely reported in literature. Previously, Nigam et al, 1996 demonstrated that enrichment anaerobic mixed cultures were capable of decolourising azo dye mixtures containing up-to nine structurally different dyes. In the view of large structural diversity and wide range of molecular weights of azo dyes, it can be expected that their decolourisation may benefit from the use of adapted anaerobic microbial consortia rather than the use of pure cultures.

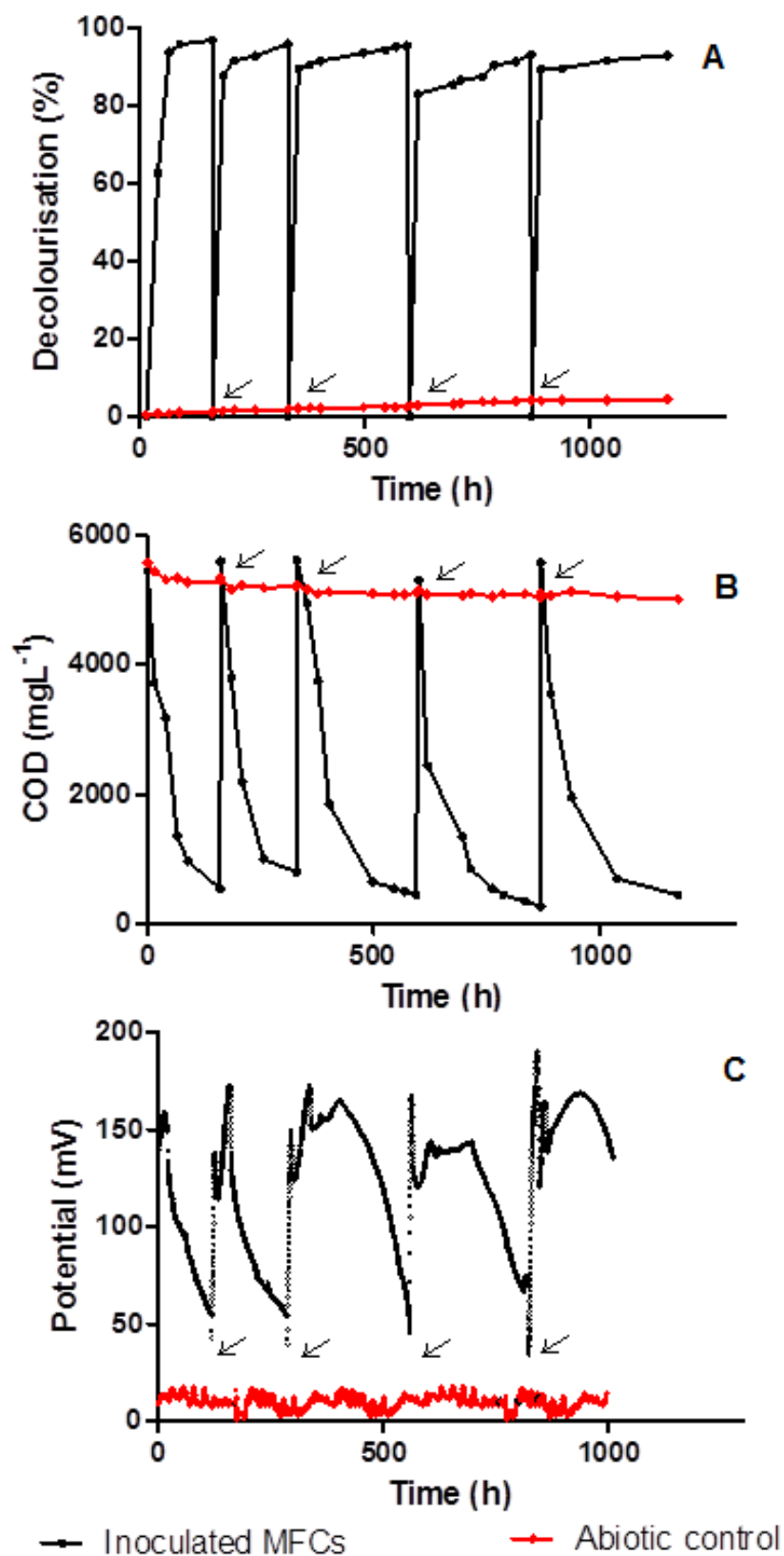


**Figure 4.2** (A): Decolourisation of azo dye mixtures (B) COD reduction of the feed solution and (C) MFC voltage generation during fed-batch operation (arrows indicate the fresh medium feeding and start of new fed-batch cycles- Experiment-1; temperature- 30°C).

Harazono and Nakamura, 2005 demonstrated that azo dye mixtures comprising of three component dyes can be decolourised using purified fungal manganese peroxidase (MnP) and in liquid fermentations of basidiomycete fungus *Phanerochaete sordida*. The decolourisation of azo dye mixtures observed in the aforementioned study was attributed to the MnP activity of the culture. Similarly, in a study by Selvam et al, 2003, dye industry effluents containing azo dye mixtures were decolourised by white rot fungus *Thielephora* sp. In this case, decolourisation was attributed to the fungal extracellular production of lignin peroxidase (LiP), laccase and MnP. Although white rot fungi are shown to non-specifically degrade a wide variety of poly aromatic compounds including azo dyes, the lignolytic oxidative enzyme production in liquid fermentations is known to be inconsistent (Robinson et al, 2001). This could be mainly due to the unfamiliar environment of liquid fermentations for wood degrading fungi as opposed to solid-state fermentations (SSF) where their natural environment is more closely simulated. Therefore, the use of adapted bacterial cultures rather than fungal cultures for rapid colour removal in colour industry effluent would be advantageous in operational standpoint.

The results of this study indicates that it is possible to achieve over 90% colour and COD removal in azo dye mixtures in a repeatable manner during fed-batch MFC operation (Figures 4.2A and 4.2B). This highlights the potential advantages of using an adapted mixed microbial consortium for azo dye removal. The use of the electrochemically active environment of MFCs could confer additional benefits such as enhancing azo dye removal kinetics and concomitant bio-electricity production (Figure 4.2C).

### **4.2.3. Decolourisation and bio-electrochemical system performances under thermophilic and saline conditions**

#### **4.2.3.1. The effect of operating temperature (Experiment-2)**

The kinetic constants for colour and COD removal indicated approximately a 6.5 fold and 3.5 fold enhancements respectively when the operating temperature was raised from 20°C to 50°C (Table 4.1). This suggests that the adapted microbial consortium prefers thermophilic operation for dye decolourisation and COD reduction over mesophilic operation. The composition of the adapted microbial consortium determined by 16s rDNA analysis suggests that bacteria belonging to genera *Clostridium* and *Eubacterium* are predominant (Table 4.3). Many bacteria belonging to aforementioned genera are known to produce thermostable enzymes (Gomes and Steiner, 1998) and known to function under thermophilic conditions (Lo et al, 2011). The effect of operating temperature was also reflected in the electrochemical performance of the MFC system where, peak power density obtainable from the system increased approximately two-fold from  $13.22 \pm 2.42 \text{ mWm}^{-2}$  to  $25.6 \pm 2.77 \text{ mWm}^{-2}$  when the operating conditions were changed from sub-mesophilic (20°C) to thermophilic (50°C) (Table 4.1).

**Table 4.1:** The effect of operating temperature on colour removal, COD removal and electrochemical performance (peak power densities obtainable from the MFC system). Values are means of duplicate experiments  $\pm$  SD (Experiment-2) (ND – no detectable change)

Operating temperature ( $^{\circ}\text{C}$ )	K-decolourisation ( $\text{h}^{-1}$ )	K-COD removal ( $\text{h}^{-1}$ )	Peak power density ( $\text{mWm}^{-2}$ )
20	$0.0412 \pm 0.001$	$0.0114 \pm 0.004$	$13.22 \pm 2.42$
30	$0.132 \pm 0.021$	$0.0236 \pm 0.007$	$16.18 \pm 3.12$
40	$0.22 \pm 0.016$	$0.036 \pm 0.011$	$19.67 \pm 3.44$
50	$0.27 \pm 0.029$	$0.04 \pm 0.009$	$25.6 \pm 2.77$
Abiotic control	ND	ND	$0.21 \pm 0.1$

#### 4.2.3.2. The effect of salinity (Experiment-3)

The common auxiliary salts present in textile wet processing processes were added in this study by addition of varying (w/v %) amounts of NaCl and  $\text{Na}_2\text{SO}_4 \cdot 10\text{H}_2\text{O}$  (Glauber's salt) in a ratio of 1.1.

**Table 4.2:** The effect of salinity on colour removal, COD removal and electrochemical performance of the MFC system (temperature -  $30^{\circ}\text{C}$ ). Values are means of duplicate experiments  $\pm$  SD (Experiment-3) (ND – no detectable change).

Salt content (w/v %)	K-decolourisation ( $\text{h}^{-1}$ )	K-COD removal ( $\text{h}^{-1}$ )	Peak power density ( $\text{mWm}^{-2}$ )
0	$0.1831 \pm 0.024$	$0.0466 \pm 0.006$	$14.568 \pm 1.21$
1	$0.28 \pm 0.043$	$0.0644 \pm 0.01$	$22.27 \pm 4.77$
2.0	$0.0975 \pm 0.007$	$0.0301 \pm 0.009$	$27.65 \pm 2.11$
2.5	$0.064 \pm 0.009$	$0.0197 \pm 0.003$	$13.58 \pm 2.9$
Abiotic control	ND	ND	$0.16 \pm 0.15$

The results indicated that reasonable decolourisation and COD removal kinetic rates can be maintained up-to a solution salt content of 2% (w/v). This performance deteriorated about 4.4 fold and 3.3 fold respectively in terms of colour and COD removal when the solution salt content was raised from 1% (w/v) to 2.5% (w/v). The high power densities of the MFC system observed at high salt content (1% - 2% w/v) could be due to the better electrochemical performance of electrochemically active bacteria at high ionic strength. Similar to these findings, Liu et al, 2005 reported that high power densities yielded in single chamber MFCs inoculated with anaerobic mixed cultures at high (salt content- 0.6% - 2.3% w/v) ionic strengths. However, the salt content appears to indicate an inhibitory effect on power output of the MFC system at 2.5% (w/v), suggesting that it may be out of the tolerable range (Table 4.2). Colour industry wastewater often contains mixtures of azo dyes with a vast chemical structural diversity. Moreover, during textile wet processing, large amounts of sodium sulphate decahydrate (Glauber's salt) and sodium chloride are added to improve the migration and fixation of dye molecules into the textile substrate. The temperature during textile wet processing is maintained at around 90°C and the effluent is often hot when discharged (Schlaeppli, 1998). A previous study aimed at characterising textile effluent generated from textile wet processing plants in south-east Asia reported salinities between 1% (w/v) – 3.3% (w/v) (Roy et al, 2010). Therefore, the findings of this study indicating the potential industrial applicability of such systems employing robust, azo dye adapted mixed microbial consortia are promising.

### 4.2.3. Bacterial 16s rDNA community analysis of the original anaerobic digested sludge and azo dye/MFC adapted dye degrading culture

Comparison of DGGE fingerprints of the original anaerobic digested sludge and azo dye/MFC adapted microbial cultures indicate different banding patterns; suggesting that a different microbial community becomes selected under the conditions used in this study (Figure 4.3).

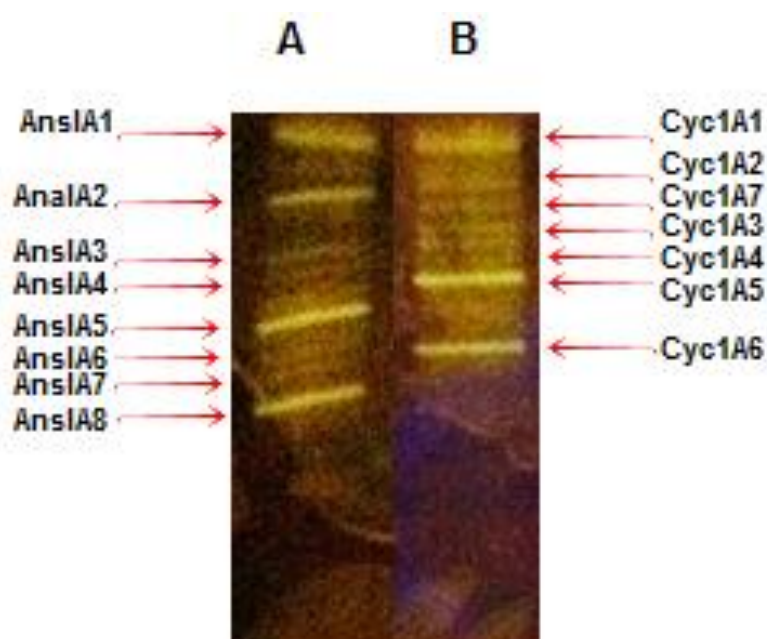


**Figure 4.3:** 16s rDNA PCR-DGGE profiles of (A) original un-acclimated anaerobic digested sludge (B) azo dye/MFC acclimated microbial culture after approximately 50 days of fed-batch operation (temperature-30°C).

Phylogenetic analysis of 16s rDNA sequences obtained from the original anaerobic culture revealed that majority (87%) comprised of bacterial species belonged to genera *Clostridium* and *Eubacterium* (Figure 4.4A). Phylogenetic affiliations of the identified bacterial species are shown in table 4.3. Many substrate types suitable for fermentative hydrogenic and methanogenic growth are



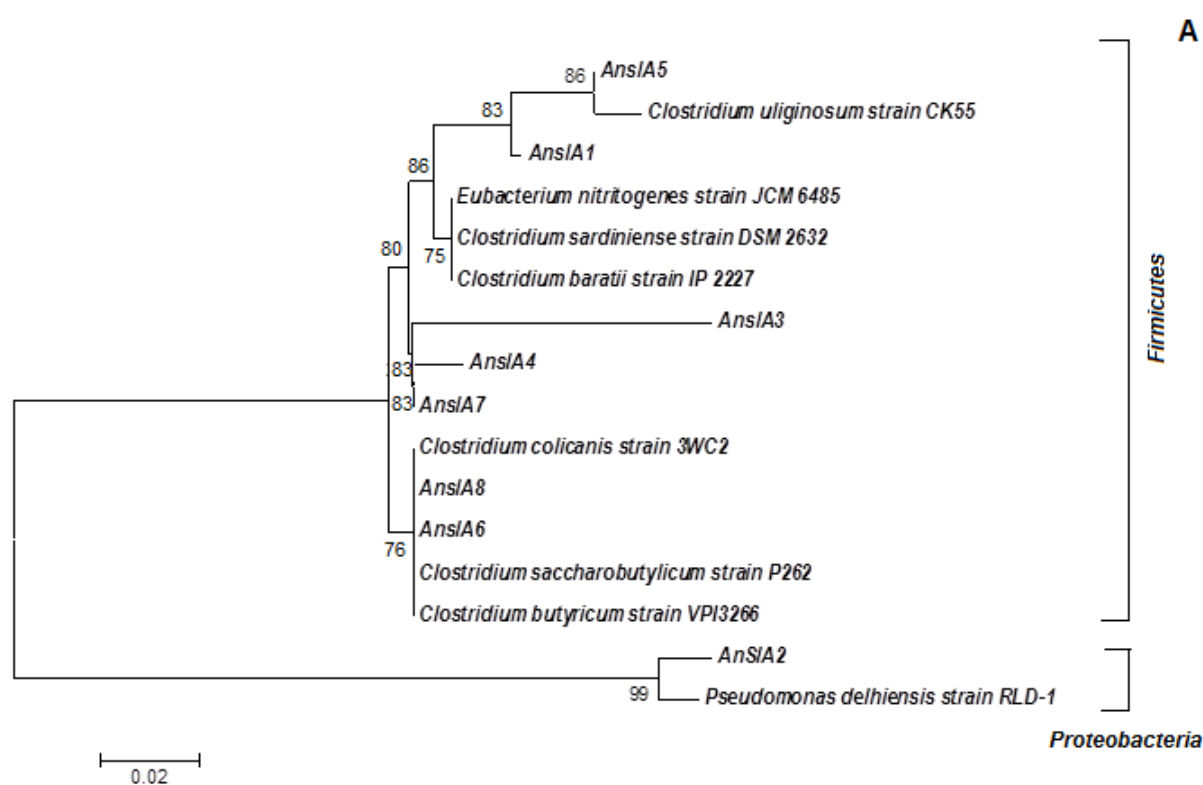
encountered in anaerobic wastewater treatment plants (Venkata Mohan, 2009). Therefore, a high proportion of such Firmicutes can be expected in anaerobically digested sludge.

Clear differences in phylogenetic relationships can be observed between the original anaerobic microbial community and the dye/MFC adapted microbial consortium capable of bio-decolourisation of azo dye mixtures. More Gram negatives belonging to phyla Bacteroidetes and Proteobacteria were selected under these conditions (43%) (Figure 4.4B). This may be attributed to the electrochemically active environment provided to the microbial community in the form of a microbial fuel cell. In earlier studies, Gram negative organisms such as *Pseudomonas* sp. and *Flavobacterium* sp. are reported to be responsible for extracellular electron transfer (EET) in MFCs (Rabaey and Verstraete, 2005 and Nien et al, 2011). Some *Flavobacterium* sp. are also known to be moderately halotolerant (Saha et al, 2006 and Yoshie et al, 2006).

**Table 4.3:** Phylogenetic affiliations of PCR-DGGE sequences of the un-adapted anaerobic culture (designated AnslA) and azo dye adapted culture (designated Cyc1A) based on the 16s rDNA sequences in the NCBI 16s rDNA sequence repository

Sample	Closest relative (% similarity)	GenBank accession number	Phylogenetic affiliation
<b>AnslA1</b>	<i>Clostridium saccharobutylicum</i> strain P262 (98)	<a href="#">NR_036951.1</a>	Firmicutes
<b>AnslA2</b>	<i>Pseudomonas delhiensis</i> strain RLD-1 (96)	<a href="#">NR_043731.1</a>	Proteobacteria
<b>AnslA3</b>	<i>Eubacterium nitritogenes</i> strain JCM 6485 (96)	<a href="#">NR_024684.1</a>	Firmicutes
<b>AnslA4</b>	<i>Clostridium sardiniense</i> strain DSM 2632 (100)	<a href="#">NR_041006.1</a>	Firmicutes
<b>AnslA5</b>	<i>Clostridium butyricum</i> strain VPI3266 (99)	<a href="#">NR_042144.1</a>	Firmicutes
<b>AnslA6</b>	<i>Clostridium colicanis</i> strain 3WC2 (99)	<a href="#">NR_028964.1</a>	Firmicutes
<b>AnslA7</b>	<i>Clostridium baratii</i> strain IP 2227 (97)	<a href="#">NR_029229.1</a>	Firmicutes
<b>AnslA8</b>	<i>Clostridium uliginosum</i> strain CK55 (99)	<a href="#">NR_028920.1</a>	Firmicutes
<b>Cyc1A1</b>	<i>Clostridium saccharobutylicum</i> strain P262 (100)	<a href="#">NR_036951.1</a>	Firmicutes
<b>Cyc1A2</b>	<i>Pseudomonas</i>	<a href="#">NR_028987.1</a>	Proteobacteria

	<i>trivialis</i> strain P		
	513/19 (100)		
<b>Cyc1A3</b>	<i>Flavobacterium</i>	<a href="#">NR_044208.1</a>	Bacteroidetes
	<i>lindanitolerans</i> strain		
	IP10 (94)		
<b>Cyc1A4</b>	<i>Sedimentibacter</i>	<a href="#">NR_029146.1</a>	Firmicutes
	<i>hydroxybenzoicus</i>		
	strain JW/Z-1 (96)		
<b>Cyc1A5</b>	<i>Clostridium baratii</i>	<a href="#">NR_029229.1</a>	Firmicutes
	strain IP 2227 (99)		
<b>Cyc1A6</b>	<i>Clostridium colicanis</i>	<a href="#">NR_028964.1</a>	Firmicutes
	strain 3WC2 (95)		
<b>Cyc1A7</b>	<i>Pseudomonas poae</i>	<a href="#">NR_028986.1</a>	Proteobacteria
	strain P 527/13(99)		



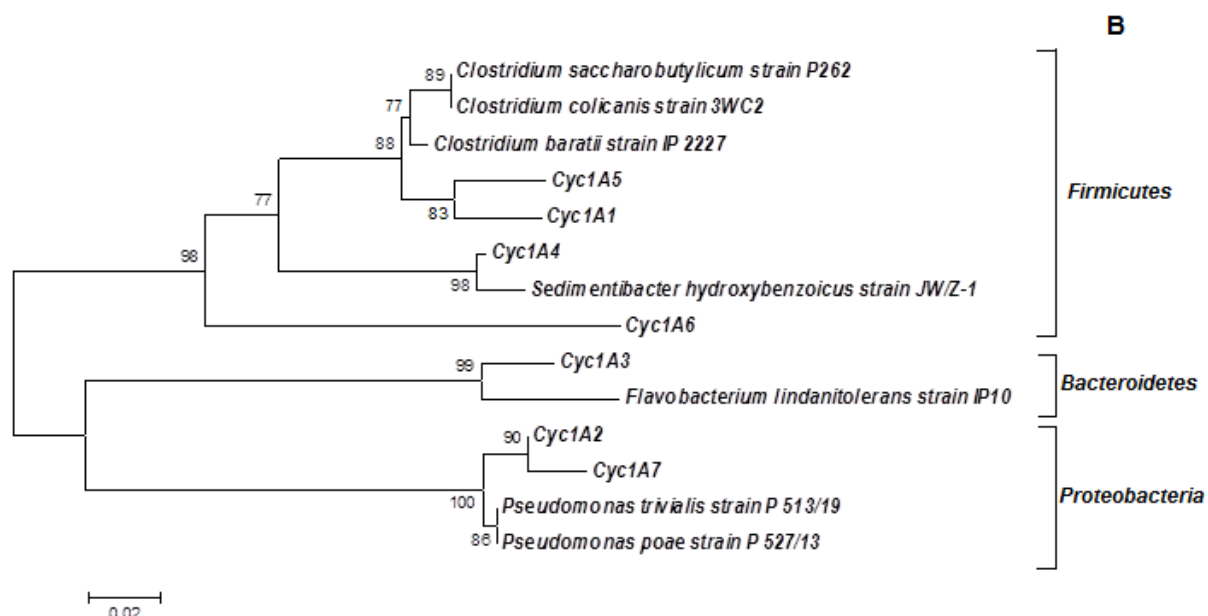


**Figure 4.4:** Phylogenetic relationships of (A) 16s rDNA sequences from the original un-adapted anaerobic digested sludge and (B) 16s rDNA sequences from azo dye/MFC adapted microbial consortium after 50 days of fed-batch operation. Numbers above or below branches indicate bootstrap values ( $\geq 75\%$ ) from 1000 replicates and scale bars indicate the number of nucleotide substitutions per site.

The high proportion of Firmicutes such as *Clostridium* sp. and *Eubacterium* sp. found both in the un-adapted original anaerobic culture and the dye/MFC adapted bacterial consortium may explain the ability of the microbial community to operate efficiently under thermophilic conditions. *Clostridium* species are well known for fermentative growth under thermophilic conditions (Lo et al, 2009 and Zverlov et al, 2010).

Previous work by Park et al, 2001 was able to isolate and characterise a *Clostridium* sp. closely related to *Clostridium butyricum* from MFCs fed with starch processing wastewater. Further characterisation of the isolate revealed that the organism was capable of fermentative growth as well as neutral red reduction and Fe (III) reduction; suggesting that organism is electrochemically active and capable of carrying out extracellular electron transfer. These findings implies that the Firmicutes that became selected during dye fed cycles within the

electrochemically active environment of MFCs in this study may also be capable of extracellular electron transfer onto the electrode as well as the azo moiety of the dye compounds, leading to their effective reductive decolourisation.

### **4.3. Concluding remarks**

The outcomes of this work implies that wastewater containing complex azo dye mixtures can be effectively decolourised under industrially relevant conditions such as high temperature and moderately saline conditions using an adapted anaerobic microbial consortium in MFCs. Efficient colour removal of the dye mix containing simulated wastewater and concomitant bio-electricity production was achieved using the unrefined co-substrate molasses as the electron donor. The molecular phylogenetic analysis conducted in this study demonstrated that bacteria belonging to phylum Firmicutes was predominant in planktonic MFC anode solutions following long-term MFC operation. This work demonstrates that MFCs could potentially be employed as an efficient system for reductive colour removal from azo dye contaminated wastewater.

# **Chapter 5 - An integrated MFC – aerobic bioreactor process for complete degradation of Acid Orange-7**

## Summary

The objective of this study was to fully biodegrade the azo dye AO-7 using an integrated MFC-aerobic system into non-toxic intermediates. Simulated wastewater containing AO-7 and the cheap, sustainable co-substrate molasses as the electron donor was continuously fed to the integrated set up of MFC-aerobic bioreactor system during experiments.

In this study, the commercially used azo dye Acid Orange-7 (AO-7) was fully degraded into less toxic intermediates using an integrated microbial fuel cell (MFC) and aerobic bioreactor system. The integrated bioreactor system was operated at ambient temperature and continuous-flow mode. AO-7 loading rate was varied during experiments from  $70 \text{ gm}^{-3}\text{day}^{-1}$  to  $210 \text{ gm}^{-3}\text{day}^{-1}$ . Colour and soluble COD removal rates reached  $> 90\%$  under all AO-7 loading rates. The MFC treatment stage prompted AO-7 to undergo reductive degradation into its constituent aminobenzenes. HPLC-MS analysis of metabolite extracts from the aerobic stage of the bioreactor system indicated further oxidative degradation of the resulting aminobenzenes into simpler compounds. Eco-toxicity testing of the effluents using bioluminescent *Vibrio fischeri* cells indicated that aerobic stage effluent indicated toxicity reductions of approximately five-fold and ten-fold respectively compared to the dye wastewater influent and MFC-stage effluent.

The experimental outcomes of the work described in this chapter were published in, Fernando, E., Keshavarz, T., Kyazze, G., 2014a. Complete degradation of the azo dye Acid Orange-7 and bioelectricity generation in an integrated microbial fuel cell, aerobic two-stage bioreactor system in continuous flow mode at ambient temperature. *Bioresource Technology* 156, 155-162.

## **5.2. Results and discussion**

### **5.2.1. AO7 degradation, colour removal and soluble COD reduction during two-stage reactor operation**

The AO-7 loading rate was incrementally varied over the course of reactor operation from  $70 \text{ gm}^{-3}\text{day}^{-1}$  to  $210 \text{ gm}^{-3}\text{day}^{-1}$ . However, the effluent AO-7 concentrations measured at both the MFC stage and the aerobic stages of the integrated bioreactor were below  $8 \text{ mgL}^{-1}$ , indicated a high (>90%) AO-7 removal efficiency throughout the reactor operation. The incremental variation of AO-7 feeding during continuous reactor operation did not adversely affect the AO-7 removal efficiency of the integrated reactor system and >90% removal efficiencies were reached even at the highest AO-7 loading rate ( $210 \text{ gm}^{-3}\text{day}^{-1}$ ). This indicates the robustness of the integrated reactor system and the ability to deal with high pollutant loading rates. The reactor system was capable of sustaining the high removal rates throughout the long-term operation (more than 150 days) without noticeable deterioration to colour removal or soluble COD removal performances. The open circuit control reactor (analogous to a conventional anaerobic process) was unable to reach the same level of AO-7 decolourisation compared to continuous MFC reactors under the same HRT at any of the three dye loading rates tested (Figure 5.1A).

The removal of AO-7 during the two-stage operation suggests that largest proportion of AO-7 was degraded during the anoxic MFC stage of the reactor operation. No noticeable AO-7 removal and hence, colour removal can be observed at the aerobic stage of the integrated reactor system. This suggests that AO-7 is only amenable to reductive biotransformation at the anoxic MFC stage but



the residual AO-7 is recalcitrant under aerated latter stage of the reactor (Figure 5.1A). These observations corroborate well with the results of numerous other studies that demonstrated the reductive colour removal of various azo dyes and the recalcitrance of the unreduced azo dyes under aerobic conditions (O'Neill et al, 2000, Rajaguru et al, 2000, Shaul, 1991).

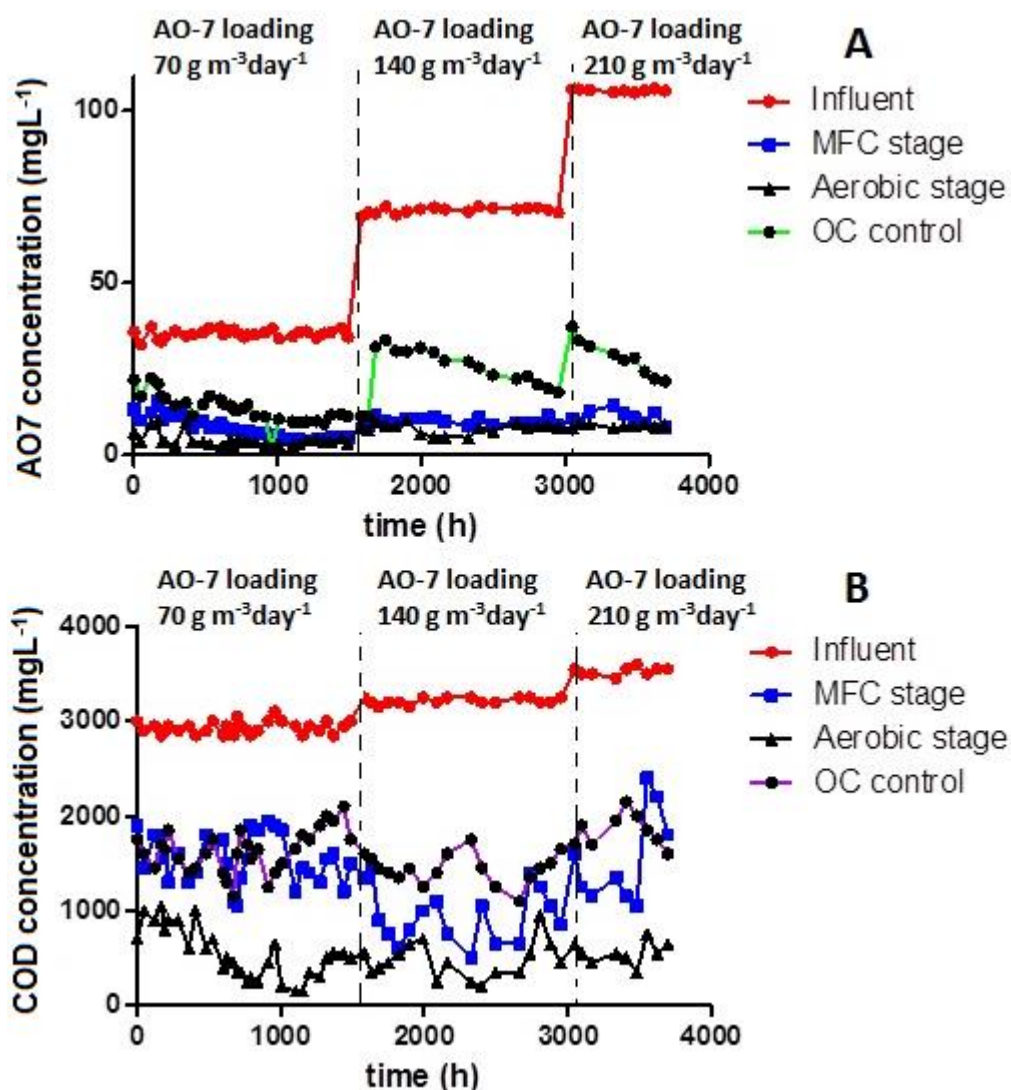


**Figure 5.1:** (A) AO-7 removal during the two stage operation at various AO-7 loading rates over a period of 150 days and (B) COD removal performance of the integrated bioreactor system at each stage

Soluble COD reduction was observed during both MFC stage and the aerobic stage. However, the COD reduction during the MFC stage was only partial. The relatively high concentrations of soluble COD at the end of the MFC stage can be

attributed to the residual co-substrate (molasses) from the MFC stage and recalcitrant aminobenzenes resulting from the biological reduction process of AO-7. The further reduction of COD during the subsequent aerobic stage of the integrated reactor suggests that a larger proportion of the molasses co-substrate and the amine biotransformation products have been consumed during the sequential MFC – aerobic treatment stages (Figure 5.1B). The total COD loading in the reactor system ranged from  $1.044 \text{ kgCODm}^{-3}\text{day}^{-1}$  (at  $70 \text{ g m}^{-3}\text{day}^{-1}$  AO-7 loading rate) to  $1.26 \text{ kgCODm}^{-3}\text{day}^{-1}$  (at  $210 \text{ gm}^{-3}\text{day}^{-1}$  AO-7 loading rate). This indicates that the integrated reactor system was capable of effectively dealing with high COD loading rates over prolonged operational periods (over 150 days) without suffering a substantial reduction in COD removal efficiency. The COD value of molasses containing blank medium without AO-7 was measured to be  $2950 \pm 60 \text{ mg CODL}^{-1}$ . Although the contribution of AO-7 to total COD concentration was relatively small (approximately 10% of total soluble COD at  $210 \text{ gm}^{-3}\text{day}^{-1}$  AO-7 loading rate), high COD removal efficiencies achieved (often above 90% removal) throughout the aerobic treatments stage suggests that refractory amines have been utilised by the bacterial mixed population for their carbon and energy needs. The integrated bioreactor system was operated at ambient temperature and temperature fluctuations had little or no apparent effect on colour removal efficiency or soluble COD reduction in the combined bioreactor stages. Particularly, during winter months where the temperature was lower, no adverse effects on aforementioned parameters could be observed.

### **5.2.2. Aminobenzene formation during the MFC stage and amine removal in the subsequent aerobic stage**

Effluent samples collected subsequent to the anoxic MFC stage indicated that both constituent aminobenzenes of AO-7 (4-aminobenzenesulfonic acid and 1-

amino-2-naphthol) were formed as a result of reductive azo bond cleavage. Increasing concentrations of both aminobenzenes were detected when the AO-7 loading rate was elevated from  $70 \text{ g m}^{-3} \text{ day}^{-1}$  to  $210 \text{ g m}^{-3} \text{ day}^{-1}$  (Figures 5.2A and 5.2B).

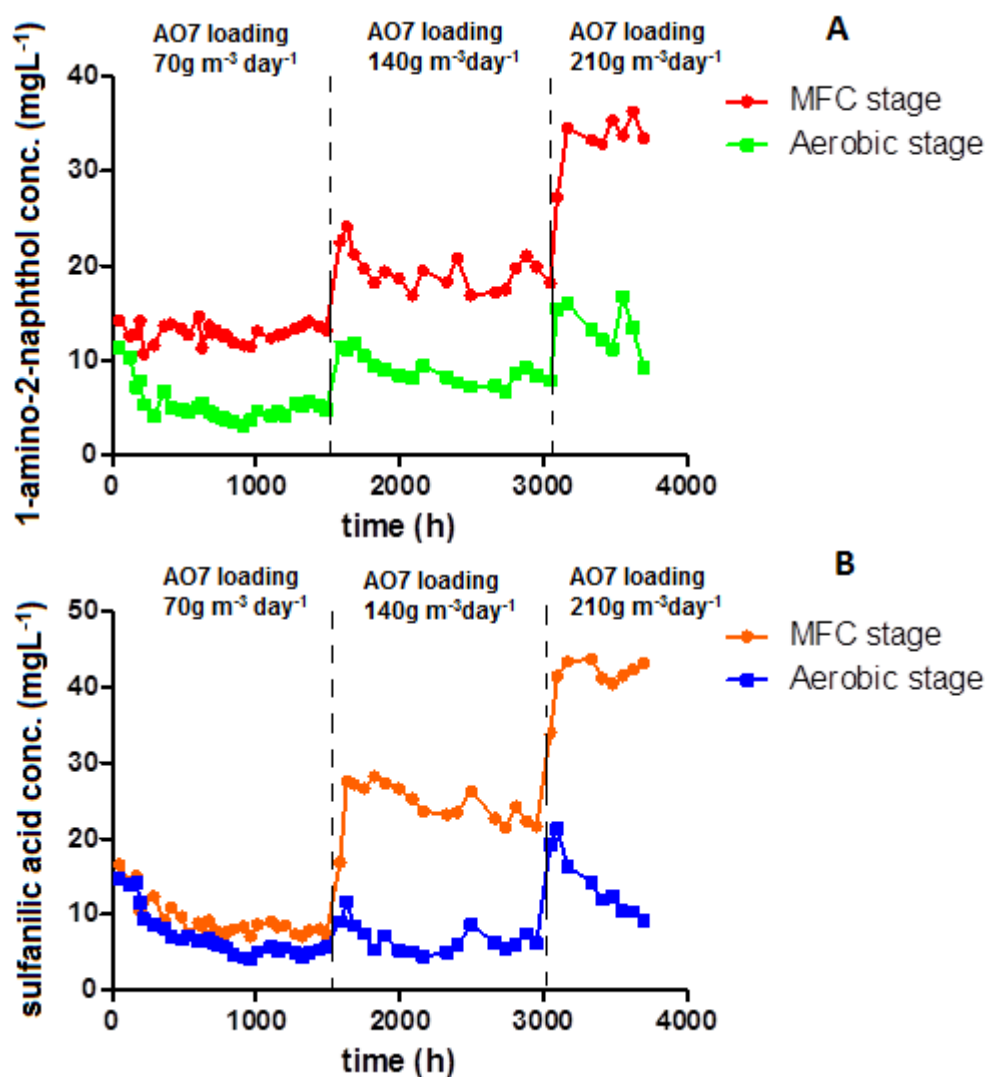


**Figure 5.2:** (A) Removal of 1-amino-2-naphthol within the MFC stage and aerobic stages of integrated bioreactor operation and (B) removal of 4-aminobenzenesulfonic acid (Sulfanilic acid) during the integrated bioreactor operation over a period of 150 days.

The prevalent high concentrations of both amines at the anoxic MFC stage suggests that under the hydraulic retention time (HRT) the MFCs operate at, the MFC stage treatment is unable to degrade both aminobenzenes effectively and

hence are washed out into the effluent entering the subsequent aerobic treatment stage of the reactor system.

Effluent samples collected at the end of the aerobic treatment stage of the integrated reactor system however, indicated considerably smaller concentrations of both aminobenzenes. This suggested that both constituent amines 4-aminobenzenesulfonic acid and 1-amino-2-naphthol were amenable to further degradation under the aerobic conditions utilised in the latter stage of the integrated bioreactor in this study. The observed additional reduction of soluble COD in the second aerobic stage of the reactor (Figure 5.1B) corroborates well with the data presented in figures 5.1A and 5.1B.

Ortho-substituted aminophenols such as 1-amino-2-naphthol are known for undergoing autoxidation reactions to form more refractory and highly coloured polymeric products upon exposure to oxygen (Kudlich et al, 1999). In this study however, no such accumulation of coloured, polymeric autoxidation products were observed. Especially at high AO-7 loadings ( $210 \text{ gm}^{-3}\text{day}^{-1}$ ) the effluent of the second stage was colourless and indicated no accumulation of coloured polymeric residues. This indicates that the aerobic stage of the reactor system is capable of effectively degrading autoxidation prone aminophenols such as 1-amino-2-naphthol. Sulfonated aminobenzenes such as 4-aminobenzoic acid are particularly known for their refractory nature (Gan et al, 2012). The use of azo dye adapted mixed microbial population in this study however, enabled 4-aminobenzenesulfonic acid removal rates up-to 74% even at the highest AO-7 loading ( $210 \text{ gm}^{-3}\text{day}^{-1}$ ) (Figure 5.2B).

In a very recent similar study, Cui et al, 2013 utilised a microbially assisted electrolysis system coupled to a subsequent aerobic stage to treat model wastewater containing the azo dye Alizarin Yellow – R (AYR). However, this

process utilised by Cui et al, 2013 being an electrolysis system, it required the use of an exogenous power supply and was unable to operate effectively in the absence of power. Electrolysis processes for azo dye treatment are not favoured due to high operational costs. Furthermore, a toxicity assessment about the end products of the aerobic stage was not conducted by Cui et al, 2013 in that study.

### **5.2.3. Toxicity reduction during the two stage reactor operation**

Achieving low environmental toxicity of the effluents is important for any biotreatment strategy used for recalcitrant waste removal (Ayed et al, 2011). Some aminobenzenes resulting from azo dye reductive biotransformation are demonstrated to be highly toxic to humans and other organisms including microorganisms (Skipper et al, 2010, Chen et al, 2009). Results of this study indicate that the amines formed at the end of the anoxic MFC stage induce a bioluminescence reduction toxicity effect on *V.fischeri* cells (Figure 5.3). The half maximal luminescence inhibition value ( $EC_{50}$ ) for the AO-7 containing synthetic wastewater influent and MFC effluent were  $127 \text{ mgCODL}^{-1}$  and  $63.3 \text{ mgCODL}^{-1}$  respectively. The effluent of the MFC stage indicated a marked increase in the  $EC_{50}$  value ( $637 \text{ mgCODL}^{-1}$ ) suggesting a significant ( $p < 0.01$ , ANOVA) reduction in toxicity compared to both MFC stage influent and MFC stage effluent. Interestingly, the low  $EC_{50}$  value (high toxicity) of the dye wastewater influent suggests that the presence of unreduced AO-7 itself in high concentrations may contribute to high environmental toxicity.

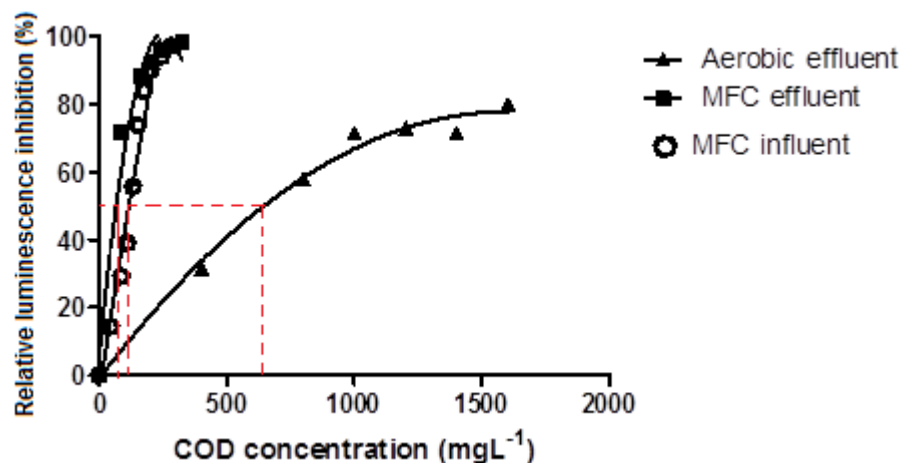


**Figure 5.3:** *Vibrio fischeri* luminescence based toxicity determinations of MFC influent, MFC effluent and aerobic stage effluent at the highest AO-7 loading rate ( $210 \text{ gm}^{-3}\text{day}^{-1}$ ).

Therefore, the results suggest that environmental toxicity of the samples were considerably reduced by subjecting the MFC stage effluent to aerobic post-treatment. The toxicity of the aerobic stage effluent was approximately 5-fold lower compared to synthetic wastewater influent and 10-fold lower compared to amine containing MFC stage effluent. These findings corroborate well with few other previous studies where a reduction of toxicity was observed following aerobic treatment of decolourised azo dye wastewater (Gottlieb et al, 2003, Kalme et al, 2007).

#### 5.2.4. Biogenic electricity generation during AO-7 degradation

Tubular type MFC operation during AO-7 removal resulted in concomitant biogenic electricity production. Current density reached approximately  $125 \text{ mA m}^{-2}$  during MFC operation (across a  $500 \text{ }\Omega$ ). Current output during reactor operation was subject to fluctuation, most likely due to wide temperature variations in the laboratory during the long operational periods (Figure 5.4).

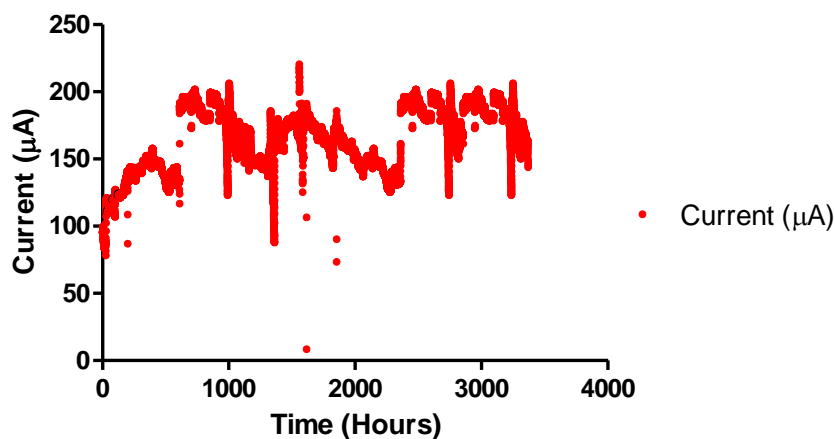


**Figure 5.4:** MFC current production (mean of duplicate MFCs) during the tubular MFC operation ( $R_{\text{ext}} = 500\Omega$ ).

Open circuit control indicated an OCV of  $641 \pm 37$  mV throughout the study (data not shown). Subsequent electrochemical performance characterisation of the MFCs at the end of the operational run using polarisation tests indicated maximum power densities of  $51.9 \pm 4$   $\text{mWm}^{-2}$  (Figure 5.5).

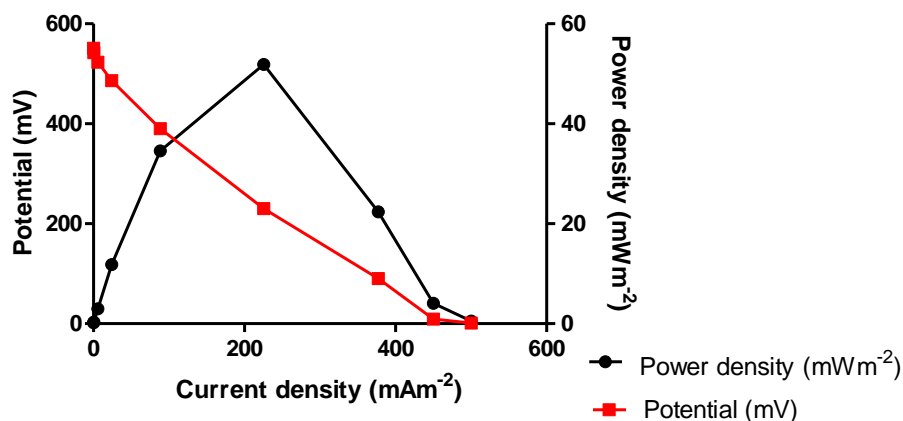


**Figure 5.5:** Current-power plot and a polarisation curve indicating the tubular MFC electrochemical performance at the end of the long term continuous MFC run.

This demonstrates the ability of the two-stage bioreactor system to generate bioelectricity while degrading recalcitrant AO-7. The electron donor used in this study was a waste material and the anolyte medium did not include a buffering

system. Instead, common textile wastewater auxiliary salts  $\text{Na}_2\text{SO}_4 \cdot 10\text{H}_2\text{O}$  and  $\text{NaCl}$  was added to adjust the ionic strength. This demonstrates the potential practical applications of an MFC-aerobic reactor system for complete degradation of colour industry wastewater and concomitant bioelectricity production.

#### **5.2.5. Degradation of aminobenzenes in the aerobic second stage**

HPLC analysis of the metabolite extracts of effluent samples from the aerobic stage of the two-stage reactor indicated that numerous degradation products were formed (Figure 5.6A). The aminobenzenes were degraded into several different simpler metabolites during the aerobic treatment stage and this suggests that oxidative degradation of aminobenzenes is the most effective way of removing them from colour industry wastewater. These findings are further reinforced by the COD removal and toxicity reduction data. A further reduction of COD from the anoxic first stage (MFC stage) effluent was observed in the aerobic second stage. A concomitant and marked reduction of toxicity was also observed in the aerobic stage effluent compared to the MFC stage effluent, suggesting that aminobenzene reductive biotransformation products were degraded into simpler non-toxic metabolites.



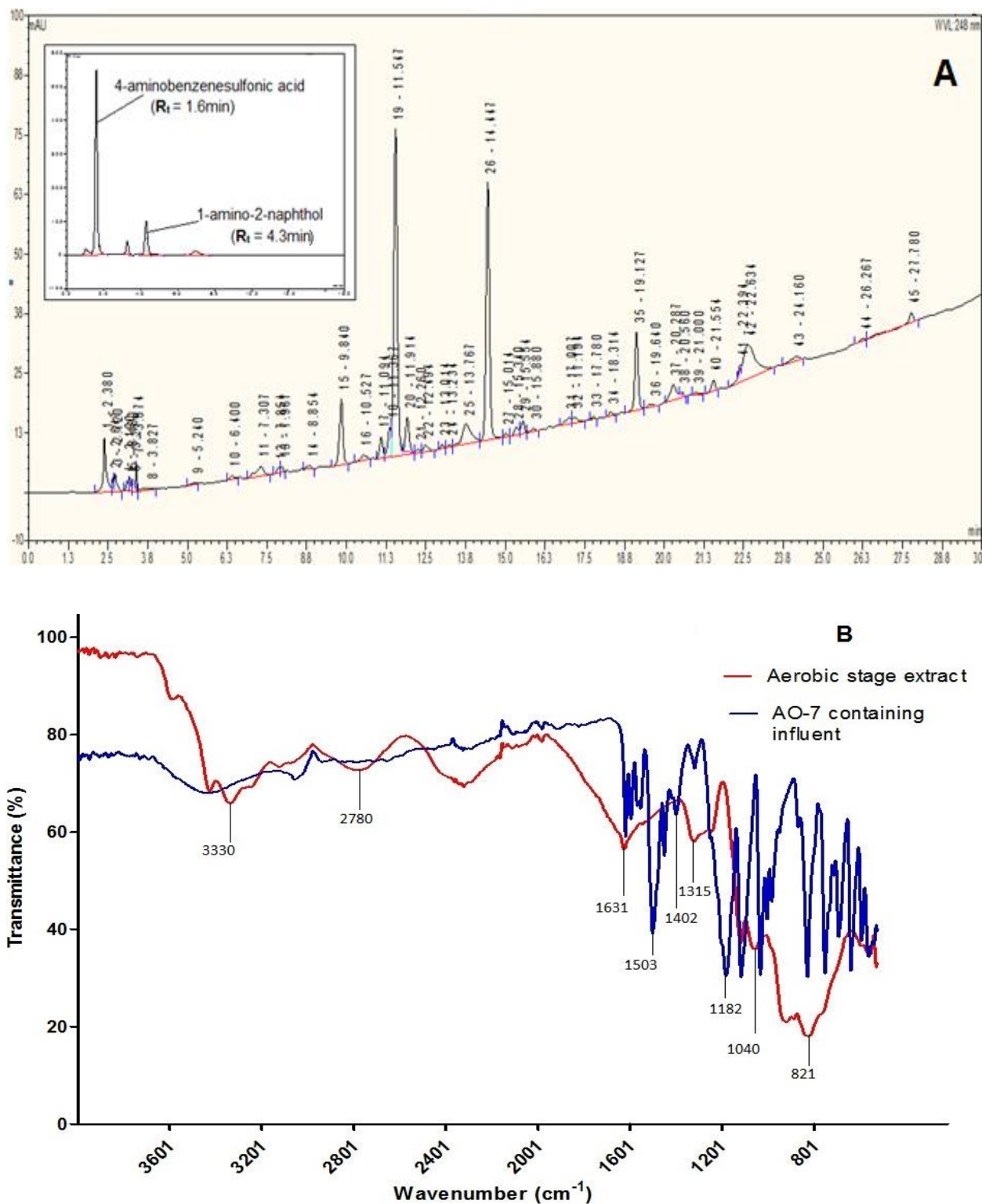
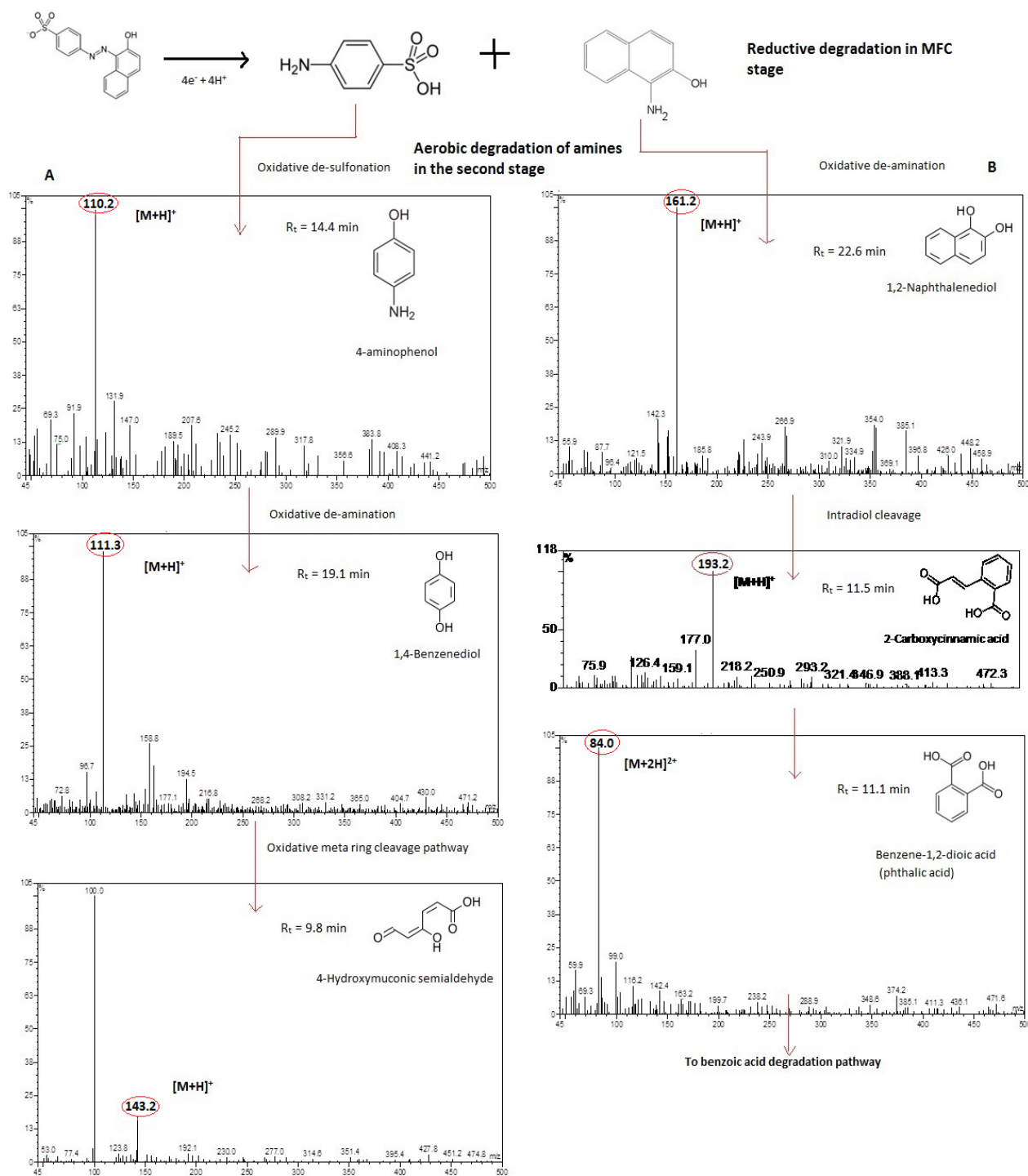


**Figure 5.6:** (A) HPLC gradient elution profile of the effluent of the aerobic treatment stage of the integrated reactor system and inset: isocratic flow HPLC profile of the effluent from the anoxic MFC stage, indicating the formation of amines 4-aminobenzenesulfonic acid ( $R_t = 1.6$  min) and 1-amino-2-naphthol ( $R_t = 4.3$  min) and (B) FTIR spectra overlay of the extracts of AO-7 containing influent and the aerobic stage effluent

### **5.2.6. Putative biodegradation pathway of AO-7**

Based on the HPLC-MS identification of the AO-7 biotransformation metabolites, a putative biodegradation pathway is suggested. Products of reductive biotransformation (MFC stage) of AO-7 were identified as 1-amino-2-naphthol and 4-aminobenzenesulfonic acid by HPLC peaks compared to authentic standard compounds (Figure 5.6A – inset). These biotransformation products are further catabolised into simpler and less toxic metabolites at the latter aerobic stage of the integrated bioreactor system. The suggested biodegradation pathways based on identified HPLC-MS intermediates for 4-aminobenzenesulfonic acid and 1-amino-2-naphthol are depicted in figures 5.7A and 5.7B respectively.



The formation of 4-aminophenol ( $M+H^+ = 110.2$ ,  $R_t = 14.4$  min) from 4-aminobenzenesulfonic acid under aerobic conditions suggests an aerobic de-sulfonation reaction, probably due to the action of mono-oxygenase enzymes. Similar de-sulfonation reactions on sulfonated aminobenzenes catalysed by mono-

oxygenase enzymes were earlier reported by Kalme et al, 2007. They demonstrated that *Pseudomonas desmolyticum* NCIM 2112 was capable of carrying out a series of oxidative de-sulfonation reactions using mono-oxygenase enzymes on azo dyes carrying multiple sulfonic acid groups. Formation of 1, 4-benzenediol ( $M+H^+ = 111.3$ ,  $R_t = 19.1$  min) from 4-aminophenol suggests that oxidative de-amination to form a benzenediol derivative. Mono-oxygenases are also known to catalyse de-amination reactions of aminobenzenes to form catechol derivatives (Junker et al, 1994). The sequential de-sulfonation and de-amination of 4-aminobenzenesulfonic acid to form 1, 4-benzenediol indicates the action of mono-oxygenases and further suggests that di-oxygenases may not be involved in the aromatic ring activation reactions. The sequential aromatic ring activation reactions catalysed by mono-oxygenase could eventually lead to oxidative aromatic ring opening (formation of 4-hydroxymuconic semialdehyde) ( $M+H^+ = 143.2$ ,  $R_t = 9.8$  min) (Takenaka et al, 2003).

Similar to the oxidative deamination of 4-aminobenzenesulfonic acid by the action of mono-oxygenase, the formation of 1, 2-naphthalenediol ( $M+H^+ = 161.2$ ,  $R_t = 22.6$  min) suggests that 1-amino-2-naphthol undergoes oxidative de-amination, most probably due to the action of a mono-oxygenase. Following the activation of one aromatic ring in the form of a naphthalenediol structure, it becomes susceptible to further oxidative catabolism. The intradiol cleavage of 1, 2-naphthalenediol leads to the formation of 2-carboxycinnamic acid ( $M+H^+ = 193.2$ ,  $R_t = 11.5$  min). Beta-oxidation-like two-carbon shortening of the opened aromatic ring of 2-carboxycinnamic acid may eventually lead to the formation of Benzene-1, 2-dioic acid (Phthalic acid) ( $[M+2H]^{2+} = 84.0$ ,  $R_t = 11.1$  min). In an earlier study conducted by Annweiler et al, 2000 on aerobic naphthalene degradation by *Bacillus thermoleovorans*, it was demonstrated that naphthalene is catabolised by

the bacterium for its carbon and energy needs via the intermediates 2, 3-naphthalenediol, 2-carboxycinnamic acid, phthalic acid and benzoic acid. Benzoic acid can be further catabolised and its intermediates can be fed into TCA cycle relatively easily in benzoate degradation pathways (Nogales et al, 2010). Therefore, the intermediates of AO-7 degradation entering TCA cycle could lead to mineralisation.

The use of an azo dye adapted mixed microbial population in this study gives an additional advantage of a larger diversity of aerobic degradation pathways for recalcitrant compounds such as aminobenzenes (Saratale et al, 2009). The dye adapted mixed microbial culture used in this study has been characterised in the work described in chapter 4, and several *Pseudomonas* species were identified. Earlier studies indicated that many *Pseudomonas* species are capable of converting recalcitrant sulfonated aminobenzenes to more biodegradable compounds with the action of mono and di-oxygenase enzymes (Kalme et al, 2000). The possible action of mono-oxygenases in de-sulfonation and de-amination reactions of sulfonated aminobenzenes observed in this study could be due to the production of such enzymes by numerous Pseudomonads present in the mixed microbial population.

The FTIR spectroscopy of the influent sample indicated a characteristic peak for the aromatic azo bond (-N=N-) stretch at  $1503\text{ cm}^{-1}$ . Furthermore, peaks characteristic for the S=O stretch and S-O stretch of sulfonic acid groups were evident at wavenumbers  $1402\text{ cm}^{-1}$  and  $1182\text{ cm}^{-1}$ . In the FTIR spectra of the extracts from the aerobic stage effluent however, the peaks for the azo moiety at  $1503\text{ cm}^{-1}$  and the sulfonic acid groups at  $1402\text{ cm}^{-1}$  and  $1182\text{ cm}^{-1}$  were absent; suggesting that the unreduced azo moieties and intact sulfonic acid groups were absent in the treated effluent. Aerobic stage effluent produced peaks characteristic

for the carbonyl stretch ( $\text{C}=\text{O}$ ) of the carboxylic acids and aldehydes (at  $1626\text{ cm}^{-1}$ ), O-H stretch of carboxylic acids ( $3330\text{ cm}^{-1}$ ), C-H stretch of aldehydes and C-O stretch of catechols and naphthols (at  $1040\text{ cm}^{-1}$ ). Additional peaks characteristic of N-H<sub>2</sub> wagging of aminobenzenes (at  $821\text{ cm}^{-1}$ ) and O-C stretch of carboxylic acids were also identifiable in the aerobic stage extracts. The FTIR spectra indicate that the aerobic stage extracts are distinctly different to the AO-7 containing influent with regards to its chemical nature. The formation of catechol and naphthalenediol derivatives, aldehydes and carboxylic acids with the concomitant elimination of the azo moieties and sulfonic acid groups of AO-7 is further supported by FTIR analysis of the samples (Figure 5.6B).

Sequential reduction of soluble COD in the two stages of the integrated bioreactor system, the formation of numerous metabolites in the aerobic degradation stage and the marked reduction of environmental toxicity suggests that AO-7 is completely degraded to non-toxic intermediates by the mixed microbial population in the combined MFC-aerobic bioreactor. The use of continuous bioreactors utilising waste materials such as molasses for the treatment of recalcitrant wastes are particularly favoured due to industrial applicability and cost considerations. Moreover, the use of unbuffered anode medium for the continuous MFC anode further enhances the cost effectiveness of this reactor system because the use of buffered media for wastewater treatment is highly disadvantageous in cost and operational standpoints. The prospect of biogenic electricity production during azo dye removal is an added advantage of using tubular MFC systems such as the ones used in the current study. The integrated bioreactor system tested in this study was also capable of operating successfully under wide temperature fluctuations ( $14.6^{\circ}\text{C}$  -  $26^{\circ}\text{C}$ ). This is another potential advantage for industrial applications because exogenous temperature regulation is known to be costly and

hence, a bioreactor system that could tolerate a wide temperature range would be advantageous. The findings of this study further implies that MFC technology can be used in combination with activated sludge communal wastewater treatment systems in order to sustainably deal with recalcitrant colour industry wastewater.

### 5.2.7. The effect of shock AO-7 loadings on MFC operation

For a continuous bioreactor being developed for potential colour industry waste treatment applications, it is necessary to possess the ability to withstand shock loadings of xenobiotics and COD levels. In colour industry waste streams, it is likely to encounter very high dye concentrations and COD levels. Therefore, any potential MFC based system developed for this purpose must be robust enough to withstand such conditions. Hence, as part of this study, shock AO-7 loadings of  $400 \text{ mgL}^{-1}$  were introduced in order to monitor the response of the MFC stage from such a shock load.

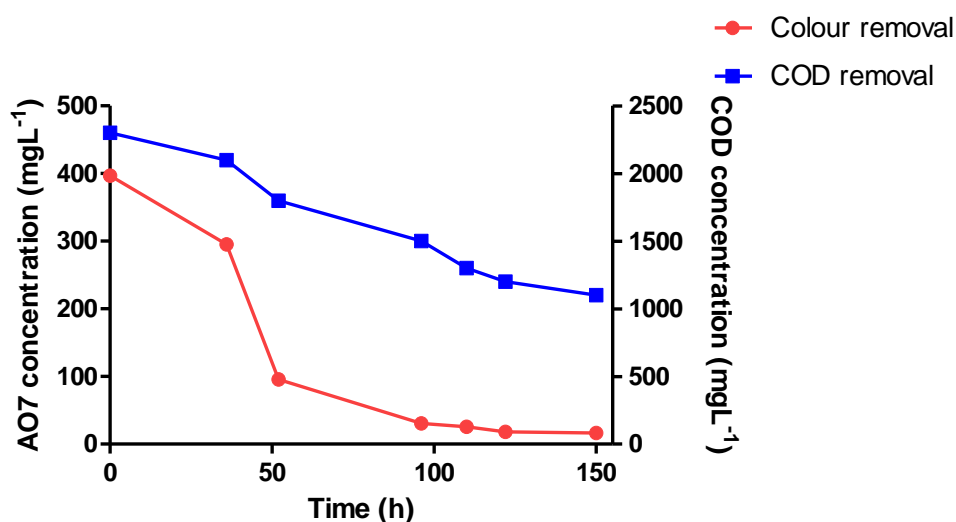


**Figure 5.8:** The recovery of the MFC stage from a shock AO-7 loading ( $400 \text{ mgL}^{-1}$ )

Following an initial lag of about 10 hours, the AO-7 concentration indicated a rapid decrease (Figure 5.8) suggesting that the MFC stage was capable of withstanding shock loadings of AO7. However, the AO-7 concentration to fall below 50 mgL<sup>-1</sup> took approximately 75 hours. This could be due to the high level of cytotoxicity originating from the formation of very high quantities of aminobenzenes during the reductive decolourisation process.

### **5.3. Concluding remarks**

The findings of this study demonstrate that an integrated MFC-aerobic bioreactor configuration is capable of achieving complete biodegradation of the model azo dye AO-7. The two-stage process was capable of bringing about significant reductions in environmental toxicity, colour and soluble COD of the model wastewater, coupled with simultaneous bio-electricity generation. The aminobenzenes generated at the end of the anaerobic MFC stage were effectively converted to non-toxic and simpler compounds at the end of the aerobic reactor operation. This integrated bioreactor system was capable of using a cheap and sustainable electron donor (molasses), mixed microbial populations, sustain longer operational periods (150 days) in continuous flow mode and was able to operate at ambient temperature under wide temperature fluctuations (often low temperatures). Therefore, this indicates the potential colour industry wastewater treatment applications of the integrated bioreactor system described in this study.



## **Chapter 6 - The scale up tubular air-breathing MFCs and treatment of real colour industry wastewater**

## Summary

The scalability of any MFC based system is of vital importance if they are to be utilised for potential field applications. In this study, an MFC – aerobic integrated bioreactor system was investigated for its scalability for the purpose of treatment of simulated colour industry wastewater containing the model azo dye AO-7 and two types of real colour industry wastewater. A volumetric MFC scale-up factor of 6 (200 mL to 1200 mL reactor volume at MFC stage) from the previous study (reactor system described in chapter-5) was used. The real colour industry wastewater originated from acid dyebaths for wool colouring and leather tanning. The influent containing real wastewater was fed to the reactor in continuous mode at ambient temperature. Three MFC units were integrated to act in unison as a single module for wastewater treatment and an aerobic bioreactor mimicking an activated sludge system operating downstream to the MFC module was installed in order to ensure more complete degradation of colouring agents found in the real wastewater. Total colour removal in the final effluent exceeded 90% in all experiments where both synthetic (AO-7 containing) and real wastewater was used as the influent feed. The COD reduction also exceeded 80% in all experiments under the same conditions. The MFC modules connected in parallel configuration allowed obtaining higher current densities than that can be obtained from a single MFC unit. The maximum current density of the MFC stack reached  $1150 \text{ mA m}^{-2}$  when connected in parallel configuration. The outcome of this work implies that suitably up-scaled MFC – aerobic integrated bioprocesses could be used for colour industry wastewater treatment in industrially relevant conditions with possible prospects of bio-electricity generation.

## 6.2. Results and discussion

### 6.2.1. Decolourisation and COD removal in AO-7 containing model wastewater in the scaled up MFC-aerobic reactor system

It was demonstrated earlier (Chapter 5) that MFC- aerobic integrated reactor system was capable of fully degrading AO-7 containing simulated colour industry wastewater into non-toxic simpler metabolites. The modular scale – up of the same two – stage system was tested initially in continuous mode in this study using the same synthetic medium containing AO-7 ( $35 \text{ mgL}^{-1}$ ).

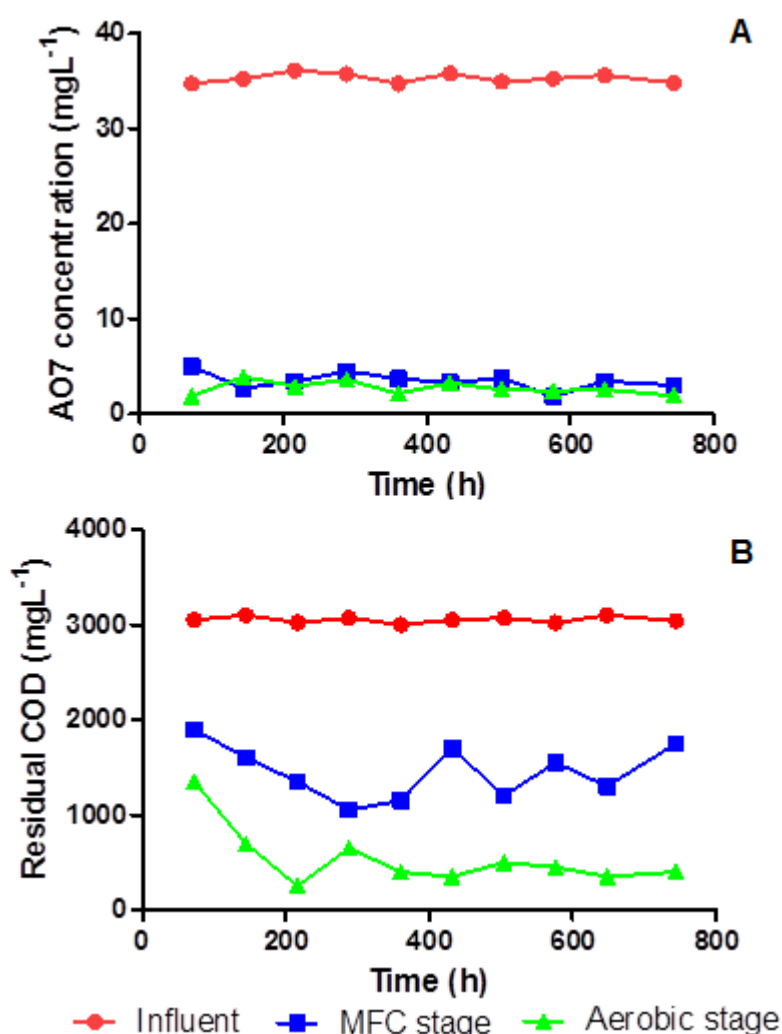


**Figure 6.1:** (A) Colour removal of the model wastewater containing AO-7 ( $35 \text{ mgL}^{-1}$ ) fed into the scaled-up MFC system in the MFC and aerobic stages and (B) residual COD of the samples taken in the MFC and aerobic stages

The results indicate that the colour and COD removal reached above 90% and therefore, the performance of the scaled-up two-stage MFC-aerobic reactor system was comparable to the similar but smaller reactor system (200 mL working volume) utilised in the previous study described in chapter 5 (Figure 6.1A and 6.1B). This suggests that the integrated MFC-aerobic two-stage reactor system is capable of operating without any deterioration of its colour and COD removal performances when it is scaled-up by a volume scale factor of 6 (1200 mL total working volume in the three integrated MFC modules) and operating on the same synthetic wastewater medium containing AO-7. Previously (chapter 5) it was demonstrated that an MFC – aerobic two stage reactor set – up was the ideal configuration for more complete degradation and toxicity removal of azo dyes such as AO-7. Therefore, the same two – stage MFC aerobic reactor set up was used in the up-scaled model reactor.

### **6.2.2. Decolourisation of real colour industry wastewater in the scaled up system**

For any potential wastewater treatment system tested for field application, it is essential to possess the capability to effectively deal with real wastewater types. This is especially relevant to biological wastewater treatment systems developed for the removal of xenobiotic compounds. Although the use of model wastewater often containing a single dye is ubiquitous in many studies done in this area, the use of real colour industry wastewater is relatively rare. It is not always possible and adequate to extrapolate the information obtained from studies utilising model wastewater into a scenario where real colour industry wastewater is encountered. Therefore, it is essential to conduct experiments utilising real colour industry wastewater when attempting to scale up prospective wastewater treatment

systems. Therefore, in this study, two types of real colour industry wastewater were tested; namely, acid dyebath wastewater from wool colouring and acid dyebath wastewater from leather tanning.

When using real colour industry wastewater from wool colouring, the effluent from the MFC stage and the aerobic stage indicated a slow, sequential colour reduction during the start – up phase (Figure 6.2). Subsequently however, both MFC and aerobic stages reached high colour removal performances exceeding 90% decolourisation (Figure 6.3A).

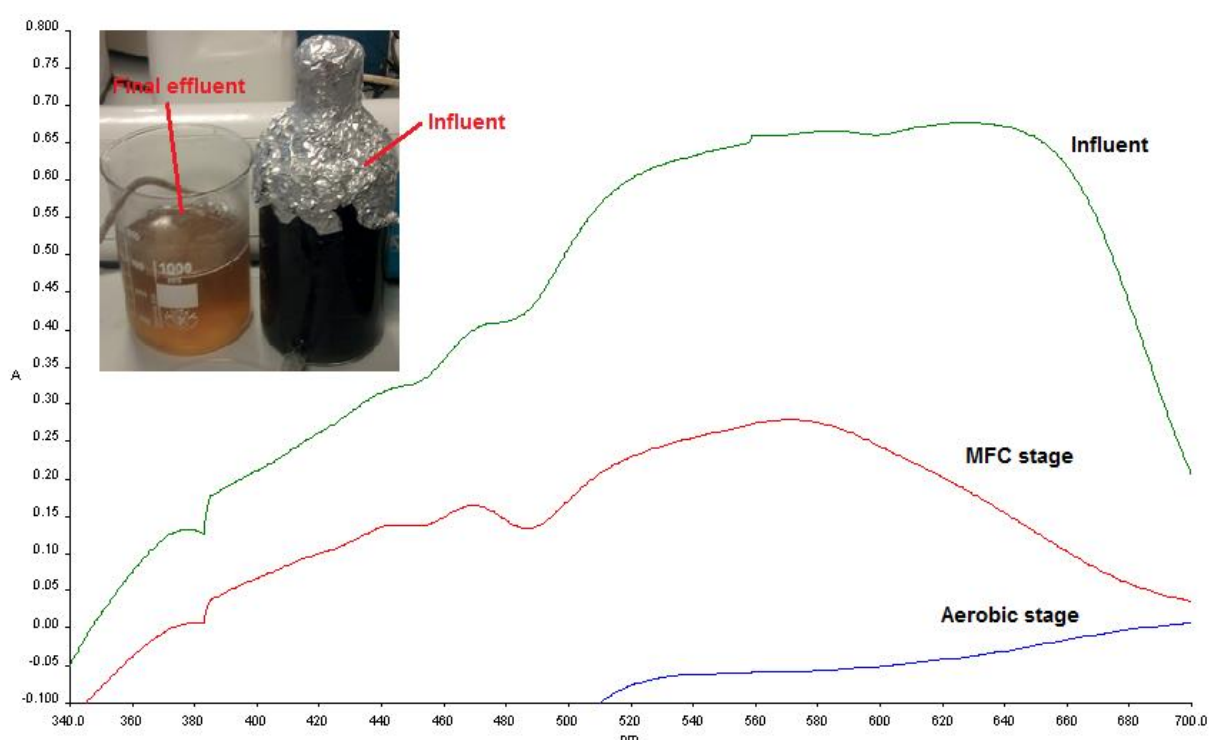


**Figure 6.2:** Absorption spectra showing the decolourisation of real colour industry wastewater from an acid dyebath for wool in the scaled-up MFC system at the MFC stage and the aerobic stage. Inset – clear visible colour difference between the influent real dye wastewater and the final effluent.

Furthermore, COD reduction indicated a stepwise reduction compared to the influent COD, indicating a COD level below  $500 \text{ mgL}^{-1}$  for the final effluent (Figure 6.3B).

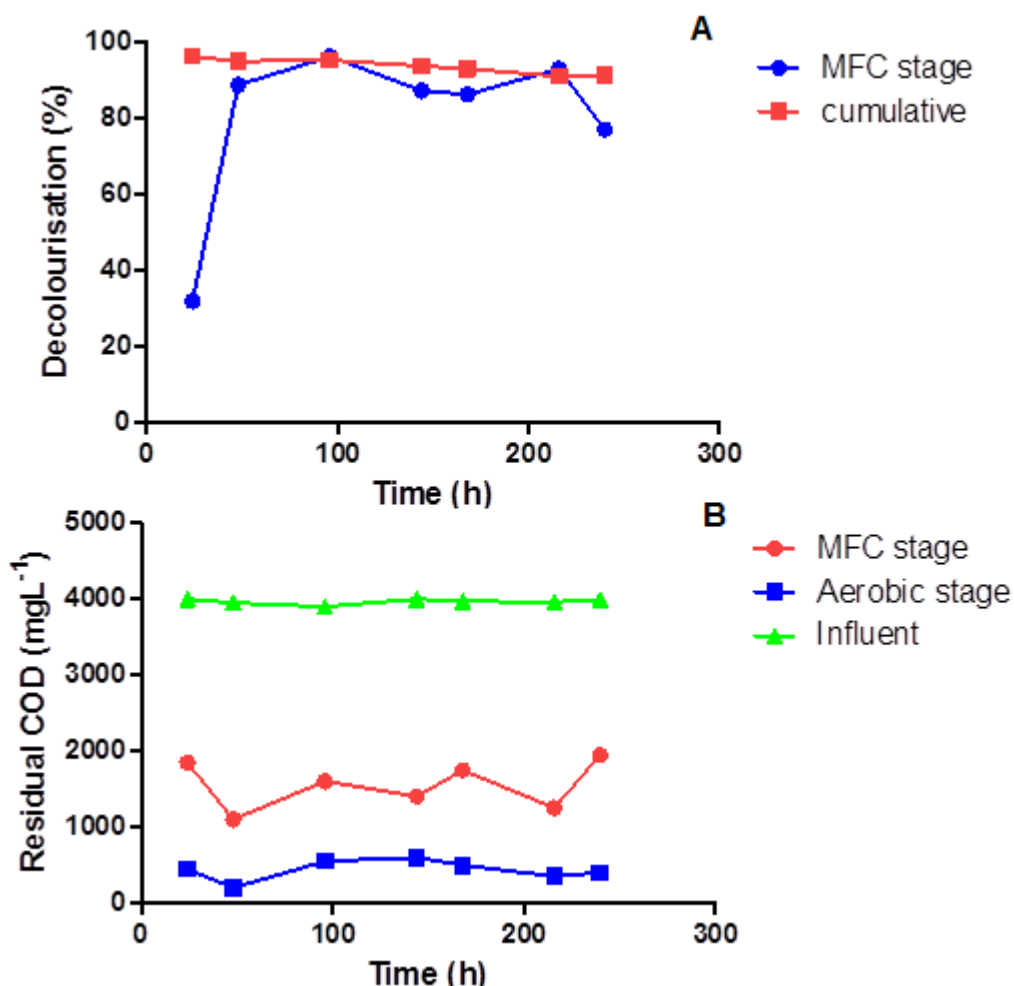


**Figure 6.3:** (A) Colour removal performance of scaled up MFC reactor system treating real wastewater originating from an acid dyebath for wool at the MFC stage and aerobic stage (B) residual COD of the samples obtained from the MFC stage

Therefore, similar to the previous study that used an integrated MFC – aerobic process (chapter 5), it can be expected that due to the stepwise and sequential COD reduction, some of the decolourisation metabolites formed in the anaerobic MFC stage are further oxidised into simpler compounds during the aerobic stage.

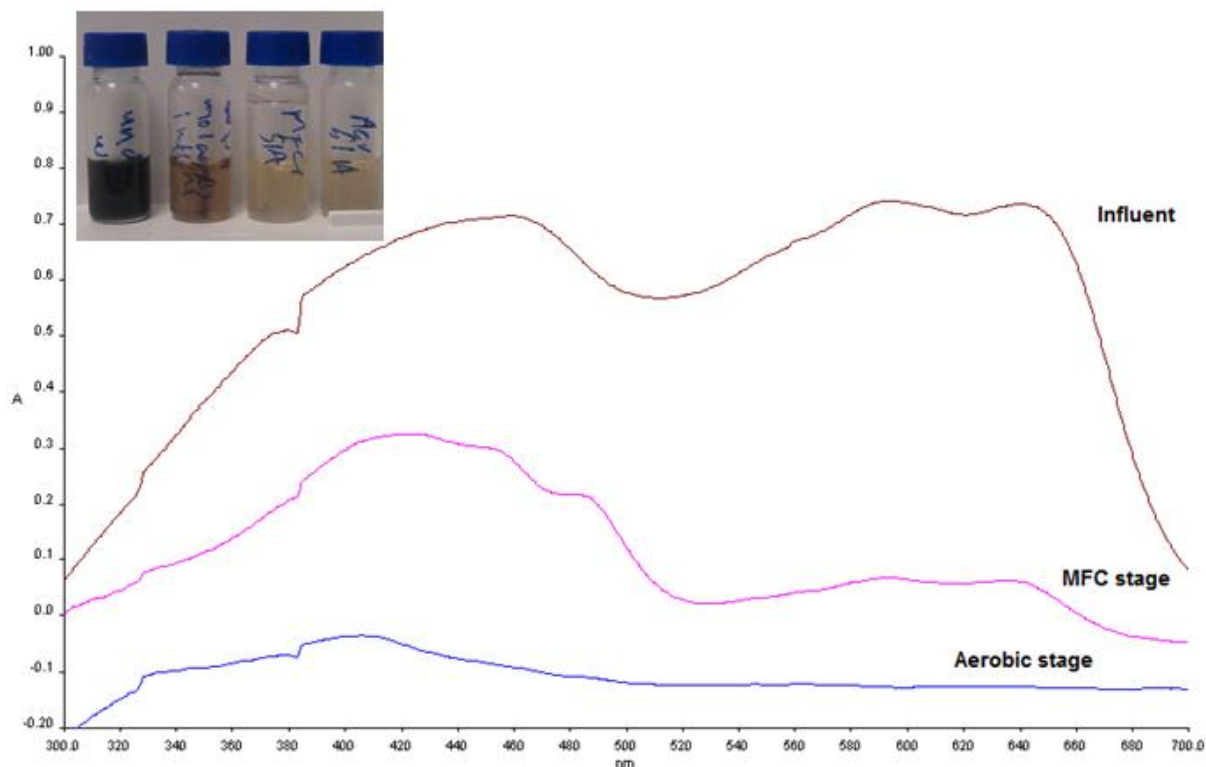


**Figure 6.4:** Absorption spectra showing decolourisation of real colour industry wastewater from leather tanning in the scaled – up MFC – aerobic bioreactor during the MFC stage and aerobic stage. Inset – comparison of vials from left to right containing leather tanning real wastewater influent, MFC stage effluent, aerobic stage effluent and model wastewater containing only molasses

Similar to the previous observations with real colour industry wastewater from wool colouring, the intense colour of the influent was almost completely removed from real wastewater originating from leather tanning when it was used as the influent feed for the scaled-up integrated MFC – aerobic reactor system (figure 6.4). This clearly suggests that the scaled-up integrated MFC module coupled to the aerobic reactor system is capable of effectively removing colour from both types of real colour industry wastewater tested in this study. The final colour removal efficiency of the combined MFC-aerobic stages of the reactor reached over 90% (Figure 6.5A) when leather tanning wastewater was used as the influent. This clearly demonstrates that the scaled-up integrated MFC – aerobic system is a versatile bioreactor system that can effectively deal with different types of real colour industry wastewater.

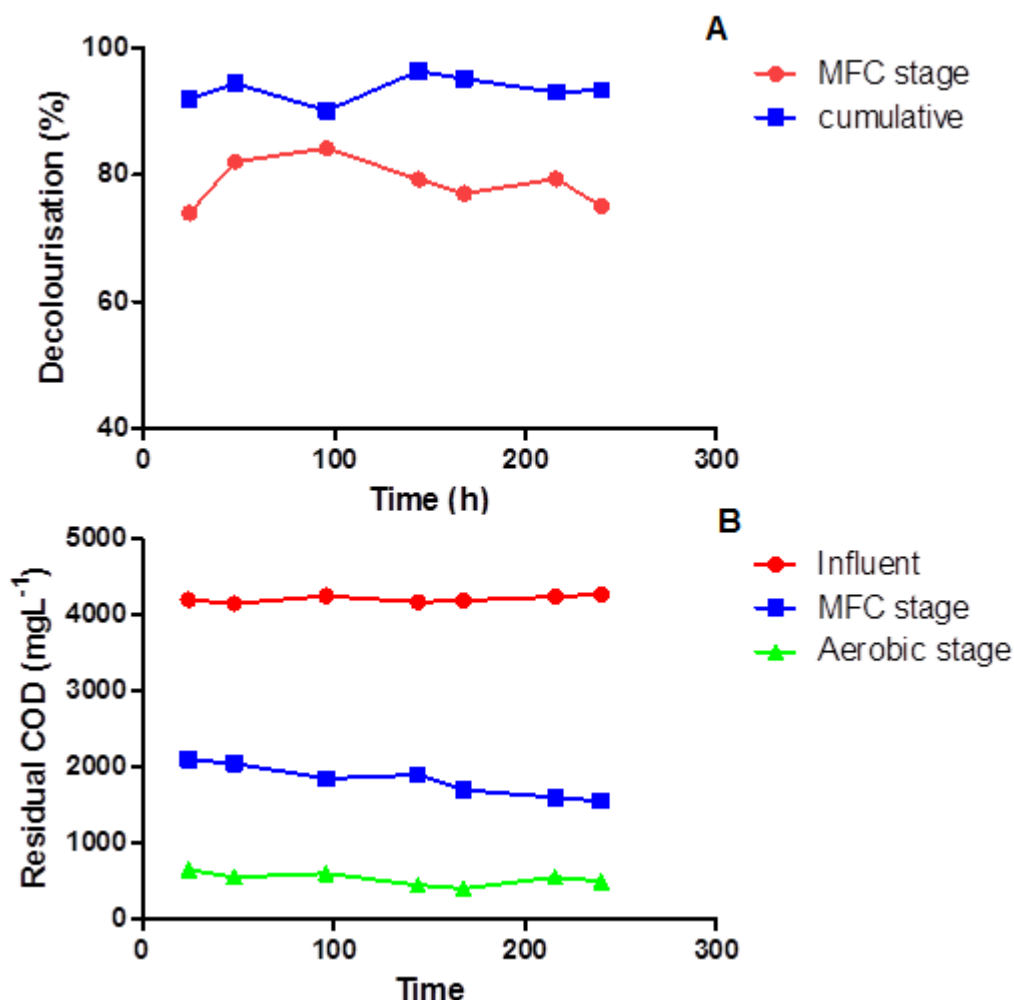


**Figure 6.5:** (A) Decolourisation performance of the scaled up MFC-aerobic reactor system when using real colour industry wastewater originating from leather tanning during the MFC stage and aerobic stage (B) COD removal performance during MFC stage and aerobic stage.

Residual COD levels of the samples also indicated a stepwise reduction at the end of the MFC stage and the aerobic stage compared to the influent COD when real leather tanning wastewater was used as the influent. This suggests that decolourisation metabolites were further oxidised into simpler compounds at the aerobic reactor stage of the integrated system. The unmodified (without the addition of the co-substrate molasses) COD values for the two types of real wastewaters were  $1000 \pm 60 \text{ mgL}^{-1}$  and  $1280 \pm 40 \text{ mgL}^{-1}$  respectively for wool colouring wastewater and leather tanning wastewater. The residual COD values of the final effluent exiting from the aerobic stage when both types of real wastewater



were used in the scaled – up reactor system were below  $500 \text{ mgL}^{-1}$  (figures 6.3B and 6.5B). This clearly suggests that organic components contained in the two types of wastewater (including colouring agents) were oxidised in a stepwise manner during the process into simpler and colourless compounds. When leather tanning wastewater was used as the influent, colour removal at the end of the MFC stage remained at 80% or below, but the overall colour removal of the combined MFC + aerobic process was over 90%. This is in contrast to other work done using this two stage system. When azo dyes (i.e. AO-7) was used as the model compounds in synthetic wastewater, most of the colour removal ( $> 90\%$ ) occurred at the MFC stage rather than at the aerobic stage because most azo moieties ( $-\text{N}=\text{N}-$ ) undergo reductive degradation in the anaerobic MFC stage. However, contrary to the observations relating to azo dyes such as AO-7, when leather tanning wastewater was used as the influent, the aerobic stage accounted for more than 10% of the total decolourisation (Figure 6.5A). This suggests that leather tanning real wastewater used here may contain other types of dyes belonging to dye classes such as anthraquinone or triphenylmethane dyes which could be amenable to degradation in the aerobic reactor stage.

### **6.2.3. Electrochemical performance of the parallel connected MFC modules during real and simulated wastewater treatment**

Connecting stacked MFCs in series configuration could lead to undesirable energy losses due to effects such as voltage reversal and potential drop across each MFC unit when connected in series. Voltage reversal is thought to occur due to sudden fuel starvation in the anode of one or more MFCs in an MFC stack and as a result, a sudden loss of bacterial catalytic activity transferring electrons to the anode (Aelterman et al, 2006, Ieropoulos et al, 2008, Oh and Logan, 2006). However,

voltage reversal is mainly encountered during batch operation of MFC stacks and hence, operating MFCs in continuous mode and by ensuring good mixing, the undesirable energy losses of voltage reversal could be circumvented. The voltage drop across each MFC during a series connection of an MFC stack mainly occurs due to the internal resistance of MFCs (Zhuang et al, 2012). MFC systems when used as a single unit, suffer from the intrinsic theoretical maximum voltage output upper limit of about 1.2 Volts. However, due to various internal energy losses as discussed in chapter 1, the actual voltage obtained under field conditions is lower than 1.2 V. Therefore, when scaling up MFC systems, it is essential to connect multiple MFC units in either series or parallel configurations in order to obtain useful and high enough voltage or current outputs. Parallel connection of multiple MFCs is useful in terms of obtaining high current densities.

The current production of an MFC module during AO-7 containing simulated wastewater is depicted in figure 6.6. Current densities across a  $R_{\text{ext}}$  of 500  $\Omega$  reached a maximum of approximately 200  $\text{mA m}^{-2}$  and stayed relatively stable throughout continuous reactor operation.

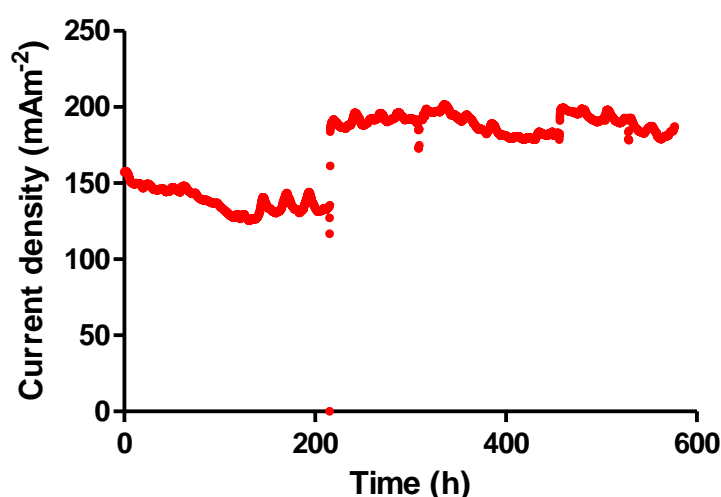


**Figure 6.6:** Current production in scaled – up MFC modules during AO-7 containing simulated wastewater treatment ( $R_{\text{ext}} = 500 \Omega$ )

Polarisation curves and power current plots of individual scaled-up MFC units indicated average maximum current and power densities of  $550 \text{ mA m}^{-2}$  and  $49 \text{ mW m}^{-2}$  respectively during real colour industry wastewater treatment (Figure 6.7). The average open circuit potential (OCP) of an individual MFC module of the integrated MFC stage reached  $297 \pm 31 \text{ mV}$  during the same operational period.

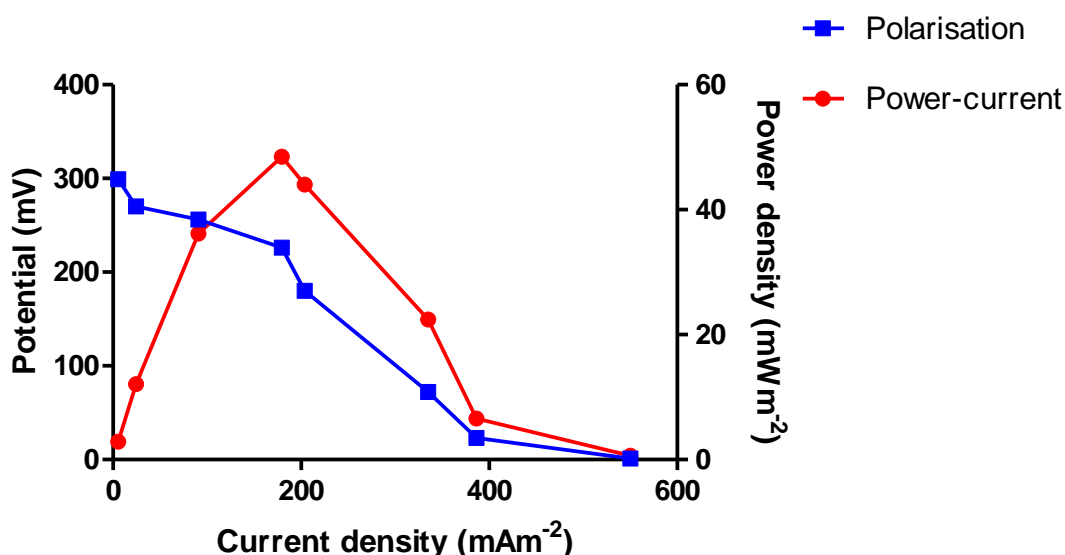


**Figure 6.7:** The average individual electrochemical performance of the three parallel connected MFC modules during real dye wastewater treatment.

When the MFC modules were connected in parallel configuration, maximum current densities as high as  $1150 \text{ mA m}^{-2}$  could be obtained while the maximum power density obtainable from the parallel connected MFC modules remained a modest  $54 \text{ mW m}^{-2}$  (Figure 6.8). However, the OCP remained at  $275 \text{ mV}$ . This indicates that the parallel connected MFC units allows drawing a larger maximum current while the maximum power density obtainable from such parallel connected MFC units is not notably different to the maximum power that can be drawn compared to a single MFC unit. The OCP of the parallel connected MFCs ( $275 \text{ mV}$ ) remained close to that of a single MFC unit ( $297 \text{ mV}$ ), indicating that no significant enhancement of voltage output is possible in parallel MFC

configuration. These findings are in agreement with an earlier study conducted by Zhuang et al, 2012 in which they used parallel and series connected MFC stacks and found that current outputs can be enhanced when the MFC units are stacked in parallel configuration with no significant enhancement to the voltage output or power density.

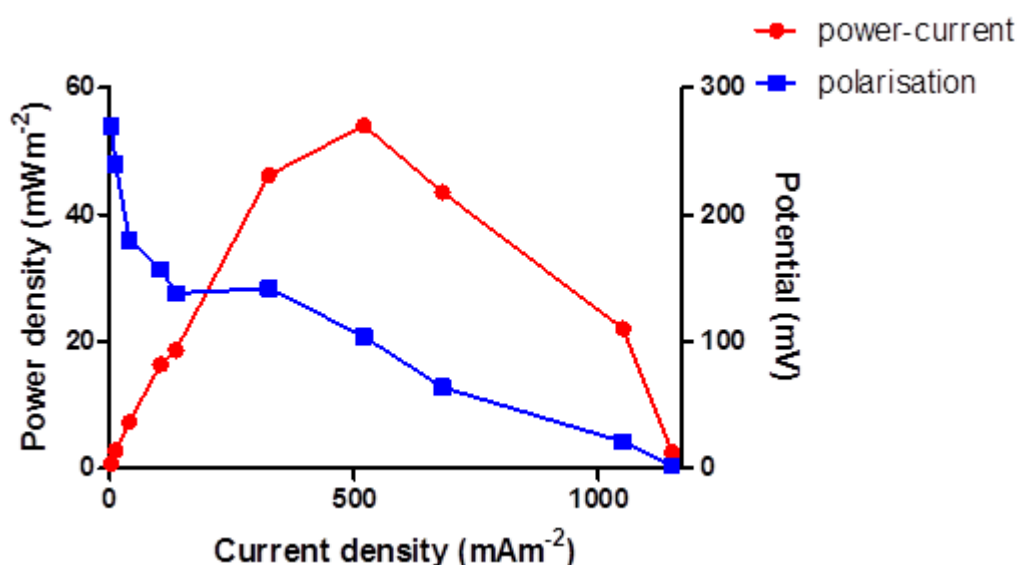


**Figure 6.8:** The power – current plot and polarisation curve of the parallel connected integrated MFC module while treating real colour industry wastewater from an acid dye bath for wool.

#### 6.2.4. Degradation of colouring agents in real colour industry wastewater in the MFC – aerobic two stage process

Effective colour removal from both types of colour industry wastewater was achieved using the scaled – up MFC-aerobic bioreactor system as shown in figures 6.3 and 6.5. However, it is necessary to assess the degradation of various colouring components contained within real colour industry wastewater during the two stage treatment process. Comparison of HPLC elution profiles of the influents and the effluents at various stages of the two stage process was carried out for this purpose.

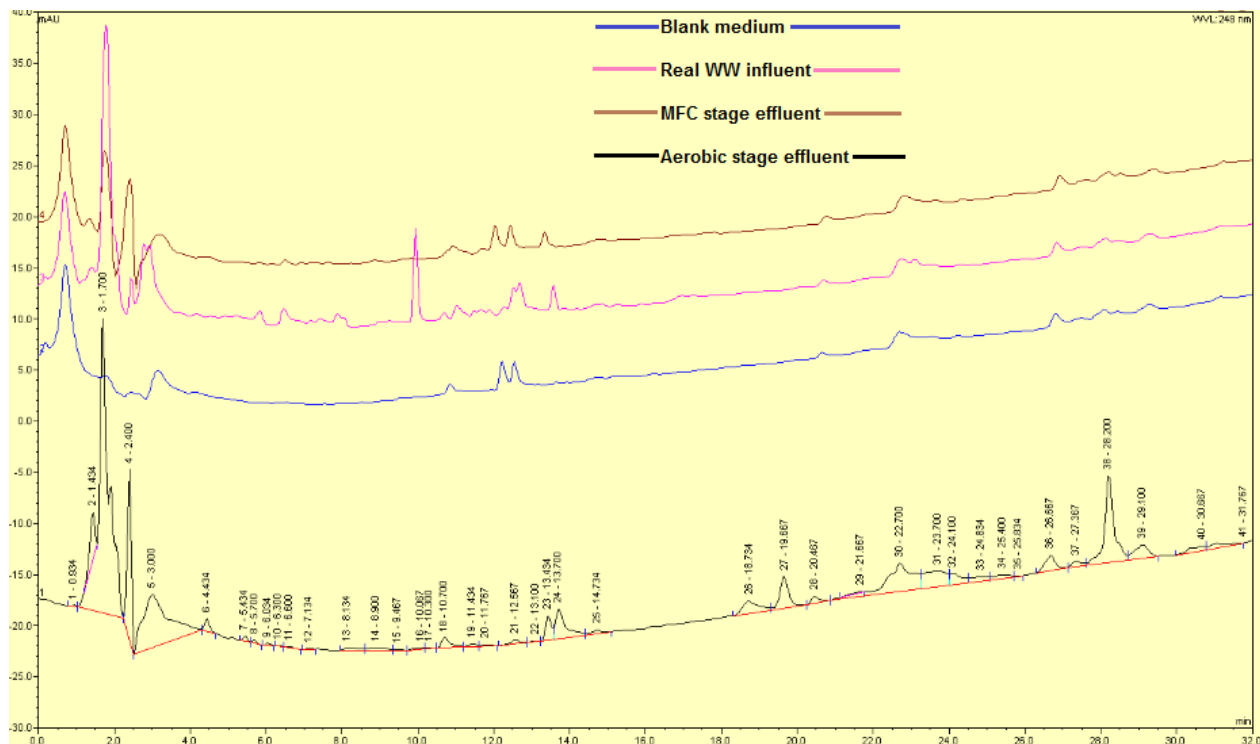


**Figure 6.9:** overlay of HPLC chromatograms of real colour industry wastewater from leather tanning. Compared chromatograms indicate the blank media (i.e. molasses without colour industry wastewater), real leather tanning wastewater supplemented with molasses (influent), the effluent from MFC stage and the effluent from the aerobic stage of the integrated scaled – up bioreactor system

HPLC analysis of the samples obtained from the two-stage operation reactor when leather tanning wastewater was used as the reactor feed indicates that numerous metabolites were produced at the end of the aerobic stage of the treatment process (Figure 6.9). The HPLC spectrum of the aerobic stage effluent (final effluent) was markedly different from the HPLC spectra of the blank medium, real wastewater influent feed and the MFC stage effluent.

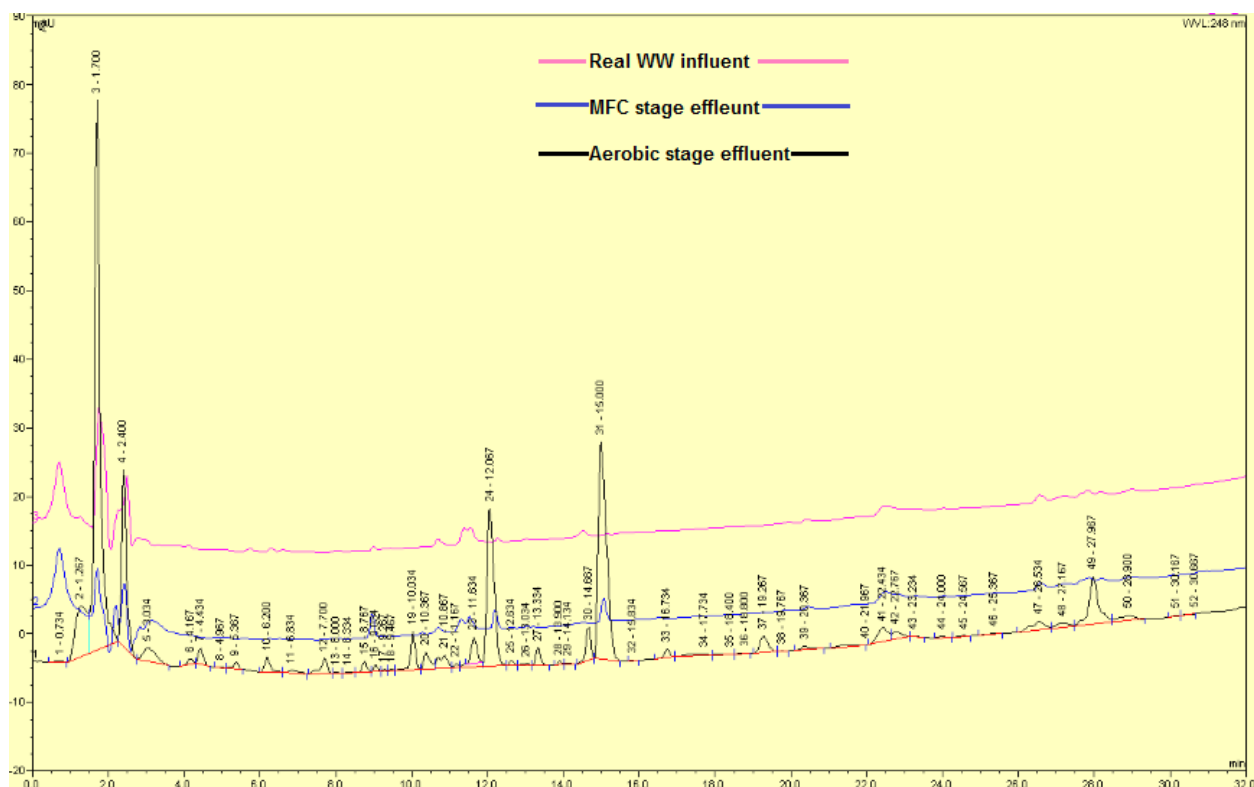


**Figure 6.10:** Overlay of HPLC chromatograms of real colour industry wastewater from wool colouring. Compared chromatograms indicate real colour industry wastewater from wool colouring, MFC stage effluent and aerobic stage effluent of the integrated scaled- up bioreactor system.

HPLC chromatograms of the samples obtained from the integrated bioreactor system operating on wool colouring real wastewater being used as the influent feed also indicated that many metabolites were produced at the end of the decolourisation process in the final effluent (aerobic stage effluent) (Figure 6.10). The chromatograms indicate that during the decolourisation process of both types of wastewater, a clear biotransformation of the colouring agents contained in the wastewater takes place. Furthermore, the number of metabolites produced at the end of the aerobic stage is greater than the number of metabolites present at the end of anaerobic MFC stage in both instances where two different types of colour industry wastewater was used (Figures 6.9 and 6.10). This clearly indicates that decolourisation metabolites produced as a result of biotransformation of colouring agents at the MFC stage undergoes further catabolism into simpler compounds in

the aerobic stage. These findings are similar to earlier findings presented in chapter 5, where simulated colour industry wastewater containing AO-7 as the model azo dye compound underwent a sequential biotransformation into aminobenzenes and then other simpler organic compounds in a similar MFC – aerobic combined bioreactor process.

### **6.3. Concluding remarks**

The findings of this study indicate that the MFC – aerobic integrated bioreactor system could be successfully scaled up to suitable scales using numerous MFC modules in order to handle larger colour industry wastewater volumes. The system was capable of effectively handling real wastewater originating from acid dyebaths for wool colouring and leather tanning in continuous flow mode at ambient temperature. The parallel configured MFC connection of numerous MFC modules allowed the current that can be drawn from the system to be enhanced. The findings of this study implies that suitably scaled – up MFC stacks operating in continuous flow mode could potentially be incorporated with aerobic processes such as activated sludge systems in order to treat complex colour industry wastewater. This brings about possibilities of effective colour industry wastewater treatment, good colour removal, detoxification and potential energy recovery with the use of MFCs during wastewater treatment.

## **Chapter 7 - External resistance and redox mediators as potential tools for influencing azo dye reductive decolourisation kinetics in MFCs**



## Summary

Azo moieties of polar and highly charged dyes are thought to undergo reductive degradation into constituent amines in the extracellular milieu of bacterial cells due to their inability to penetrate into cellular interior. The aims of this study were to investigate the influence of MFC external resistance on azo dye reductive degradation kinetics, to investigate microbial community shifts under various  $R_{ext}$ s and to investigate the influence of exogenous addition of synthetic redox mediators on azo dye reductive degradation in MFC anodes. In this study, experiments were conducted in MFCs to investigate the influence of applied external resistance on the reductive decolourisation kinetics of three structurally different commercial azo dyes. The results indicate that at very high current densities (low  $R_{ext}$ ) and very low current densities (high  $R_{ext}$ ), the reductive decolourisation kinetic constants were lower for all three tested azo dyes in comparison to a moderate optimum  $R_{ext}$  (2.2 k $\Omega$ ), close to the internal resistance of the MFC systems. PCR-DGGE of the 16s rRNA gene microbial community fingerprints were distinctly different between experiments that utilised different  $R_{ext}$ s. Molecular phylogenetic microbial profiling indicated that the microbial communities selected at different  $R_{ext}$ s were distinctly different. Exogenous supplementation of the two synthetic electron shuttling compounds Anthraquinone-2,6-disulfonic acid (AQDS) and Anthraquinone-2-sulfonic acid (AQS) was found to enhance decolourisation kinetic constants of AO-7 reductive degradation. The enhanced decolourisation kinetic constants obtained using a moderate  $R_{ext}$  indicates that  $R_{ext}$  can be used as a potential tool for influencing azo dye reductive degradation in MFCs.

The experimental outcomes of the work described in this chapter were published in, Fernando, E., Keshavarz, T., Kyazze, G., 2014b. External resistance as a potential tool for influencing azo dye reductive decolourisation kinetics in microbial fuel cells. *International Biodeterioration & Biodegradation* 89, 7-14

## 7.2. Results and discussion

### 7.2.1. Azo dye degradation kinetics and MFC external resistance

The reductive azo dye degradation constants were significantly higher ( $p < 0.05$ ) compared to open circuit controls under all tested external resistances. This was observed for all three azo dyes used in this study (Figures 7.1A, 7.1B and 7.1C). This suggests that the transfer of reducing equivalents to the azo moiety is more efficient in the electrochemically active environment of an MFC anode in comparison to open circuit controls. A similar trend was observed in a previous study conducted by Kalathil et al, 2012 who reports that a MFC system treating real textile wastewater ( $R_{\text{ext}} = 50 \Omega$ ) indicated 75% colour removal in 48 hours compared to 62% colour removal in a similar time-scale in an open circuit MFC. The open circuit controls (infinite  $R_{\text{ext}}$ ) are analogous to an anaerobic reactor, where the microbes must resort to utilising alternative terminal electron acceptors due to the absence of a functional anode. The highest reductive azo dye degradation constants ( $k$ ) were observed for all tested dyes at the external resistance 2.2 k $\Omega$  and the ( $k$ ) values were significantly higher ( $p < 0.05$ , ANOVA) compared to ( $k$ ) values at other tested external resistances. Moreover, this trend was observed for all three structurally different azo dyes tested in this study. Considering the large molecular weight of the tested azo dyes and their highly charged nature, it can be expected that these dyes are incapable of crossing non-polar biological membranes and penetrating into cellular interior of anolyte microorganisms. Therefore, the transfer of reducing equivalents to reduce azo moieties would occur extracellularly. The experimental evidence in this study suggests that the efficient exo-electrogenic nature of anode microorganisms enhances the rate of azo dye reductive degradation under an optimum external

resistance. The internal resistance of the MFC systems (estimated using polarisation slope method) used in this study varied between  $655 \pm 2.2 \Omega$  -  $1020 \pm 3.7 \Omega$  at all tested external resistances. Menicucci et al, 2006 reported that maximum sustainable current and power obtainable from an MFC system is greatly influenced by the applied external resistance. Therefore, this 'optimum' external resistance may affect the external electron transfer efficiency of the anodic exo-electrogens and may eventually influence azo dye reductive degradation kinetics as observed in the current study. In terms of terminal electron acceptor availability for microbial metabolism, it could be expected that under higher  $R_{ext}$ , more reducing equivalents will be transferred to azo moieties utilised as alternative terminal electron acceptors. But interestingly, in this study, low azo dye reductive decolourisation rates under high  $R_{ext}$  (10 k $\Omega$  and 46 k $\Omega$ ) for all three azo dyes tested were observed. Under high external resistances, mostly fermentative and methanogenic microbial communities become selected in MFCs and the environment for exo-electrogenic bacteria becomes unfavourable (Jung and Regan, 2011). Therefore, this unfavourable environment for exo-electrogens under high  $R_{ext}$  may account for the low azo dye reductive decolourisation rates observed in this study. Conversely, under low  $R_{ext}$  (high current densities), the anode and the azo moieties are competitive terminal electron acceptors and therefore, may account for the low azo dye decolourisation rates observed at low  $R_{ext}$  (10  $\Omega$  and 510  $\Omega$ ) in this study. This is also reflected in the 16s rRNA PCR-DGGE microbial community fingerprints where less microbial diversity is observed at very high and very low  $R_{exts}$  (Figure 7.4A).

Findings of a previous study by Cai et al, 2011 utilising the well-known electrochemically active microorganism *Shewanella oneidensis* MR-1 and sulfonated azo dye Methyl Orange (MO) as the electron acceptor for anaerobic

growth, indicated that *S.oneidensis* can utilise its Mtr respiratory pathway in order to transfer electrons extra cellularly on-to the azo moiety. Mtr respiratory pathway is demonstrated to be essential for reversibly reducing electron carriers such as flavins and electrodes poised at a suitable potential in MFC environments (Coursolle et al, 2010). The findings of the current study indicates that the efficiency of direct/mediated extracellular electron transfer by the MFC anode exoelectrogenic bacteria on-to the azo moiety of structurally diverse azo dyes can be conveniently varied by applied external resistance.

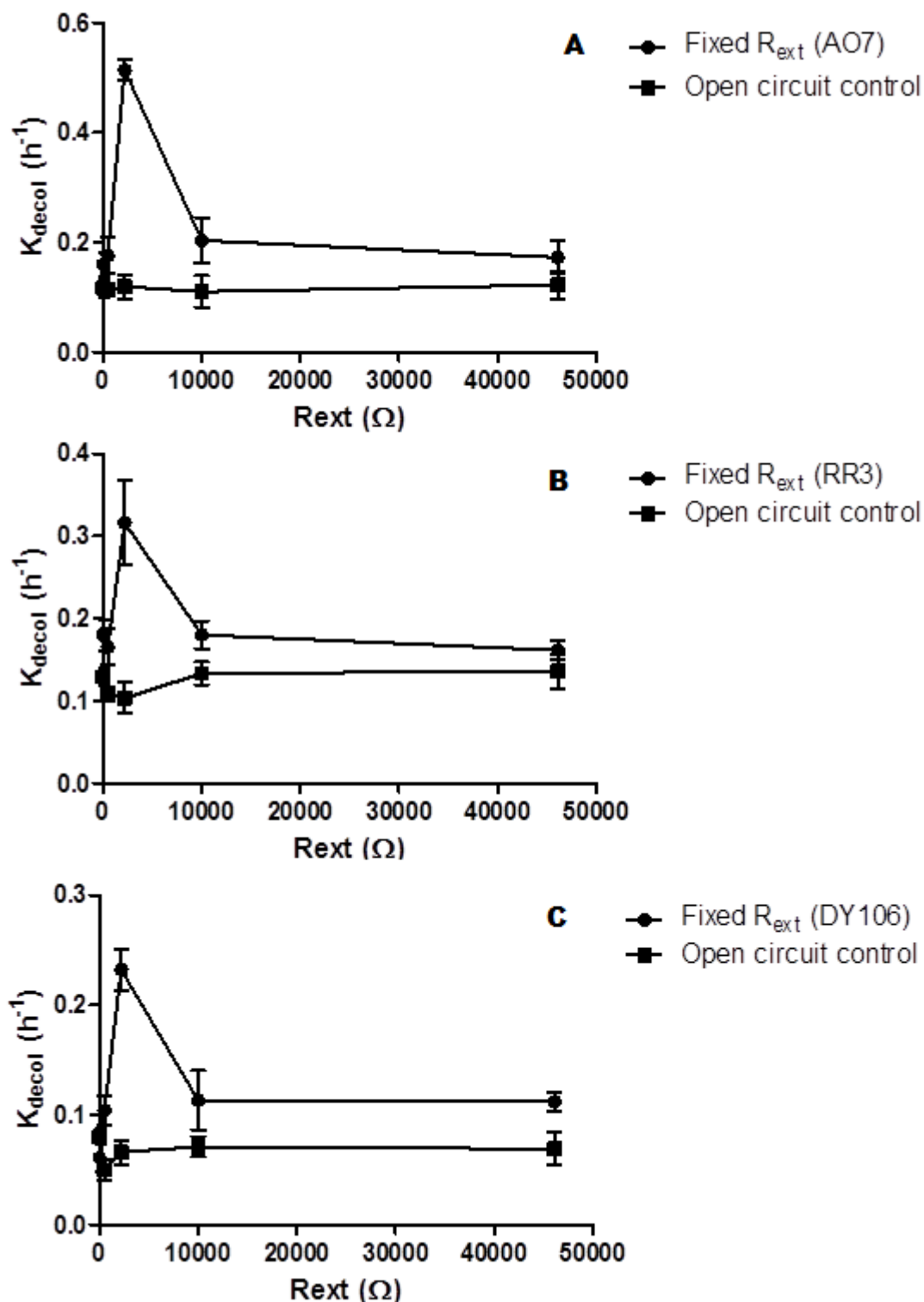


**Figure 7.1:** Decolourisation kinetic constants of azo dyes at various external resistances compared to open circuit controls of A) AO7 B) RR3 and C) DY106 (starting dye concentration for all dyes is 50  $mgL^{-1}$ ).

The decolourisation kinetic constants ( $k$ ) at 2.2  $k\Omega$  indicated 3.2 fold, 1.75 fold and 3.8 fold enhancements compared to ( $k$ ) values of experiments conducted at low

$R_{\text{ext}}$  (10 $\Omega$ ), for AO7, RR3 and DY106 respectively. Similarly, (k) values of decolourisation for AO7, RR3 and DY106 respectively, at 2.2 k $\Omega$  were 3 fold, 1.95 fold and 2.1 fold higher compared to (k) values at high  $R_{\text{ext}}$  (46 k $\Omega$ ).

### **7.2.2. Simultaneous power production in MFCs coupled to azo dye degradation under various external resistances**

The power densities of MFCs operating under various external resistances indicate a similar trend to the decolourisation kinetic constants observed in this study. In the three experiments utilising AO7, RR3 and DY106 in the anodes, their highest power densities were observed when an external resistance of 2.2 k $\Omega$  was applied.  $P_{\text{max}}$  values at 2.2 k $\Omega$   $R_{\text{ext}}$  reached 52 mWm<sup>-2</sup>, 48.3 mWm<sup>-2</sup> and 40.4 mWm<sup>-2</sup> respectively during AO7, RR3 and DY106 reductive degradation in the anode (Figure 7.2). The maximum power densities obtained at 2.2k $\Omega$  external resistance for all three azo dyes were significantly higher ( $P < 0.05$ ) than those obtained at external resistances 10  $\Omega$  and 46 k $\Omega$ . These findings on power densities observed at high current densities (low  $R_{\text{ext}}$ ) are in agreement with the findings of the earlier study conducted by Menicucci et al, 2006. Contrary to findings of this study and the findings by Menicucci et al, 2006 however, Lyon et al, 2010 found that external resistance has little effect on MFC power production. Furthermore, the findings of this study on power densities from the MFCs produced under different external resistances during concomitant reductive degradation of all three azo dyes corroborate with the findings by Katuri et al, 2011.

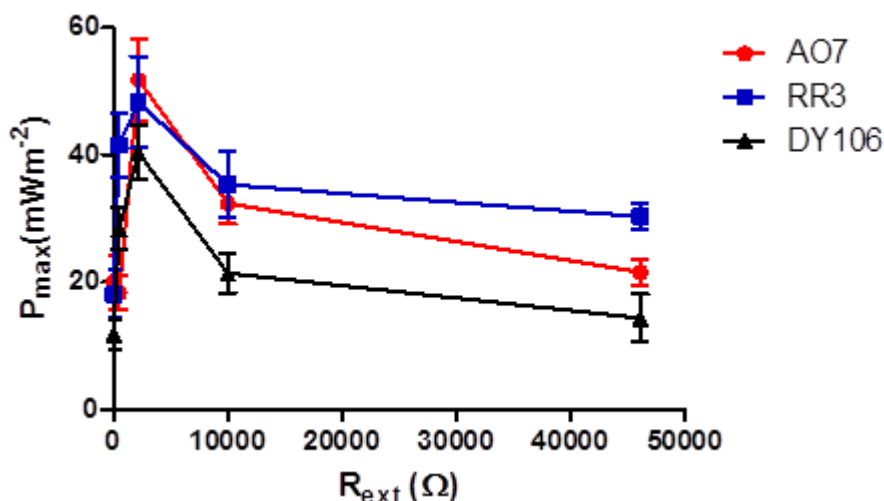


**Figure 7.2:** The variation of maximum power densities obtainable from MFCs during concomitant azo dye degradation in the MFC anode with different applied external resistances.

### 7.2.3. COD reduction in MFCs during azo dye reductive decolourisation under various external resistances

COD reduction (after 72 hours of MFC operation) during azo dye degradation indicated that at high current densities (low  $R_{ext}$  -10 $\Omega$ ), the effluent quality was significantly better ( $p < 0.01$ , one way ANOVA with Tukey post-test) compared to open circuit controls for all tested azo dyes (Figure 7.3). In experiments conducted with three model azo dyes, the COD reduction under all tested external resistances was better compared to open circuit controls.

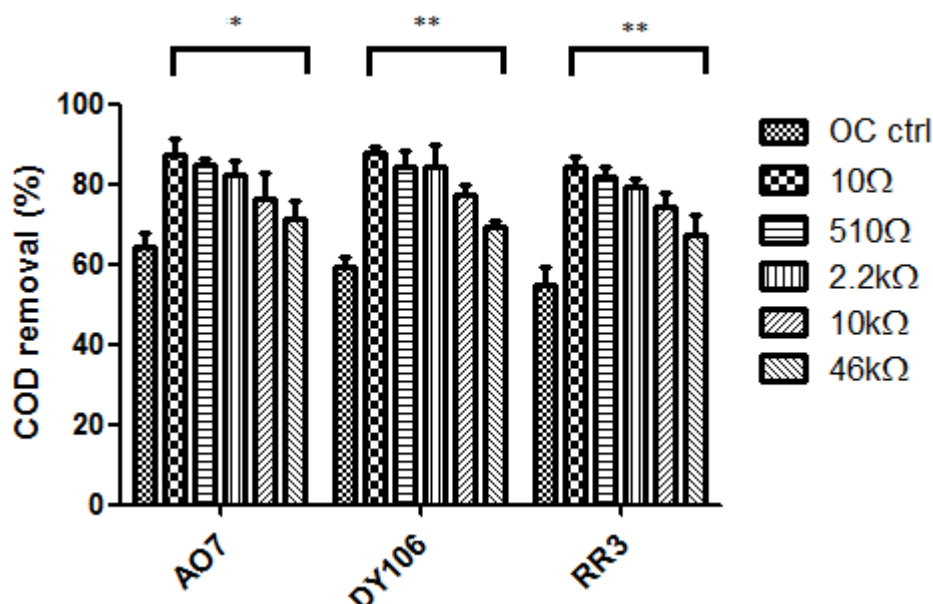


**Figure 7.3:** COD reduction performance of MFC systems at 72 hours of operation during decolourisation experiments of three model azo dyes under various  $R_{ext}$  (\* and \*\* indicates  $p < 0.05$  and  $p < 0.01$  respectively; one way ANOVA and Tukey post-test).

However, the differences in COD removal between low  $R_{ext}$  (10  $\Omega$ ) and 2.2 k $\Omega$   $R_{ext}$  were not statistically significant in all experiments ( $p < 0.05$ , one way ANOVA with Tukey post-test). This clearly indicates that enhanced azo dye decolourisation rates can be achieved by using an ‘optimum’  $R_{ext}$  for a given MFC system without any significant deterioration of COD removal and MFC power production.

#### 7.2.4. Microbial community variations in MFCs under different external resistances

DGGE fingerprints reflecting the different microbial communities selected under different  $R_{exts}$  were distinctly different from each other (Figure 7.4A shows the DGGE fingerprints of MFCs operated under different  $R_{exts}$  utilising AO-7 as the model azo dye). Interestingly, the microbial community DGGE profiles did not significantly differ from each other when different dyes were used. DGGE fingerprint profiles of MFCs operating under the same  $R_{ext}$  but different azo dyes (i.e. AO-7, RR-3 and DY-106) did not differ from each other (DGGE fingerprints



are not shown for RR-3 and DY-106 experiments). Moreover, UPGMA cluster analysis indicates that the bacterial community profiles developed under different  $R_{\text{exts}}$  distinctly differ from each other and from the open circuit control (Figure 7.4B).

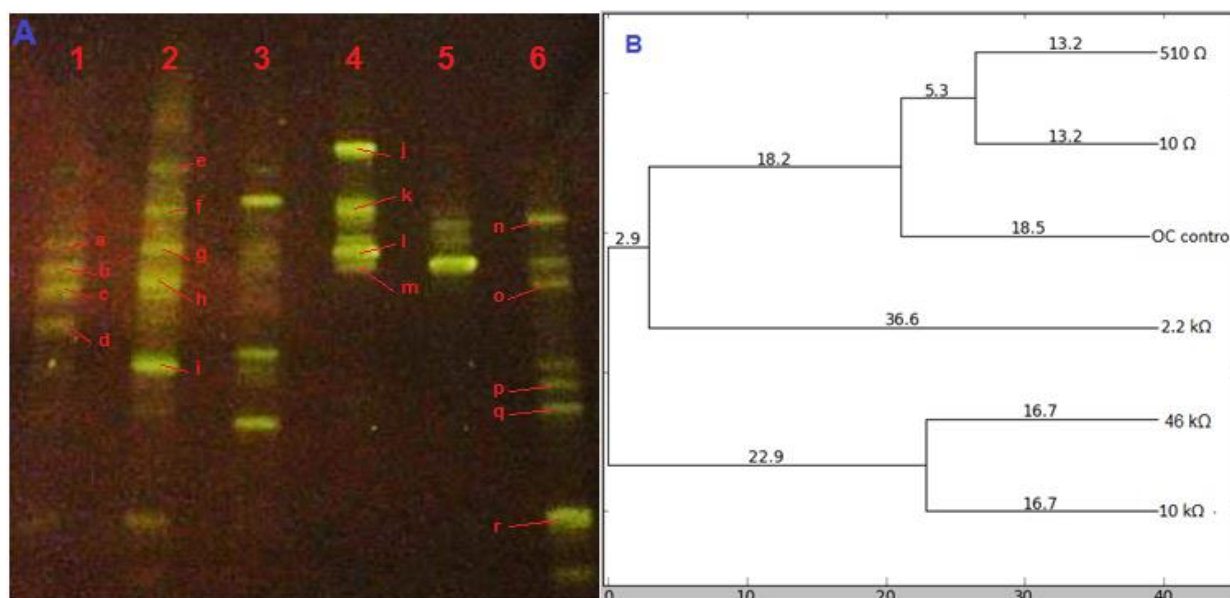


**Figure 7.4:** (A) DGGE fingerprints during AO-7 decolourisation in MFCs operating under various  $R_{\text{exts}}$ . Lanes 1-6 respectively were MFCs operating under 1- 10  $\Omega$ , 2- 510  $\Omega$ , 3- 2.2 k $\Omega$ , 4- 10 k $\Omega$ , 5- 46 k $\Omega$  and 6- open circuit (OC) control. (B) UPGMA cluster dendrogram using Jaccard's coefficient generated from the DGGE fingerprints. The scale bar at the bottom indicates percentage similarity based on Jaccard's coefficient and the figures on the branches represent the distance between the clusters generated.

This further suggests that the different azo dye used has little or no influence on the microbial community selected, whereas the applied external resistance exerts a major effect on the selection of different microbial communities in the MFC anode. Furthermore, the microbial diversity appeared to be enhanced at moderate external resistances (510  $\Omega$  and 2.2 k $\Omega$   $R_{\text{exts}}$  – lanes 2 and 3) compared to extreme low (10  $\Omega$  – lane -1) extreme high (46 k $\Omega$  – lane -5)  $R_{\text{exts}}$ . These enhancements in bacterial diversity observed at moderate  $R_{\text{exts}}$  may account for the enhanced colour removal and power performances observed when the MFC systems are operated at moderate external resistances (close to  $R_{\text{int}}$ ) in this study.

Identification of various bacterial communities selected under various external resistances were identified and profiled using 16s rDNA fingerprinting (Table 7.1).

**Table 7.1:** Phylogenetic affiliations of the 16s rDNA sequences obtained from experiments conducted under various  $R_{\text{exts}}$  and open circuit (OC) control experiments based on the sequences in the 16s ribosomal DNA repository of NCBI.

<b>Band (experiment)</b>	<b>Closest relative (% similarity)</b>	<b>GenBank accession</b>	<b>Phylogenetic affiliation</b>
a (10 $\Omega$ )	<i>Sphingobacterium</i> <i>multivorum</i> strain IAM14316 (100)	NR_040992.1	Bacteroidetes
b (10 $\Omega$ )	<i>Sphingobacterium</i> <i>thalpophilum</i> strain DSM 11723 (95)	NR_042135.1	Bacteroidetes
c (10 $\Omega$ )	<i>Rhodococcus</i> <i>erythropolis</i> strain PR4 (99)	NR_074622.1	Actinobacteria
d (10 $\Omega$ )	<i>Actinomyces funkei</i> strain CCUG 42773 (90)	NR_028960	Actinobacteria
e (510 $\Omega$ )	<i>Dysgonomonas mossii</i> strain DSM22836 (99)	NR_025484.1	Bacteroidetes
f (510 $\Omega$ )	<i>Pseudomonas</i> <i>protegens</i> strain Pf-5 (99)	NR_074599.1	Proteobacteria
g (510 $\Omega$ )	<i>Pseudomonas</i> <i>plecoglossicida</i> strain FPC951 (100)	NR_024662.1	Proteobacteria
h (510 $\Omega$ )	<i>Pelotomaculum</i> <i>propionicicum</i> strain MGP (88)	NR_041000.1	Firmicutes

i (510 $\Omega$ )	<i>Dickeya zeae</i> strain Ech1591 (99)	NR_102824.1	Proteobacteria
j (10 k $\Omega$ )	<i>Klebsiella variicola</i> Strain F2R9 (99)	NR_025635.1	Proteobacteria
k (10 k $\Omega$ )	<i>Klebsiella pneumoniae</i> strain DSM30104 (98)	NR_036794.1	Proteobacteria
l (10 k $\Omega$ )	<i>Pseudomonas</i> <i>plecoglossicida</i> strain FPC951 (99)	NR_024662.1	Proteobacteria
m (10 k $\Omega$ )	<i>Methylobacterium</i> <i>extorquens</i> strain AM1 (98)	NR_074138.1	Proteobacteria
n (OC control)	<i>Pseudomonas putida</i> strain F1 (98)	NR_074739.1	Proteobacteria
o (OC control)	<i>Pseudomonas poae</i> strain RE*1-1-14 (97)	NR_102514.1	Proteobacteria
p (OC control)	<i>Pseudomonas</i> <i>japonica</i> strain IAM15071	NR_074138.1	Proteobacteria
q (OC control)	<i>Clostridium</i> <i>saccharobutylicum</i> Strain P262 (97)	NR_036951.1	Firmicutes
r (OC control)	<i>Clostridium uliginosum</i> strain CK55 (96)	NR_028920.1	Firmicutes

---

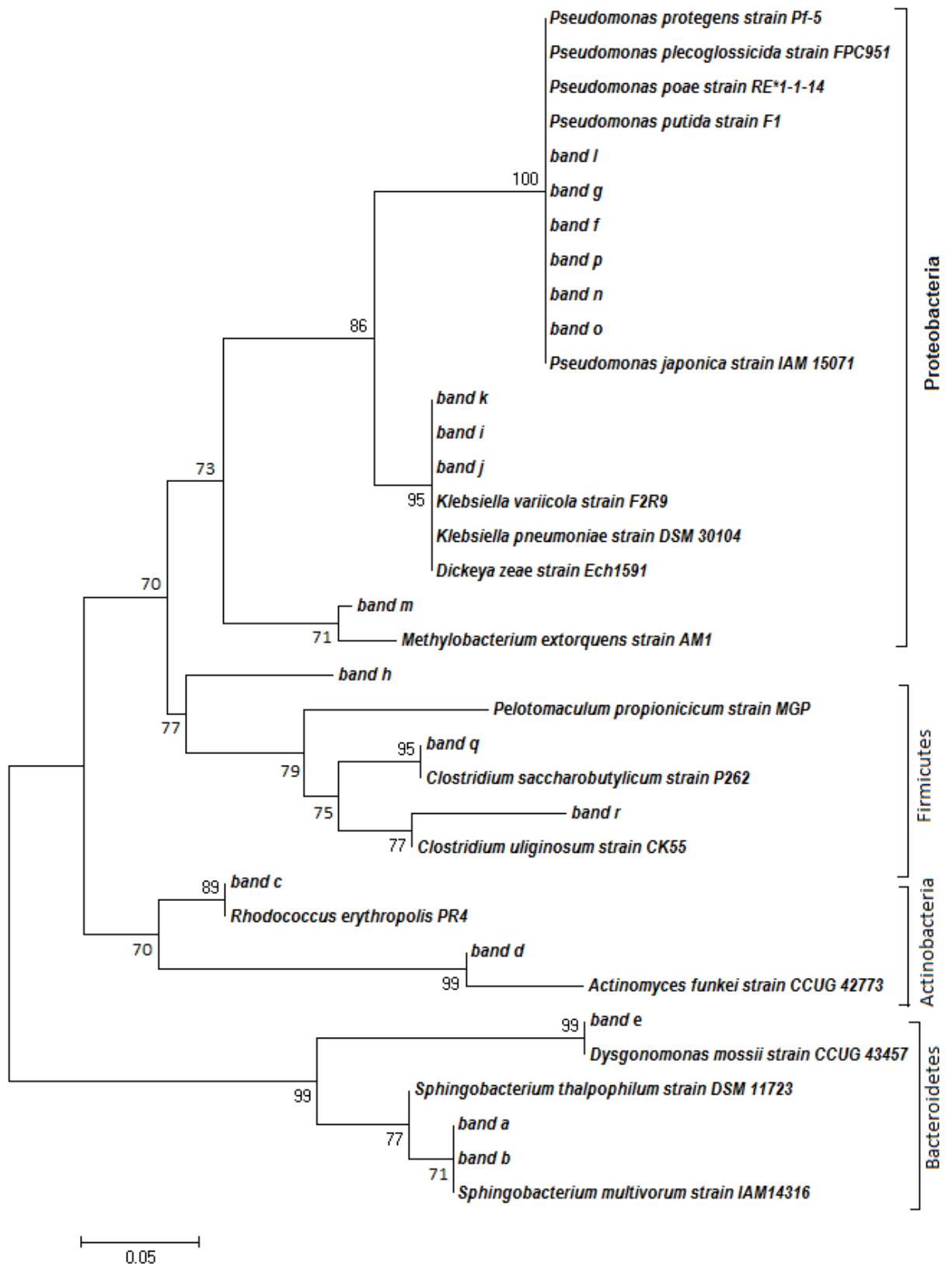


**Figure 7.5:** Phylogenetic tree of the bacterial communities selected in MFC anodes under various  $R_{\text{exts}}$  and open circuit operation constructed using the neighbour joining method. Bootstrap values  $\geq 70\%$  (from 1000 bootstrap replicates) are shown at the nodes of the tree and the scale bar indicates the number of substitutions per site.

Phylogenetic analysis of microbial communities selected at various external resistances and open circuit conditions indicate significant differences in microbial identities (Table 7.1). At open circuit conditions (controls) where the cathode is unable to accept electrons and is analogous to a conventional anaerobic reactor, fermentative anaerobes such as *Clostridium* species were observed with other facultative aerobes belonging to genus *Pseudomonas*. At moderate  $R_{\text{ext}}$  (510  $\Omega$ ), several organisms belonging to phyla such as Proteobacteria (*Pseudomonas protegens*, *Pseudomonas plecoglossicida* and *Dickeya zeae*), Firmicutes (*Pelotomaculum propionicicum*) and Bacteroidetes (*Dysgonomonas mossii*) were selected. At high  $R_{\text{exts}}$  (10 k $\Omega$ ), Proteobacteria belonging to genera such as *Klebsiella*, *Pseudomonas* and *Methylobacterium* were selected. Species belonging to the genus *Klebsiella* are especially known for fermentative growth (Cheng et al, 2010) and therefore, the selection of *Klebsiella* sp. at high  $R_{\text{exts}}$  could be reflective of the electron transfer limitations encountered by the anode organisms at high  $R_{\text{exts}}$ . The low anode potentials that prevail under high  $R_{\text{exts}}$  tend to render the anode ineffective as a terminal electron acceptor (Jung and Regan, 2011). These conditions may favour methanogenic microbial communities rather than exo-electrogenic bacteria. Organisms belonging to the genus *Methylobacterium* are known for their ability to utilise methane as the sole source of carbon and energy (Van Aken et al, 2004). The presence of methane oxidising bacteria such as *Methylobacterium extorquens* could be indicative of high prevalence of methane generating prokaryotes at high  $R_{\text{exts}}$  (10 k $\Omega$ ). No species belonging to phyla Firmicutes and Proteobacteria were identified at low  $R_{\text{ext}}$  (10  $\Omega$ ), whereas species belonging to phyla Actinobacteria (*Rhodococcus* sp. and *Actinomyces* sp) and Bacteroidetes (*Sphingomonas* sp.) were identified. A previous study conducted by Jung and Regan, (2011) found that when the MFCs were operated with an  $R_{\text{ext}}$  close to their internal resistance and subsequently changed to a higher  $R_{\text{ext}}$ ,

significant microbial community shifts do occur. Whereas, decreasing the  $R_{\text{ext}}$  below the  $R_{\text{int}}$  does not significantly influence microbial community structures in acetate fed and glucose fed MFCs. To the contrary of the latter observation however, significant changes in microbial community at low  $R_{\text{exts}}$  (10  $\Omega$ ) from the microbial community at moderately low  $R_{\text{ext}}$  (510  $\Omega$ ) were found in this study (Table 7.1 and Figure 7.5).

### **7.2.5. The effect of exogenous addition of synthetic redox mediators on azo dye decolourisation in MFC anodes**

Synthetic and natural redox mediators such as AQDS, AQS and riboflavin are known to reversibly conduct reduction/oxidation reactions by carrying electrons between various chemical species. Reductive azo dye degradation by means of electron transfer on the azo moieties is an important starting step of any bacterial azo dye degradation strategy. Therefore, it is important to investigate avenues to enhance the reductive degradation of azo dyes in order to avoid it becoming a rate-limiting factor in the process of azo dye biodegradation. Redox mediators are capable of lowering thermodynamic limitations of electron transfer reactions and were reported in several previous studies to be capable of enhancing azo dye reductive degradation kinetics (Dos Santos et al, 2003, Dos Santos et al, 2004, Rodriguez et al, 2012).

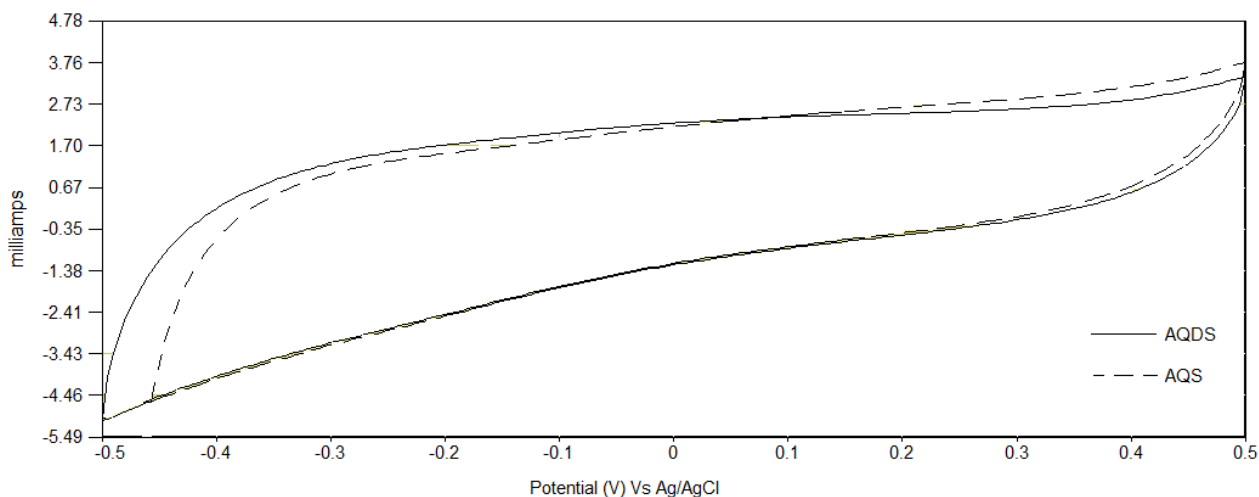
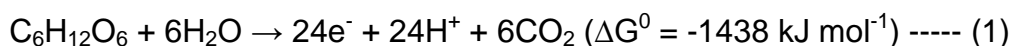


**Figure 7.6:** Cyclic voltammograms of AO-7 containing MFC anodes following the addition of synthetic redox mediators AQDS (solid line) and AQS (dashed line) indicating reversible oxidation-reduction peaks characteristic of redox mediatory role played by these compounds.

Cyclic voltammograms of AQDS and AQS redox mediator containing MFC anodes indicate that these two compounds are indeed capable of ferrying electrons reversibly from and to the anode electrode (Figure 7.6). This suggests that the two synthetic redox compounds used in this study carry out oxidation/reduction reactions in a reversible manner. This further suggests that the presence of such synthetic electron shuttling compounds would assist ferrying electrons to the azo moieties of various azo dyes if they were included in the MFC anode.

In this view, the presence of compounds that are capable of ferrying electrons reversibly to azo moieties of various azo dyes would be beneficial in enhancing reductive degradation kinetics and faster attenuation of dyes from synthetic wastewater. The two synthetic redox mediators AQDS and AQS were used in a range of concentrations in this study in order to investigate the possible azo dye degradation kinetic enhancements in microbial fuel cells. A portion of the reducing equivalents released as a result of oxidation of organic substrate (glucose in this study) will be diverted to reducing the azo moieties while the remainder of the

reducing equivalents will be transferred to the anode by the exo-electrogenic bacteria (assuming that no other electron sinks are present in the anode medium).



The thermodynamic barriers of electron transfer on to the azo moieties leading to their reductive degradation are expected to be lowered by the presence of the two redox mediators AQDS and AQS.

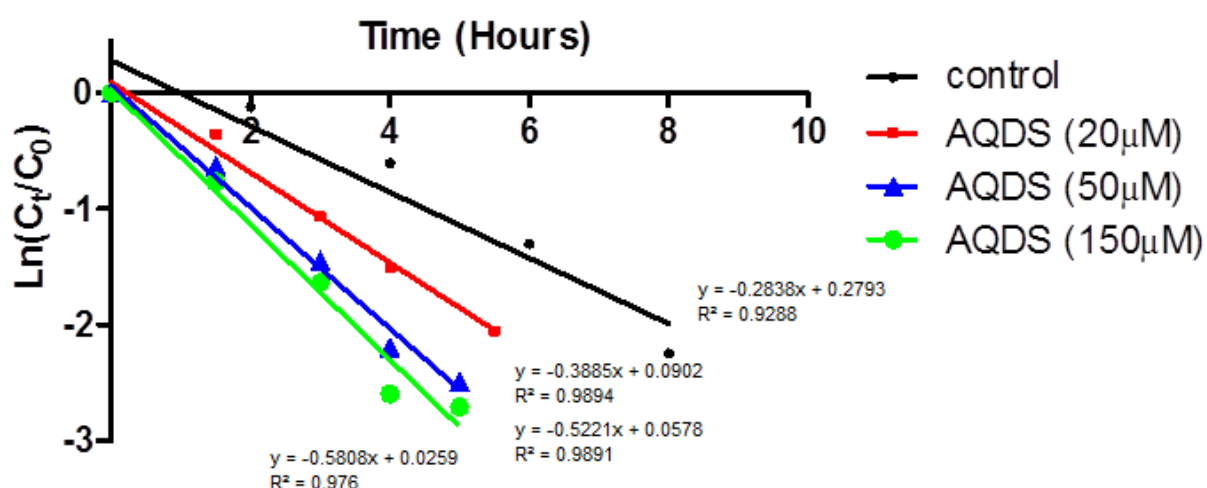


**Figure 7.7:** The concentration dependant effect of the exogenous supplementation of the redox mediator AQDS on the first-order decolourisation kinetic constants ( $k$ ) of the azo dye AO-7 in MFC anodes (AO-7 concentration =  $210 \text{ mgL}^{-1}$ )



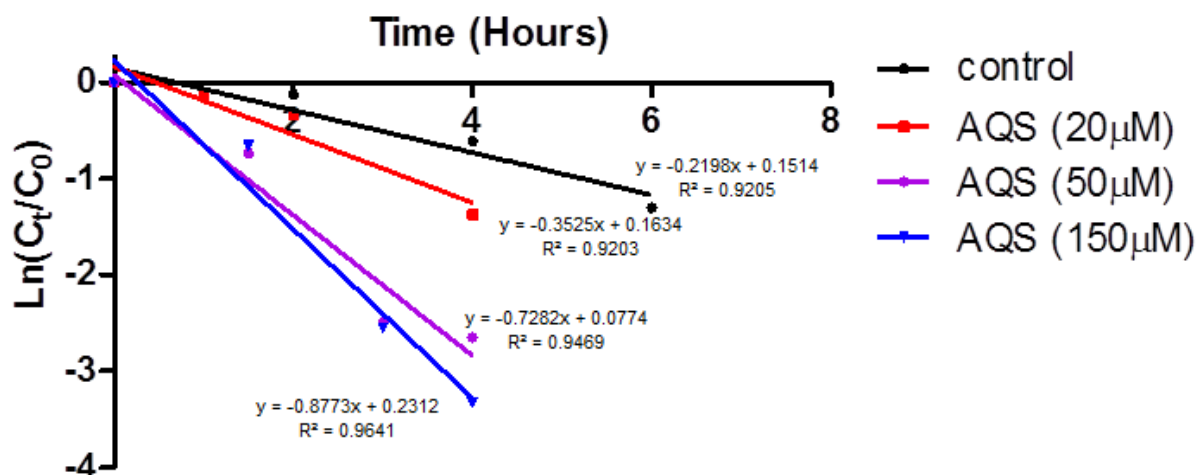


**Figure 7.8:** The concentration dependant effect of the exogenous supplementation of the redox mediator AQS on the first-order decolourisation kinetic constants ( $k$ ) of the azo dye AO-7 in MFC anodes (AO-7 concentration = 210 mgL<sup>-1</sup>)

The enhancement of AO-7 decolourisation observed in this study as a result of the addition of synthetic redox mediators indicated a concentration-dependant effect. The first order kinetic constants were significantly enhanced in both experiments where AQDS and AQS were utilised as electron shuttles. The AO-7 decolourisation kinetic constants were significantly improved ( $p < 0.05$ , ANOVA) compared to controls (no mediator) from 0.28 h<sup>-1</sup> and 0.22 h<sup>-1</sup> to 0.58 h<sup>-1</sup> and 0.88 h<sup>-1</sup> (mediator concentration – 150 μM) respectively for AQDS and AQS (Figures 7.7 and 7.8).

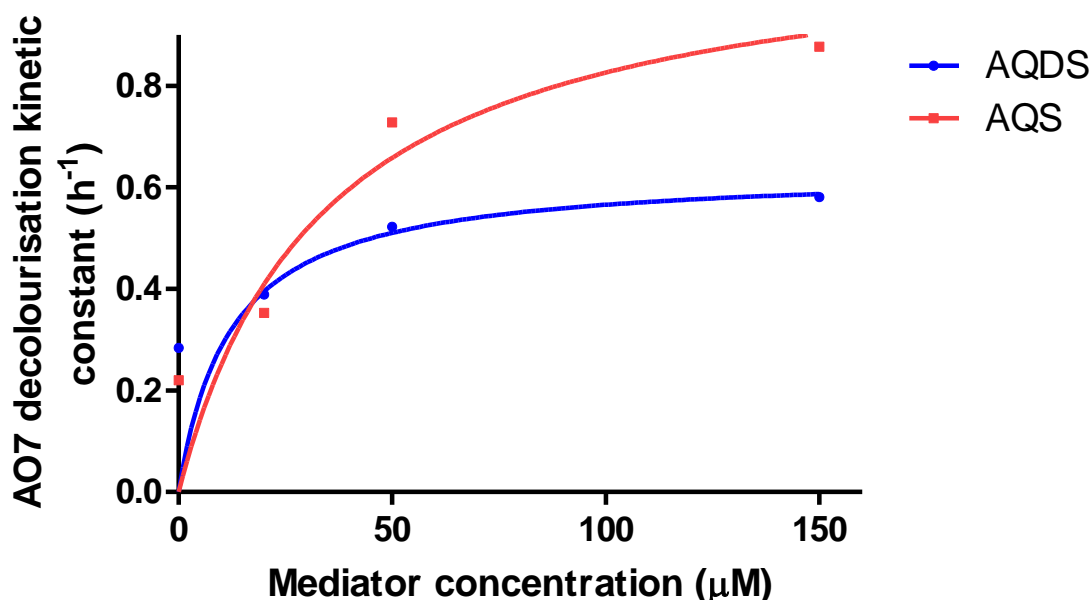


**Figure 7.9:** The non-linear saturation – type relationship between the mediator concentration in MFC anodes and AO-7 decolourisation kinetic constants ( $k$ ) for AQDS and AQS

The relationship between the AO-7 decolourisation kinetic constant ( $k$ ) and the mediator concentration (in both experiments where AQDS or AQS were utilised) was not linear, but rather exhibited a saturation-type hyperbolic relationship (Figure 7.9). It is widely accepted that a reductive-oxidative sequential biodegradation approach is suitable for achieving full degradation of azo dyes in potential industrial applications (O'Neill et al, 2000, Pandey et al, 2007). Therefore, avoiding kinetic limitations in the initial reductive degradation step of azo dyes is extremely important in order to circumvent any possible bottlenecks in the overall process. Therefore, when MFCs are considered for potential industrial or pilot scale azo dye removal applications, optimisation of the anode potential by means of optimising the  $R_{\text{ext}}$  and exogenous addition of synthetic or natural electron shuttling compounds may assist in enhancing the overall efficiency of azo dye removal process.

### 7.3. Concluding remarks

The outcome of the work indicates that microbial fuel cell external resistance can be used as a potential tool for influencing azo dye reductive degradation kinetics. The influence of  $R_{\text{ext}}$  on exo-electrogenic bacteria for optimum power production can be utilised to enhance the efficiency of reductive degradation of azo moieties of various azo dye compounds. The choice of the external resistance for achieving optimum azo dye reductive degradation kinetics did not significantly deteriorate the effluent quality in terms of COD removal. Apart from influencing azo dye degradation kinetics and MFC power outputs, the variations in  $R_{\text{ext}}$  significantly influenced the selection of significantly diverse microbial communities in the MFC anodes. Furthermore, exogenous supplementation of electron shuttling compounds could further enhance azo dye reductive decolourisation kinetics. Therefore, these approaches for azo dye reductive degradation kinetic enhancement could potentially be used in the initial stage of the reductive-oxidative two-stage bioprocesses involving microbial fuel cells.

## **Chapter 8 - Conclusions**

The initial study (Chapter 3) utilising AO-7 as the model azo dye in two-chamber MFC anodes demonstrated that enhanced azo dye reductive degradation kinetics can be achieved by employing either *S.oneidensis* pure cultures or mixed anaerobic microbial populations. At the four dye concentrations tested ( $35 \text{ mgL}^{-1}$ ,  $70 \text{ mgL}^{-1}$ ,  $195 \text{ mgL}^{-1}$  and  $350 \text{ mgL}^{-1}$ ), colour removal efficiencies exceeding 98% were reached within 30 hours of MFC operation. The decolourisation kinetic constants ( $k$ ) indicated a concentration – dependant decrease from  $0.709 \pm 0.05 \text{ h}^{-1}$  to  $0.05 \pm 0.01 \text{ h}^{-1}$  when the azo dye concentration was raised from  $35 \text{ mgL}^{-1}$  to  $350 \text{ mgL}^{-1}$ . The two constituent amines formed during the decolourisation process were identified as sulfanilic acid (4-aminobenzenesulfonic acid) and 1-amino-2-naphthol. It can be inferred from these results that when the amine degradation products were formed in increasing concentration (i.e. when high concentrations of AO-7 is introduced into MFC anodes), the decolourisation kinetic constants are adversely affected probably due to their toxic effects to the anode microorganisms. The Ames mutagenicity tests subsequently carried out using two Histidine auxotroph strains of *S.typhimurium* confirmed that the mutagenic potential of the decolourisation products increase in a concentration – dependent manner. This clearly indicates that it is potentially dangerous to discharge reductively decolourised AO-7 contaminated wastewater into the environment due to its mutagenic potential and toxicity. Simultaneous bioelectricity generation was achieved during AO-7 reductive degradation at all dye concentrations. This study further demonstrated that cheaper and sustainable substrate types such as molasses and corn-steep liquor can be used as the electron donor for azo dye reductive degradation and concomitant bioelectricity generation in MFC anodes. Fast AO-7 reductive degradation kinetics achieved in this study holds promise for utilising MFC based systems as the initial step of a two-stage anaerobic-aerobic sequential treatment regimen for complete degradation of azo dyes. However, the

toxic and mutagenic amines generated in MFC anodes during AO-7 reductive degradation suggest that the decolourised effluent is not suitable to be released without further aerobic treatment.

In the second study (Chapter 4), the reductive degradation of complex azo dye mixtures under industrially relevant conditions such as high salinities and high temperatures was investigated in two-chamber MFCs. Azo dye contaminated wastewater is more likely to contain many different structurally different dye compounds and may also contain various auxiliary salts such as  $\text{Na}_2\text{SO}_4$  and  $\text{NaCl}$  used during the dyeing process. Hence, it is imperative for any potential wastewater treatment system to be capable of effectively dealing with multiple azo dyes under industrially relevant conditions. A potential system would ideally be capable of operating utilising cheap and sustainable electron donors such as molasses. The azo dye adapted mixed microbial consortium used in this study was capable of effective colour and organic load removal over 90% using molasses as the electron donor during MFC operation with concomitant bioelectricity generation ( $P_{\text{max}} = 16 \text{ mWm}^{-2}$ ). Thermophilic operation at  $50^\circ\text{C}$  allowed for enhanced performances in terms of azo dye degradation kinetic constants ( $k = 0.27\text{h}^{-1}$ ) and MFC bioelectricity generation ( $P_{\text{max}} = 25.6 \text{ mWm}^{-2}$ ) compared to mesophilic operation of MFCs at  $30^\circ\text{C}$ . Furthermore, the MFC systems were capable of effectively removing colour and COD at moderate salinities. The outcome of this study implies that MFC based systems could successfully be employed for effective colour and COD removal from complex azo dye mixtures. The microbial communities selected during azo dye degradation were distinctly different to the microbial communities found in the original mixed bacterial population. It can be inferred that microbial community structure is markedly influenced by the presence of azo dyes in MFC anodes and this may

potentially play an important role in effective degradation of complex azo dye mixtures by the azo dye adapted mixed bacterial population.

In the third study (Chapter 5), the possibility of complete degradation of the model azo dye AO-7 using an integrated MFC – aerobic sequential biotreatment process was investigated. Tubular mono-chamber MFCs operated in continuous mode fed with AO-7 containing synthetic wastewater medium was used in this study. The synthetic wastewater medium was supplemented with molasses to act as the electron donor for azo dye reductive degradation and MFC operation and the reactor system was operated at ambient temperature. The synthetic wastewater medium did not include a buffering system but was instead adjusted with common colour industry wastewater auxiliary salts  $\text{Na}_2\text{SO}_4$  and  $\text{NaCl}$ , in order to provide necessary ionic strength for MFC operation. Colour and soluble COD removal rates in excess of 90% in the final effluent were achieved even when the AO-7 loading rates were incrementally varied from  $70 \text{ gm}^{-3}\text{day}^{-1}$  to  $210 \text{ gm}^{-3}\text{day}^{-1}$ . This suggests that the two-stage integrated bioreactor system is capable of effective colour and organics removal even at high azo dye loading rates. HPLC-MS analysis indicated that aminobenzenes were further degraded into simpler and non-toxic (determined using the *V.fischeri* toxicity assessment procedure) metabolites at the end of the MFC-aerobic two-stage reactor operation. The two-stage system was capable of operating at ambient temperature, often encountering low temperatures and was capable of operating effectively for long operational periods (in excess of 150 days) in continuous mode. This highlights the robustness of such MFC-aerobic integrated reactor systems and therefore, would suit potential industrial scale colour industry wastewater treatment processes. Furthermore, the MFC stage was capable of continues bioelectricity production during azo dye degradation and therefore highlights the additional benefits of such systems in

terms of sustainable bioenergy production. Outcomes of this study implies that MFC based technologies in conjunction with existing wastewater treatment technologies such as activated sludge systems can effectively be used for colour industry wastewater treatment.

In the penultimate study (Chapter 6), an up-scaled version of the MFC – aerobic two stage bioreactor system was used in order to treat real colour industry wastewater originating from acid dyebaths for wool colouring and leather tanning. The system comprised of several mono-chamber MFC units acting in unison in continuous flow mode and had a working volume of 1.2 L. The MFC stage was hydraulically connected to a subsequent aerobic bioreactor stage (2 L working volume) mimicking an activated sludge system in order to achieve more complete degradation of colouring agents found within colour industry wastewater used in the study. The individual MFC modules used in the scaled-up MFC system were connected in parallel configuration with the aim of attaining higher current densities. Colour and COD removal in the final effluents when synthetic wastewater (containing AO-7 as the azo dye) was used, reached over 90% and 85% respectively, suggesting that the scaled up two-stage reactor was in par in terms of performance with the smaller two- stage reactor used in the previous study. When both types of synthetic wastewater were used, colour and COD removal efficiencies of the final effluents exceeded 95% and 80% respectively. Current output ( $1150 \text{ mA m}^{-2}$ ) of the parallel connected MFC modules was found to be an enhancement from single MFC modules ( $550 \text{ mA m}^{-2}$ ), whereas the power densities remained relatively unchanged when the MFC modules were stacked in parallel configuration ( $54 \text{ mW m}^{-2}$  from parallel stacked MFCs compared to  $49 \text{ mW m}^{-2}$  from individual modules). Comparison of HPLC chromatograms of dye contaminated influent wastewater and decolourised final effluent from the aerobic



stage suggested that numerous degradation products were formed during the two-stage biotreatment process. It can be inferred from these findings that modular MFC scale-up could potentially be used in conjunction with other existing wastewater treatment technologies such as activated sludge systems for effective colour and organic removal from colour industry wastewater and concomitant bioelectricity generation.

In the final study (Chapter 7), the influence of applied external resistance ( $R_{\text{ext}}$ ) and exogenous addition of synthetic electron shuttling compounds Anthraquinone-2-sulfonic acid (AQS) and Anthraquinone-2,6-disulfonic acid (AQDS) on the decolourisation kinetics of three model azo dyes AO-7, Reactive red -3 (RR-3) and Direct yellow-106 (DY-106) was investigated in two-chamber MFCs. The  $R_{\text{ext}}$  is known to significantly influence the anode potential and hence, the metabolism of the microbial populations residing in the MFC anode. The reductive decolourisation kinetic constants ( $k$ ) of all three tested azo dyes in MFC anodes were found to be enhanced at moderate  $R_{\text{exts}}$ , whereas application of extremely low ( $10\ \Omega$ ) and extremely high ( $46\ \text{k}\Omega$ )  $R_{\text{exts}}$  considerably hindered decolourisation kinetic constants of all three model dyes. Microbial community dynamic studies indicated that microbial populations being selected under different  $R_{\text{exts}}$  were markedly different. Maximum power densities obtained from the two chamber systems during dye degradation were also found to be higher when moderate  $R_{\text{exts}}$  were used, as opposed to extreme high or extreme low  $R_{\text{exts}}$ . This suggests that application of moderate  $R_{\text{exts}}$  (between  $500\ \Omega$  to  $2.2\ \text{k}\Omega$  in this study) would enhance the selection of exo-electrogenic bacteria, whereas the application of extremes of  $R_{\text{exts}}$  would promote mostly the selection of fermentative microorganisms, eventually leading to a deterioration of azo dye reductive degradation kinetics and MFC power outputs. The addition of synthetic electron

shuttling compounds such as AQDS and AQS enhanced  $k$  values of AO-7 reductive degradation in a concentration-dependant manner. However, at very high mediator concentrations (150  $\mu\text{M}$ ), the  $k$  values indicated a saturation-type non-linear relationship in relation to the mediator concentration. The outcomes of this work demonstrates that  $R_{\text{ext}}$  and the exogenous supplementation of electron shuttling compounds are capable of influencing azo dye reductive degradation kinetics in MFC based colour industry wastewater treatment systems.

## **Chapter 9 - Future work**

The final outcome of this research underscores several areas of potential further study. These may allow further optimisation and improvement of the developed bioelectrochemical systems for colour industry wastewater treatment.

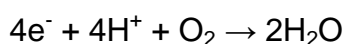
## **9.1. Development of biocathodes for colour industry wastewater treatment**

When two-chamber bioelectrochemical systems are considered, biocathodes are an exciting new prospect in terms sustainability of BES and cost reduction of using abiotic cathode catalysts (i.e. precious metal catalysts). The use of biocathodes eliminates the need for the use of precious metals such as platinum in MFC cathodes (He and Angenent, 2006). Many previous studies demonstrated the potential of biocathodes utilising various microorganisms as the cathode catalyst for the cathodic oxygen reduction reaction in MFCs (Clauwaert et al, 2007, Freguia et al, 2010, Lefebvre et al, 2008, You et al, 2009). The outcomes of current work demonstrated that in order to achieve complete biodegradation of azo dyes in colour industry wastewater by MFC based systems utilising various types of bacteria, a two stage sequential strategy comprising of reductive and oxidative degradation steps is necessary. Therefore, if these reductive and oxidative stages are to be combined in a two-chamber MFC system, the utilisation of a biocathode would be the ideal strategy for the final oxidative degradation step. The colourless but toxic amines generated in the reductive degradation step in MFC anode would be fed into the biocathodes where the amines would undergo further degradation oxidatively in the biocathode. Very few previous studies investigated this possibility of using biocathodes of BES for the treatment of aminobenzenes generated from azo dye reductive degradation (Hou et al, 2012, Liu et al, 2009, Sun et al, 2011, Wang et al, 2013). Therefore, additional work could be carried out in this area in

order to investigate the possibility of utilising biocathodes for the purpose of efficient degradation and detoxification of azo dyes and their harmful transformation products and for simultaneous bioelectricity generation.

## **9.2. The use of enzymes as the cathode catalyst in MFCs for simultaneous azo dye degradation and bioelectricity generation**

The use of peroxidase and phenol oxidase enzymes for the purpose of dye degradation including azo dyes is well documented in previous research (Kwang-Soo and Chang-Jin, 1998, Chivukula and Renganathan, 1995, Spadaro and Ranganathan, 1994). Phenol oxidase enzymes such as laccases and many other peroxidases possess high redox potentials (Xu et al, 1996). Therefore, they could be used for the purpose of electron abstraction from the cathode and subsequent reduction of oxygen to water in the cathodic compartment in MFCs.



This has been demonstrated in several previous studies where the noble metal catalyst cathode was replaced by a laccase catalysed cathode in MFCs (Schaetzle et al, 2009, Szczupak et al, 2012). Considering the ability of phenol oxidases such as laccases to non-specifically degrade dye compounds such as azo dyes, these enzymes could potentially be utilised in MFC cathodes in the twin-role of degrading azo compounds as well as carrying out the vital oxygen reduction reaction without the assistance of any noble metal catalyst. Furthermore, enzyme immobilisation on electrode surfaces could enhance the catalytic efficiency and the longevity of the active form of the enzyme than when suspended in solution. Hence the use of laccase, other phenol oxidases and peroxidase enzymes as the

cathode catalysts in MFCs and dye degrading agents in biocathodes would be an exciting area of further study.

### **9.3. Integrating advanced oxidation processes (AOP) with MFCs for complete azo dye degradation**

Many AOP based processes have previously been studied and demonstrated to possess the capability to degrade dye compounds. The use of MFC's for *in-situ* generation of  $\text{H}_2\text{O}_2$  and hydroxyl radical has been demonstrated in a few recent studies (Fu et al, 2010, Liu et al, 2011, Zhu and Logan, 2013). *In-situ* generation of Fenton's reagent or hydroxyl radicals holds great potential for degradation and detoxification of dye compounds and their biological transformation products such as aminobenzenes. Controlling the cathode half-cell potential to around 600 mV in two chamber MFCs would lead to the generation of  $\text{H}_2\text{O}_2$  in the catholyte. When combined with a suitable source of  $\text{Fe}^{3+}$  in the catholyte, *in-situ* generation of the Fenton's reagent at the cathode end of MFCs can be achieved for wastewater treatment purposes. Hence, more research into MFC/AOP integrated systems would be beneficial in view of developing bioelectrochemical systems that are capable of effectively dealing with colour industry wastewater.

## **9.4. Incorporating molecular and synthetic biology approaches for engineering microbes that are better capable of extracellular electron transfer**

Engineering microbes that are capable of efficient extracellular electron transfer is considered as an attractive and novel way of enhancing the performance of BES including MFCs. It could also be expected that employing such microbes with enhanced capabilities of extracellular electron transfer (EET) could also be beneficial in reductive degradation of various azo dye pollutants. In this view, the heterologous expression of proteins that are thought to be involved in external electron transfer in hosts such as *Escherichia coli* seems very attractive. Particularly, the membrane-bound cytochromes such as Mtr, Cym and Omc proteins that are demonstrated to be linked to extracellular electron transfer in hosts such as *E.coli* confers several benefits. Firstly, high rates of EET could be achieved when rapid growth rates of organisms such as *E.coli* are modified to express fully functional EET related proteins. Secondly, the heterologous expression of such proteins in hosts such as *E.coli* would be more convenient because a highly developed molecular toolkit is already available for genetically manipulating organisms such as *E.coli*. Hitherto, only a few reports of published work can be found relating to heterologous expression of EET proteins in *E.coli*. Many of the EET proteins that were heterologously expressed were *S.oneidensis* cytochromes such as MtrA (Pitts et al, 2003), CymA (Gescher et al, 2008) and OmcA (Donald et al, 2008). All of these EET genes that were heterologously expressed in *E.coli* were demonstrated to be functional and were shown to reduce electron acceptors such as  $\text{Fe}^{3+}$  and other insoluble electron acceptors such as poised electrodes. Hence, this suggests that heterologous expression of one or

several EET capable genes in hosts such as *E.coli* would be beneficial in improving electrochemical performance in BES including MFCs.



# References

Aelterman, P., Rabaey, K., Pham, H.T., Boon, N., Verstraete, W., 2006.

Continuous Electricity Generation at High Voltages and Currents Using Stacked Microbial Fuel Cells. *Environmental science & technology* 40, 3388-3394.

Aeschbacher, M., Sander, M., Schwarzenbach, R.P., 2009. Novel electrochemical approach to assess the redox properties of humic substances. *Environmental science & technology* 44, 87-93.

Al-Kdasi, A., Idris, A., Saed, K., Guan, C.T., 2004. Treatment of textile wastewater by advanced oxidation processes—a review. *Global Nest Int J* 6, 222-230.

Aleboyeh, A., Moussa, Y., Aleboyeh, H., 2005. Kinetics of oxidative decolourisation of Acid Orange 7 in water by ultraviolet radiation in the presence of hydrogen peroxide. *Separation and Purification Technology* 43, 143-148.

Annweiler, E., Richnow, H.H., Antranikian, G., Hebenbrock, S., Garms, C., Franke, S., Francke, W., Michaelis, W., 2000. Naphthalene Degradation and Incorporation of Naphthalene-Derived Carbon into Biomass by the Thermophile *Bacillus thermoleovorans*. *Applied and Environmental Microbiology* 66, 518-523.

Antolini, E., Passos, R.R., Ticianelli, E.A. 2002. Effects of the cathode gas diffusion layer characteristics on the performance of polymer electrolyte fuel cells. *Journal of Applied Electrochemistry* 32, 383-388.

Ayed, L., Mahdhi, A., Cheref, A., Bakhrouf, A., 2011. Decolorization and degradation of azo dye Methyl Red by an isolated *Sphingomonas paucimobilis*: Biotoxicity and metabolites characterization. *Desalination* 274, 272-277.

- Banat, I.M., Nigam, P., Singh, D., Marchant, R., 1996. Microbial decolorization of textile-dyecontaining effluents: A review. *Bioresource Technology* 58, 217-227.
- Berk, R.S., Canfield, J.H., 1964. Bioelectrochemical energy conversion. *Applied microbiology* 12, 10-12.
- Brás, R., Isabel A. Ferra, M., Pinheiro, H.M., Gonçalves, I.C., 2001. Batch tests for assessing decolourisation of azo dyes by methanogenic and mixed cultures. *Journal of Biotechnology* 89, 155-162.
- Cai, P.-J., Xiao, X., He, Y.-R., Li, W.-W., Chu, J., Wu, C., He, M.-X., Zhang, Z., Sheng, G.-P., Lam, M.-W., Xu, F., Yu, H.-Q., 2012. Anaerobic biodecolorization mechanism of methyl orange by *Shewanella oneidensis* MR-1. *Applied Microbiology and Biotechnology* 93, 1769-1776.
- Capar, G., Yetis, U., Yilmaz, L., 2006. Membrane based strategies for the pre-treatment of acid dye bath wastewaters. *Journal of Hazardous Materials* 135, 423-430.
- Carvalho, C., Fernandes, A., Lopes, A., Pinheiro, H., Gonçalves, I., 2007. Electrochemical degradation applied to the metabolites of Acid Orange 7 anaerobic biotreatment. *Chemosphere* 67, 1316-1324.
- Cervantes, F., Dos Santos, A., 2011. Reduction of azo dyes by anaerobic bacteria: microbiological and biochemical aspects. *Reviews in Environmental Science and Bio/Technology* 10, 125-137.
- Chacón, J.M., Teresa Leal, M., Sánchez, M., Bandala, E.R., 2006. Solar photocatalytic degradation of azo-dyes by photo-Fenton process. *Dyes and Pigments* 69, 144-150.

Chen, B.-Y., Lin, K.-W., Wang, Y.-M., Yen, C.-Y., 2009. Revealing interactive toxicity of aromatic amines to azo dye decolorizer *Aeromonas hydrophila*. *Journal of Hazardous Materials* 166, 187-194.

Chen, S., Liu, G., Zhang, R., Qin, B., Luo, Y., 2012. Development of the Microbial Electrolysis Desalination and Chemical-Production Cell for Desalination as Well as Acid and Alkali Productions. *Environmental science & technology* 46, 2467-2472.

Cheng, K.-K., Liu, Q., Zhang, J.-A., Li, J.-P., Xu, J.-M., Wang, G.-H., 2010. Improved 2,3-butanediol production from corncob acid hydrolysate by fed-batch fermentation using *Klebsiella oxytoca*. *Process Biochemistry* 45, 613-616.

Cheng, S., Liu, H., Logan, B.E., 2005. Power Densities Using Different Cathode Catalysts (Pt and CoTMPP) and Polymer Binders (Nafion and PTFE) in Single Chamber Microbial Fuel Cells. *Environmental science & technology* 40, 364-369.

Chengalroyen, M., Dabbs, E., 2013. The microbial degradation of azo dyes: minireview. *World Journal of Microbiology and Biotechnology* 29, 389-399.

Chequer, F.M.D., Angeli, J.P.F., Ferraz, E.R.A., Tsuboy, M.S., Marcarini, J.C., Mantovani, M.S., de Oliveira, D.P., 2009. The azo dyes Disperse Red 1 and Disperse Orange 1 increase the micronuclei frequencies in human lymphocytes and in HepG2 cells. *Mutation Research/Genetic Toxicology and Environmental Mutagenesis* 676, 83-86.

Chequer, F.M.D., Lizier, T.M., de Felício, R., Zanoni, M.V.B., Debonsi, H.M., Lopes, N.P., Marcos, R., de Oliveira, D.P., 2011. Analyses of the genotoxic and mutagenic potential of the products formed after the biotransformation of the azo dye Disperse Red 1. *Toxicology in Vitro* 25, 2054-2063.

- Chiou, M.S., Li, H.Y., 2003. Adsorption behavior of reactive dye in aqueous solution on chemical cross-linked chitosan beads. *Chemosphere* 50, 1095-1105.
- Chivukula, M., Renganathan, V., 1995. Phenolic Azo Dye Oxidation by Laccase from *Pyricularia oryzae*. *Applied and Environmental Microbiology* 61, 4374-4377.
- Chou, W.-L., Wang, C.-T., Chang, C.-P., 2011. Comparison of removal of Acid Orange 7 by electrooxidation using various anode materials. *Desalination* 266, 201-207.
- Christie, R.M., 2001. *Colour chemistry*. Royal Society of Chemistry.
- Clauwaert, P., van der Ha, D., Boon, N., Verbeken, K., Verhaege, M., Rabaey, K., Verstraete, W., 2007. Open Air Biocathode Enables Effective Electricity Generation with Microbial Fuel Cells. *Environmental Science & Technology* 41, 7564-7569.
- Cohen, 1931. The bacterial culture as an electrical half-cell. *Journal of Bacteriology* 21, 18-19.
- Coursolle, D., Baron, D.B., Bond, D.R., Gralnick, J.A., 2010. The Mtr Respiratory Pathway Is Essential for Reducing Flavins and Electrodes in *Shewanella oneidensis*. *Journal of Bacteriology* 192, 467-474.
- Cui, D., Guo, Y.-Q., Lee, H.-S., Cheng, H.-Y., Liang, B., Kong, F.-Y., Huang, L.-P., Xu, M.-Y., Wang, A.-J., 2013. Efficient azo dye removal in bioelectrochemical system and post-aerobic bioreactor: optimization and characterization. *Chemical Engineering Journal* 243, 355 -363.
- Ding, H., Li, Y., Lu, A., Jin, S., Quan, C., Wang, C., Wang, X., Zeng, C., Yan, Y., 2010. Photocatalytically improved azo dye reduction in a microbial fuel cell with rutile-cathode. *Bioresource Technology* 101, 3500-3505.

Doble, M., Kumar, A., 2005. Biotreatment of industrial effluents. Butterworth-Heinemann.

dos Santos, A.B., Bisschops, I.A.E., Cervantes, F.J., van Lier, J.B., 2004. Effect of different redox mediators during thermophilic azo dye reduction by anaerobic granular sludge and comparative study between mesophilic (30 °C) and thermophilic (55 °C) treatments for decolourisation of textile wastewaters. *Chemosphere* 55, 1149-1157.

dos Santos, A.B., Cervantes, F.J., Yaya-Beas, R.E., van Lier, J.B., 2003. Effect of redox mediator, AQDS, on the decolourisation of a reactive azo dye containing triazine group in a thermophilic anaerobic EGSB reactor. *Enzyme and Microbial Technology* 33, 942-951.

Donald, J.W., Hicks, M.G., Richardson, D.J., Palmer, T., 2008. The c-Type Cytochrome OmcA Localizes to the Outer Membrane upon Heterologous Expression in *Escherichia coli*. *Journal of Bacteriology* 190, 5127-5131.

El-Desoky, H.S., Ghoneim, M.M., Zidan, N.M., 2010. Decolorization and degradation of Ponceau S azo-dye in aqueous solutions by the electrochemical advanced Fenton oxidation. *Desalination* 264, 143-150.

Engel, E., Ulrich, H., Vasold, R., König, B., Landthaler, M., Süttinger, R., Bäuml, W., 2007. Azo pigments and a basal cell carcinoma at the thumb. *Dermatology* 216, 76-80.

Erkurt, H.A., 2010. Biodegradation of Azo Dyes. Springer.

Espantaleón, A.G., Nieto, J.A., Fernández, M., Marsal, A., 2003. Use of activated clays in the removal of dyes and surfactants from tannery waste waters. *Applied Clay Science* 24, 105-110.

- Fan, Y., Sharbrough, E., Liu, H., 2008. Quantification of the Internal Resistance Distribution of Microbial Fuel Cells. *Environmental Science & Technology* 42, 8101-8107.
- Fang, Z., Song, H.-L., Cang, N., Li, X.-N., 2013. Performance of microbial fuel cell coupled constructed wetland system for decolorization of azo dye and bioelectricity generation. *Bioresource Technology* 144, 165-171.
- Ferraz, E.R.A., Grando, M.D., Oliveira, D.P., 2011. The azo dye Disperse Orange 1 induces DNA damage and cytotoxic effects but does not cause ecotoxic effects in *Daphnia similis* and *Vibrio fischeri*. *Journal of Hazardous Materials* 192, 628-633.
- Foley, J.M., Rozendal, R.A., Hertle, C.K., Lant, P.A., Rabaey, K., 2010. Life Cycle Assessment of High-Rate Anaerobic Treatment, Microbial Fuel Cells, and Microbial Electrolysis Cells. *Environmental science & technology* 44, 3629-3637.
- Freguia, S., Tsujimura, S., Kano, K., 2010. Electron transfer pathways in microbial oxygen biocathodes. *Electrochimica Acta* 55, 813-818.
- Fu, L., You, S.-J., Zhang, G.-q., Yang, F.-L., Fang, X.-h., 2010. Degradation of azo dyes using in-situ Fenton reaction incorporated into H<sub>2</sub>O<sub>2</sub>-producing microbial fuel cell. *Chemical Engineering Journal* 160, 164-169.
- Fu, Y., Viraraghavan, T., 2001. Fungal decolorization of dye wastewaters: a review. *Bioresource Technology* 79, 251-262.
- Gan, H.M., Chew, T.H., Tay, Y.-L., Lye, S.F., Yahya, A., 2012. Genome Sequence of *Ralstonia* sp. Strain PBA, a Bacterium Involved in the Biodegradation of 4-Aminobenzenesulfonate. *Journal of Bacteriology* 194, 5139-5140.

- Gaudet, I., 1994. Standard procedure for MICROTOX analysis. Alberta Environmental Centre.
- Gescher, J.S., Cordova, C.D., Spormann, A.M., 2008. Dissimilatory iron reduction in *Escherichia coli*: identification of CymA of *Shewanella oneidensis* and NapC of *E. coli* as ferric reductases. *Molecular microbiology* 68, 706-719.
- Gomes, J., Steiner, W., 1998. Production of a high activity of an extremely thermostable  $\beta$ -mannanase by the thermophilic eubacterium *Rhodothermus marinus*, grown on locust bean gum. *Biotechnology Letters* 20, 729-733.
- Gottlieb, A., Shaw, C., Smith, A., Wheatley, A., Forsythe, S., 2003. The toxicity of textile reactive azo dyes after hydrolysis and decolourisation. *Journal of Biotechnology* 101, 49-56.
- Guivarch, E., Trevin, S., Lahitte, C., Oturan, M., 2003. Degradation of azo dyes in water by Electro-Fenton process. *Environmental Chemistry Letters* 1, 38-44.
- Guzman, J.J., Cooke, K.G., Gay, M.O., Radachowsky, S.E., Girguis, P.R., Chiu, M.A., 2010. Benthic microbial fuel cells: long-term power sources for wireless marine sensor networks, SPIE Defense, Security, and Sensing. *International Society for Optics and Photonics*, pp. 76662M-76662M-76612.
- HaoYu, E., Cheng, S., Scott, K., Logan, B., 2007. Microbial fuel cell performance with non-Pt cathode catalysts. *Journal of Power Sources* 171, 275-281.
- Harazono, K., Nakamura, K., 2005. Decolorization of mixtures of different reactive textile dyes by the white-rot basidiomycete *Phanerochaete sordida* and inhibitory effect of polyvinyl alcohol. *Chemosphere* 59, 63-68.
- Hawkes, F. R., Kim, J., Kyazze, G., Premier, G. C, Guwy, A. 2010. "Feedstocks for BES conversions". In: Rabaey, K., Angenent, L. T., Shroeder, U., Keller, J.

Bioelectrochemical systems: From extracellular electron transfer to biotechnological application. London: IWA Publishing, pp- 369-388.

He, Z., Angenent, L.T., 2006. Application of Bacterial Biocathodes in Microbial Fuel Cells. *Electroanalysis* 18, 2009-2015.

Hou, B., Hu, Y., Sun, J., 2012. Performance and microbial diversity of microbial fuel cells coupled with different cathode types during simultaneous azo dye decolorization and electricity generation. *Bioresource Technology* 111, 105-110.

Ieropoulos, I., Greenman, J., Melhuish, C., 2008. Microbial fuel cells based on carbon veil electrodes: Stack configuration and scalability. *International Journal of Energy Research* 32, 1228-1240.

Ieropoulos, I.A., Greenman, J., Melhuish, C., Hart, J., 2005. Comparative study of three types of microbial fuel cell. *Enzyme and Microbial Technology* 37, 238-245.

Inan Beydilli, M., Pavlostathis, S., 2005. Decolorization kinetics of the azo dye Reactive Red 2 under methanogenic conditions: effect of long-term culture acclimation. *Biodegradation* 16, 135-146.

Jain, K., Shah, V., Chapla, D., Madamwar, D., 2012. Decolorization and degradation of azo dye – Reactive Violet 5R by an acclimatized indigenous bacterial mixed cultures-SB4 isolated from anthropogenic dye contaminated soil. *Journal of Hazardous Materials* 213–214, 378-386.

Jung, S., Regan, J.M., 2011. Influence of External Resistance on Electrogenesis, Methanogenesis, and Anode Prokaryotic Communities in Microbial Fuel Cells. *Applied and Environmental Microbiology* 77, 564-571.

Junker, F., Field, J.A., Bangerter, F., Ramsteiner, K., Kohler, H.-P., Joannou, C.L., Mason, J.R., Leisinger, T., Cook, A.M., 1994. Oxygenation and spontaneous



deamination of 2-aminobenzenesulphonic acid in *Alcaligenes* sp. strain O-1 with subsequent meta ring cleavage and spontaneous desulphonation to 2-hydroxymuconic acid. *Biochem. J* 300, 429-436.

Kalathil, S., Lee, J., Cho, M.H., 2012. Efficient decolorization of real dye wastewater and bioelectricity generation using a novel single chamber biocathode-microbial fuel cell. *Bioresource Technology* 119, 22-27.

Kalme, S., Ghodake, G., Govindwar, S., 2007. Red HE7B degradation using desulfonation by *Pseudomonas desmolyticum* NCIM 2112. *International Biodeterioration & Biodegradation* 60, 327-333.

Katuri, K.P., Scott, K., Head, I.M., Picioreanu, C., Curtis, T.P., 2011. Microbial fuel cells meet with external resistance. *Bioresource Technology* 102, 2758-2766.

Khehra, M.S., Saini, H.S., Sharma, D.K., Chadha, B.S., Chimni, S.S., 2006. Biodegradation of azo dye CI Acid Red 88 by an anoxic–aerobic sequential bioreactor. *Dyes and Pigments* 70, 1-7.

Kolekar, Y.M., Pawar, S.P., Gawai, K.R., Lokhande, P.D., Shouche, Y.S., Kodam, K.M., 2008. Decolorization and degradation of Disperse Blue 79 and Acid Orange 10, by *Bacillus fusiformis* KMK5 isolated from the textile dye contaminated soil. *Bioresource Technology* 99, 8999-9003.

Kudlich, M., Hetheridge, M.J., Knackmuss, H.-J., Stolz, A., 1999. Autoxidation Reactions of Different Aromatic o-Aminohydroxynaphthalenes That Are Formed during the Anaerobic Reduction of Sulfonated Azo Dyes. *Environmental Science & Technology* 33, 896-901.

- Kwang-Soo, S., Chang-Jin, K., 1998. Decolorisation of artificial dyes by peroxidase from the white-rot fungus, *Pleurotus ostreatus*. *Biotechnology Letters* 20, 569-572.
- Lefebvre, O., Al-Mamun, A., Ng, H., 2008. A microbial fuel cell equipped with a biocathode for organic removal and denitrification. *Water Science & Technology* 58, 881-885.
- Li, Z., Zhang, X., Lin, J., Han, S., Lei, L., 2010. Azo dye treatment with simultaneous electricity production in an anaerobic–aerobic sequential reactor and microbial fuel cell coupled system. *Bioresource Technology* 101, 4440-4445.
- Liang, P., Huang, X., Fan, M.-Z., Cao, X.-X., Wang, C., 2007. Composition and distribution of internal resistance in three types of microbial fuel cells. *Applied microbiology and biotechnology* 77, 551-558.
- Liu, H., Cheng, S., Logan, B.E., 2005. Power Generation in Fed-Batch Microbial Fuel Cells as a Function of Ionic Strength, Temperature, and Reactor Configuration. *Environmental science & technology* 39, 5488-5493.
- Liu, L., Li, F.-b., Feng, C.-h., Li, X.-z., 2009. Microbial fuel cell with an azo-dye-feeding cathode. *Applied microbiology and biotechnology* 85, 175-183.
- Liu, L., Yuan, Y., Li, F.-b., Feng, C.-h., 2011. In-situ Cr(VI) reduction with electrogenerated hydrogen peroxide driven by iron-reducing bacteria. *Bioresource Technology* 102, 2468-2473.
- Lo, Y.C., Huang, C.-Y., Fu, T.-N., Chen, C.-Y., Chang, J.-S., 2009. Fermentative hydrogen production from hydrolyzed cellulosic feedstock prepared with a thermophilic anaerobic bacterial isolate. *International Journal of Hydrogen Energy* 34, 6189-6200.

- Logan, B.E., Hamelers, B., Rozendal, R., Schröder, U., Keller, J., Freguia, S., Aelterman, P., Verstraete, W., Rabaey, K., 2006. Microbial Fuel Cells: Methodology and Technology†. *Environmental science & technology* 40, 5181-5192.
- Logan, B.E., Murano, C., Scott, K., Gray, N.D., Head, I.M., 2005. Electricity generation from cysteine in a microbial fuel cell. *Water Research* 39, 942-952.
- Lopes, A., Martins, S., Morão, A., Magrinho, M., Gonçalves, I., 2004. Degradation of a Textile Dye C. I. Direct Red 80 by Electrochemical Processes. *Portugaliae Electrochimica Acta* 22, 279-294.
- Luo, H., Jenkins, P.E., Ren, Z., 2010a. Concurrent Desalination and Hydrogen Generation Using Microbial Electrolysis and Desalination Cells. *Environmental science & technology* 45, 340-344.
- Luo, Y., Liu, G., Zhang, R., Zhang, C., 2010b. Power generation from furfural using the microbial fuel cell. *Journal of Power Sources* 195, 190-194.
- Lyon, D.Y., Buret, F., Vogel, T.M., Monier, J.-M., 2010. Is resistance futile? Changing external resistance does not improve microbial fuel cell performance. *Bioelectrochemistry* 78, 2-7.
- Mansour, H., Mosrati, R., Corroler, D., Ghedira, K., Barillier, D., Chekir, L., 2009. In vitro mutagenicity of Acid Violet 7 and its degradation products by *Pseudomonas putida* mt-2: Correlation with chemical structures. *Environmental Toxicology and Pharmacology* 27, 231-236.
- Maron, D.M., Ames, B.N., 1983. Revised methods for the *Salmonella* mutagenicity test. *Mutation Research/Environmental Mutagenesis and Related Subjects* 113, 173-215.

Marsili, E., Baron, D.B., Shikhare, I.D., Coursolle, D., Gralnick, J.A., Bond, D.R., 2008. Shewanella secretes flavins that mediate extracellular electron transfer. *Proceedings of the National Academy of Sciences* 105, 3968-3973.

Martínez-Huitle, C.A., Brillas, E., 2009. Decontamination of wastewaters containing synthetic organic dyes by electrochemical methods: a general review. *Applied Catalysis B: Environmental* 87, 105-145.

Méndez-Paz, D., Omil, F., Lema, J., 2003. Modeling of the Acid Orange 7 anaerobic biodegradation. *Water Science & Technology* 48, 133-139.

Méndez-Paz, D., Omil, F., Lema, J.M., 2005. Anaerobic treatment of azo dye Acid Orange 7 under fed-batch and continuous conditions. *Water Research* 39, 771-778.

Menicucci, J., Beyenal, H., Marsili, E., Veluchamy, Demir, G., Lewandowski, Z., 2005. Procedure for Determining Maximum Sustainable Power Generated by Microbial Fuel Cells. *Environmental science & technology* 40, 1062-1068.

Mu, Y., Rabaey, K., Rozendal, R.A., Yuan, Z., Keller, J.r., 2009a. Decolorization of Azo Dyes in Bioelectrochemical Systems. *Environmental science & technology* 43, 5137-5143.

Mu, Y., Rozendal, R.A., Rabaey, K., Keller, J.r., 2009b. Nitrobenzene Removal in Bioelectrochemical Systems. *Environmental science & technology* 43, 8690-8695.

Murali, V., Ong, S.-A., Ho, L.-N., Wong, Y.-S., 2013. Evaluation of integrated anaerobic–aerobic biofilm reactor for degradation of azo dye methyl orange. *Bioresource Technology* 143, 104-111.

- Mutafov, S., Avramova, T., Stefanova, L., Angelova, B., 2007. Decolorization of Acid Orange 7 by bacteria of different tinctorial type: a comparative study. *World Journal of Microbiology and Biotechnology* 23, 417-422.
- Neamtu, M., Yediler, A., Siminiceanu, I., Macoveanu, M., Kettrup, A., 2004. Decolorization of disperse red 354 azo dye in water by several oxidation processes—a comparative study. *Dyes and Pigments* 60, 61-68.
- Nien, P.-C., Lee, C.-Y., Ho, K.-C., Adav, S.S., Liu, L., Wang, A., Ren, N., Lee, D.-J., 2011. Power overshoot in two-chambered microbial fuel cell (MFC). *Bioresource Technology* 102, 4742-4746.
- Nigam, P., Banat, I.M., Singh, D., Marchant, R., 1996. Microbial process for the decolorization of textile effluent containing azo, diazo and reactive dyes. *Process Biochemistry* 31, 435-442.
- Nogales, J., Canales, Á., Jiménez-Barbero, J., Serra, B., Pingarrón, J.M., García, J.L., Díaz, E., 2011. Unravelling the gallic acid degradation pathway in bacteria: the gal cluster from *Pseudomonas putida*. *Molecular Microbiology* 79, 359-374.
- O'Neill, C., Lopez, A., Esteves, S., Hawkes, F.R., Hawkes, D.L., Wilcox, S., 2000. Azo-dye degradation in an anaerobic-aerobic treatment system operating on simulated textile effluent. *Applied microbiology and biotechnology* 53, 249-254.
- Ogram, A., Saylor, G.S., Barkay, T., 1987. The extraction and purification of microbial DNA from sediments. *Journal of microbiological methods* 7, 57-66.
- Oh, S.-E., Logan, B., 2006. Proton exchange membrane and electrode surface areas as factors that affect power generation in microbial fuel cells. *Applied microbiology and biotechnology* 70, 162-169.

- Ooi, T., Shibata, T., Sato, R., Ohno, H., Kinoshita, S., Thuoc, T.L., Taguchi, S., 2007. An azoreductase, aerobic NADH-dependent flavoprotein discovered from *Bacillus* sp.: functional expression and enzymatic characterization. *Applied microbiology and biotechnology* 75, 377-386.
- Ozkan-Yucel, U.G., Gokcay, C.F., 2013. Effect of anaerobic azo dye reduction on continuous sludge digestion. *CLEAN – Soil, Air, Water*, (in-press).
- Pandey, A., Singh, P., Iyengar, L., 2007. Bacterial decolorization and degradation of azo dyes. *International Biodeterioration & Biodegradation* 59, 73-84.
- Pant, D., Singh, A., Van Bogaert, G., Irving Olsen, S., Singh Nigam, P., Diels, L., Vanbroekhoven, K., 2012. Bioelectrochemical systems (BES) for sustainable energy production and product recovery from organic wastes and industrial wastewaters. *RSC Advances* 2, 1248-1263.
- Park, H.S., Kim, B.H., Kim, H.S., Kim, H.J., Kim, G.T., Kim, M., Chang, I.S., Park, Y.K., Chang, H.I., 2001. A Novel Electrochemically Active and Fe(III)-reducing Bacterium Phylogenetically Related to *Clostridium butyricum* Isolated from a Microbial Fuel Cell. *Anaerobe* 7, 297-306.
- Petrova, S., Volodarskii, M., Makarov, S., Li, L.Z., 2008. Oxidation of azo dyes with inorganic peroxides in the presence of cationic surfactants. *Russian Journal of Applied Chemistry* 81, 1573-1577.
- Pham, H., Boon, N., Marzorati, M., Verstraete, W., 2009. Enhanced removal of 1,2-dichloroethane by anodophilic microbial consortia. *Water Research* 43, 2936-2946.
- Pilatz, S., Breitbach, K., Hein, N., Fehlhaber, B., Schulze, J., Brenneke, B., Eberl, L., Steinmetz, I., 2006. Identification of *Burkholderia pseudomallei* Genes

Required for the Intracellular Life Cycle and In Vivo Virulence. *Infection and Immunity* 74, 3576-3586.

Pitts, K.E., Dobbin, P.S., Reyes-Ramirez, F., Thomson, A.J., Richardson, D.J., Seward, H.E., 2003. Characterization of the *Shewanella oneidensis* MR-1 Decaheme Cytochrome MtrA: Expression in *Escherichia coli* confers the ability to reduce soluble Fe(III) chelates. *Journal of Biological Chemistry* 278, 27758-27765

Potter, M.C., 1911. Electrical effects accompanying the decomposition of organic compounds. *Proceedings of the Royal Society of London. Series B, Containing Papers of a Biological Character* 84, 260-276.

Rabaey, K., Angenent, L., Shroeder, U., Keller, J., 2010. *Bio-electrochemical Systems: From Extracellular Electron Transfer to Biotechnological Application*. IWA publishing.

Rabaey, K., Lissens, G., Verstraete, W., 2005. Microbial fuel cells: performances and perspectives. *Biofuels for fuel cells: renewable energy from biomass fermentation*, 377-399.

Rabaey, K., Van de Sompel, K., Maignien, L., Boon, N., Aelterman, P., Clauwaert, P., De Schamphelaire, L., Pham, H.T., Vermeulen, J., Verhaege, M., Lens, P., Verstraete, W., 2006. Microbial Fuel Cells for Sulfide Removal. *Environmental science & technology* 40, 5218-5224.

Rabaey, K., Verstraete, W., 2005. Microbial fuel cells: novel biotechnology for energy generation. *Trends in Biotechnology* 23, 291-298.

Rajaguru, P., Kalaiselvi, K., Palanivel, M., Subburam, V., 2000. Biodegradation of azo dyes in a sequential anaerobic–aerobic system. *Applied Microbiology and Biotechnology* 54, 268-273.

Razo-Flores, E.a., Donlon, B., Lettinga, G., Field, J.A., 1997. Biotransformation and biodegradation of N-substituted aromatics in methanogenic granular sludge. FEMS microbiology reviews 20, 525-538.

Ringeisen, B.R., Henderson, E., Wu, P.K., Pietron, J., Ray, R., Little, B., Biffinger, J.C., Jones-Meehan, J.M., 2006. High Power Density from a Miniature Microbial Fuel Cell Using *Shewanella oneidensis* DSP10. Environmental science & technology 40, 2629-2634.

Rismani-Yazdi, H., Christy, A.D., Dehority, B.A., Morrison, M., Yu, Z., Tuovinen, O.H., 2007. Electricity generation from cellulose by rumen microorganisms in microbial fuel cells. Biotechnology and Bioengineering 97, 1398-1407.

Robinson, T., McMullan, G., Marchant, R., Nigam, P., 2001. Remediation of dyes in textile effluent: a critical review on current treatment technologies with a proposed alternative. Bioresource Technology 77, 247-255.

Rodrigues da Silva, M.E., Firmino, P.I.M., dos Santos, A.B., 2012. Impact of the redox mediator sodium anthraquinone-2,6-disulphonate (AQDS) on the reductive decolourisation of the azo dye Reactive Red 2 (RR2) in one- and two-stage anaerobic systems. Bioresource Technology 121, 1-7.

Rosenkranz, H.S., Klopman, G., 1990. Structural basis of the mutagenicity of 1-amino-2-naphthol-based azo dyes. Mutagenesis 5, 137-146.

Roy, R., Fakhruddin, A., Khatun, R., Islam, M., Ahsan, M., Neger, A., 2010. Characterization of Textile Industrial Effluents and its Effects on Aquatic Macrophytes and Algae. Bangladesh Journal of Scientific and Industrial Research 45, 79-84.



Rozendal, R.A., Hamelers, H.V.M., Rabaey, K., Keller, J., Buisman, C.J.N., 2008. Towards practical implementation of bioelectrochemical wastewater treatment. *Trends in Biotechnology* 26, 450-459.

Ruiz-Arias, A., Juárez-Ramírez, C., Cobos-Vasconcelos, D., Ruiz-Ordaz, N., Salmerón-Alcocer, A., Ahuatz-Chacón, D., Galíndez-Mayer, J., 2010. Aerobic Biodegradation of a Sulfonated Phenylazonaphthol Dye by a Bacterial Community Immobilized in a Multistage Packed-Bed BAC Reactor. *Applied Biochemistry and Biotechnology* 162, 1689-1707.

Saha, P., Chakrabarti, T., 2006. *Flavobacterium indicum* sp. nov., isolated from warm spring water in Assam, India. *International Journal of Systematic and Evolutionary Microbiology* 56, 2617-2621.

Sanromán, M.A., Pazos, M., Ricart, M.T., Cameselle, C., 2004. Electrochemical decolourisation of structurally different dyes. *Chemosphere* 57, 233-239.

Saratale, R.G., Saratale, G.D., Chang, J.S., Govindwar, S.P., 2010. Decolorization and biodegradation of reactive dyes and dye wastewater by a developed bacterial consortium. *Biodegradation* 21, 999-1015.

Saratale, R.G., Saratale, G.D., Kalyani, D.C., Chang, J.S., Govindwar, S.P., 2009. Enhanced decolorization and biodegradation of textile azo dye Scarlet R by using developed microbial consortium-GR. *Bioresource Technology* 100, 2493-2500.

Schaetzle, O., Barriere, F., Schroder, U., 2009a. An improved microbial fuel cell with laccase as the oxygen reduction catalyst. *Energy & Environmental Science* 2, 96-99.

Schaetzle, O., Barrière, F., Schröder, U., 2009b. An improved microbial fuel cell with laccase as the oxygen reduction catalyst. *Energy & Environmental Science* 2, 96-99.

Schlaeppli, F., 1998. Optimizing textile wet processes to reduce environmental impact. *Text Chem Color* 30, 19-26.

Schröder, U., 2007. Anodic electron transfer mechanisms in microbial fuel cells and their energy efficiency. *Physical Chemistry Chemical Physics* 9, 2619-2629.

Selvam, K., Swaminathan, K., Chae, K.-S., 2003. Decolourization of azo dyes and a dye industry effluent by a white rot fungus *Thelephora* sp. *Bioresource Technology* 88, 115-119.

Shah, C., Jain, D., 1983. Dyeing of modified polypropylene: cationic dyes on chlorinated polypropylene. *Textile Research Journal* 53, 274-281.

Shaul, G.M., Holdsworth, T.J., Dempsey, C.R., Dostal, K.A., 1991. Fate of water soluble azo dyes in the activated sludge process. *Chemosphere* 22, 107-119.

Skipper, P.L., Kim, M.Y., Sun, H.-L.P., Wogan, G.N., Tannenbaum, S.R., 2010. Monocyclic aromatic amines as potential human carcinogens: old is new again. *Carcinogenesis* 31, 50-58.

Spadaro, J.T., Renganathan, V., 1994. Peroxidase-Catalyzed Oxidation of Azo Dyes: Mechanism of Disperse Yellow 3 Degradation. *Archives of Biochemistry and Biophysics* 312, 301-307.

Stiborová, M., Martínek, V., Rýdlová, H., Hodek, P., Frei, E., 2002. Sudan I Is a Potential Carcinogen for Humans Evidence for Its Metabolic Activation and Detoxication by Human Recombinant Cytochrome P450 1A1 and Liver Microsomes. *Cancer research* 62, 5678-5684.

- Sun, J., Bi, Z., Hou, B., Cao, Y.-q., Hu, Y.-y., 2011. Further treatment of decolorization liquid of azo dye coupled with increased power production using microbial fuel cell equipped with an aerobic biocathode. *Water Research* 45, 283-291.
- Sun, J., Hu, Y.-y., Bi, Z., Cao, Y.-q., 2009. Simultaneous decolorization of azo dye and bioelectricity generation using a microfiltration membrane air-cathode single-chamber microbial fuel cell. *Bioresource Technology* 100, 3185-3192.
- Sun, J., Li, W., Li, Y., Hu, Y., Zhang, Y., 2013a. Redox mediator enhanced simultaneous decolorization of azo dye and bioelectricity generation in air-cathode microbial fuel cell. *Bioresource Technology* 142, 407-414.
- Sun, J., Li, Y., Hu, Y., Hou, B., Zhang, Y., Li, S., 2013b. Understanding the degradation of Congo red and bacterial diversity in an air-cathode microbial fuel cell being evaluated for simultaneous azo dye removal from wastewater and bioelectricity generation. *Applied microbiology and biotechnology* 97, 3711-3719.
- Szczupak, A., Kol-Kalman, D., Alfonta, L., 2012. A hybrid biocathode: surface display of O<sub>2</sub>-reducing enzymes for microbial fuel cell applications. *Chemical Communications* 48, 49-51.
- Takenaka, S., Okugawa, S., Kadowaki, M., Murakami, S., Aoki, K., 2003. The metabolic pathway of 4-aminophenol in *Burkholderia* sp strain AK-5 differs from that of aniline and aniline with C-4 substituents. *Applied and Environmental Microbiology* 69, 5410-5413.
- Tarr, M.A., 2003. Chemical degradation methods for wastes and pollutants: environmental and industrial applications. CRC Press.

Teerapatsakul, C., Bucke, C., Parra, R., Keshavarz, T., Chitradon, L., 2008. Dye decolorisation by laccase entrapped in copper alginate. *World Journal of Microbiology and Biotechnology* 24, 1367-1374.

Thygesen, A., Poulsen, F.W., Min, B., Angelidaki, I., Thomsen, A.B., 2009. The effect of different substrates and humic acid on power generation in microbial fuel cell operation. *Bioresource Technology* 100, 1186-1191.

Towns, A.D., 1999. Developments in azo disperse dyes derived from heterocyclic diazo components. *Dyes and Pigments* 42, 3-28.

Tsujimura, S., Fujita, M., Tatsumi, H., Kano, K., Ikeda, T., 2001.

Bioelectrocatalysis-based dihydrogen/dioxygen fuel cell operating at physiological pH. *Phys. Chem. Chem. Phys.* 3, 1331-1335.

Tyagi, O.D., Yadav, M., 1990. *A Text Book of Synthetic Dyes: (for B.Sc. (Hons.) and M.Sc. Students)*. Anmol Publications Pvt. Limited.

Van Aken, B., Peres, C.M., Doty, S.L., Yoon, J.M., Schnoor, J.L., 2004.

*Methylobacterium populi* sp. nov., a novel aerobic, pink-pigmented, facultatively methylotrophic, methane-utilizing bacterium isolated from poplar trees (*Populus deltoides* × *nigra* DN34). *International Journal of Systematic and Evolutionary Microbiology* 54, 1191-1196.

Van der Zee, F., Lettinga, G., Field, J., 2000. The role of (auto) catalysis in the mechanism of an anaerobic azo reduction. *Water Science & Technology* 42, 301-308.

van der Zee, F.P., Lettinga, G., Field, J.A., 2001. Azo dye decolourisation by anaerobic granular sludge. *Chemosphere* 44, 1169-1176.

- Vandevivere, P.C., Bianchi, R., Verstraete, W., 1998. Review: Treatment and reuse of wastewater from the textile wet-processing industry: Review of emerging technologies. *Journal of Chemical Technology & Biotechnology* 72, 289-302.
- Velasquez-Orta, S.B., Head, I.M., Curtis, T.P., Scott, K., Lloyd, J.R., von Canstein, H., 2010. The effect of flavin electron shuttles in microbial fuel cells current production. *Applied microbiology and biotechnology* 85, 1373-1381.
- Venkata Mohan, S., 2009. Harnessing of biohydrogen from wastewater treatment using mixed fermentative consortia: Process evaluation towards optimization. *International Journal of Hydrogen Energy* 34, 7460-7474.
- Virdis, B., Rabaey, K., Yuan, Z., Keller, J., 2008. Microbial fuel cells for simultaneous carbon and nitrogen removal. *Water Research* 42, 3013-3024.
- von Canstein, H., Ogawa, J., Shimizu, S., Lloyd, J.R., 2008. Secretion of Flavins by *Shewanella* Species and Their Role in Extracellular Electron Transfer. *Applied and Environmental Microbiology* 74, 615-623.
- Wang, X., Cai, Z., Zhou, Q., Zhang, Z., Chen, C., 2012. Bioelectrochemical stimulation of petroleum hydrocarbon degradation in saline soil using U-tube microbial fuel cells. *Biotechnology and Bioengineering* 109, 426-433.
- Wang, Y.-Z., Wang, A.-J., Liu, W.-Z., Kong, D.-Y., Tan, W.-B., Liu, C., 2013. Accelerated azo dye removal by biocathode formation in single-chamber biocatalyzed electrolysis systems. *Bioresource Technology* 146, 740-743.
- Weber, E.J., 1991. Studies of benzidine-based dyes in sediment-water systems. *Environmental Toxicology and Chemistry* 10, 609-618.
- Wolin, E.A., Wolin, M.J., Wolfe, R.S., 1963. Formation of Methane by Bacterial Extracts. *Journal of Biological Chemistry* 238, 2882-2886.

Westwood, D., 2007. The Determination of Chemical Oxygen Demand in Waters and

Effluents. Environment Agency, National Laboratory Service, UK

Wu, J., Eiteman, M.A., Law, S.E., 1998. Evaluation of membrane filtration and ozonation processes for treatment of reactive-dye wastewater. *Journal of environmental engineering* 124, 272-277.

Xie, Y.B., Li, X.Z., 2006. Interactive oxidation of photoelectrocatalysis and electro-Fenton for azo dye degradation using TiO<sub>2</sub>-Ti mesh and reticulated vitreous carbon electrodes. *Materials Chemistry and Physics* 95, 39-50.

Xu, F., Shin, W., Brown, S.H., Wahleithner, J.A., Sundaram, U.M., Solomon, E.I., 1996. A study of a series of recombinant fungal laccases and bilirubin oxidase that exhibit significant differences in redox potential, substrate specificity, and stability. *Biochimica et Biophysica Acta (BBA) - Protein Structure and Molecular Enzymology* 1292, 303-311.

Yoshie, S., Makino, H., Hirose, H., Shirotani, K., Tsuneda, S., Hirata, A., 2006. Molecular analysis of halophilic bacterial community for high-rate denitrification of saline industrial wastewater. *Applied microbiology and biotechnology* 72, 182-189.

You, S.J., Ren, N.Q., Zhao, Q.L., Wang, J.Y., Yang, F.L., 2009. Power Generation and Electrochemical Analysis of Biocathode Microbial Fuel Cell Using Graphite Fibre Brush as Cathode Material. *Fuel Cells* 9, 588-596.

Zhao, F., Rahunen, N., Varcoe, J.R., Chandra, A., Avignone-Rossa, C., Thumser, A.E., Slade, R.C.T., 2008. Activated Carbon Cloth as Anode for Sulfate Removal in a Microbial Fuel Cell. *Environmental science & technology* 42, 4971-4976.

Zhu, X., Logan, B.E., 2013. Using single-chamber microbial fuel cells as renewable power sources of electro-Fenton reactors for organic pollutant treatment. *Journal of Hazardous Materials* 252–253, 198-203.

Zhu, X., Ni, J., 2009. Simultaneous processes of electricity generation and p-nitrophenol degradation in a microbial fuel cell. *Electrochemistry Communications* 11, 274-277.

Zhuang, L., Zheng, Y., Zhou, S., Yuan, Y., Yuan, H., Chen, Y., 2012. Scalable microbial fuel cell (MFC) stack for continuous real wastewater treatment. *Bioresource Technology* 106, 82-88.

Zille, A., Ramalho, P., Tzanov, T., Millward, R., Aires, V., Cardoso, M.H., Ramalho, M.T., Gübitz, G.M., Cavaco-Paulo, A., 2004. Predicting Dye Biodegradation from Redox Potentials. *Biotechnology Progress* 20, 1588-1592.

Zverlov, V.V., Hiegl, W., Köck, D.E., Kellermann, J., Köllmeier, T., Schwarz, W.H., 2010. Hydrolytic bacteria in mesophilic and thermophilic degradation of plant biomass. *Engineering in Life Sciences* 10, 528-536.

### **Web references**

<http://www.biofuture.ie/>

[http://en.wikipedia.org/wiki/William\\_Henry\\_Perkin](http://en.wikipedia.org/wiki/William_Henry_Perkin)

<http://blast.ncbi.nlm.nih.gov/Blast>

# List of publications

## **Peer – reviewed journal articles**

Fernando, E., Keshavarz, T., Kyazze, G., 2012. Enhanced bio-decolourisation of acid orange 7 by *Shewanella oneidensis* through co-metabolism in a microbial fuel cell. *International Biodeterioration & Biodegradation* 72, 1-9.

Fernando, E., Keshavarz, T., Kyazze, G., 2013. Simultaneous co-metabolic decolourisation of azo dye mixtures and bio-electricity generation under thermophilic (50°C) and saline conditions by an adapted anaerobic mixed culture in microbial fuel cells. *Bioresource Technology* 127, 1-8.

Fernando, E., Keshavarz, T., Kyazze, G., 2014a. Complete degradation of the azo dye Acid Orange-7 and bioelectricity generation in an integrated microbial fuel cell, aerobic two-stage bioreactor system in continuous flow mode at ambient temperature. *Bioresource Technology* 156, 155-162.

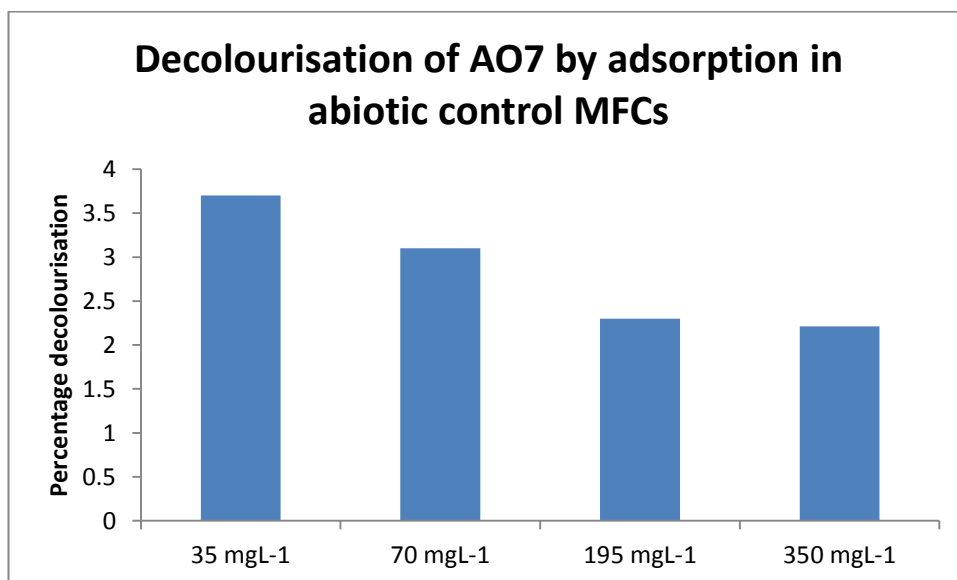
Fernando, E., Keshavarz, T., Kyazze, G., 2014b. External resistance as a potential tool for influencing azo dye reductive decolourisation kinetics in microbial fuel cells. *International Biodeterioration & Biodegradation* 89, 7-14 (Short communication).

## **Conference publications**

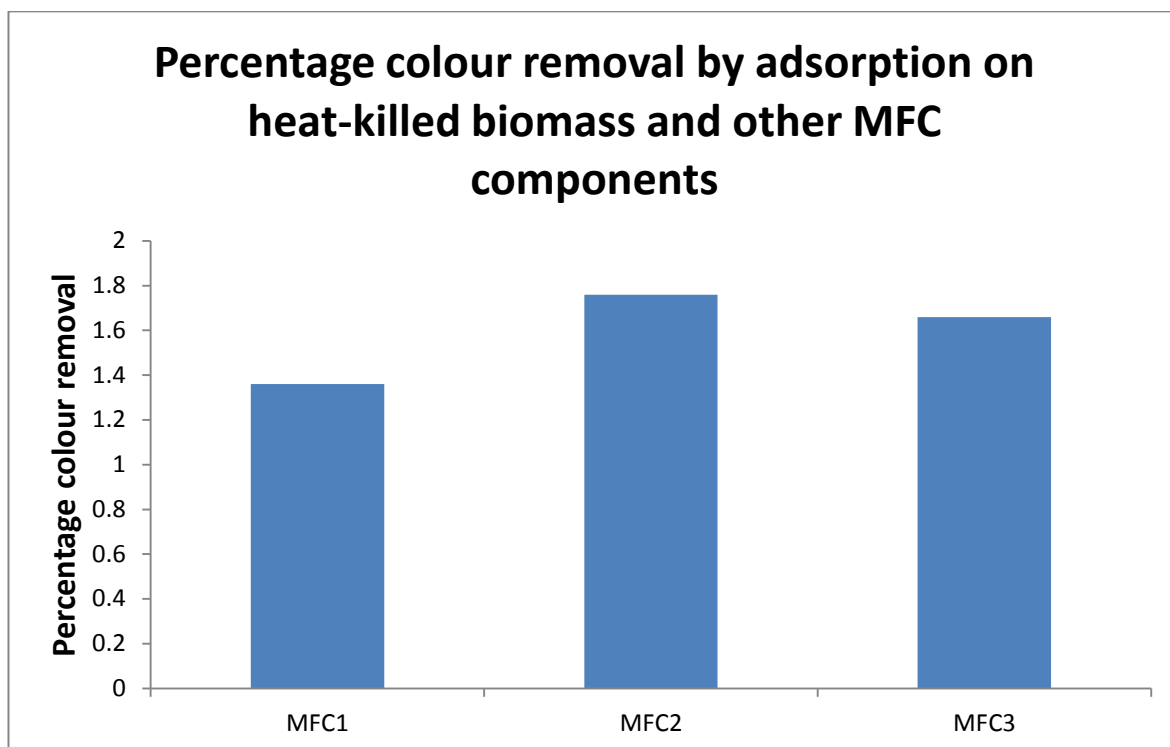
Eustace Fernando, Godfrey Kyazze, Taj Keshavarz. (2012). Simultaneous co-metabolic azo dye decolourisation and bio-electricity generation in microbial fuel cells, in - *Electron transfer at the microbe-mineral interface*, P-036.



## Appendix 1



## Appendix 2



Test	Percent adsorption
MFC1	1.36
MFC2	1.76
MFC3	1.66
mean	1.59
STDEV	0.208